Investigating the role of Class Ia phosphoinositide-3 kinase isoforms in Mantle Cell Lymphoma.

Iyengar, Sunil

Investigating the role of Class Ia phosphoinositide-3 kinase isoforms in Mantle Cell Lymphoma

Sunil Iyengar

Submitted in partial fulfilment of the requirements
of the Degree of Doctor of Philosophy

2013

Centre for Haemato-Oncology
Barts Cancer Institute
Queen Mary University of London
Charterhouse Square
London

To my family for their love, support and patience

ABSTRACT

Mantle Cell Lymphoma (MCL) is a rare but aggressive Non-Hodgkin Lymphoma (NHL). Although t(11;14) is a hallmark of MCL, it is insufficient for lymphomagenesis. The phosphoinositide-3 kinase (PI3K) pathway is thought to play an important role in MCL pathogenesis and the PI3K p110δ isoform is enriched in leucocytes making it an attractive target. Early phase trials evaluating the p110δ selective inhibitor GS-1101 however demonstrate inferior responses in MCL compared to chronic lymphocytic leukaemia and indolent NHL.

The relative contribution of the class Ia PI3K isoforms p110α (*PIK3CA*), p110β (*PIK3CB)* and p110δ (*PIK3CD*) was therefore evaluated in MCL. Immunohistochemistry on MCL tissue microarrays revealed that while p110δ was highly expressed, p110α showed wide variation and p110β expression was the weakest. A significant increase in p110α expression was found with disease progression. Although GS-1101 was sufficient to abolish B-cell receptor mediated PI3K activation, additional p110α inhibition was necessary to abolish constitutive PI3K activation in MCL exhibiting high p110α expression. Compared to GS-1101, GDC-0941 (p110α and p110δ inhibitor) had greater *in vitro* toxicity and a high *PIK3CA*/*PIK3CD* mRNA ratio (> twice ratio in healthy B-cells) was able to identify primary MCL samples that were resistant to GS-1101 but significantly more sensitive to GDC—0941. This ratio also increased with disease progression. No *PIK3CA* or *PIK3R1* activating mutations were found. In summary, blockade of both p110α and p110δ appears to be necessary for effective PI3K inhibition in MCL, particularly with relapse. The *PIK3CA*/*PIK3CD* mRNA ratio may help identify those patients that are most likely to respond.

Finally, a disseminated xenograft model of human primary MCL was established in NSG mice. Engraftment of primary MCL was demonstrated by peripheral blood flow cytometry, tissue immunohistochemistry and FISH for t(11;14). This model is potentially valuable for pre-clinical *in vivo* testing of novel drugs for this incurable disease.

Table of Contents

LIST OF TABLES

Chapter 1

Chapter 2

Chapter 3

Chapter 4

Chapter 5

APPENDIX

LIST OF FIGURES

Chapter 1

Chapter 2

Chapter 3

Chapter 4

Chapter 5

CHAPTER 6

APPENDIX

ACKNOWLEDGEMENTS

I was first made aware of the research post that I was appointed to at the Centre for Haemato-Oncology, Barts Cancer Institute by Simon Hallam and I am grateful to him for this. Throughout my period at the Institute Lynn Haddon, Carol Jennings and David Williamson were very kind and helpful with administrative and laboratory issues. My supervisors Dr Simon Joel and Prof John Gribben provided valuable guidance, support and encouragement to explore my ideas and also achieve my goals within the timeframe I had. I am extremely grateful to them for this. It was a pleasure to work with Andrew Clear and Csaba Bodor and I am grateful to them for sharing their knowledge and laboratory expertise with me. I had the privilege of working closely with the Centre for Cell Signalling and would like to thank Prof Bart Vanhaesebroeck, Ezra Aksoy and Benoit Bilanges for sharing their expertise in the field of PI3K signalling. In the second year of my research I was fortunate to be awarded the EHA-ASH translational research training fellowship in haematology (TRTH). I would like to acknowledge all the members of the TRTH small working group for their support, particularly Donna Neuberg for her statistical input. I received valuable assistance from Rebecca Auer, Janet Matthews, Jacek Marzec, Sameena Iqbal and Thomas Dowe in gathering clinical data and samples from patients with Mantle Cell Lymphoma and am indebted to the patients themselves for providing these. I would like to acknowledge the helpful advice I received (often by the coffee machine!) from Jude Fitzgibbon, David Taussig and Jeff Davies and the mentorship I received from Prof Andrew Lister's before his retirement and his advice and encouragement afterwards. I also consider myself very fortunate to have had the opportunity to collaborate with Dr Dominique Bonnet and Linda Ariza-McNaughton at the Haematopoietic Stem Cell Laboratory, CRUK, Lincoln's Inn Fields in the final year of my research. This collaboration opened up exciting possibilities and I am grateful for their advice and input towards this research.

This work was funded by the David Pitblado Fellowship, Barts and the London Charity and I would like to thank Katherine Priesley for her kindness and generosity. Additional funding for animal studies was secured from the Roger Counter Foundation Early Stage Research Grant awarded by the British Society of Haematology.

Finally, I would like to thank my family for all the sacrifices they have made and my daughter Rachna for providing me a constant source of joy that I have often needed through this work. Above all, I would like to thank my wife Sneha and her family who have been extremely patient and supportive through the long evenings and weekends that were spent doing this research.

CHAPTER 1: INTRODUCTION

1.1 MANTLE CELL LYMPHOMA

1.1.1 Introduction

Mantle cell lymphoma (MCL) is a B-cell non-Hodgkin lymphoma (NHL) that was first recognised as a distinct entity in 1994,[1] although the concept of a 'mantle zone lymphoma' was introduced by Weisenburger *et al* as far back as 1982.[2] MCL is relatively rare and constitutes about 2-10% of all NHL with an incidence of approximately 0.5 per 100,000 in the western world.[3] The majority of patients are elderly males with a median age of approximately 70 years at diagnosis and a male to female ratio of 2-3:1 (Figure 1.1). Advanced stage disease with bone marrow and extranodal involvement, particularly of the gastrointestinal tract, where it is often seen as multiple lymphomatous polyps, is frequently found and approximately a third of all patients present with lymphocytosis in the peripheral blood. Central nervous system involvement is not uncommon in MCL and is more frequent with blastoid morphology and advanced disease.[4,5]

Figure 1.1 Estimated age-specific incidence of Mantle Cell Lymphoma in the United Kingdom

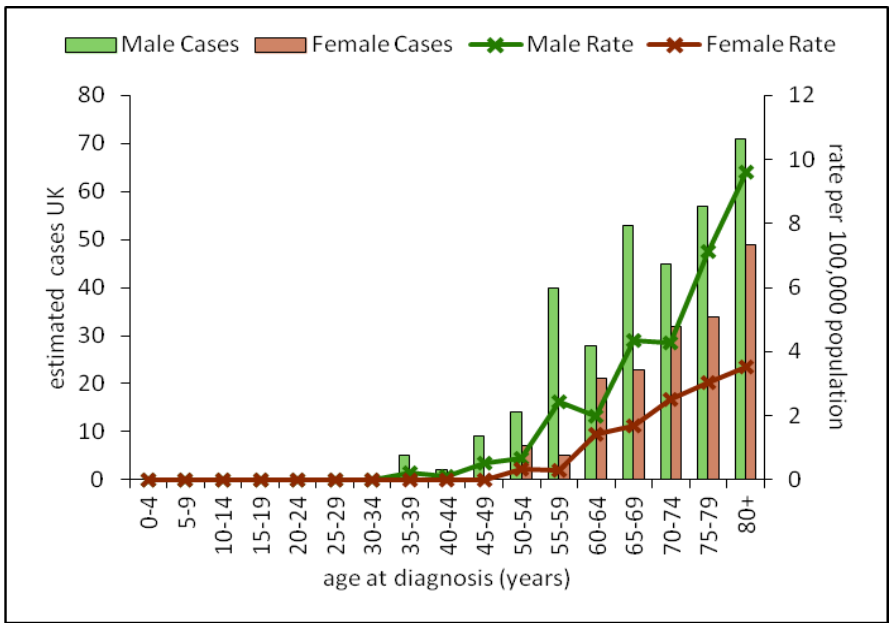

Source: www.hmrn.org

Although there has been an improvement in overall survival from the 2-4 year range cited in earlier series to between 5 and 7 years in more recent studies,[6] MCL remains incurable with conventional treatment. Apart from better supportive care, improvement in overall survival of patients is attributable to aggressive treatment of younger and/or fitter patients with high dose cytarabine containing regimens, such as hyperCVAD and maxiCHOP/Ara-C, as well as the use of autologous and allogeneic stem-cell transplantation, all of which are associated with significant toxicity and can adversely impact on quality of life. The Kaplan-Meier curve in figure 1.2, derived from the overall survival of 120 patients with MCL treated at Barts between 1975 and 2010, emphasises the need for improved management of this condition.

In recent years, a better understanding of the genetic and molecular basis of MCL has revealed a number of promising targets, including the phosphoinositide-3 kinase (PI3K) pathway. Given the relative rarity of MCL, pre-clinical evaluation of these drugs in parallel with biomarker discovery is essential for effective targeting of this aggressive and incurable neoplasm.

Figure 1.2 Kaplan-Meier survival estimate for patients treated at Barts hospital between 1975 and 2010 (N=120)

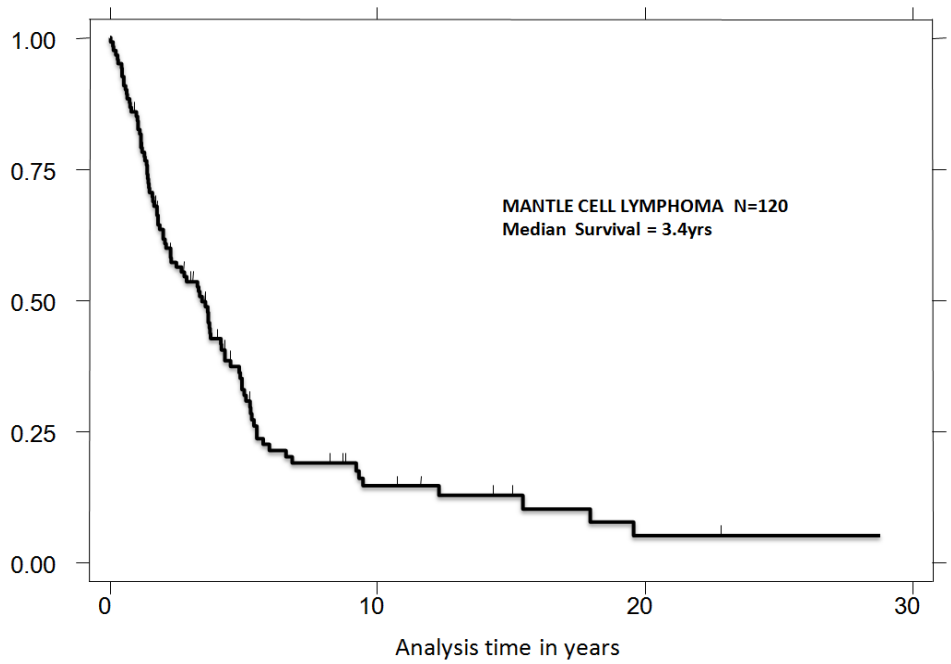

1.1.2 Genetic and molecular basis

MCL likely originates from B-cells of the inner mantle zone of secondary lymphoid follicles. The cell of origin in MCL is not restricted to the naive pre-germinal centre B-cell as previously thought and 15 - 40% of cases are found to have hypermutated immunoglobulin heavy chain variable region (IGHV) genes.[7-10] Morphologically, MCL consists of small to medium sized lymphocytes with irregular nuclear contours in the majority of cases. Although a number of morphological variants have been described, only the small cell (classical) and blastoid variants are of potential clinical significance. Blastoid morphology, which is found in about 20% of patients at presentation, can be recognised by an increase in nuclear size and chromatin dispersal along with prominent nucleoli and pleomorphism in some cases (Figure 1.3). The risk of transformation to blastoid MCL for those presenting with small cell morphology is approximately 42% over 5 years.[11] MCL cells exhibit a mature B-cell phenotype with expression of CD19, CD20, CD22 and CD79a. CD5 is co-expressed in the majority of cases but, in contrast to chronic lymphocytic leukaemia (CLL), CD20 expression is strong, FMC7 is expressed and CD23 is usually absent. The germinal centre markers CD10 and BCL6 are absent.[12]

Figure 1.3 Classical and blastoid morphological variants in MCL

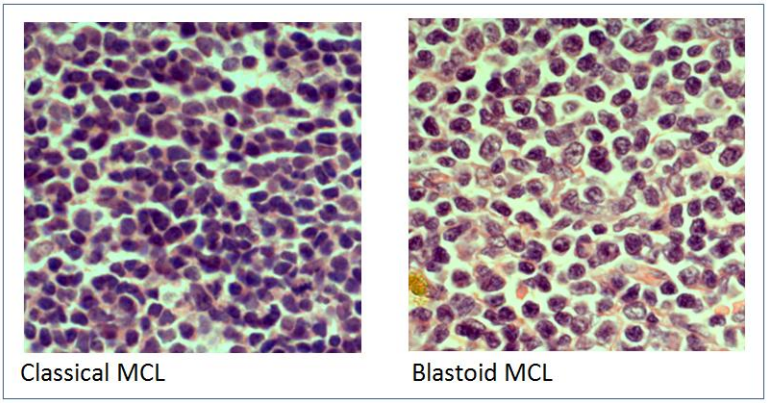

The diagnostic hallmark and primary event in MCL pathogenesis is t(11;14) which results in fusion of the immunoglobulin heavy chain (*IGH)* promoter at 14q32 to the gene encoding cyclin D1 (*CCND1*), at 11q13, leading to the characteristic over-expression of cyclin D1.[13] Approximately 6% of MCLs are

negative for this translocation but are found to over-express cyclin D2, D3 or E.[14] This primary event leads to deregulation of the cell cycle at the G_1/S phase transition but is unlikely to be sufficient for MCL tumorigenesis as suggested by observations that Eμ-cyclin D1 transgenic mice fail to develop tumours spontaneously. However, exposing these mice to a mitogenic stimulus (isoprane) over a period of time, leads to development of a CD20 and cyclin D1 expressing MCL-like lymphoma involving the spleen, bone marrow and lymph nodes.[15] Similarly double transgenic mice with Eμ-linked co-expression of cyclin D1 and MYC develop spontaneous lymphomas implying secondary hits are necessary for mantle cell lymphomagenesis.[16]

A number of secondary genetic events have now been described in MCL, consisting of recurrent copy number amplifications and chromosomal gains and losses. These events primarily converge on pathways involving the cell cycle and DNA damage response.[17] Deletions involving the INK4a/ARF locus and mutations involving TP53 and the PI3K domain of the DNA damage response gene ATM (found in 40-75% of cases) are some common examples.[18,19] MCL therefore shows high genetic instability with more complex karyotypes often associated with blastoid morphology[20] and aggressive behaviour. In addition to genetic aberrations, both gene expression profiling and proteomic studies have implicated the PI3K/Akt/mTOR,[21-24], NFκB[25] and WNT[21,26] signalling pathways in proliferation and survival of MCL. More recently, whole transcriptome sequencing has revealed recurrent mutations in NOTCH1, primarily involving the PEST domain, with a frequency of 12%. In the same study NOTCH inhibition with a gamma-secretase inhibitor was shown to inhibit growth and induce apoptosis in two MCL cell lines.[27]

Studies of the microenvironment in MCL are few compared to other lymphomas but interaction with the surrounding cellular and chemical components almost certainly plays an important role in conjunction with signalling pathways in the survival of neoplastic cells. MCL carrying hypermutated IGHV genes show a strong bias in the IGHV gene repertoire and therefore, similar to CLL, antigen

selection may be an important driver of clonal expansion.[10] Reports of constitutive SYK activation and the identification of SYK and BTK among the most abundant phosphoproteins in a recent phosphoproteomic study further emphasize the importance of B-cell receptor (BCR) signalling in MCL.[24,28] In addition, tumour cells have been found to express high levels of CXCR4, CXCR5 and VLA-4 and have been observed to proliferate in response to CD40 ligand as well as interleukin-4 (IL4) stimulation in vitro.[29] Furthermore, a chemo-protective role for mesenchymal stromal cells has been demonstrated in co-culture studies with MCL cells.[30] More recently, autocrine and paracrine secretion of IL-6 has been reported to be key to MCL survival through activation of the PI3K/Akt and JAK-STAT pathways.[31] The role of T-cells and macrophages in MCL is less clear. In one study a macrophage infiltration (CD68+ cells) of greater than 5% was reported as being associated with a significantly worse overall survival but, similar to observations in follicular lymphoma, the significance of this finding was lost in rituximab treated patients.[32]

1.1.3 Prognostic markers

MCL is an aggressive neoplasm in the vast majority of patients. However, in a small minority this lymphoma behaves indolently and can even be managed expectantly with no detrimental effects on survival.[33,34] A number of studies have analysed clinical and molecular characteristics that may predict for indolent disease. It is now becoming clear that most patients with indolent MCL present with isolated leukaemic (non-nodal) disease whereas patients with nodal disease are more likely to have more aggressive lymphoma.[35,36] Molecular markers such as SOX11,[37,38] IGHV mutation status[39-41] and 17p deletions/TP53 mutations [42,43] continue to be controversial as independent prognostic markers, but may have a better predictive value when evaluated in conjunction with clinical characteristics. For example, nodal MCL with unmutated or minimally mutated IGHV and positive SOX11 is very likely to have a significantly worse prognosis than isolated leukaemic disease with mutated IGHV, negative SOX11 and a wild type TP53. Leukaemic disease with mutated TP53, on the other hand, is more likely to follow an aggressive clinical course.[44,45] A recent study of somatic

hypermutation in MCL evaluated a >97% homology cut-off, as opposed to the 98% cut-off used in CLL studies, for differentiating IGHV mutated from unmutated MCL and demonstrated that this was able to clearly define a unmutated/minimally mutated cohort with a significantly worse prognosis.[45] Nevertheless, a combination of these clinical and molecular characteristics is likely to be superior for defining indolent disease than any single marker.

The Ki-67 tumour proliferation fraction, MIPI (MCL international prognostic index) and minimal residual disease (MRD) analysis are three well established independent prognostic markers that have a strong predictive value in MCL. Using gene expression profiling, the Leukemia Lymphoma Molecular Profiling group demonstrated that a signature of proliferation genes was able to identify MCL subsets differing in median survival by over 5 years.[46] This led to the evaluation of Ki-67, a non-histone nuclear protein found exclusively in proliferating cells, as a prognostic marker using immunohistochemistry. The percentage Ki67-positivity has now been shown to be highly predictive of outcome in multivariate analysis and retains its validity in the rituximab era[47-49] (Table 1.1). Consensus guidelines have been published recently on the use of Ki-67 as a marker of proliferation in MCL.[50]

The MIPI was formulated by the European MCL network following data evaluation from over 450 patients with advanced stage MCL treated in 3 clinical trials and incorporates patient age, ECOG status, LDH and white cell count to provide a predictive score.[51] Patients can be divided into three distinct categories with significantly different survival based on this score. A simplified MIPI and a 'biological MIPI' (incorporating the Ki-67 index) have also been described and are detailed in table 1.2. Another important independent prognostic marker is PCR based sequential minimal residual disease (MRD) monitoring. In two large MCL clinical trials, significantly improved response duration was seen in patients who achieved molecular remission independent of the degree of clinical

remission (CR, CRu or PR).[52] The predictive value of MRD monitoring has recently been confirmed in an independent study by the Cancer and Leukemia Group B (CALGB).[53]

Table 1.1 Prognostic value of Ki67 proliferation index

Ki67 proliferation index	Median survival
<10%	42 months
11-40	30 months
>40%	15 months

Tiemann *et al* 2005[49]

Table 1.2 Mantle cell lymphoma international prognostic index (MIPI)

Mantle cell lymphoma international prognostic index (MIPI)

MIPI = [0.03535 x age (years)]
+ 0.6978 (if ECOG>1)
+ 1.367 x $\log_{10}$ (LDH/ULN)
+ 0.9393 x $\log_{10}$ (WBC count)

$MIPI_b$ = MIPI + (0.02142 x Ki-67%)

Simplified MIPI

Points	Age (y)	ECOG	LDH/ULN	WBC x10^9/L
0	<50	0-1	<0.67	<6.7
1	50-59	-	0.67-0.99	6.7-9.9
2	60-69	2-4	1.000-1.49	10-14.9
3	>70	-	>1.5	>15

Risk	MIPI	$MIPI_b$	Simplified MIPI	Median OS (based on MIPI)
Low risk	<5.7	<5.7	0-3	Not reached*
Intermediate risk	5.7 – 6.2	5.7-6.5	4-5	54 months
High risk	>6.2	>6.5	6-11	29 months

*5year OS = 60 %

Other prognostic markers that have been described in MCL include the five-gene model (*RAN*, *MYC*, *TNFRSF10B*, *POLE2*, and *SLC29A2)*[54] and more recently, methylation profiles,[55] NOTCH mutations,[27] microRNA signatures[56] and serum free light chain ratios.[57] These will need further validation, but have contributed to our understanding of this biologically complex disease.

1.1.4 Current management

Until recently patients with MCL were treated heterogeneously with treatments ranging from expectant management to a variety of chemotherapy regimens and stem cell transplant. In the last 10 years, collaborative efforts like the European MCL network have been able to provide evidence-based recommendations to guide first-line treatment through large clinical trials. The treatment of relapsed disease remains a difficult challenge but the number of novel agents with proven clinical efficacy has grown rapidly in the last few years and has created an exciting platform for future studies.

As discussed briefly in the previous section, patients with asymptomatic MCL can be managed expectantly with no detrimental effect on survival. While Martin et al demonstrated a significant survival advantage in those patients in whom treatment was deferred,[34] Eve et al did not find any significant difference between these two approaches in an independent cohort[33] suggesting that a watch and wait approach is at least non-inferior in these patients, as long as they are closely monitored for progression.

Over 90% of patients with MCL present with stage III or IV (modified Ann-Arbor) disease but in the small proportion who present with limited stage disease, radiotherapy with or without chemotherapy may be indicated. There is good evidence that MCL is radiosensitive and localised disease can be treated with involved field radiotherapy to satisfactory responses that are, in some cases, sustained for several years.[58-60]

A handful of studies, particularly the recently reported National Cancer Research Institute (NCRI) phase III study comparing FC (fludarabine, cyclophosphamide) and R-FC,[61] have provided evidence for improved response rates and progression free survival (PFS) with the addition of rituximab to chemotherapy in front line treatment of MCL.[62-64] In younger, fitter patients it is now widely accepted that a chemotherapy regimen containing high dose Ara-C, such as R+maxiCHOP/Ara-C or R-DHAP (dexamethasone, cytarabine, cisplatin), followed by autologous stem cell transplant (ASCT) is likely to provide the most benefit in terms of PFS. This significant prolongation of PFS with upfront ASCT was first demonstrated by Dreyling et al in the landmark first randomised study of the European MCL network.[65] Subsequently the Nordic lymphoma group MCL 2 study showed there was a significant improvement in response rates and PFS from addition of high dose Ara-C and rituximab to the maxiCHOP induction, compared to the same group's previous MCL1 study of maxiCHOP and BEAM ASCT.[66] The benefit of high dose Ara-C in significantly improving response rates, time to treatment failure and, for the first time, overall survival (OS) was recently reported at the 2012 ASH annual meeting in the final analysis of the European MCL network randomised study (*MCL younger trial*) that compared 6 cycles of R-CHOP to alternating cycles of R-DHAP (x3) and R-CHOP (x3) followed by ASCT.[67] Another very active regimen is R-hyperCVAD/Ara-C and methotrexate that has been shown to achieve high response rates in younger patients without the need for ASCT but the significant toxicities associated with this regimen have discouraged more widespread use.[68,69] Table 1.3 summarises selected regimens from clinical trials that have achieved high response rates and progression free survival.

The treatment of elderly patients is guided by performance status and co-morbidities, and a number of chemo-immunotherapy options such as R-FC, R-CHOP, R-CVP, R-bendamustine and R-chlorambucil have been evaluated. Although R-CHOP is often included in the standard arm in randomised trials there is no evidence for benefit with addition of anthracycline and R-CVP may be equally effective.[70,71] A recent landmark study for the treatment of elderly patients with MCL (>60

years and not eligible for high dose therapy, median age 70 years) was reported by the European MCL network[72] providing evidence in favour of R-CHOP followed by rituximab maintenance for front-line treatment in this cohort. This trial evaluated an initial induction randomisation between R-CHOP and R-FC followed, in responding patients, by a maintenance randomisation between rituximab and interferon alpha (given until progression). Patients who received R-CHOP induction had a significantly better OS and PFS compared to R-FC while rituximab maintenance significantly reduced the risk of progression or death compared to interferon alpha maintenance.

Relapsed MCL has a dismal prognosis with a median survival of 1-2 years. There is evidence for graft-versus-lymphoma effect in MCL and reduced intensity conditioning allogeneic stem cell transplantation (AlloSCT) has a role in eligible patients who have an appropriate donor and chemo-sensitive disease.[73,74]. Myeloablative conditioning regimens have high treatment related mortality (30-40%) and experience with AlloSCT in refractory disease is limited. In patients not eligible for AlloSCT, in addition to the use of another standard regimen to which the patient has not previously been exposed, a number of alternative chemotherapy regimens have been evaluated with varying efficacy. These include cladiribine,[75] R-FCM (additional mitoxantrone),[76] PEP-C (prednisone, etoposide, procarbazine, cyclophosphamide),[77] temsirolimus,[78] bortezomib[79,80] and gemcitabine/dexamethasone/cisplatin.[81] Clinical trial data for these regimens along with some of the promising newer agents that have significant activity in relapsed/refractory MCL are summarised in table 1.4. The activity of PI3K pathway inhibitors in MCL is discussed in greater detail in section 1.3. Other novel inhibitors including Flavopiridol (pan cyclin-dependent kinase inhibitor), Enzastausrin (PKCβ inhibitor) and Fostamatinib (SYK inhibitor) have shown disappointing activity in MCL despite the potential importance of their targets in MCL pathogenesis.

In summary, while there has been a significant improvement in our understanding of how to use conventional chemotherapy in frontline treatment to improve responses and outcomes in MCL,

further improvements are only likely to come from a better understanding of which novel therapies to use and also how and when to use them. A number of these therapies have already shown great promise in early phase trials with significant prolongation of progression free survival and very favourable toxicity profiles,. The challenge now lies with effectively evaluating this armamentarium of novel therapies in a rare lymphoma like MCL but this can potentially be overcome with increased emphasis on models for pre-clinical evaluation and biomarker discovery.

Table 1.3 Selected data from clinical trials in front-line MCL showing the best progression-free and overall survival rates achieved with current chemo-immunotherapy and dose-intense regimens

	Regimen	N	ORR (CR/Cru)	Median PFS (months)	Median OS (months)	Reference
Immuno-chemotherapy regimens	R-Chlorambucil	14	64% (36%)	26	-	Bauwens *et al* 2005
	R-CHOP	62	94% (34%)	20	Not reached	Lenz *et al* 2005
	R-FC	186	91% (65%)	31	-	Rule *et al* 2011
	R-CHOP / R maintenance	87	86% (34%) With induction	Not reached	87% at 48mths	Kluin-Nelemans *et al* 2012
Dose-intense regimens	HyperCVAD / high dose methotrexate + Ara-C	45	93.5% (38%)	72% at 36mths	92% at 36mths	Khouri *et al* 1998
	MaxiCHOP / high dose Ara-C / ASCT	160	90% CR	56% at 72mths	75% at 48mths	Geisler *et al* 2008
	R-HyperCVAD / high dose methotrexate + Ara-C	97	97% (87%)	4.6 yrs	Not reached	Romaguera *et al* 2010
	R-HyperCVAD / high dose methotrexate + Ara-C	60	83% (72%)	61% at 5yrs (estimated)	73% at 5 yrs (estimated)	Merli *et al* 2012
	R-CHOP / ASCT	455	90% (40%)	49	82mths	Hermine *et al* 2012
	R-DHAP / R-CHOP / ASCT		95% (54%)	84	Not reached	

Table 1.4 Selected clinical trial data with conventional regimens and novel therapies in relapsed/refractory MCL

Therapy		N	ORR (CR/Cru)	Median PFS (months)	Median OS (months)	Median lines of previous therapy	Reference
Purine analogues	R-FC	16	75%	11	-	2(1-6)	Thomas *et al* 2005
	R-FCM	24	58% (29%)	8	Not reached	1	Forstpointner *et al* 2004
	Cladiribine	25	46% (21%)	5.4	22.8	-	Inwards *et al* 2008
Other cytotoxics	Gemcitabine-dexamethasone-cisplatin	18	44.4% (9%)	8.5	Not reached	1 (1-3)	Morschhauser *et al* 2007
	R-bendamustine	16	75% (50%)	18	-	1 (1-3)	Rummel *et al* 2005
	PEP-C	22	82% (46%)	-	-	-	Coleman 2008
Proteasome inhibitor	Bortezomib	155	32% (8%)	6.7	23.5	2 (1-3)	Goy *et al* 2009
	Bortezomib-gemcitabine	26	58% (12%)	11.4	-	1 (1-3)	Kouroukis *et al* 2011
	R-Bortezomib	19	58% (16%)	-	-	-	Agathocleous *et al* 2010
mTOR inhibitor	Temsirolimus	35	38% (3%)	6.5	12	3 (1-11)	Witzig *et al* 2005
	R-Temsirolimus	69	59% (19%)	9.7	29.5	2 (1-9)	Ansell *et al* 2011
Immunomodulatory agents	R-Thalidomide	16	81% (31%)	20.4	Not reached	1	Kaufmann *et al* 2004
	Lenalidomide	57	24% (12%)	5.7	-	3	Witzig *et al* 2011
PI3K inhibitor	GS-1101	21	48%	4	-	5 (1-12)	Kahl *et al* 2010
BTK inhibitor	Ibrutinib	109	66% (19%)	Not reached	Not reached	3 (1-6)	Wang et al 2012

1.2 THE PHOSPHOINOSITIDE-3 KINASE PATHWAY

1.2.1 Introduction

The term phosphoinositide-3 kinase (PI3K) refers to lipid kinases that can phosphorylate the 3-hydroxyl position of the inositol ring of the phosphatidylinositol membrane lipids (PtdIns). PI3Ks and the 3-phosphoinositides they generated were first discovered in the late 1980s in studies examining the transformation of 3T3 fibroblasts by the polyoma virus middle T (PMT) antigen.[82,83] The observation that association of PMT with PI3K correlated with transformation and that PMT mutants that failed to associate with PI3K did not result in transformation, indicated an essential role for this enzyme in the transformation process.[84] Until this discovery, the existence of 3-OH phosphorylated PtdIns was not known and interest in PtdIns had focussed on receptor-stimulated hydrolysis of phosphoinositide (3,4) biphosphate (PIP_2) by phospholipase C (PLC) leading to inositol (1,4,5) triphosphate (IP_3) and diacylglycerol (DAG)[85] production. The discovery of this new class of enzymes and the 3-phosphoinositides they generated [PI[86] monophosphate, PI(3,4) diphosphate and PI(3,4,5) triphosphate] placed PI3Ks in a new pathway, now known as the PI3K signalling pathway, distinct from PLC-dependent signalling. Further milestones in PI3K research led to better understanding of the heterodimeric structure and isoforms of the enzyme,[87-93] mechanisms of regulation,[94-97] downstream targets[98-102] and its role in healthy and malignant cells.[103-107] Some of these milestones, including the development of mutant/knockout mouse models[108-113] and pharmacological inhibitors,[114-117] which have been central in establishing a better understanding of this pathway, are detailed in the timeline in figure 1.4. This timeline is not exhaustive, but it provides a snapshot of the transition from basic science discoveries to bedside applications in the field of PI3K research. PI3Ks are part of a complex signalling network with multiple inputs and downstream effects and our knowledge of this pathway is far from complete, but the entry of PI3K inhibitors into the clinic and the impressive single agent effects observed in some haematological malignancies provides ultimate evidence for the importance of this pathway in cancer cell survival.

Figure 1.4 Timeline of milestones in PI3K research

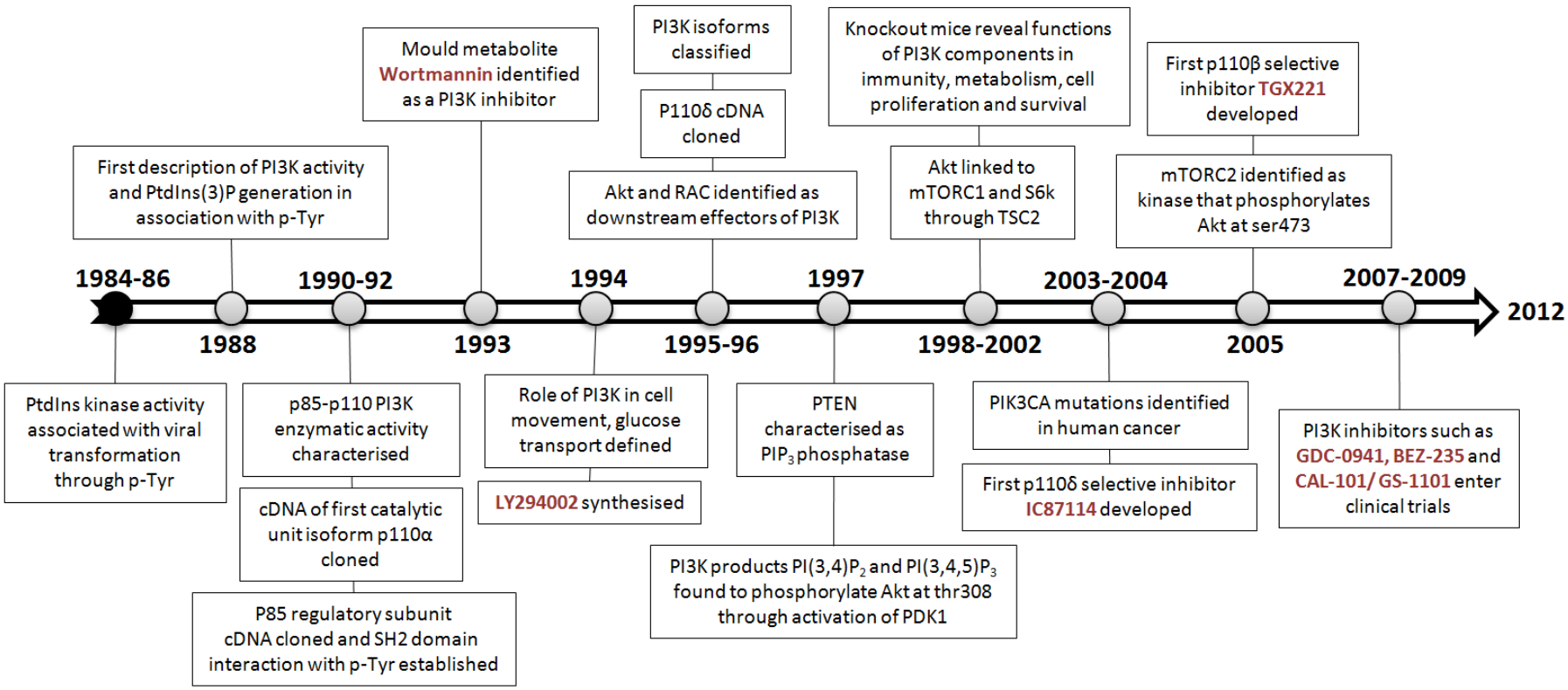

Abbreviations: PtdIns = phosphatidylinositol, p-Tyr = phosphorylated tyrosines, PI3K=phosphoinositide-3 kinase, SH2=Src homology 2, PTEN=phosphatase and tensin homolog, PDK-1=phosphoinositide dependent kinase 1, mTORC=mammalian target of rapamycin complex, TSC2=tuberous sclerosis complex2. Pharmacological PI3K inhibitors are highlighted in red.

1.2.2 Classification of the PI3K enzymes

PI3Ks are divided into three classes – I, II and III, on the basis of their structure and lipid substrate preferences.[92,93] Class I PI3Ks are primarily linked to oncogenesis because of their ability to convert PI(4,5)diphosphate to the important second messenger PI(3,4,5)triphosphate, which from here on will be referred to as PIP2 and PIP3. PI3K classes II and III convert PI to PI(3) monophosphate, and PI(4)monophosphate to PI(3,4)diphosphate but little is known about the role of these 2 classes of enzymes in oncogenesis, if any, and hence they will not be discussed further. PTEN (phosphatase and tensin homolog) is an antagonist phosphatase that converts PIP3 back to PIP2 (Figure 1.5). Class I enzymes have four 110kD catalytic unit isoforms - p110α, p110β, p110δ and p110γ. These isoforms show differential tissue expression in that p110δ and p110γ are highly enriched in leukocytes while p110α and p110β are expressed in all tissues.[90,118] All class I enzymes are obligate heterodimers and have a p85 regulatory subunit, apart from p110γ which binds to a p101 or p87 subunit (Figure 1.6). On the basis of their regulatory subunits class I enzymes are further divided into class Ia and Ib (Figure 1.6) with class Ia PI3Ks signalling downstream of activated receptor tyrosine kinase (RTKs) and class Ib downstream of G-protein coupled receptors (GPCRs).[93] This functional distinction is now becoming less clear with evidence that molecules such as Ras, which can be activated by either RTKs or GPCRs, can in turn activate class Ia and class Ib isoforms.[119,120] However this classification is still useful, as for instance in the context of p85 activating mutations which result in activation of only class Ia isoforms.[121]

Class Ia isoforms form the main focus of this research for three main reasons. Firstly, p110δ is highly enriched in leucocytes[90,91] and is the primary isoform involved in B-cell receptor (BCR) signalling.[122, 123] Secondly, although p110γ is also enriched in leucocytes, p110γ-deficient mice are found to primarily suffer T-cell defects while p110δ-deficient mice primarily suffer B-cell defects.[124] Finally, activating oncogenic mutations of PI3K have only been described in relation to class Ia isoforms.[107,121]

1.2.3 Class Ia PI3K: Role in normal and malignant cells

PI3Ks were first discovered in the context of oncogenic cellular transformation but we now know that class I PI3Ks play an important role in a number of physiological processes such as immunity, metabolism, proliferation and survival. Most of these processes are enhanced or altered in malignant cells to provide them an advantage over normal cells. PI3K activation in healthy cells is mostly agonistic and driven by growth factors, antigenic stimuli (in B and T-lymphocytes) and metabolic changes. In malignant cells, in addition to agonistic signalling, a number of mechanisms for constitutive PI3K activation have been described and some of these are discussed below in relation to the components of the PI3K signalling machinery.

The p85 regulatory subunit: The class Ia regulatory subunit genes reside on the long arm of chromosome 5. *PIK3R1* encodes the isoforms p85, p55α and p50α through differential promoter usage while *PIK3R2* and *PIK3R3* encode p85β and p55γ respectively. The inter-SH2, p110 binding domain links the regulatory subunit to the catalytic subunit and as a result stabilises as well as inhibits the kinase activity of the enzyme. On growth factor stimulation, class Ia PI3Ks are recruited to the cell membrane and the p85 subunits bind to phosphorylated tyrosine motifs or Ras through their respective binding domains. This binding releases the inhibitory effect of P85 on the catalytic subunits while also approximating them to their substrate PIP2, thereby triggering the PI3K signalling cascade.

It is not known whether each of the p85 isoforms have distinct roles but there is evidence for differential binding to receptors. It has also been demonstrated that p85 regulatory subunits can bind any of the class Ia p110 isoforms and there is no evidence for preferential binding.[90] It is therefore likely that this pairing depends, at least to some extent, on the relative abundance of the p110 isoforms.

Figure 1.5 Conversion of PIP2 to PIP3 by class I PI3K and antagonism by the phosphatase PTEN

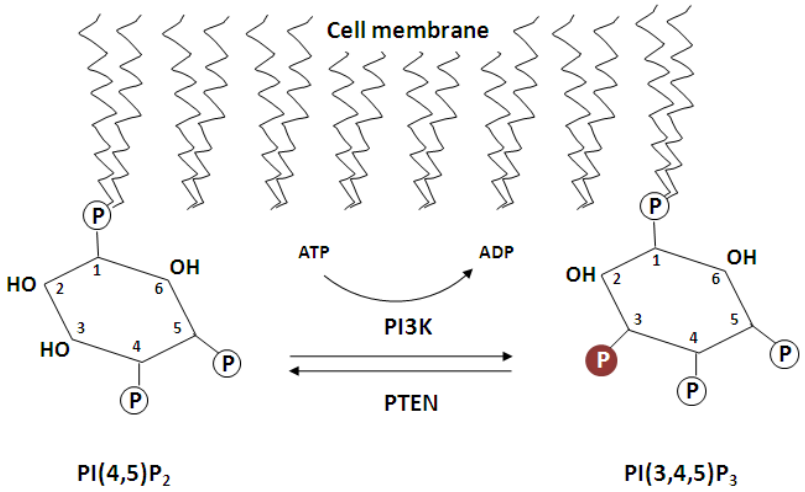

Figure 1.6 Classification of class I PI3K isoforms

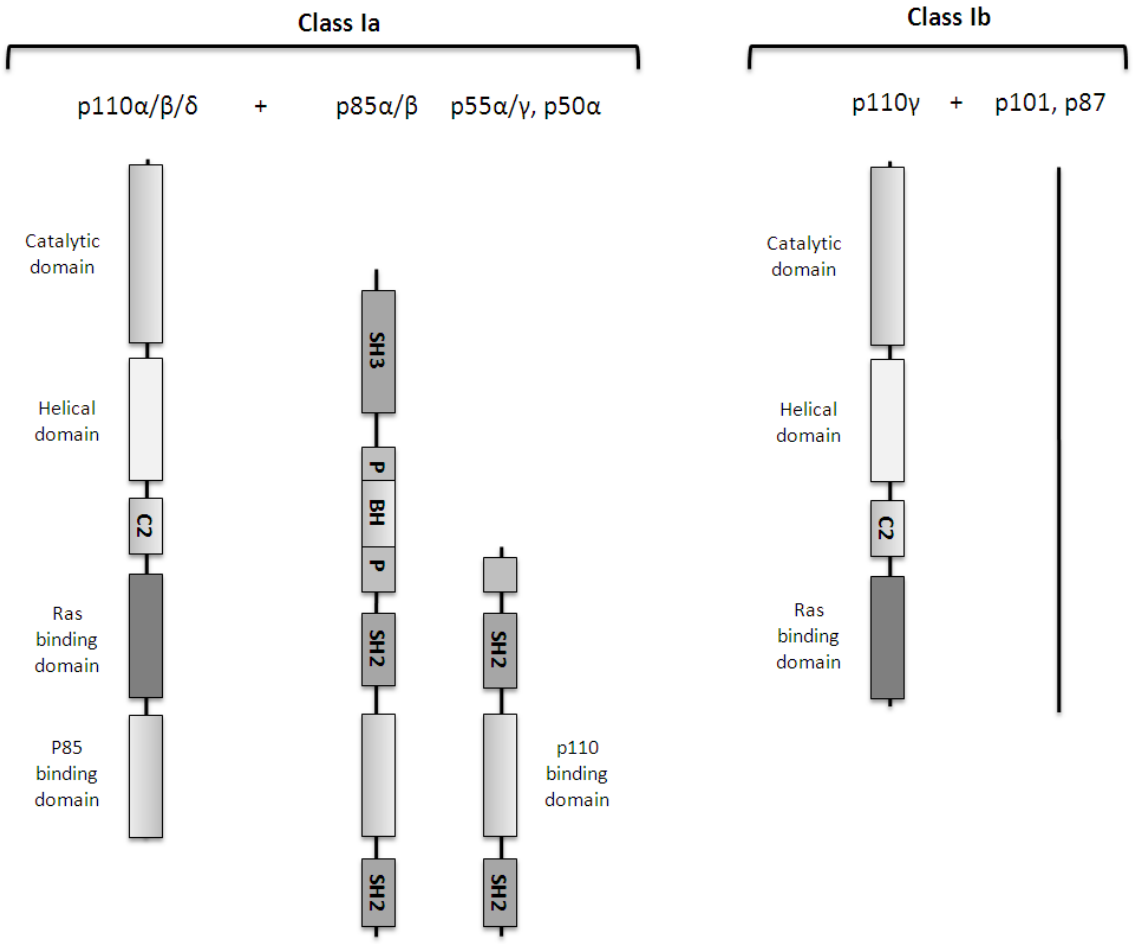

Somatic mutations in *PIK3R1*, the gene encoding p85, p55α and p50α, were first described in association with ovarian and colorectal carcinomas[125]. These mutations were found to be predominantly localised to the inter SH2, p110 binding domain and were shown to constitutively activate PI3K, thereby establishing their oncogenic potential. This was confirmed more recently when frequent somatic mutations in the inter-SH2 regions of *PIK3R1* were described in colon cancer (9/108) and were shown to promote cell survival in a p110-dependent manner[121]. Moreover, it was recognised that these mutations may provide a mechanism for global class Ia activation.

The class Ia p110 catalytic subunits: The genes encoding p110α *(PIK3CA*), p110β (*PIK3CB*) and p110δ *(PIK3CD*) reside on chromosome 3. As mentioned previously, p110α and β are widely expressed in mammalian tissue. Genetic lack of p110α or p110β in mice is associated with embryonic lethality.[110,126] However, selective conditional knock out/ knock-in models and pharmacological inhibitors of p110α have demonstrated an important role for this isoform in proliferation, growth factor and insulin signalling.[112,127,128] This isoform has also been reported to play an important role in angiogenesis.[129] Studies of the *PIK3CA* promoter have observed that expression of this isoform can be regulated positively by FOXO3a[130] and NF-κB[131] and negatively by p53.[132] Conditional p110β knockout mice demonstrate similar defects in insulin signalling, cell trafficking and proliferation.[133] In addition p110β plays an important role in PI3K activation in platelets and thrombus formation.[117,134] Little is known about the factors controlling the expression of *PIK3CB*.

In contrast to p110α and p110β isoforms, p110δ knockout mice are viable but show an immune defect. The details of the immune defects observed in p110δ knockout mice compared to the class IB p110γ knockout genotype are detailed in table 1.5. The reason for the enrichment of p110δ in leucocytes is not entirely clear but is likely to be a combination of lineage specific hypomethylation of specific promoter regions in the *PIK3CD* gene together with leukocyte specific trans-acting factors.[135,136]

Table 1.5 Characteristics of p110δ and p110γ knockout mice

Mouse genotype	Immunological features	Biochemical features
P110δ knock out	B-cells: •Reduced numbers of mature B cells •Decreased proliferation upon IgM or CD40 stimulation •Decreased T-cell-dependent and T-cell-independent antibody production Neutrophils: •Decreased chemotaxis	B-cells: •Reduced PIP3 and p-Akt(Ser473) production upon IgM stimulation Neutrophils: •Reduced PIP3 production upon GPCR stimulation
P110γ knock out	B cells: not affected T cells: •CD4:CD8 ratio increased •Decreased proliferation of mature T cells in response to anti-CD3 Mast cells: •Decreased degranulation downstream of FcεRI •*In vivo* resistance to (IgE-Ag) allergic challenge Dendritic cells: •Reduced *in vivo* and *ex vivo* migration Neutrophils: •Increased numbers; •Decreased oxidative burst; •*Decreased in vitro* chemokine-induced chemotaxis; Macrophages: •Reduced *in vitro* chemokine-induced chemotaxis •Decreased *in vitro* VEGF-induced migration •Decreased *in vivo* recruitment (septic peritonitis)	Neutrophils, macrophages and mast cells: •Reduced PIP3 and p-Akt(Ser473) production upon GPCR stimulation

Vanhaesebroeck et al. 2005[124]

Studies have demonstrated that the PI3K pathway is a critical survival pathway downstream of the BCR[137] and p110δ has an essential role in B-cell development and B-cell receptor (BCR) signalling.[138,139] The BCR in mammalian cells consists of a ligand binding moiety linked to a heterodimeric (Ig-α, Ig-β) signal transduction moiety that has a cytoplasmic immunoreceptor tyrosine-based activation motif (ITAM). Antigen recognition and binding by the BCR, leads to ITAM induced phosphorylation of SYK and LYN which in turn activate a number of downstream pathways that mediate B-cell growth, anti-apoptotic effects, proliferation, and increased cell metabolism. Phosphorylated SYK and LYN in turn phosphorylate the cytoplasmic YXXM motifs (where X is any amino acid) of CD19 and B-cell adaptor for PI3K (BCAP). As mentioned previously, these phopshorylated tyrosine motifs are recognised by the p85 regulatory subunit of PI3K resulting in

recruitment of the PI3K heterodimer to the cell membrane thereby leading to conversion of PIP2 to PIP3. PIP3 recruits proteins that have a pleckstrin homology domain, such as AKT, PDK1 and BTK to the cell membrane. This leads to phosphorylation of AKT by PDK1 at threonine 308 (thr308). Full activation of AKT is achieved by phosphorylation at serine 473 (ser473) by mTOR complex 2 (Figure 1.7). AKT and its downstream targets such as mTOR are key effectors in the PI3K pathway and are discussed further in the next section. In addition to BCR signalling, an important role for p110δ has also been described in IL4 receptor signalling in B cells,[140] regulation of allergic responses[141] and in regulatory T-cell function.[142] In summary, at least in healthy cells, there appears to be a degree of non-redundancy in the functions of the individual PI3K isoforms.

Figure 1.7 Activation of the PI3K signalling cascade downstream of the B-cell receptor

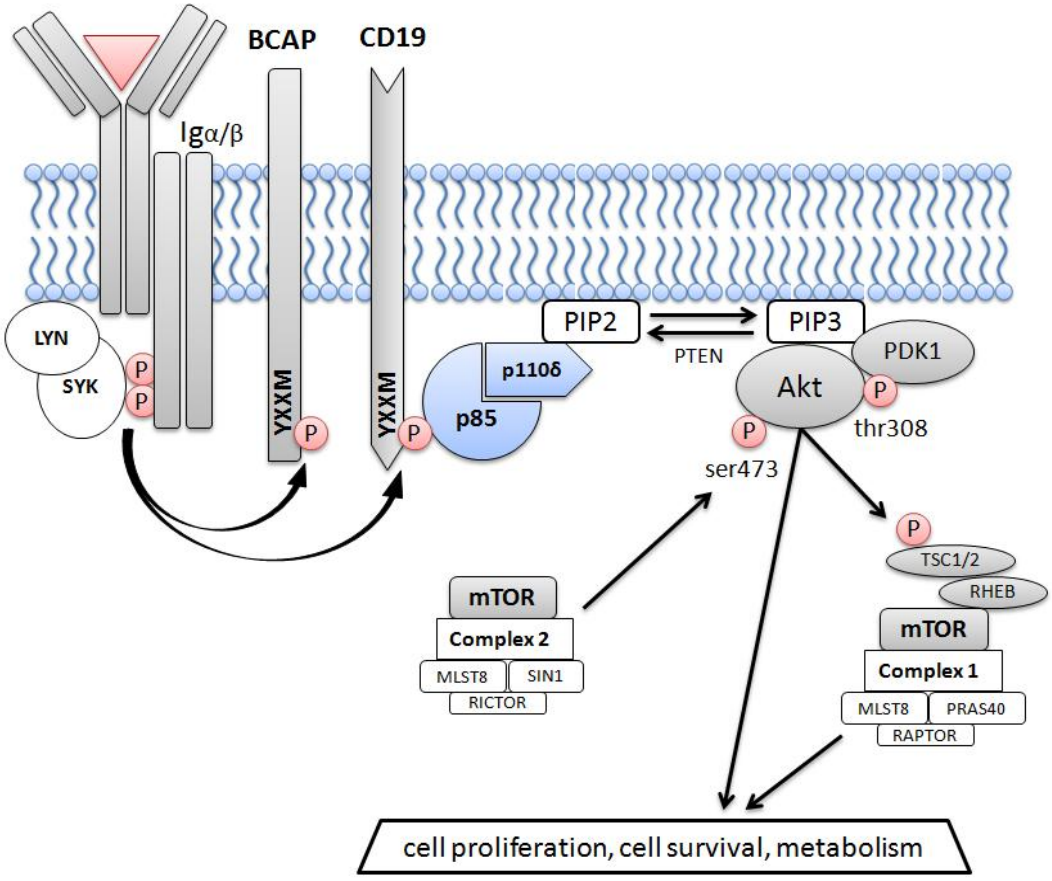

The role of PI3K in cancer has been studied best in relation to the class Ia isoforms. *PIK3CA* is the only isoform that has cancer-associated somatic mutations.[107] These gain of function mutations were initially described in solid tumours and are associated with increased lipid kinase activity, constitutive pathway activation and the ability to transform normal cells *in vitro* and *in vivo.*[143] 80% of these mutations arise from three hotspots (in exons 9 and 20), two located in the helical domain and one in the kinase domain of p110α. Evidence thus far suggests that *PIK3CA* mutations are rare or absent in haematological malignancies. Increased copy number of *PIK3CA* has been described in a number of solid tumours such as breast, thyroid and squamous cell carcinoma and is associated with a worse outcome. As discussed later, *PIK3CA* gene amplification has also been described in mantle cell lymphoma and is thought to contribute to pathogenesis.[144] The role of *PIK3CB* in oncogenesis has mainly been described in the context of loss of PTEN expression where this isoform appears to gain an important role.[145] Once again this has only been studied in solid tumours. As previously mentioned, similar to *PIK3CB*, no cancer associated mutations are found with *PIK3CD*. However, both *PIK3CB* and *PIK3CD* have been observed to induce oncogenic transformation when over-expressed in avian cells in culture.[146]

Signalling outputs: PIP3 is the key product generated by lipid kinase activity of PI3K. An increase in PIP3 production, as a result of growth factor or antigenic stimulation, leads to an increase in recruitment of proteins that have a PH domain to the cell membrane. These include serine-threonine kinases such as AKT, PDK1 and tyrosine kinases such as BTK. AKT is the best studied downstream target of PI3K and phosphorylation of AKT at thr308 and ser473 is commonly used as a marker of PI3K activation. Upon activation, AKT phosphorylates a number of downstream targets leading to a net positive effect on cell metabolism, growth, survival and proliferation. Several downstream targets of AKT have been described but some of the well described ones are TSC (tuberous sclerosis complex), GSK-3β (Glycogen synthase kinase), FOXO1 (forkhead box O transcription factor), BAD and MDM2, all of which are inactivated by AKT mediated phosphorylation.

Inactivation of TSC leads to mTORC1 mediated phosphorylation of S6K and 4EBP-1 leading to increased protein translation. Akt can also activate mTORC1 through inactivation of PRAS40 which otherwise inhibits mTORC1 activity. GSK-3β regulates the potentially oncogenic transcription factors JUN and MYC and also phosphorylates and mediates nuclear export of cyclin D1, while FOXO1 has a positive effect on the growth attenuating factor p27 and pro-apoptotic BIM. Akt inactivates the pro-apoptotic BCL2 family member BAD and also phosphorylates MDM2 allowing its translocation to the nucleus to inhibit p53.[147]

Figure 1.8 Important downstream targets of the serine-threonine kinase Akt

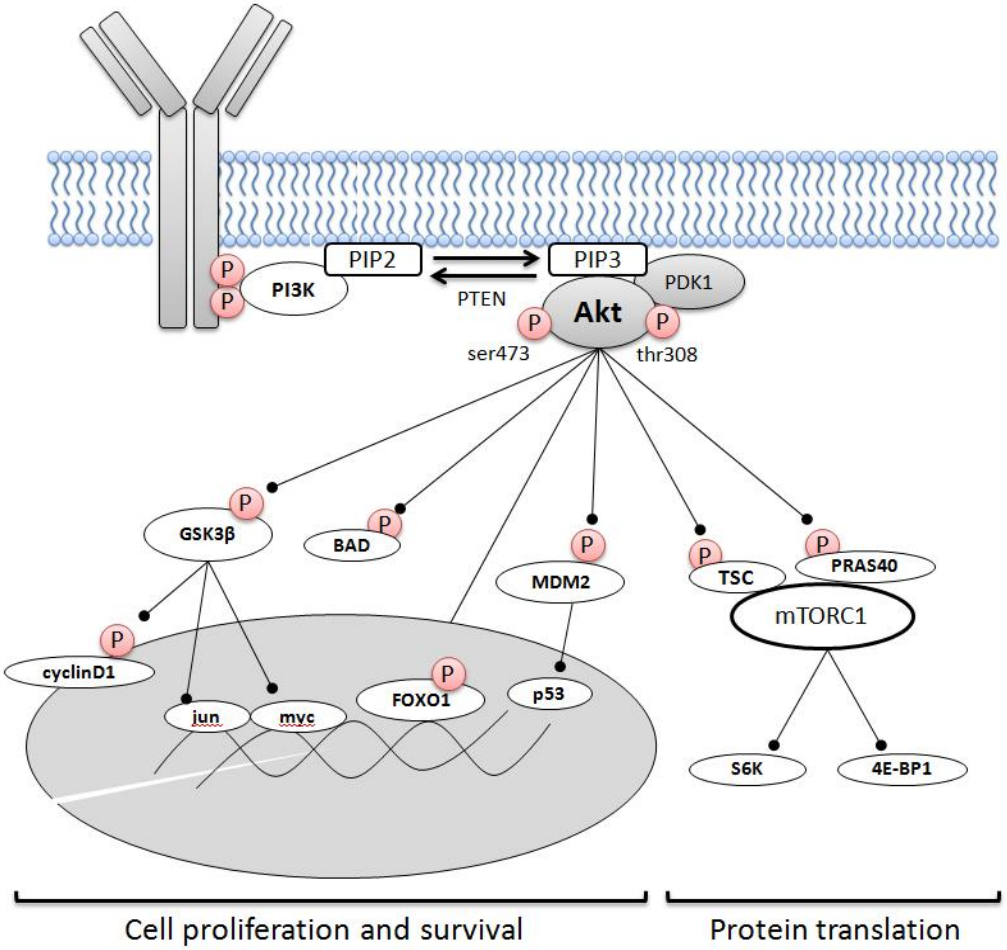

1.3 MANTLE CELL LYMPHOMA AND THE PI3K PATHWAY

1.3.1 Pre-clinical studies

Initial evidence for the importance of PI3K signalling in MCL was found in a study comparing gene expression profiles in purified MCL cells to their normal counterparts.[21] Following this, a study by Rudelius et al in 2006 observed that constitutive activation of AKT and its downstream targets was commonly found in MCL particularly with the blastoid variant. They found loss of PTEN expression in 6/31 primary samples but did not detect any mutations in exons 9 and 20 of *PIK3CA*. They also demonstrated that LY294002, wortmannin and an AKT inhibitor were able to block phosphorylation of downstream targets and induce growth arrest as well as apoptosis in 2 MCL cell lines Granta 519 and Z138C.[22] A further study by Dal Col et al suggested that a phosphorylated inactive form of PTEN correlated with constitutive activation of Akt in MCL. Using LY294002 and the mTORC1 inhibitor Rapamycin, they demonstrated that while both inhibitors were able to antagonise IL4 and CD40L induced proliferation of MCL, PI3K inhibition was also able to induce apoptosis in primary samples.[23] Both studies described reduction in cyclin D1 levels in response to these inhibitors as a result of reduction in mTOR induced protein translation of cyclin D1 but also enhanced GSK-3β mediated nuclear export of cyclin D1. In addition it has been suggested that Akt can stabilise cyclin D1 mRNA by inactivating proteins that bind to mRNA ARE (AU rich elements) to mediate decay.[148]

Subsequently, while studying the role of *PIK3CA* in MCL, Psyrri et al found gene amplification of *PIK3CA* in 15/22 primary MCL (68%) and 2 cell lines (Granta519 and REC-1) related to a gain of *PIK3CA* copy number ($\geq$3). Once again, no *PIK3CA* mutations were detected but loss of PTEN expression was found using IHC in 5/33 MCL. Only one of the five samples with loss of PTEN expression also had *PIK3CA* gene amplification. Constitutive AKT phosphorylation was found in 7 out of 12 cases with *PIK3CA* gene amplification. This study was limited by the fact that other class Ia

isoforms were not studied, the role of isoform selective inhibition was not evaluated and findings were not correlated with clinical status of the patient.

Although there is no direct evidence for the oncogenic role of p110δ, its key role in B-cell survival and high expression in leucocytes make it an attractive target in lymphoid malignancy. The first highly selective p110δ inhibitor CAL-101 or GS-1101, now known as Idelalisib, was shown to significantly inhibit constitutive Akt phosphorylation (p-AKT) to a similar extent in primary MCL and CLL cells in vitro.[149] It was also shown to attenuate increases in p-AKT induced by BCR and soluble CD40 ligand stimulation. In addition GS-1101 was shown to counteract chemotactic signals and overcome the protective effect of nurse-like cells in CLL co-culture models.[150,151]

There is therefore good pre-clinical evidence for PI3K signalling in the pathogenesis and survival of MCL. *PIK3CA* amplification appears to be an important aberration but the reasons for and implications of this aberration have not been studied. Loss of PTEN expression appears to be a relatively common mechanism for constitutive activation of this pathway and is thought to occur in 15-20% of cases. More recently, 13q31-q32 amplification, one of the common secondary genetic alterations in MCL, has been shown to lead to PTEN inactivation via microRNAs miR 17~92 providing another mechanism for PI3K activation.[152] However, these studies do not address the relative role of the class Ia isoforms in MCL or biomarkers that may predict sensitivity to isoform-selective or pan-PI3K inhibition. The pre-clinical data discussed above is summarised in Table 1.6.

Table 1.6 Pre-clinical evidence for the role of PI3K signalling in MCL survival and pathogenesis

Study	Details	Key findings
Rizzatti *et al* 2005	21 diagnostic MCL PBMCs compared to naive B-cells extracted from normal tonsils.	PI3K/Akt signalling pathway genes upregulated compared to normal controls
Rudelius *et al* 2006	4 cell lines – Granta519, NCEB-1, Z138C, REC-1 12 aggressive blastoid variants 19 typical MCL PI3K pathway inhibitors -LY294002, Wortmannin, Akt inhibitor	Constitutive PI3K activation seen preferentially in blastoid variant Loss of PTEN expression in 3/4 cell lines and 6/31 primary MCL by western blotting No PIK3CA activating mutations Pathway inhibition, growth attenuation and apoptosis seen with PI3K inhibitors.
Dal Col *et al 2008*	3 cell lines - Granta 519, Jeko-1, SP53 5 primary MCL (1 blastoid lymph node cell suspension, 4 PBMCs) 12 lymph nodes (1 blastoid) used for IHC PI3K pathway inhibitors -LY294002, Wortmannin, Rapamycin	Constitutive PI3K activation associated with phosphorylated inactive PTEN PI3K and mTOR inhibition antagonise proliferative effect of IL4 and sCD40L Superior therapeutic effect with PI3K inhibition compared to mTOR inhibition
Psyrri *et al* 2009	2 cell lines – Granta519 and REC-1 35 MCL primaries PI3K pathway inhibitors -LY294002	No PIK3CA activating mutations Loss of PTEN expression in 5/33 (15%) by IHC PI3K α gene amplification (≥3 copy number) in 15/22 primaries -68% associated with elevated mRNA Growth inhibition and apoptosis seen in cell lines with LY294002.
Lanutti et al 2011	5 MCL PBMCs PI3K pathway inhibitor -CAL-101/ GS-1101	Attenuation of constitutive Akt phosphorylation as well as IgM and sCD40L induced Akt phosphorylation.

1.3.2 Clinical activity of GS-1101 in MCL

Results from phase I trials of the first PI3K p110δ selective inhibitor GS-1101 were reported at the annual meeting of the American Society of Hematology in 2010.[153] The study included patients with relapsed/ refractory indolent and aggressive NHL (Table 1.6). A dose escalation starting at 50mg BID and going up to 350mg BID was undertaken. Plasma C_{max} and AUC did not increase significantly beyond a dose of 150mg BID and MTD was not reached. An interesting redistribution of lymphocytes resulting in lymph node shrinkage and transient peripheral blood lymphocytosis was observed and is thought, at least in CLL, to be due to abrogation of chemokine mediated migration and homing of tumour cells.[151] This phenomenon was also observed subsequently in early phase studies with the BTK inhibitor Ibrutinib, another key 'second messenger' in BCR signalling. Apart from a reversible transaminitis seen in some patients, GS-1101 was well tolerated in the majority of patients.

Table 1.7 Clinical characteristics of patients enrolled in the phase I study of CAL-101/GS-1101

Characteristics	MCL (N=21)	iNHL (N=30)	CLL (N=54)
Age, median	71	61.5	62.5
[range], years	[52-82]	[32-85]	[37-82]
Bulky disease, %	57	50	81
Adverse genetics (del 17p), %	--	--	36
Prior therapies, median	5	4	5
[range]	[1-12]	[1-10]	[2-15]
Prior therapy type, %			
Rituximab	100	100	98
Alkylating agent	100	87	87
Anthracycline	95	50	--
Purine analog	--	30	100
Bortezomib (MCL)/Alemtuzumab (CLL)	76	--	31

Kahl *et al* ASH annual meeting 2010

In relation to MCL, responses with GS-1101 were reported for 21 patients with relapsed/refractory disease. The median number of prior therapies in patients with MCL included in this study was 5 (range 1-12). The best on-treatment change in tumour size in MCL compared to CLL and indolent NHL (follicular lymphoma, small lymphocytic lymphoma, marginal zone lymphoma and lymphoplasmacytic lymphoma) along with the median duration of response in these groups of patients is depicted in the waterfall plot in figure 1.9A. While the response rates in MCL (best on-treatment response) with single agent GS-1101 in this heavily pre-treated cohort is still impressive, a markedly greater proportion of patients with CLL and indolent NHL achieved a greater than 50% reduction in tumour size with fewer progressions while on treatment (Hallek criteria 2008). In addition, the duration of response was markedly shorter in MCL patients compared to both CLL and indolent NHL (Figure 1.9B).

Figure 1.9 Best on-treatment response (A) and duration of response (B) with CAL-101/ GS-1101 in MCL, CLL and indolent NHL (iNHL)

A.

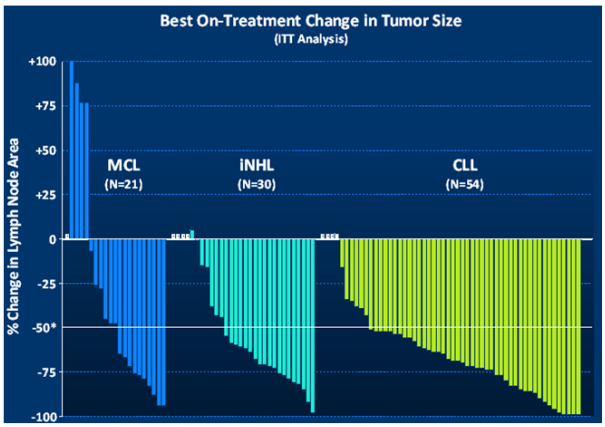

B.

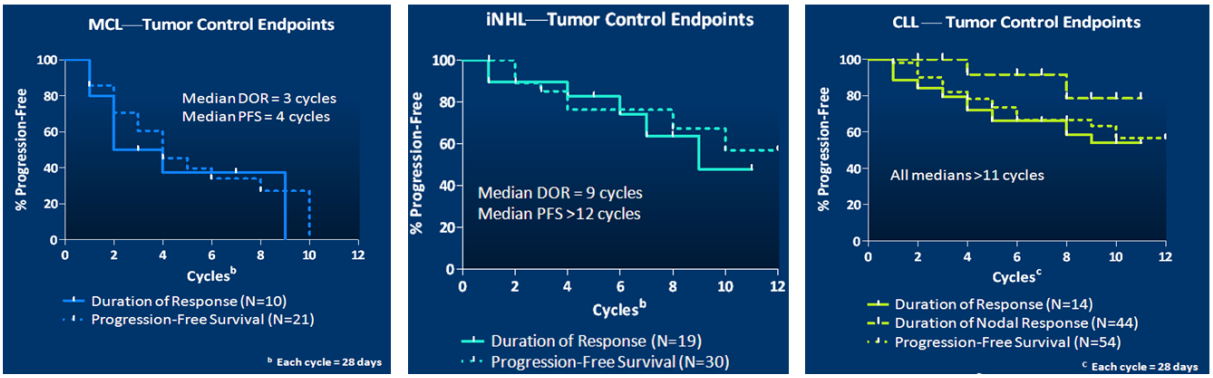

Kahl *et al.* ASH Annual meeting 2010

1.3.3 Summary and rationale for studies presented

While pre-clinical studies provide good evidence for a role for the PI3K pathway in the pathogenesis of MCL, the relative role of the class Ia isoforms, which are the best studied isoforms in PI3K mediated oncogenesis, is not clear in this disease. B-cell receptor signalling is important for healthy B-cell survival but also appears to play a role in malignant B-cell survival as shown not only by evidence of bias in the IGHV repertoire and constitutive activation of BCR activation related pathways, but also from the clinical activity of highly selective small molecule inhibitors of the BCR signalling cascade. Some of these inhibitors have been evaluated in MCL and are depicted in figure 1.10.

Figure 1.10 The BCR signalling cascade and targets under evaluation in MCL

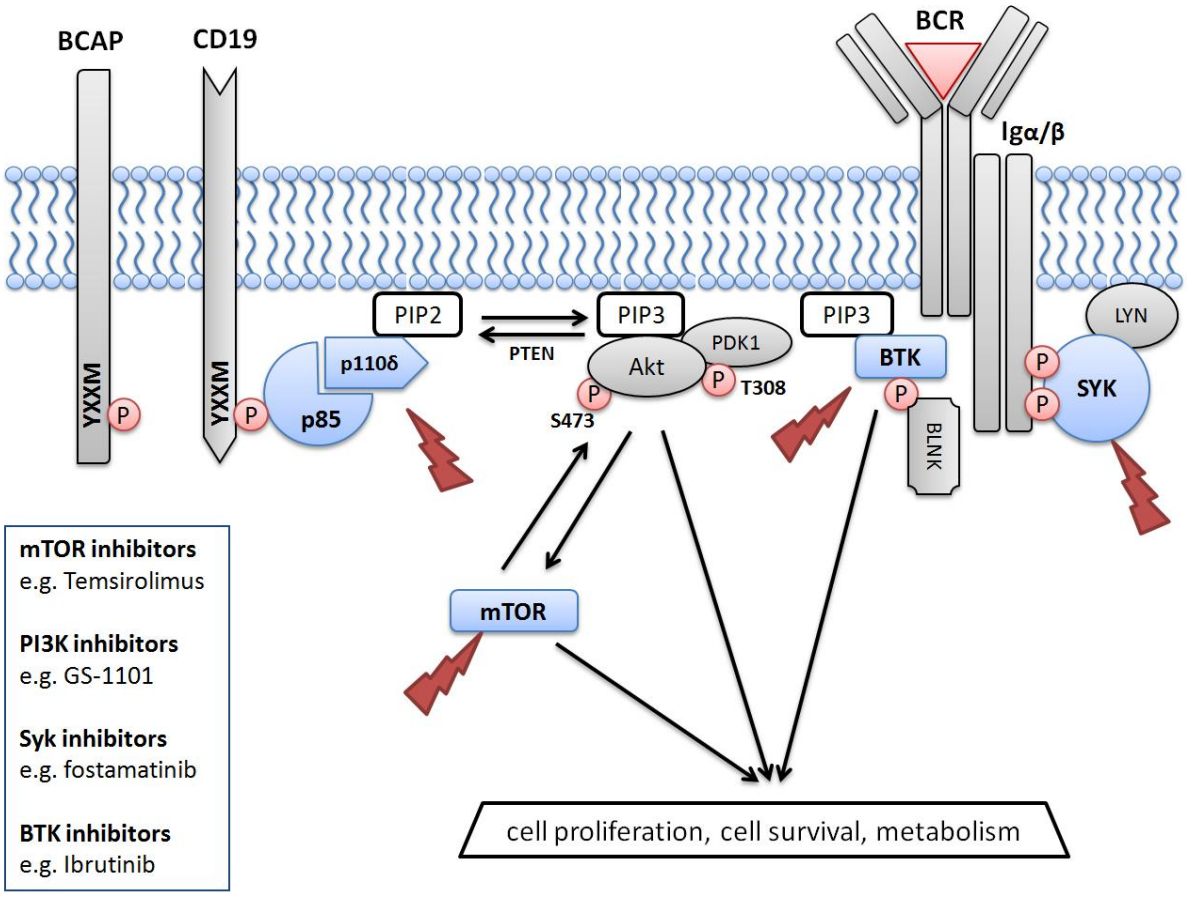

The p110δ isoform is a key component of BCR signalling and is enriched in leucocytes making it an attractive target. However, phase I studies with the highly selective p110δ inhibitor CAL-101/GS-1101 have demonstrated relatively inferior activity in MCL compared to CLL and indolent NHL. With evidence that loss of PTEN expression and gene amplification of *PIK3CA* are relatively common in MCL, it is important to investigate the relative role of the class Ia isoforms in this disease.

Targeting more isoforms is likely to be associated with greater toxicity but although genetic deletion of p110α and p110β knock out in mice is associated with embryonic lethality, pharmacological inhibition with PI3K inhibitors that target multiple isoforms appear to be well tolerated in patients. This may be the result of a more selective effect on the 'PI3K' addicted tumour cells. One such example is GDC-0941, an orally bioavailable PI3K inhibitor that was designed for use in solid tumours on the basis that *PIK3CA* mutations occur at a high frequency of in this group of patients. GDC-0941 has activity against both wild-type and mutated *PIK3CA* but is equally selective for *PIK3CD/*p110δ. In early phase trials, GDC-0941 has been reasonably well tolerated with grade 1-2 gastro-intestinal symptoms, fatigue and in some cases hyperglycaemia as the main side-effects.[154] We therefore elected to evaluate this inhibitor in our studies.

While *in vitro* studies of these drugs are valuable, there is also a need for a pre-clinical *in vivo* model to study drug delivery and activity of these PI3K inhibitors. An in vivo model of MCL would be particularly valuable for evaluation of rational drug combinations and biomarkers that emerge from *in vitro* studies. The currently available murine models of human MCL are xenografts (subcutaneous and disseminated) of MCL cell lines in severe combined immunodeficient (SCID) mice. [155,156] The only primary human MCL mouse model described in the literature was established by injection of CD19 selected primary MCL cells into human embryonic bone grafts that were implanted subcutaneously in SCID mice (SCID-Hu).[157] SCID mice without the bone grafts did not show engraftment. This is not easily reproducible because of the difficulty and cost involved in obtaining human embryonic bone

grafts. Another factor that may have limited the development of a mouse model of human MCL could be the availability of adequate tumour cells for injection into mice. The unique position of being in a centre with access to a large tissue bank of MCL patient samples and access to NSG mice (non-obese diabetic/severe combined immunodeficient/interleukin-2 receptor γ chain–null) through collaboration with Dominique Bonnet's group led us to evaluate this model as a host for primary MCL in our studies. NSG mice lack NK cells in addition to mature T or B cells and have been shown to permit engraftment of a wider range of primary human cells compared to earlier strains.[158] The following section details the hypothesis and aims of this research based on the issues highlighted above.

HYPOTHESES AND AIMS

Hypothesis 1: The relative expression of class Ia PI3K isoforms and mechanism of PI3K activation can inform the use of isoform-selective inhibitors in mantle cell lymphoma.

Aims

1. Evaluate expression of the class Ia isoforms in MCL by immunohistochemistry and real-time PCR.
2. Evaluate mechanisms of constitutive activation – *PIK3CA* mutations, *PIK3R1* mutations and loss of PTEN expression.
3. Using isoform-selective inhibitors, examine the relative contribution of the class Ia isoforms in BCR signalling and constitutive PI3K activation.
4. Evaluate the cytotoxicity of isoform-selective inhibitors in MCL cell lines and primary samples in relation to isoform expression and mechanisms of constitutive activation.

Hypothesis 2: A disseminated xenograft model of human primary mantle cell lymphoma can be established in NSG mice.

Aims

1. Study the kinetics and distribution of luciferase transduced MCL cell lines injected into pre-irradiated NSG mice using bioluminescent imaging.
2. Study the fate of T-cell depleted primary MCL samples injected into irradiated mice.

CHAPTER 2: MATERIALS AND METHODS

2.1 TISSUE CULTURE

2.1.1 Cell lines

All cell lines were grown in sterile flasks under normoxic conditions (21% O_2) with 5% CO_2 at 37°C. Cells were passaged two or three times a week, depending on doubling time, to maintain optimal cell concentration. Aliquots of cell lines were frozen down and thawed at regular intervals of 3-4 months and mycoplasma testing was carried out every 8 weeks. Cells were harvested in their logarithmic growth phase for experiments. The cell lines listed in Table 2.1 were used in construction of a cell-block microarray as discussed later.

The MCL cell lines, Jeko-1 and Granta519, were obtained from Dr. Rebecca Auer and their identity was confirmed with short tandem repeat (STR) profiling (LGC standards, Teddington, UK). The lymphoblastoid cell line NcNc was purchased from ATCC (LGC standards). These three cell lines were used in further experiments as detailed later. All culture media and fetal calf serum (FCS) was purchased from Sigma-Aldrich (St Louis, MO, USA) while Gentamicin was purchased from GIBCO (Life technologies, Paisley, UK).

2.1.2 Primary samples

In accordance with the updated Declaration of Helsinki, all samples were obtained under current regulatory approval from the local research ethics committee (East London and the City), and after informed consent, from patients treated at St Bartholomew's Hospital. Patient information was treated with strict confidentiality and was stored electronically in password protected spreadsheets.

Table 2.1 Details of cell lines used for cell-block micro-array construction

Cell line	Origin	Growth medium
CTS	Acute Myeloid Leukaemia	RPMI + 10% FCS + 1% Gentamicin
Fuji	Acute Myeloid Leukaemia	RPMI + 10% FCS + 1% Gentamicin
THP1	Acute Myeloid Leukaemia	RPMI + 10% FCS + 1% Gentamicin
MEC-1	High grade transformation of CLL	IMDM + 10% FCS + 1% Gentamicin
Jeko-1	Mantle Cell Lymphoma t(11;14)	RPMI + 10% FCS + 1% Gentamicin
GRANTA519	Mantle Cell Lymphoma t(11;14)	DMEM + 10% FCS + 1% Gentamicin
U266	Multiple Myeloma	RPMI + 10% FCS + 1% Gentamicin
RPMI	Multiple Myeloma	RPMI + 10% FCS + 1% Gentamicin
OPM2	Multiple Myeloma	RPMI + 10% FCS + 1% Gentamicin
DoHH2	Diffuse Large B Cell Lymphoma t(14;18)	RPMI + 10% FCS + 1% Gentamicin
SUDHL-6	Diffuse Large B Cell Lymphoma t(14;18)	RPMI + 10% FCS + 1% Gentamicin
SUDHL-8	Diffuse Large B Cell Lymphoma t(8;14)	RPMI + 20% FCS + 1% Gentamicin

Mantle cell lymphoma: Solid tissue used in tissue microarray (TMA) construction was fixed in formalin and embedded in paraffin (FFPE). Snap-frozen tissue used in experiments was evaluated for tumour content using CD20 immunohistochemistry (IHC) and then homogenised using the Qiagen TissueLyserII (Qiagen, Hilden, Germany) for DNA, RNA and protein extraction. Mononuclear cell suspensions were prepared from peripheral blood (PBMCs) and bone marrow (BM) using Ficoll-Paque (Miltenyi biotech, Cologne, Germany) density gradient centrifugation. Splenic tissue was

dissected on a pre-cooled thermal tray at 4°C (Biocision, Larkspur, CA) and homogenised by mashing over 70µm filters (BD biosciences, Franklin Lakes, NJ, USA). Cells were then washed with phosphate buffered saline (PBS) prior to density gradient centrifugation to isolate mononuclear cells.

Samples for density gradient centrifugation were diluted 1:1 in sterile PBS. 35mls of this solution was carefully layered over 15 ml of Ficoll-Paque in a 50ml conical tube. Tubes were centrifuged at 400xg for 25 minutes after which the upper layer of fluid was carefully aspirated out and the mononuclear layer carefully transferred to another 50ml conical tube using a pipette. After performing cell counts, cells were cryopreserved in 90% FCS and 10% Di-Methyl Sulphoxide (DMSO, Sigma-Aldrich) at -80°C. Cryopreserved cells were thawed in a water bath at 37°C, washed immediately and re-suspended at a concentration of 10^6 cells per ml in Iscove's modified Dulbecco's medium (IMDM) with 1mM pyruvate, insulin-transferrin-selenium (Life technologies, Paisley, UK), 10% human serum (Sigma-Aldrich) and 1% Gentamicin, for use in experiments. A total of 22 primary MCL cell suspensions confirmed to have more than 85% CD20 positive cells by flow cytometry were used in experiments.

Healthy controls: Healthy B-cells were isolated from healthy volunteer PBMCs using negative selection with the B-cell isolation kit II (Miltenyi Biotec). Following density gradient centrifugation and determination of cell number, 40µl MACS (Magnetic Cell Separation) buffer (Miltenyi Biotec) was added for every 10^7 cells. 10µl of a biotin antibody cocktail (per 10^7 cells) against non B cells (CD2, CD14, CD16, CD36 and glycophorin A) was added and incubated after mixing at 4°C. Following addition of a further 30µl of MACS buffer, cells were incubated with anti-biotin beads (20µl per 10^7 cells) for a further 15 minutes at 4°C. Cells were then washed and re-suspended in 500µl MACS buffer. LS columns (Miltenyi Biotec) were primed with buffer in the magnetic field of a MACS separator (Miltenyi Biotec). Cells were applied gently to the top of the column and the effluent consisting of negatively selected B-cells was collected in a 15ml conical tube. Cell counts were performed after which cells were either re-suspended in culture medium and used immediately for

experiments or cryopreserved at -80°C in 90% FCS and 10% DMSO. Snap frozen or FFPE tonsils used as healthy controls were obtained from tonsillectomies performed for non-malignant pathology.

2.2 IMMUNOHISTOCHEMISTRY

2.2.1 Cell block preparation

Antibodies against p110α, p110β, PTEN and Ki67 have previously been validated for IHC on FFPE tissue[159] but there was no literature describing the use of a p110δ selective antibody for IHC at the time of performing these experiments. In order to evaluate a commercially available p110δ antibody (Santa Cruz Biotech, Santa Cruz CA) for use in FFPE tissue, cell blocks were prepared from the cell lines listed previously and incorporated into a cell block microarray.

We compared two previously described methods for cell block preparation - one using 2% agar and the other involving the use of thrombin or fibrin clot as a matrix. The thrombin cell block preparation method [160] was relatively quicker and easier. It was also superior in preserving the morphology of cells compared to the agar method. Appendix A contains details of the protocols and a comparison of the two methods. 1mm cores in duplicate from formalin-fixed, paraffin-embedded thrombin cell blocks were incorporated into a cell block microarray which was then used to validate and optimize the p110δ antibody by comparing expression by IHC to that seen by western blotting in the same cell lines (Figure 2.1).

Three dilutions, 1:100, 1:250 and 1:500, of the p110δ antibody were evaluated (manufacturer's recommendation 1:50-1:500). A dilution of 1:250 was found to provide optimal staining and was able to differentiate high p110δ expressing cell lines from low expressing ones (Figure 2.2).

Figure 2.1 Optimisation and validation of an antibody against p110δ: A panel of cell lines (A) were used to prepare a thrombin cell block FFPE microarray (B). Simultaneous western blotting was performed on the lymphoma and myeloma cell lines included in this panel (C).

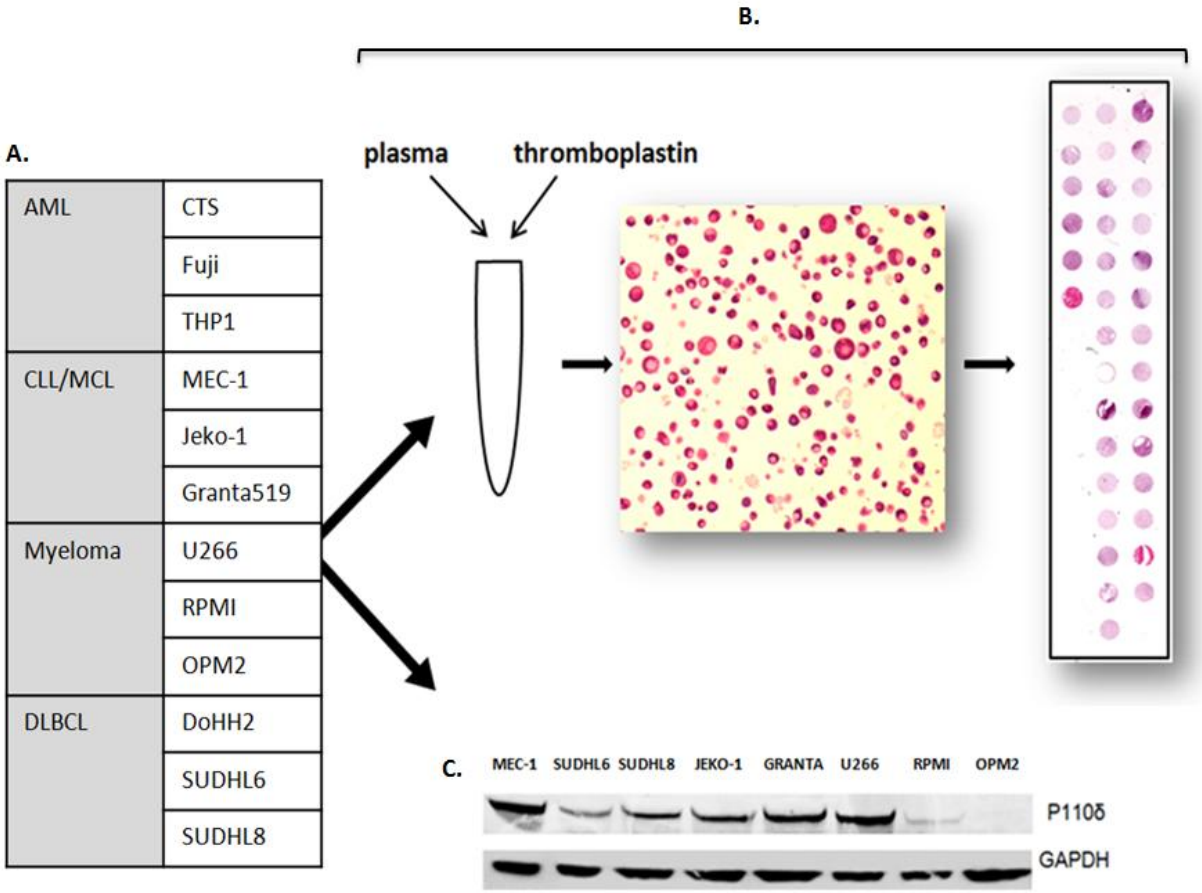

Figure 2.2 Optimisation and validation of an antibody against p110δ: A) Bar graph of IHC scores obtained from staining of the cell block microarray with **a** p110δ antibody concentration of 1:250. B) Western blot (same as in figure 2.1) showing comparable intensities of p110δ in the corresponding cell lines. MEC-1 (green arrow) exhibits strong expression while OPM2 has little or no expression of p110δ similar to the IHC results. C) Images of p110δ staining of cell blocks (original magnification x400) in 3 cell lines MEC-1, THP-1 and OPM2 exhibiting different intensities of staining.

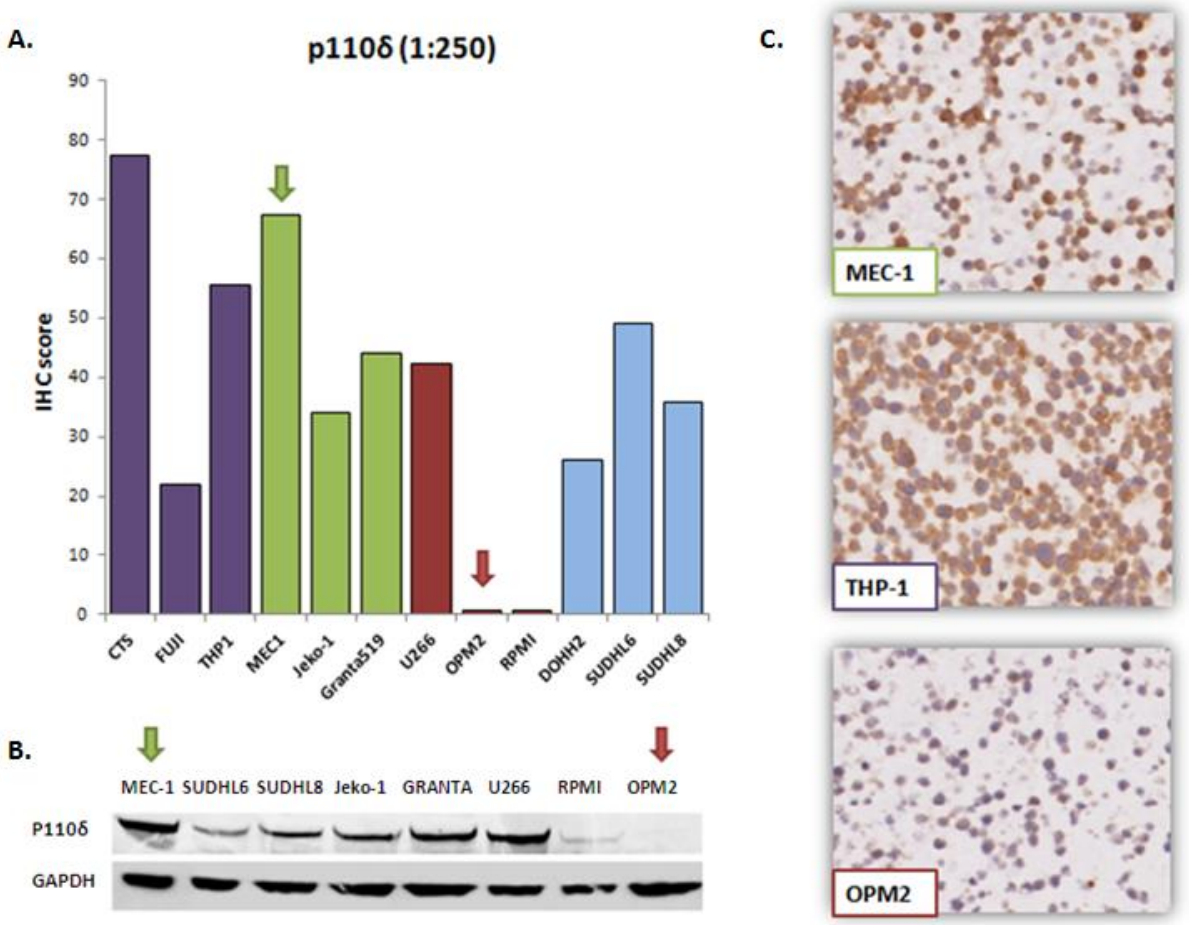

2.2.2 Tissue microarray (TMA) preparation, staining and scoring

1mm cores from 175 FFPE biopsies taken from 121 patients were arrayed in triplicate onto 6 slides (TMA 03A-F). In addition to tumour samples, 3 tonsil controls (TON) and 3 orientation cores (ORI - cardiac muscle) were incorporated into each tissue micro-array slide (Figure 2.3A).

TMA slides were heated overnight in an oven at 60°C. Slides were de-waxed with xylene prior to antigen retrieval by pressure cooking in a citrate buffer at pH 6. A hydrophobic pen was used to mark around the arrays after which slides were loaded onto the Dako Autostainer Plus machine (Dako, Glostrup, Denmark). The appropriate volumes of antibodies and reagents were placed in the machine which was then programmed to sequentially incubate slides with primary antibody, super enhancer reagent, super sensitive horse radish peroxidise (HRP) labelled polymer and finally a diamino benzidine (DAB) substrate (Biogenex, Fremont, CA, USA) at room temperature. Details of primary antibodies used are listed in table 2.2. Incubation times for the other reagents are listed in table 2.3. Slides were then counterstained with haematoxylin and cover slips were mounted using DPX (Di-N-Butyl Phthalate in Xylene).

Table 2.2 Details of primary antibodies and conditions used for immunohistochemistry on MCL TMA

Primary antibody	Supplier/ code	Species (clone)	Antigen retrieval	Concentration	Incubation
P110α	Cell Signaling #4249	Rabbit polyclonal (C73F8)	Citrate pH6	1:250	40”
P110β	Abcam ab55593	Mouse monoclonal	Citrate pH6	1:250	40”
P110δ	Santa Cruz sc-55589	Mouse monoclonal (A-8)	Citrate pH6	1:500	40”
PTEN	Cascade ABM-2052	Mouse monoclonal (6H2.1)	Citrate pH6	1:25	60”
Ki-67	Dako M7240	Mouse monoclonal (MIB1)	Citrate pH6	1:1000	40”

Table 2.3 Incubation times for IHC reagents

IHC Reagent	Incubation time
Super enhancer	20”
SS HRP labelled polymer	30”
DAB	10”

Phosphoprotein markers of PI3K pathway activation such as phospho-Akt were deliberately excluded from IHC analysis as the stability of phosphoproteins has been shown to be highly reliant on the interval between removal from the body and fixation. Rapid de-phosphorylation has been observed within minutes in the absence of prompt fixation making IHC analysis of phosphoprotein expression in FFPE tissue unreliable.[161,162]

All TMA slides were scanned using an Olympus scanning microscope to obtain high-resolution images which were then analyzed using the Ariol SL-50 visual analysis software version 3.2 (Genetix, San Jose, CA, USA). Images of cores were screened individually to exclude non-tumor tissue and tonsillar germinal centers were selected as controls. The software was trained to calculate the percentage of positive cells and mean staining intensity of cores. The immunohistochemistry (IHC) score was calculated as the product of percentage positive cells and mean intensity. Maps of tissue microarrays were created in order to match tissue cores to the corresponding patient biopsy (Figure 2.3B). The Ariol visual analysis software assigns an X-Y co-ordinate to each core and the final analysis parameters are displayed against the respective X-Y co-ordinate. The parameters were matched to the corresponding patient biopsy using the TMA slide map and the X-Y co-ordinate (Figure 2.3C). Biopsies with only one evaluable core on the TMA were excluded and IHC scores for duplicates and triplicates were averaged for final analysis.

Figure 2.3 Example of a MCL TMA slide with the corresponding map designed to match cores on the TMA to patient biopsies and clinical information

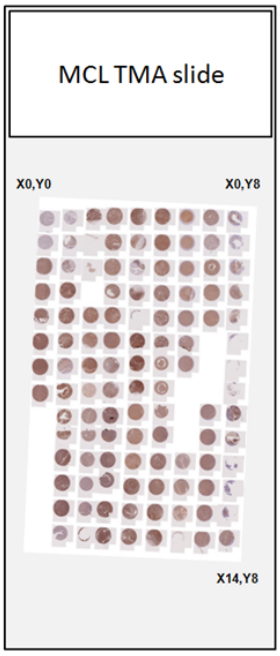

TMA SLIDE MAP

X0,Y0 X0,Y8

I1	H1	G1	F1	E1	D1	C1	B1	A1
I2	H2	G2	F1	E2	D2	C2	**ORI**	A2
I3	H3	G3	F3	**TON**	D3	C3	B3	A3
I4	H4	G4	F4	E4	D4	C4	B4	A4
I5	H5	G5	F5	E5	D5	C5	B5	A5
I6	H6	G6	F6	E6	D6	C6	B6	A6
I7	**TON**	G7	F7	E7	D7	C7	B7	A7
I8	H8	**ORI**	F8	E8	D8	C8	B8	A8
	H9	G9	F9	E9	D9	C9	B9	A9
	H10	G10	F10	E10	D10	C10	B10	A10
	H11	G11	F11	E11	D11	C11	B11	A11
	H12	G12	F12	E12	D12	C12	B12	A12
	H13	G13	F13	E13	D13	C13	B13	A13
	H14	G14	F14	E14	D14	**TON**	B14	A14

X14,Y8

Patient	Episode	Cores	X, Y on Ariol
Pt 1	1st relapse	A1-3	(0, 8) (1, 8) (2, 8)
Pt 1	3rd relapse	A4-6	(3, 8) (4, 8) (5, 8)
Pt 2	Diagnosis	A7-9	(6, 8) (7, 8) (8, 8)
Pt 3	2nd relapse	A10-12	(9, 8) (10, 8) (11, 8)
Pt 4	1st relapse	A13-B1	(12, 8) (13, 8) (14, 8)

The IHC score was validated by arranging images from randomly selected TMA cores in the order of increasing IHC scores. Cores from TMA slides stained with p110α were used for validation as they showed the widest variation (Figure 2.4). PTEN expression was scored independently by Dr. Abigail Lee and myself as 0 (no expression), 1+ (weaker than adjacent normal tissue) or 2+ (same as or stronger than normal tissue). Ki-67 was also scored by Dr Abigail Lee and myself, in line with the guidance published by the European MCL network.[50] Blastoid morphology of MCL biopsies was verified by Dr Maria Calaminici.

Figure 2.4 Validation of the IHC score (percentage positive x mean intensity) in 16 random TMA cores stained with p110α

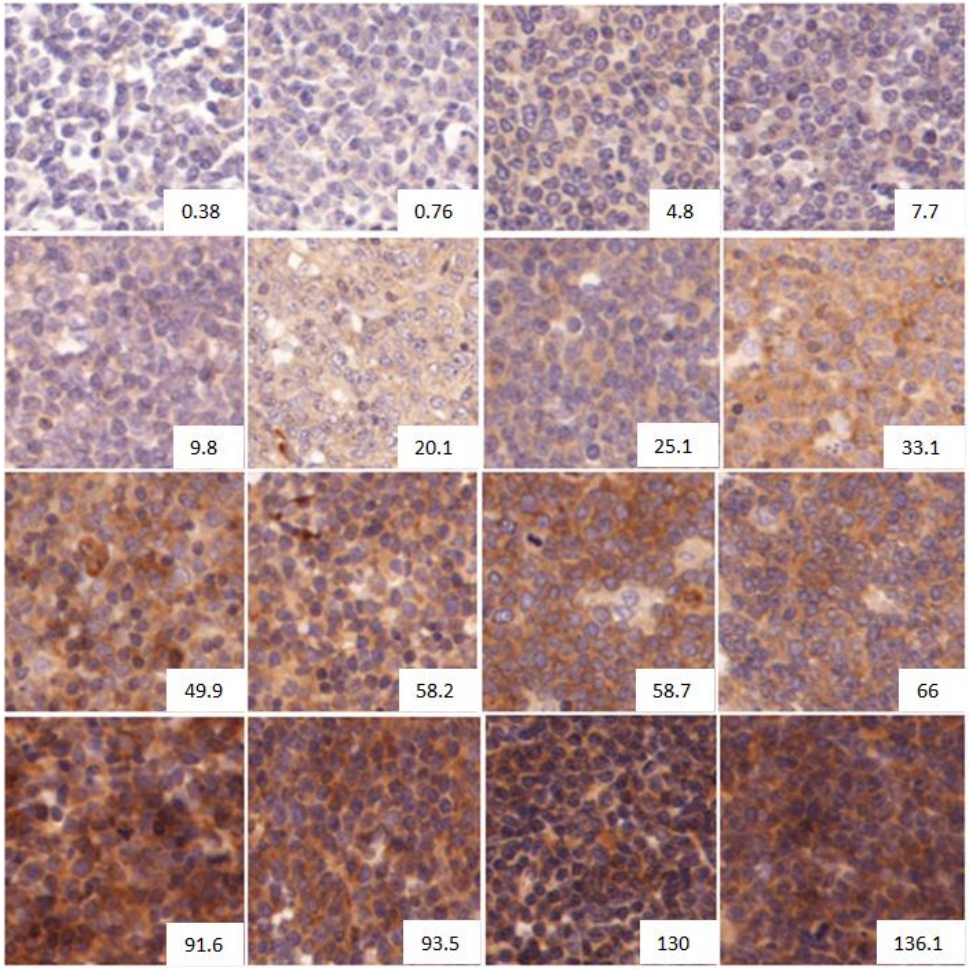

IHC score = percentage positive x mean intensity

MCL TMA slide ID	X, Y Co-ordinates	p110α IHC score	Rank
TMA-03A	X0, Y0	0.76	2
	X0, Y1	0.38	1
	X1, Y10	93.5	14
TMA-03B	X0, Y2	136.1	16
	X2, Y2	91.6	13
	X7, Y0	130.1	15
TMA-03C	X1, Y0	25.1	7
	X3, Y3	7.7	4
	X4, Y1	58.7	11
TMA-03D	X2,Y12	49.9	9
	X4, Y6	66	12
	X2, Y0	4.8	3
TMA-03E	X3, Y1	58.2	10
	X4, Y0	20.1	6
TMA-03F	X1, Y1	33.1	8
	X1, Y3	9.8	5

2.3 WESTERN BLOTTING

2.3.1 Protocol

Cell lysis buffer was prepared by addition of phosphatase and protease inhibitors (Roche, Basel, Switzerland) to cell lysis reagent (CelLyticM, Sigma-Aldrich). Lystaes were prepared by washing cells once with ice cold sterile Hank's solution (Sigma-Aldrich) and centrifuging at 400xg for 5 minutes at 4°C in pre-cooled Eppendorf vials. Supernatant was aspirated and pellets were dissolved in cell lysis buffer (100µl for $5x10^6$) followed by incubation for 20 minutes on ice. Samples were vortexed and centrifuged at 20000xg in a pre-cooled centrifuge for 10 minutes at 4°C. Supernatant was carefully aspirated and either used immediately for total protein estimation and western blotting, or stored at -80°C. For frozen tissue, a scalpel was used to take shavings from the tissue on a thermal tray (Biocision) placed over dry ice. These were added to 200µl cell lysis buffer in 2ml Eppendorf vials along with a stainless steel bead and homogenised using the Qiagen TissueLyserII (Qiagen). This machine uses two oscillating arms, each capable of holding up to 30 Eppendorf vials. The vials were placed in pre-cooled vial holders (4°C) and the machine was programmed to oscillate at 20-30 Hz for 2 minutes or until the tissue was homogenised.

Total protein was estimated using the Pierce BCA protein assay kit (Thermo Scientific, Waltham, MA, USA). This assay employs the colorimetric detection of cuprous ions that are formed by reduction of the cupric ion in an alkaline medium in the presence of protein. Samples were transferred to a 96 well plate along with increasing concentrations of bovine serum albumin (BSA) standard. A reagent containing bicinchonic acid supplied with the kit was added to the wells following which plates were incubated for 20 minutes at 37°C. Absorbance of samples was measured at 562nm on a plate reader and total protein was estimated by the software in relation to the BSA standard curve. Volumes of samples for equal protein loading were calculated and mixed with NuPage LDS sample buffer (4X) (Invitrogen, Life technologies, Paisley, UK) in a ratio of 3:1. Samples were then heated at 95°C for 5

minutes and loaded, along with a protein ladder (Magic Mark XP, Invitrogen), into wells of a NuPage 4-12% Bis-Tris polyacrylamide pre-cast gel (Invitrogen) for electrophoresis. Gels were placed in MOPS running buffer (Invitrogen), resolved at 200 volts and then transferred onto a PVDF membrane using the iBlot dry transfer device and transfer stacks (Invitrogen). Following a blocking step with 5% BSA, membranes were incubated with primary antibody either overnight at 4°C or at room temperature for 2 hours at the recommended dilutions. Membranes were then washed with TBS-T (Tris-buffered saline with tween) and incubated with horse radish peroxidase (HRP) labelled secondary antibody (Dako) for an hour at room temperature. ECL chemiluminescent reagent (GE healthcare, Uppsala, Sweden) was applied to visualize the blots using the Fuji LAS 2000 digital imager (Fujifilm, Japan). Membranes were stripped using Restore Plus stripping buffer (Thermo Scientific), blocked in 5% BSA and washed prior to further probing. Membranes were stored at -20°C by drying between 2 sheets of Whatman paper and were reactivated with methanol when required.

2.3.2 Antibodies and reagents

Primary antibodies for western blotting against p110α (#4249), GAPDH (#2118), total Syk (#2712), phospho-Syk thr525/526 (#2710), total Akt (#9272), phospho-Akt ser473 and thr308 (#9271, #2965), phospho-GSK3b ser9 (#9323), total ribosomal S6 (#2217) and phospho-S6 ser235/ser236 (#2211) were purchased from Cell Signaling technologies (Danvers, MA, USA). Antibodies against p110β (sc-602) and p110δ (sc-55589) were purchased from Santa Cruz biotechnology (Santa Cruz) and anti-human PTEN (ABM-2052) from Cascade bioscience (Winchester, MA, USA). 10 X Tris buffered saline with 1% Tween 20 (TBS-T) was prepared by adding 24.1g tris HCl and 80g NaCl to 950mls of distilled water. Hydrochloric acid or sodium hydroxide was added to adjust the pH to 7.6. 5% BSA (Sigma-Aldrich) or 5% milk (Marvel, UK) in 1x TBS-T wash buffer was used to prepare antibody dilutions.

2.3.3 Densitometry

Densitometry was performed on GelScan Standard software v5.1 (BioSciTec, Frankfurt, Germany).

2.4 PI3K INHIBITORS AND CELL STIMULATION

GDC-0941 was purchased from Selleck Chem (Houston, TX, USA) while CAL-101/GS-1101 was purchased from Active Biochem (Maplewood, NJ, USA). Figure 2.5 shows the chemical structure and IC_{50} (half maximal inhibitory concentration against recombinant enzyme) values for GS-1101[149] and GDC-0941[163] against the 4 class I PI3K isoforms. In addition, a selective p110α inhibitor A66[164] and a selective p110β inhibitor TGX-221[117] were purchased from Selleck Chem. 10mM stock solutions were prepared in DMSO and stored at -20°C. Serial dilutions for drug treatment were prepared in cell growth medium and cells were treated in their logarithmic growth phase.

Figure 2.5 CAL-101/GS-1101 and GDC-0941: Chemical structures and IC_{50}values for class I PI3K

GS-1101

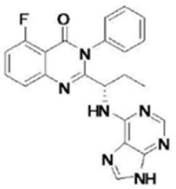

Class I PI3Ks IC50 (nM)			
p110α	p110β	p110δ	p110γ
820	565	2.5	89

GDC-0941

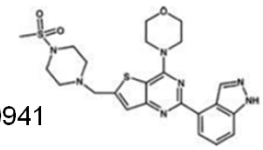

Class I PI3Ks IC50 (nM)			
p110α	p110β	p110δ	p110γ
3	33	3	75

Goat anti-human IgM $F(a'b)_2$ fragments (Southern Biotech, Cambridge, UK) were used to activate the BCR signalling cascade and study the effect of isoform-selective PI3K inhibition on downstream targets in this setting. Cells were treated with pharmacological inhibitors or vehicle for an hour prior to incubation with 10µg/ml IgM $F(a'b)_2$ for 10 minutes. Protein was extracted from cells at this point for western blotting. Recombinant interleukin 4 (IL4) (Sigma-Aldrich) was used to induce proliferation of primary MCL cells. Cells were incubated with 20ng/ml IL4 prior to treatment with

either vehicle or increasing concentrations of PI3K inhibitors in a 96-well plate. An ATP cytotoxicity assay was used at 72 hours to assess the effect of PI3K inhibition on IL4-stimulated cells.

2.5 REAL TIME QUANTITATIVE PCR MEASUREMENT OF GENE EXPRESSION

2.5.1 RNA extraction

RNA was extracted from cell lines and primary MCL cell suspensions ($5x10^6$) using the RNeasy mini kit (Qiagen, Hilden, Germany). Cells were lysed in a denaturing buffer (Buffer RLT) containing guanidine-thiocyanate to inactivate RNAses. Lysates were homogenised using QIAshredder spin columns (Qiagen) by loading up to 700µl of lysate into a column placed in a 2ml collection tube and centrifuging at full speed for 2 minutes. Ethanol was added to the homogenised lysate to facilitate binding of RNA to the silica membrane in the RNeasy spin columns. Lysates were loaded onto the spin columns and contaminants were washed off the silica membranes by centrifuging columns with the buffers provided (Buffer RW1 and Buffer RPE). Finally, total RNA was eluted from the silica membrane using RNase free water.

RNA was extracted from frozen tissue (tonsil and MCL lymph nodes) using a Trizol based method. Shavings of frozen tissue were placed in 2ml Eppendorf vials containing 1ml Trizol (Qiagen) and homogenised with the Qiagen TissueLyserII as described for protein extraction. The homogenate was allowed to rest for 5 minutes before addition of 200µl chloroform. After vortexing vigorously, the homogenate was centrifuged and the upper aqueous phase containing RNA was isolated. Isopropanol was used to precipitate the RNA by centrifugation and the pellet was washed with 1ml 75% ethanol prior to air drying and dissolution in RNAse free water. RNA quantity and purity were measured using a Nanodrop ND-1000 spectrophotometer (Nanodrop technologies, Wilmington, DE, USA) and RNA samples were stored at -80°C.

2.5.2 cDNA synthesis

The high capacity reverse transcription kit (Applied Biosystems, Life Technologies, Paisley, UK) was used to prepare a 2xRT Master Mix (10µl per reaction) as shown in table 2.4. 2µg RNA in a volume of 10µl was added to this to make up a reaction volume of 20µl per 0.2ml PCR reaction tube.

Table 2.4 Components of 2x RT Master Mix used for cDNA synthesis

2xRT master mix	**Volume per reaction (µl)**
10 x RT Buffer	2
25 x dNTP Mix (100mM)	0.8
10 x RT Random Primers	2
Multiscribe Reverse Transcriptase	1
Nuclease free water	4.2

Reverse transcription was carried out in an automated thermal cycler with initial annealing for 10min at 25°C, followed by extension for 120 min at 37°C, reverse transcriptase inactivation for 5 min at 85°C and finally cooling to 4°C.

2.5.3 Quantitative real-time PCR

Quantitative real-time PCR (qRT-PCR) was performed using TaqMan gene expression assays (Applied Biosystems) for *PIK3CA* (Hs00192399_m1), *PIK3CB* (Hs00927728_m1) and *PIK3CD* (Hs00180679_m1) with *GAPDH* (Hs99999905_m1) as endogenous control. TaqMan gene expression Master Mix (Applied Biosystems) and cDNA were added to TaqMan gene expression assays and a final volume of 20µl per reaction (Table 2.5) was added to individual wells of a Fast Optical 96 well reaction plate (Applied Biosystems).

Table 2.5 Components of PCR reaction mix for quantitative real time PCR

PCR reaction mix components	Volume per 20µl reaction (µl)
20 x Taqman gene expression assay	1
2 x TaqMan gene expression Master Mix	10
cDNA template	2
RNase free water	7

The plate was sealed with an optical adhesive cover and loaded on the ABI HT-7900 instrument (Applied Biosystems). Quantitative fast real-time PCR was performed with an initial denaturation step at 95°C for 10 minutes followed by 40 cycles at 95°C for 1 second and 60°C for 20 seconds. Data was analyzed using the SDS2.1 software (Applied Biosystems) and relative expression values were calculated using the ΔCt method with *GAPDH* as endogenous control. All reactions were run in triplicate.

2.6 *PIK3R1* AND *PIK3CA* MUTATION ANALYSIS

2.6.1 DNA extraction

Genomic DNA was extracted from cell lines, primary MCL cell suspensions and homogenised frozen sections using the DNeasy mini kit (Qiagen). Briefly, protein digestion was carried out by addition of proteinase K and buffer AL followed by incubation of samples at 56°C for 10 minutes. Samples were mixed thoroughly with 96-100% ethanol and loaded into the DNeasy spin columns. DNA was isolated on the membrane of the column by centrifugation. Contaminants and enzymes were washed off by centrifugation of columns in the presence of buffers provided (Buffer AW1 and AW2). DNA was then

eluted from the membrane using buffer AE. DNA content and purity were checked using a Nanodrop ND-1000 spectrophotometer and samples were stored at 4°C.

2.6.2 PCR, purification and sequencing

Primers used for PCR amplification of *PIK3CA* exons 9 and 20 and *PIK3R1* exons 9, 10, 11, 13, 15 and 16 were designed using the Primer3 software[165]. Primers were purchased from Sigma-Aldrich and are listed in table 2.6.

Table 2.6

Gene	Exon	Forward primer	Reverse primer
PIK3R1	**9**	CTATGTGGGCAGGAGGAATA	AACTGAAGGTTAATGGGTCAGA
	10	TGGTACGAGATGCGTCTACT	CAAAATAGCTGACATGGAAACATCT
	11	GTTACGATGTTTAGACAAGATCCTT	GCTTCAGTTATCACGTGAACTTAAT
	13	AAAATATGTTGAGCCACTCCAAA	GTTTTCATTGCCCAACCACT
	15	AAAACTCAGGTCGGGCAGA	AGCTGCTTTGGTTTCTCTTCTA
	16	TTACCTACCCAAGGCACTCG	GCCTTAGGCTGCATGTCTTC
PIK3CA	**9**	TGGCCAGTACCTCATGGATT	TAAAGCCCTAGCTTGCCTTC
	20	TTTTGGGAATTGGAGATCGT	GCTGGTTTCAATTCCTGAGC

A PCR reaction mix (20µl per reaction) consisting of 1µl of genomic DNA or non-template control, 0.5µl each of forward and reverse primers and 17µl Reddy mix (Thermo Scientific) was prepared. PCR was performed in an automated thermal cycler (MJ research, Waltham, MA USA) with initial denaturation at 95°C for 5 minutes followed by 34 cycles of denaturation for 30 seconds, annealing at 95°C for 30 seconds and extension for 72°C for 30 seconds followed by a final extension step at 72°C for 5 minutes. Amplicons were evaluated using agarose gel electrophoresis and visualized by trans-illumination under ultraviolet light. Enzymatic purification of products was carried out using

ExoSAP solution which was prepared by mixing 1µl Exonuclease1 (Promega, Madison, WI), 20µl Shrimp Alkaline Phosphatase (New England biolabs, Ipswich, MA) and 179µl distilled water. 4µl of ExoSAP was added to 5µl of PCR products and placed in an automated thermal cycler at 37°C for 30 minutes and 80°C for 15 minutes prior to storage at 4°C. Bidirectional Sanger sequencing was performed on the purified PCR products using the BigDye Terminator v3.1 cycle sequencing kit (Applied Biosystems). A 20µl sequencing reaction mix was prepared consisting of 0.5µl Big Dye Terminator mix, 3.75µl 5x Buffer and 1µl of sequencing primer added to 2µl of the purified DNA in water. This was placed in an automated thermal cycler with initial denaturation for 1 minute at 96°C followed by 26 cycles of denaturation at 96°C for 1min, annealing at 50°C for 15 seconds and extension at 60°C for 4minutes before storage at 12°C. Samples were then transferred to the CRUK sequencing services at Lincoln's Inn fields. Sequences were screened for mutations using the sequence alignment editor BioEdit version 7.1.9 (Ibis Biosciences, Carlsbad, CA, USA).

2.7 FLOW CYTOMETRY AND CYTOTOXICITY ASSAYS

2.7.1 Cell counts and viability

All cell counts for setting up experiments were performed on the Vi-Cell XR Cell Viability Analyzer (Beckman Coulter, Indianapolis, IN, USA) which is a coulter counter that incorporates automated trypan blue nuclear staining of dead cells to determine the viable cell percentage and number.

2.7.2 Immunophenotyping

Tumour content of MCL cell suspensions was verified using CD20 immunophenotyping by flow cytometry. Only samples with greater than 85% CD20 content were used in experiments. For xenograft studies, CD5/CD20 dual staining was carried out along with CD3, CD4 and CD8 staining to assess T cell content and subsets. The following fluorochrome conjugated antibodies - CD20-FITC, CD5-PE, CD3-APC, CD4-FITC and CD8-PE were purchased from Miltenyi Biotec. For flow cytometry

analysis, cells were washed with ice cold staining buffer (PBS + 2%FCS + 0.1% azide) and approximately 10^6 cells in 100µl of staining buffer were incubated with the recommended concentration of fluorochrome conjugated antibody. After incubation in the dark at 4°C for 30 minutes, cells were washed twice and re-suspended in 500µl of staining buffer. DAPI (0.5µg/ml) was added for live-dead discrimination. Data was acquired on BD LSR-Fortessa (BD biosciences) and analysed using FlowJo version 8.8.7 (TreeStar Inc, Ashland, OR, USA).

2.7.3 Annexin V / propidium iodide staining

The ApoTarget Annexin V-propidium iodide (PI) kit (Invitrogen), was used for detecting apoptosis in MCL cell lines following treatment with PI3K inhibitors. Cells were treated in their logarithmic growth phase with increasing concentrations (0.1, 1, 5 and 10µM) of PI3K inhibitors or vehicle control. After 72 hours of incubation in normoxic conditions at 37°C, cells were washed twice with PBS and re-suspended in the Annexin V binding buffer provided with the kit. Approximately $2x10^5$ cells in 100µl of staining buffer were incubated at room temperature with 5µl of FITC labelled Annexin V and 10µl propidium iodide, for 15 minutes in the dark. After this, 400µl of staining buffer was added to each tube and cells were analysed by flow cytometry. All experiments were done in triplicate.

2.7.4 Guava ViaCount

The Guava EasyCyte Plus instrument (Millipore, Billerica MA) is a bench top flow cytometer that can acquire samples from 96 well plates. The Guava ViaCount assay uses nuclear binding dyes to provide total and viable cell counts and was used to assess growth inhibition in cell lines following PI3K inhibition. Cells were treated in their logarithmic growth phase with increasing concentrations (0.1, 1, 5 and 10µM) of PI3K inhibitors or vehicle, in triplicate, in a 96 well plate. Each well was loaded with $2x10^4$ cells in a volume of 120µl. After 72 hours of incubation in normoxic conditions at 37°C, 120µl of the Guava ViaCount reagent (Millipore) was added to each well and mixed by pipetting. The 96 well plate was loaded into the EasyCyte plus instrument and the software was programmed to

acquire 2000 events per well. Acquisition and analysis were performed on the Guava Cytosoft software. All experiments were performed in triplicate.

2.7.5 ATP proliferation and cytotoxicity assay

The ATP vialight plus kit (Lonza, Basel, Switzerland) was used to assess proliferation in MCL primary samples in response to IL4 as well as cytotoxicity in response to PI3K inhibition. This luminescence assay is based on the principle that luminescence generated by luciferase in the presence of ATP and luciferin is proportional to ATP levels in the sample which in turn reflects cell number and viability.

$$\text{ATP} + \text{Luciferin} + O_2 \xrightarrow[Mg^{++}]{\text{Luciferase}} \text{Oxyluciferin} + \text{AMP} + CO_2 + \text{Light}$$

Cells were incubated in triplicate in a 96 well plate after treatment with PI3K inhibitors or vehicle using the same protocol as for the Guava ViaCount assay. However, for primary cells a concentration of $5x10^4$ cells in 100µl of medium per well was used. In order to assess the effect of PI3K inhibition on IL4 stimulation, cells were stimulated with IL4 as detailed previously and were subsequently treated with vehicle or increasing concentrations of PI3K inhibitors. Proliferation was compared with non-stimulated cells. After 72 hours of incubation in normoxic conditions at 37°C, cells were lysed in 96 well plates for 10 minutes with the lysis buffer provided in the kit and then transferred to an opaque 96 well plate. Cells were incubated with the ATP vialight plus reagent for 2 minutes and luminescence readings were acquired on a FluoStar Optima plate reader (BMG labtech, Ortenberg, Germany).

2.8 XENOGRAFT STUDIES

Xenograft studies in NSG mice were carried out in collaboration with Dominique Bonnet at the Haematopoietic stem cell laboratory, Cancer Research UK, Lincoln's Inn fields. The Jeko-1 cell line

and primary MCL samples were provided by the Centre for Haemato-Oncology. Luciferase transduction of Jeko-1, tail vein injection into NSG mice and bioluminescent imaging was carried out at Lincoln's Inn fields by Linda Ariza McNaughton (L.A.M.). Primary samples were characterised by flow cytometry, T-cell depleted and transported to our collaborators for injection into NSG mice by myself. Flow cytometry on mouse derived cells was carried out by L.A.M. while harvest of organs from NSG mice was carried out at Lincoln's Inn fields by L.A.M. and myself. Organs were transported back to Barts Cancer Institute in neutral buffered formalin for immunohistochemistry or ice cold PBS for isolating cells. Immunohistochemistry on mouse derived tissue was performed by me with assistance from Andrew Clear. Cells were isolated from spleens of NSG mice by myself and transported for *IGH: CCND1* fluorescent *in situ* hybridisation (FISH) to the cytogenetics laboratory at the Royal London hospital where FISH was performed by Amy Roe and Debra Lillington. Details of these methods are included in Chapter 6, apart from immunophenotyping of primary samples which is detailed in the flow cytometry section of this chapter.

2.9 STATISTICAL ANALYSIS

Prism version 5.03 (GraphPad, La Jolla, CA) was used for statistical analysis. Normally distributed data sets were tested with paired or unpaired t-tests, as appropriate, while for 3 data sets, one-way analysis of variance (ANOVA) followed by a Bonferroni multiple comparison post-hoc analysis was used. Data sets that were not normally distributed were analyzed using the Mann-Whitney test for unpaired samples or the Wilcoxon matched-pairs signed rank test for paired samples. P-values less than 0.05 were considered significant. Any additional statistical methods are mentioned in the relevant sections.

CHAPTER 3: IMPORTANCE OF CLASS IA PI3K ISOFORMS AND PTEN EXPRESSION IN MCL

3.1 INTRODUCTION

The expression of the three class Ia PI3K isoforms has not been evaluated simultaneously in previous studies of MCL. The study that initially reported gene amplification of *PIK3CA* in MCL did not evaluate the expression of the other class Ia isoforms and also did not study the effect of isoform selective inhibitors in the setting of *PIK3CA* gene amplification.[144] Studies reporting the activity of CAL-101/GS-1101 reported high p110δ expression in MCL but did not explore the expression of other isoforms.

Loss of expression of the tumour suppressor PTEN has been evaluated in two separate studies of MCL and has been found in 15-20% of cases.[22,144] Although, phosphorylated PTEN, evaluated by IHC, has been reported in one study as a marker of PTEN inactivation,[23] the stability of phosphoproteins in FFPE tissue is a concern[161,162] and we therefore did not evaluate this, or other phosphoproteins markers of pathway activation in our studies.

As the first step towards exploring the relative importance of the class Ia PI3k isoforms in MCL, we evaluated the protein expression of the three class Ia isoforms and PTEN using immunohistochemistry. Clinical associations of loss of PTEN expression, class Ia PI3K isoform expression, blastoid morphology and Ki-67 were explored. The effect of isoform selective inhibition was studied in relation to *PIK3CA* gene amplification and agonist-induced BCR signalling in MCL cell lines. In view of studies in solid tumours that have demonstrated an important role for p110β in cells that lack PTEN expression,[145] the value of adding a p110β inhibitor to CAL-101/GS-1101 was studied in primary MCL samples exhibiting this phenotype.

3.2 MATERIALS AND METHODS

Immunohistochemistry

As detailed in chapter 2, 175 biopsies from 121 patients were incorporated into the MCL TMA for immunohistochemical analysis using antibodies against p110α, p110β, p110δ and PTEN. Characteristics of the samples included in the TMA are listed in table 3.1. There was some attrition in the number of evaluable samples with serial sectioning of blocks due to poor quality cores, loss of cores and exclusion criteria for analysis (only biopsies with at least two evaluable cores were included). This explains the discrepancy in the number of samples described in table 3.1 and the number finally evaluated in the experiments that follow. The IHC score (product of percentage positive and mean intensity) generated with the Ariol visual analysis software was used as a measure of protein expression of PI3K isoforms in MCL biopsies and tonsil controls. PTEN and Ki-67 were scored manually as described in the previous chapter. IHC scores were matched to patient biopsies and clinical information was stored in password protected spreadsheets. Kaplan-Meier survival curves were generated using the X-tile software.[166] A KI-67 cut-off value of 30% was employed as per the recent British Committee for Standards in Haematology (BCSH) recommendations.[167] Prism version 5.03 (GraphPad, La Jolla, CA) was used for all other statistical analysis.

Quantitative real-time PCR

The Granta519 MCL cell line was used as it has been shown to exhibit gene amplification of *PIK3CA* associated with increased *PIK3CA* copy number.[144] RNA was extracted from Granta519 and the lymphoblastoid cell line NcNc using the Qiagen RNeasy mini kit (Qiagen). Gene expression of *PIK3CA* was evaluated by qRT-PCR using TaqMan gene expression assay Hs00192399_m1 (Aplied Biosystems). Data was analyzed using the SDS2.1 software (Applied Biosystems).

Table 3.1 Characteristic of MCL biopsies included in TMAs for IHC analysis

Period over which biopsies taken		1972-2008
Total biopsies evaluable (for at least one marker)		175 (121 patients)
Male: female		3.9:1 (M=85, F=22)
Median age		63yrs (38-75yrs)
Source of tissue	**Lymph node**	134
	Spleen	13
	Bone marrow	2
	Gut	8
	Other*	15
Biopsies with blastoid morphology		30
Diagnostic biopsies		48
Median overall survival of cohort		3.4yrs
Diagnostic biopsies with matched relapse biopsies		12
*Tonsil, prostate, skin, paranasal sinuses, buccal mucosa, tongue		

Western blotting

Total protein for western blotting was extracted from cell lysates prepared at the indicated time-points. Expression of p110α, PTEN, GAPDH, phosphorylated and total Syk, Akt and ribosomal S6 was evaluated by western blotting. Goat anti-human IgM $F(a'b)_2$ fragments were used for BCR stimulation of the Jeko-1 cell line.

ATP cytotoxicity assay

Two cryopreserved primary MCL samples exhibiting loss of PTEN expression by western blotting were thawed in a water bath and re-suspended in growth medium prior to treatment with PI3K inhibitors in a 96 well plate. Cells were treated with increasing concentrations of the p110δ inhibitor GS-1101 (Active Biochem) alone and in combination with 1μM of the p110β inhibitor TGX-221 (Selleck Chem). Following incubation for 72 hours, the ATP assay was performed to compare cytotoxicity of GS-1101 in these two samples with or without TGX-221.

3.3 CLASS IA PI3K EXPRESSION IN MCL

3.3.1 Expression in MCL compared to tonsil controls

A total of 144 biopsies from 109 MCL patients were evaluable for all three isoforms. P110δ was consistently expressed at high levels in MCL. P110β expression was the weakest while p110α showed wide variation in expression across biopsies (Figure 3.1). Median expression of p110α (median IHC score=44.5 vs. 33.7, p=0.15) and p110δ (median IHC scores=77.4 vs. 81.1, p=0.2) in MCL was not significantly different from that seen in the germinal centers of tonsil controls whereas P110β expression was significantly lower in MCL (median IHC score=16.1 vs. 4.9, p=0.01). Appendix B contains a summary of the clinical details and IHC scores for individual samples.

Figure 3.1 Class Ia PI3K isoform expression in MCL Dot-plot showing expression of class IA PI3K isoforms in MCL biopsies in black (144 biopsies evaluable for all 3 isoforms from 109 patients) compared to tonsil controls in grey (n=14). Each dot for MCL samples represents the average IHC score of triplicate cores and lines represent median expression. (*= p<0.05)

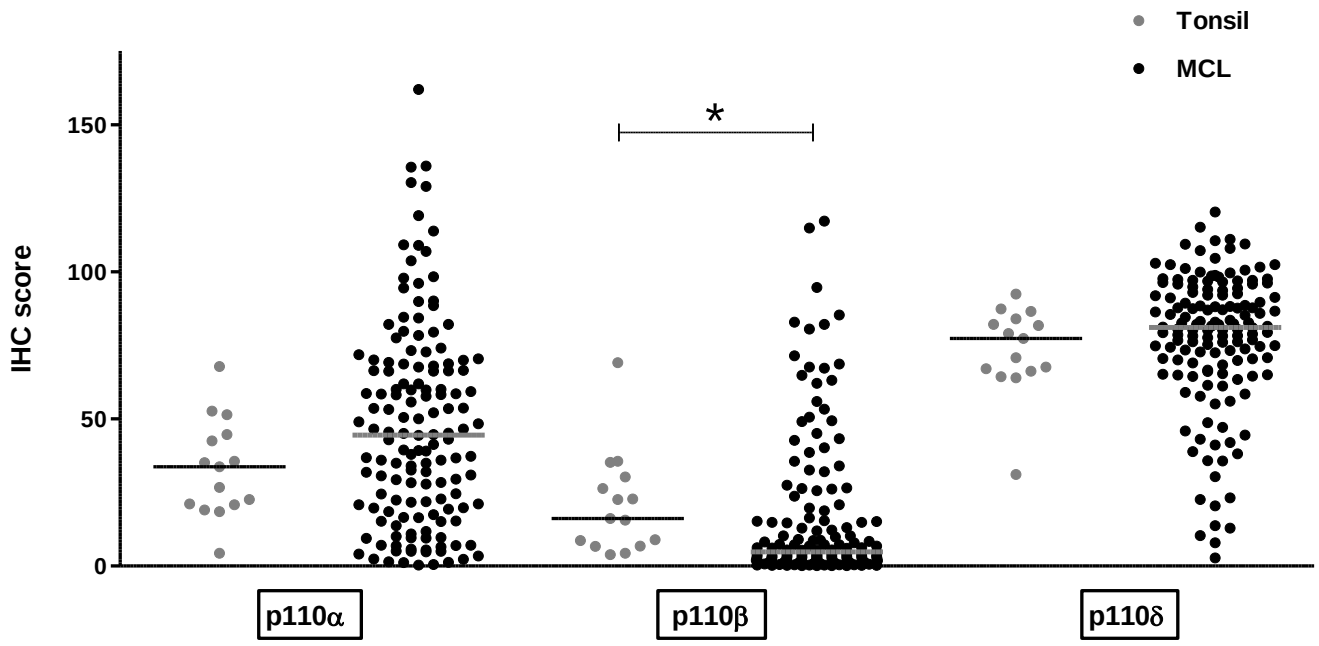

3.3.2 Expression with MCL disease progression

Based on the patient episode at which MCL biopsies were obtained, samples on the TMA were divided into those taken at diagnosis, 1st relapse and beyond 1st relapse. On comparing class Ia PI3K isoform expression between these groups, p110α expression was significantly higher in biopsies taken beyond first relapse compared to those taken at diagnosis (p=0.04) (Figure 3.2A). These differences were even more striking in sequential biopsies (p=0.008) with five out of six lymphoma samples showing significantly increased p110α expression beyond first relapse (Figure 3.2B). Images from two of the MCL sequential biopsy pairs with the greatest change between diagnosis and 1st relapse are shown in Figure 3.2C. Expression of p110α beyond first relapse was significantly higher than expression in tonsil controls (p=0.024). Neither p110β nor p110δ expression was altered significantly with relapse. (Figure 3.2 A, B)

3.3.3 Expression in relation to morphology and Ki67 proliferation index

Blastoid morphology was seen in 38 of 144 (26.4%) MCL biopsies. There was no significant difference in expression of any of the three class Ia isoforms between blastoid and non-blastoid MCL (Figure 3.3A)

Ki67 proliferative index was evaluated (using a cut off value of 30%[167]) in 30 diagnostic cases in the study cohort to determine its predictive value on disease specific survival. A significant survival benefit (p=0.0029, median survival 15.5mths vs 67.8mths) was observed in patients with Ki-67 proliferation index <30% (Figure 3.3B). This cut-off was applied to both diagnostic and relapse biopsies to assess whether expression of any of the class Ia isoforms was positively associated with a higher proliferative index. Once again, no difference was seen in class Ia isoform expression between biopsies with high and low Ki67 expression (Figure 3.3C).

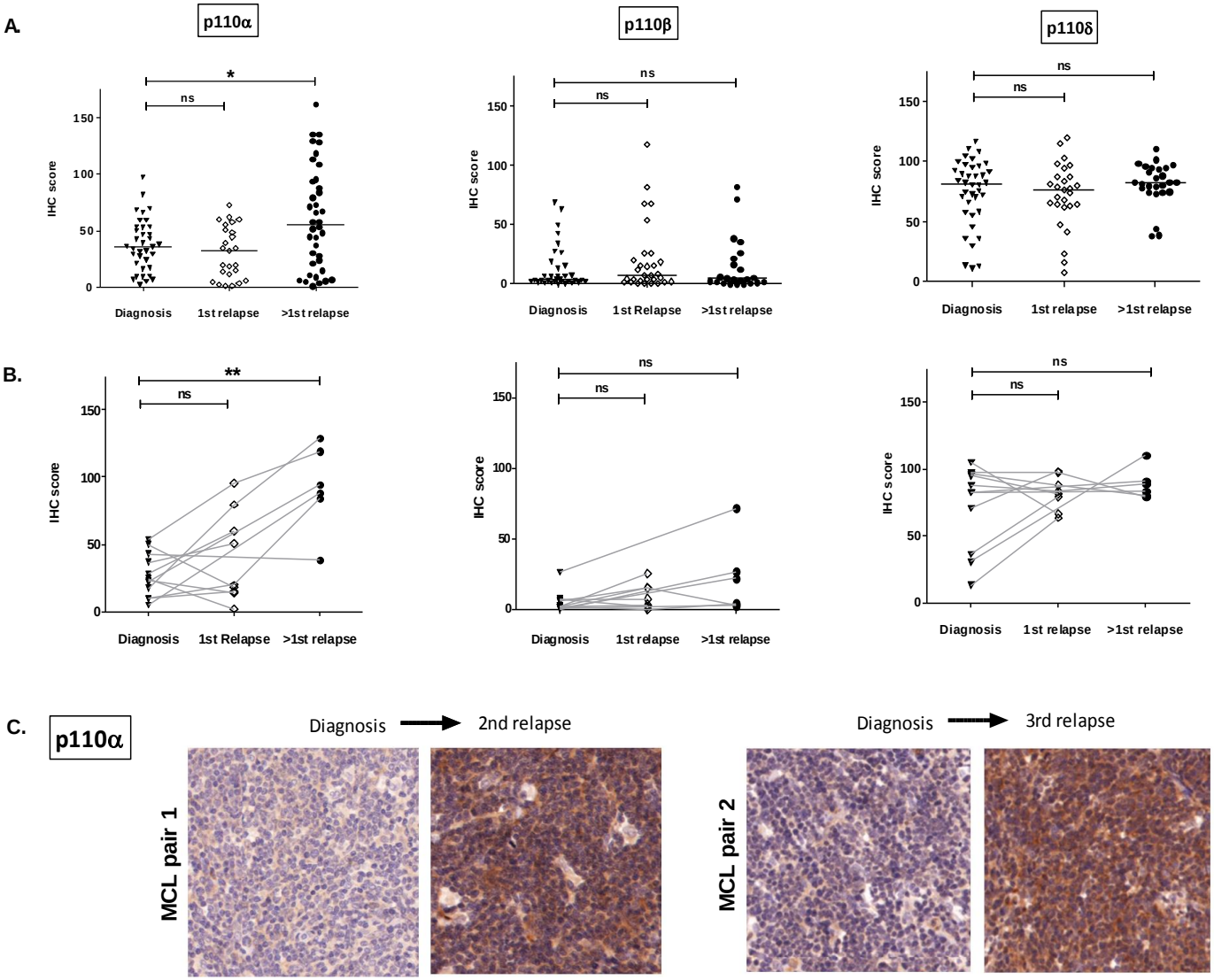

Figure 3.2 Class Ia PI3K isoform expression with MCL disease progression (A) Dot-plots showing a significant increase in p110α expression, but not p110β or p110δ, beyond first relapse. Bars represent median expression. (B) This pattern is more striking in 12 sequential cases (connected by grey lines), 6 of which had paired biopsies beyond first relapse. (C) IHC images (original magnification x200) of sequential biopsies from 2 patients showing significant increase in p110α expression beyond 1st relapse. Each dot represents the average IHC score of triplicate cores and bars represent median expression. (ns = not significant, *= p<0.05, **=p<0.01).

Figure 3.3 Class Ia PI3K isoform expression in relation to morphology and proliferative index (A) Dot plots showing no significant difference in class Ia isoform expression between blastoid and non-blastoid morphology. Bars represent median expression. (B) Kaplan-Meier disease specific survival curves demonstrating a significantly worse survival in patients with a Ki-67 proliferation index of >30% at diagnosis (N=30). (C) Class Ia PI3K expression was compared between biopsies with high or low proliferation based on a Ki-67 cut-off of 30%. As shown in the dot-plots, no significant difference was found with any of the isoforms between these two groups. Each dot represents the average IHC score of triplicate cores and lines represent median expression.

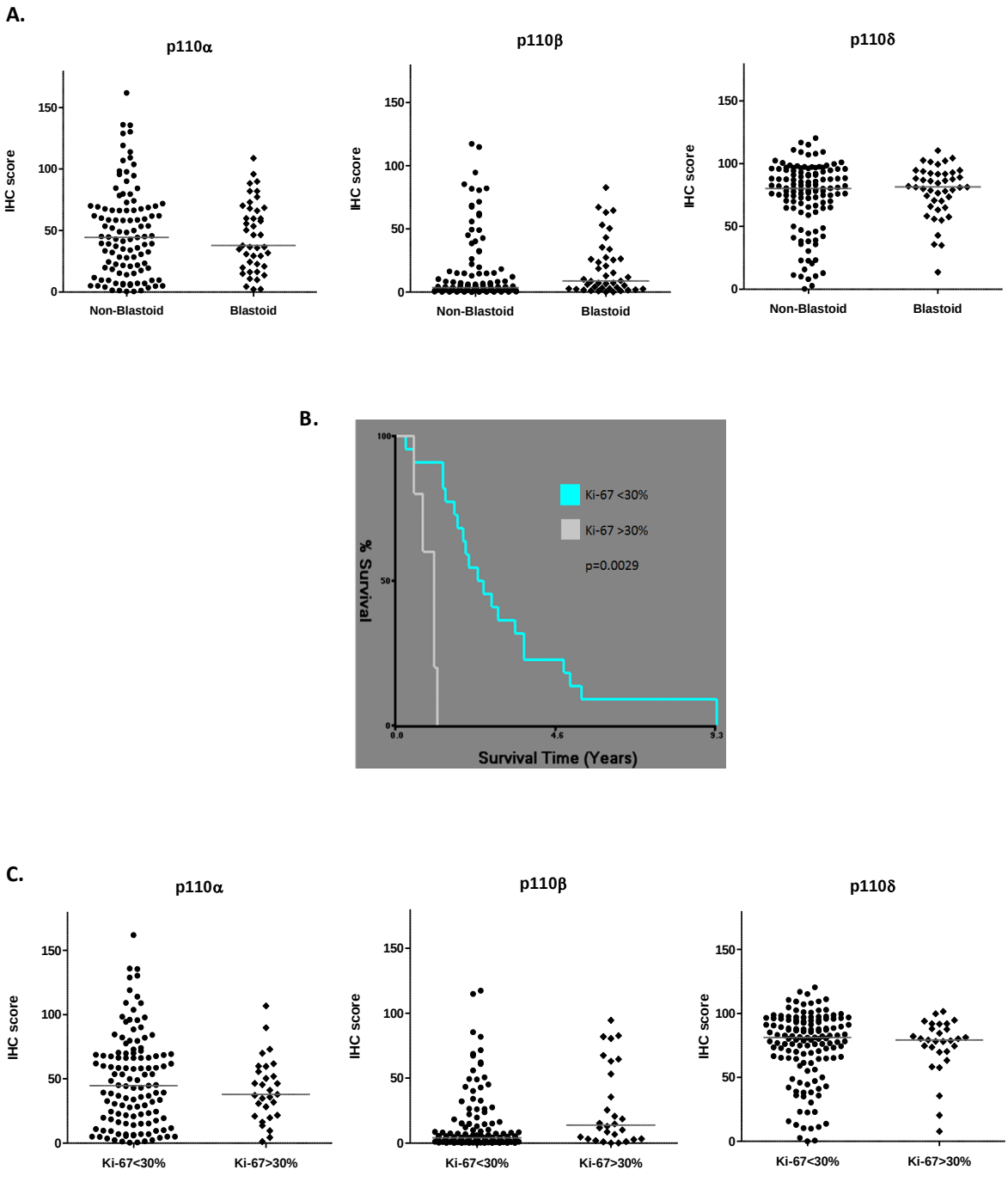

3.4 EFFECT OF ISOFORM-SELECTIVE PI3K INHIBITION ON SIGNALLING IN MCL

3.4.1 Granta519: A cell line with p110α over-expression

The Granta519 cell line was established spontaneously from the peripheral blood of a 58 year old Caucasian lady who had an aggressive relapse within 6 months of achieving a response to combination chemotherapy (high dose cyclophosphamide and methotrexate, VP16, bleomycin, vincristine and prednisolone) for stage IV MCL.[168] This cell line exhibits gene amplification of *PIK3CA* in relation to increased copy number[144] (Figure 3.4A). In view of the previous report of *PIK3CA* gene amplification in MCL and the observation that p110α expression increases with MCL disease progression, the Granta519 MCL cell line was used to study the effect of isoform selective PI3K inhibition in this setting.

Quantitative real-time PCR was used to confirm *PIK3CA* gene amplification in Granta519 by comparing it to the lymphoblastoid cell line NcNc. In keeping with this, western blotting demonstrated higher p110α expression in Granta519 compared to NcNc (Figure 3.4B). Next, the downstream effects of PI3K inhibition were compared between the p110δ inhibitor GS-1101 and a predominantly p110α and p110δ inhibitor GDC-0941, at a concentration of 1μM. Western blotting was performed 2 hours and 24 hours following treatment of Granta519 with the inhibitors. GS-1101 treatment resulted in incomplete PI3K inhibition with residual Akt phosphorylation (thr308 and ser473) detectable at 2 hours and 24 hours. At equimolar concentrations GDC-0941 blocked Akt phosphorylation in a sustained manner over 24 hours. This was reflected in reduced downstream phosphorylation of ribosomal S6 as a result of mTOR inhibition (Figure 3.4C). The relative reduction in phosphorylation of GSK-3β at both time-points was less striking between the two inhibitors.

To establish whether or not the effect of GDC-0941 was related to its activity on the p110α isoform, GS-1101 was combined separately with the p110α inhibitor A66 and the p110β inhibitor TGX221.

These combinations were tested along with single agent GS-1101 and GDC-0941. All inhibitors were used at a concentration of 1μM. Further, Granta519 cells were serum-starved by incubating them in serum-free medium for 4 hours In order to assess the effects of these inhibitors on constitutive pathway activation. Combining GS-1101 with A66 had a similar effect as GDC-0941 whereas combining GS-1101 with TGX221 made no significant difference to residual Akt phosphorylation, confirming that residual constitutive PI3K signaling in GS-1101 treated cells was attributable to p110α activity.

3.4.2 Effect on BCR signalling

The Jeko-1 MCL cell line exhibits low or undetectable levels of p-Akt and was therefore used to study the effect of isoform selective inhibition on agonist-induced BCR signaling. Cells were pre-treated for an hour with 1μM isoform selective inhibitors prior to BCR stimulation with 10μg/ml goat anti-human IgM $F(a'b)_2$ fragments for 10 minutes. Western blotting at this point showed that whereas the p110δ inhibitor GS-1101 prevented phosphorylation of Akt (thr308) in response to BCR stimulation, the p110α inhibitor A66[164] and the p110β inhibitor TGX221,[117] had minimal effects on p-Akt (thr308). Phosphorylation of Syk was used as a marker of BCR activation.

Figure 3.4 Downstream effects of isoform selective inhibition in the setting of *PIK3CA* over-expression and agonistic BCR activation - (A) Fluorescent *in situ* hybridization images (from Psyrri *et al, Clin Cancer Res 2009*) demonstrating increased copy number of *PIK3CA* in Granta519 cells compared to Raji cells (green probe=*PIK3CA*, red probe=chromosome 3) (B) Real-time PCR and western blotting confirms increased expression of *PIK3CA* and p110α in Granta519 MCL cell lines compared to the lymphoblastoid cell line NcNc. (C) Western blot comparing downstream effects of GS-1101 (1μM) and GDC-0941 (1μM), at two time points demonstrating incomplete and non-sustained effect of GS-1101 on p-Akt, p-S6 and to a lesser extent on p-GSK3β. (D) Western blot of serum-starved (4 hours) Granta519 cells treated with GS-1101, GDC-0941 and combinations of GS-1101 with A66 or TGX-221 (all 1μM), for 2 hours, confirming the contribution of p110α to constitutive PI3K activation.(E) Effect of isoform-selective PI3K inhibition on IgM stimulated Jeko-1 cells. P-Syk (tyr525/526) was used as a marker of BCR activation. GS-1101 (p110δ-selective) blocked p-Akt production while A66 (p110α-selective) and TGX-221 (p110β-selective) did not.

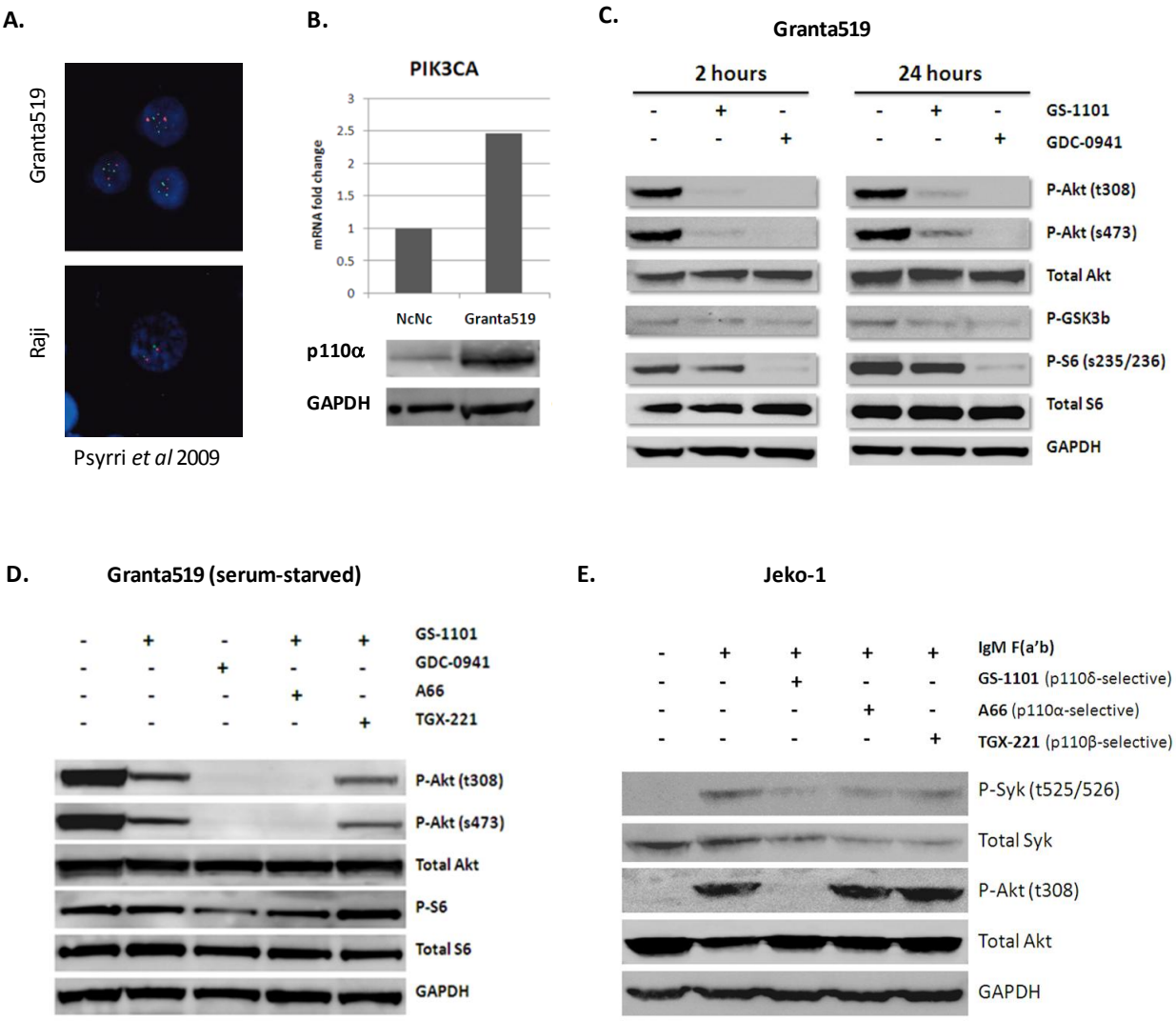

3.5 LOSS OF PTEN EXPRESSION

3.5.1 Immunohistochemistry

PTEN protein expression was evaluated by IHC on the MCL TMAs. A PTEN null adenocarcinoma control was included with the TMAs during IHC staining to confirm there was no non-specific binding of the antibody (Figure 3.5A). In keeping with previous reports,[22,144] we found loss of PTEN expression in 17% of diagnostic (6/35) and 16% of all (22/138) biopsies. A higher proportion of tumours exhibiting blastoid morphology had loss of PTEN expression compared to cases with classical histology but this difference was not significant (20% vs. 15%, p=0.55 by Fisher's exact test) (Figure 2C). No significant change was found in the pattern of isoform expression in biopsies that had loss of PTEN expression (Figure 2D).

3.5.2 Loss of PTEN expression and p110β inhibition

As both Granta519 and Jeko-1 had normal levels of PTEN protein expression, we probed 12 primary MCL samples (clinical information listed in table 4.1) for PTEN by western blotting and found loss of PTEN expression in 2 of 12 samples. A biopsy from one of the two samples was available on the TMA and confirmed the loss of PTEN expression. These two samples were treated with increasing concentrations of GS-1101, with or without the addition of 1μM of the p110β inhibitor TGX-221. The effect of these treatments at 72 hours was evaluated using an ATP cytotoxicity assay. No significant benefit was seen from the addition of TGX-221 to GS-1101 in either sample.

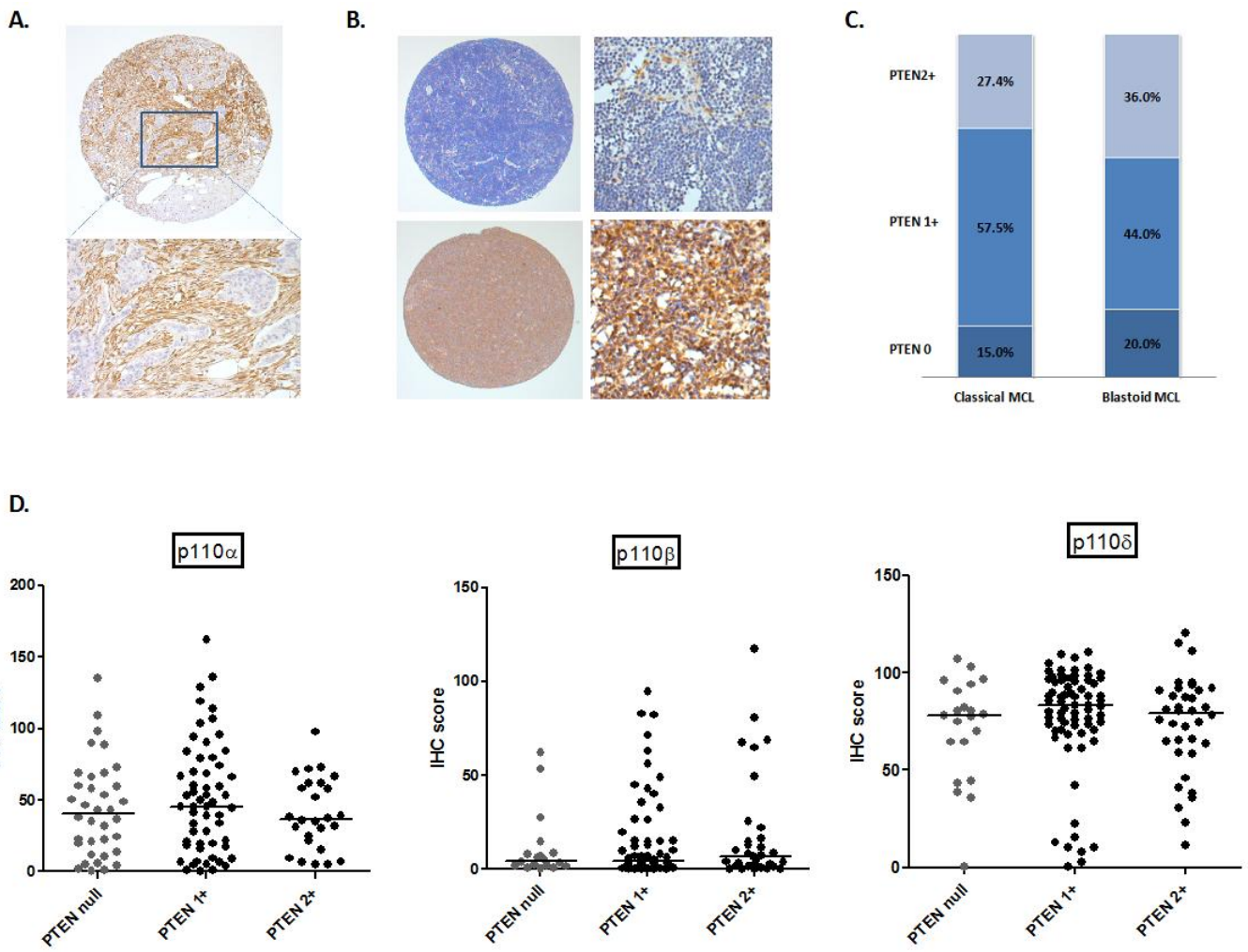

Figure 3.5 Loss of PTEN expression in MCL (A) Core from a *PTEN* null adenocarcinoma control showing PTEN negative tumor islands surrounded by PTEN positive stroma by IHC (original magnification x50 and x200). (B) Representative images of MCL cores with and without loss of PTEN expression (Original magnification x50 and x200). Macrophages and blood vessels were used as internal controls. (C) **B**ar graph of distribution of PTEN loss in blastoid and non-blastoid MCL. (D) Dot plot comparing class Ia isoform expression levels between cores with and without loss of PTEN expression showing no difference between the 3 groups (PTEN-, PTEN 1+ and PTEN2+). Bars represent median expression.

Figure 3.6 Loss of PTEN expression and p110β inhibition (A) Western blot for PTEN expression in 12 MCL primary samples showing loss of expression in 2 samples (indicated by arrows). (B) Results of ATP cytotoxicity assay after 72 hours treatment showing no benefit from addition of a p110β-selective inhibitor to GS-1101, compared to GS-1101 alone, in 2 MCL suspensions exhibiting loss of PTEN expression.

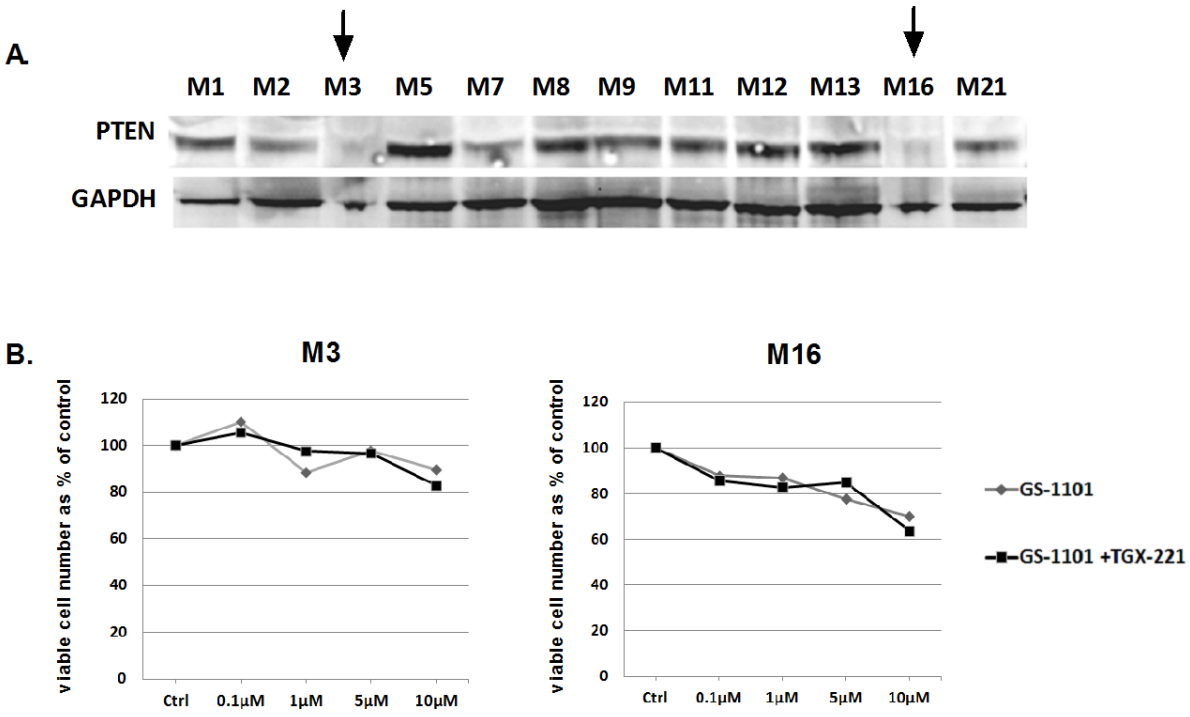

3.6 DISCUSSION

These immunohistochemistry studies confirm that, similar to healthy B-cells, p110δ is the most abundant and consistently expressed class Ia PI3K isoform in MCL. The increase in p110α expression with disease progression that we observe has not previously been described. Psyrri et al demonstrated gene amplification of *PIK3CA*, related to increased copy number, in approximately two-thirds of cases evaluated but their study did not detail the treatment episode at which these samples were taken.[144] The reason for p110α over-expression with disease progression is not clear. One theory could be that this over-expression contributes to MCL chemo-resistance with relapse. The mechanism may involve the expansion of a pre-existing clone of resistant tumour cells that have high p110α expression or induction of PIK3CA expression by cytotoxic agents. Interestingly there is evidence that prolonged activation of FOXO3a by doxorubicin can enhance survival in malignant cells through induction of *PIK3CA* expression. In the same study, increased FOXO3a induced expression of *PIK3CA* was found in chemo-resistant AML cell lines.[130]

In relation to PI3K inhibition, we find that the p110δ inhibitor GS-1101 is unable to completely abolish constitutive activation of PI3K in a cell line with p110α over-expression and this residual PI3K activity is effectively abolished by addition of a p110α inhibitor. On the other hand, p110δ inhibition is sufficient to abolish BCR mediated activation of the PI3K pathway. These observations, together with the immunohistochemistry findings, suggest an important role for additional p110α inhibition while confirming the importance of inhibiting the p110δ isoform in MCL. Of note, the p110α isoform has been shown to have a role in healthy BCR signalling.[169] It has been demonstrated that while p110δ is the key isoform in agonist-induced BCR signalling, p110α contributes to agonist-independent tonic BCR signalling. It is therefore possible that p110α over-expression increases the contribution of this isoform to agonist-independent PI3K signalling in MCL.

Similar to previous observations, we found loss of PTEN expression in approximately one-sixth (16%) of all MCL samples. Samples with loss of PTEN expression do not appear to have altered expression of class Ia isoforms. Addition of a p110β inhibitor to GS-1101 did not increase cytotoxicity in samples with loss of PTEN expression and, unlike reports in solid tumours, p110β does not appear to have an important role in this setting. However, this observation is limited to 2 samples and needs further study. Further, we only evaluated loss of PTEN expression as this was most relevant to the reports in solid tumours but, as discussed previously, other mechanisms of PTEN inactivation such as phosphorylation and micro RNA induced suppression have been described in MCL.

In summary, while inhibition of p110δ is necessary, additional p110α inhibition appears to be required for effective PI3K inhibition in MCL, particularly with relapse. Further questions that arise from these observations are, firstly, whether the effects of dual p110α/δ inhibition on PI3K signalling translate into greater cytotoxicity in MCL cells and secondly, whether biomarkers defining patient subsets that are most likely to benefit from these inhibitors can be identified. The following chapter attempts to answer these questions.

CHAPTER 4: COMPARATIVE CYTOTOXICITY OF GS-1101 AND GDC-0941 IN MCL AND PREDICTORS OF SENSITIVITY

4.1 INTRODUCTION

Studies with PI3K inhibitors LY294002 and Wortmannin have demonstrated growth inhibition and, to a lesser degree, apoptosis in MCL cell lines and primary samples. [22,23,144] These chemical inhibitors have been used widely and have advanced our understanding of this pathway but are not selective at the concentrations at which PI3K inhibition is achieved.[170] In recent years, a number of highly selective pan and isoform selective PI3K inhibitors have become available. GS-1101 was the first p110δ isoform-selective inhibitor to enter clinical trials and impressive activity was reported in early phase studies in patients with relapsed/refractory CLL and indolent NHL. The activity in relapsed/refractory MCL was less impressive.[153] The inclusion of further targets in the PI3K pathway is therefore being explored in order to achieve better responses in MCL. Recent reports have described enhanced anti-proliferative effects *in vitro* by combining GS-1101 with an mTOR inhibitor[171] or with a CDK4/CDK6 inhibitor[172] in MCL. However, inclusion of a greater number of targets is likely to result in increased toxicity. This leads on to the need for biomarkers that can guide selection of patients in whom drugs with wider activity provide significantly greater benefit.

In relation to PI3K inhibition itself, a reasonable assumption is that tumours with constitutive PI3K activation are the ones that are most likely to respond to PI3K inhibitors. Loss of PTEN expression and phosphorylation of Akt have been used widely as markers of PI3K pathway activation. Studies in pre-clinical models of breast cancer have validated *PIK3CA* mutations and amplification of epidermal growth factor receptor 2 as biomarkers for sensitivity to GDC-0941.[173] More recently, the *PIK3CA* H1047R (exon 20) mutation has been described, in early phase studies in solid tumours, to be associated with greater sensitivity to PI3K/mTOR inhibition.[174] Predictive biomarkers similar to those

described in solid tumours have not been described in lymphomas but two recent studies in haematological malignancies highlight the importance of biomarkers of resistance. The first demonstrates the association of the t(11;14) with resistance to dual PI3K/mTOR inhibition in multiple myeloma[175] whereas the second reveals the importance of NOTCH-MYC activation as a mechanism of resistance to dual PI3K/mTOR inhibition in T-acute lymphoblastic leukaemia (T-ALL).[176]

In MCL, two separate studies have described a lack of activating mutations in exons 9 and 20 of *PIK3CA.*[22,144] Somatic mutations of *PIK3R1,* the gene encoding the p85 regulatory subunit provides another mechanism of constitutive PI3K activation and their occurrence is associated with activation of all three class Ia isoforms. These have not been studied in MCL. Hotspots for somatic mutations in *PIK3R1* have been described in exons 9, 10, 11, 13, 15 and 16.[121]

Based on the findings discussed in the previous chapter, we compared the effect of the p110δ-selective inhibitor GS-1101 with the predominantly p110α and p110δ selective inhibitor GDC-0941, on MCL cell proliferation and survival. In addition, the effect of the p110α inhibitor was studied in cell lines and primary samples. PTEN expression as well as phosphorylation of Akt was evaluated, gene expression of the class Ia isoforms was determined, samples were screened for *PIK3CA* and *PIK3R1* mutations and finally the sensitivity of primary samples was studied in relation to these parameters. We found that a high *PIK3CA*/*PIK3CD* ratio was predictive of resistance of primary MCL cells to GS-1101 and that this ratio was significantly higher at relapse compared to diagnosis. In addition, mining of public gene expression profiling data revealed a significantly higher expression of *PIK3CA* in MCL compared to indolent NHL and CLL. Finally, we did not find increased expression of p110α with relapse in a study of sequential biopsies from follicular lymphoma patients, providing further evidence that the p110α isoform may have particular significance in MCL.

4.2 MATERIALS AND METHODS

Cell lines and primary samples

Two MCL cell lines (Jeko-1 and Granta519) and 12 primary MCL samples were used for initial studies of growth inhibition and cytotoxicity. An additional 10 primary MCL samples were used for validation of predictive markers identified in the experimental cohort. Table 4.1 lists the clinical details of primary samples used in these experiments.

Cell proliferation and cytotoxicity assays

MCL cells were incubated with increasing concentrations (0.1, 1, 5 and 10μM) of PI3K inhibitors GS-1101, GDC-0941 or A66 and effects on growth and survival were measured at 72 hours. AnnexinV/PI and Guava ViaCount assays were used for cell lines while the ATP cytotoxicity assay was used for primary samples. The effect of GS-1101 and GDC-0941 on IL4 stimulated proliferation was measured by pre-treating cells with 20ng/ml IL4 before incubation for 72 hours with increasing concentrations of inhibitors.

Western blotting

Total protein for western blotting was extracted from cell lysates prepared at the indicated time-points. Expression of Akt (phosphorylated thr308/ser473 and total), ribosomal S6 (phosphorylated ser235/236 and total), PTEN and GAPDH were evaluated by western blotting. Densitometry was performed using GelScan Standard software v5.1 (BioSciTec, Frankfurt, Germany).

PIK3CA and *PIK3R1* mutation analysis

DNA was extracted from 20 primary MCL samples and 2 cell lines using the DNeasy mini kit (Qiagen). PCR, DNA purification and sequencing of exons 9 and 20 of *PIK3CA* and exons 9, 10, 11, 13, 15 and 16 of *PIK3R1* were performed as detailed in chapter 2.

Gene expression

Total RNA was extracted from primary samples using the Qiagen RNeasy mini kit (Qiagen). Real-time quantitative PCR was performed using TaqMan gene expression assays Hs00192399_m1, Hs00927728_m1, Hs00180679_m1 and Hs99999905_m1 (Applied Biosystems) to determine gene expression of *PIK3CA*, *PIK3CB*, *PIK3CD* and GAPDH respectively in primary MCL samples and healthy controls. The ΔΔCt method was used for relative quantification of gene expression. Ct (cycle threshold) values for the class Ia isoforms were corrected to the endogenous control gene GAPDH by calculating the difference in thresholds values (ΔCt). The differences in ΔCt values between MCL samples and the calibrator (healthy controls) were then linearised to obtain relative gene expression values. These steps can be summarised as follows-

$\Delta Ct = Ct_{ISOFORM} - Ct_{GAPDH}$

$\Delta\Delta Ct = \Delta Ct_{MCL} - \Delta Ct_{HEALTHY\ CONTROL}$

Relative gene expression (fold change) = $2^{-\Delta\Delta Ct}$

The *PIK3CA*/*PIK3CD* ratio was calculated by dividing the relative gene expression of *PIK3CA* with that of *PIK3CD*. This ratio always approximates 1 in the calibrator samples (healthy B-cells or tonsils) but does not reflect the true ratio in these samples.

PIK3CA/PIK3CD = $2^{-\Delta\Delta Ct}$ *PIK3CA* / $2^{-\Delta\Delta Ct}$ *PIK3CD*

Gene expression of class IA PI3K isoforms at diagnosis was compared between MCL and indolent NHL using publicly available affymetrix data (European Bioinformatics Institute www.ebi.ac.uk ref: E-GEOD-16455) with the web-based software O-miner. P values were adjusted for multiple testing using the Benjamini-Hochberg correction and values <0.05 were considered significant.

Immunohistochemistry

Sequential biopsies from 10 follicular lymphoma patients were studied using immunohistochemistry for p110α using methods identical to those used for MCL TMAs. Scoring of biopsies was done using the Ariol visual analysis software as previously described.

Table 4.1 Characteristics of primary MCL samples used in PI3K inhibition studies

Experimental cohort					
Sample	**Sex**	**Source**	**Nodal disease**	**Blastoid**	**Timing of sample**
M1	M	PBMCs	No	Yes	1st relapse
M2	M	PBMCs	Yes	No	Diagnosis
M3	M	PBMCs	Yes	Yes	Diagnosis
M5	F	PBMCs	Yes	Yes	Diagnosis
M7	M	PBMCs	Yes	No	Diagnosis
M8	M	PBMCs	Yes	No	Diagnosis
M9	M	PBMCs	Yes	No	Diagnosis
M11	M	PBMCs	No	No	Diagnosis
M12	M	Spleen	Yes	No	Diagnosis
M13	M	PBMCs	Yes	No	Diagnosis
M16	M	PBMCs	Yes	No	Diagnosis
M21	M	Spleen	Yes	No	Diagnosis
Validation cohort					
Sample	**Sex**	**Source**	**Nodal disease**	**Blastoid**	**Timing of sample**
M10	M	PBMCs	Yes	No	Diagnosis
M19	M	PBMCs	No	No	1st relapse
M23	M	PBMCs	Yes	No	Progression after Rx1
M24	M	PBMCs	Yes	No	Diagnosis
M25	M	PBMCs	Yes	No	Diagnosis
M26	M	BM	Yes	No	Diagnosis
M27	M	BM	Yes	No	Diagnosis
M28	M	PBMCs	Yes	No	Diagnosis
M29	M	Spleen	Yes	No	Diagnosis
M30	F	PBMCs	Yes	No	1st relapse

4.3 COMPARATIVE TOXICITY OF GS-1101 AND GDC-0941

4.3.1 Cell lines

Expression of the class Ia PI3K isoforms, PTEN and p-Akt (T308) by western blotting, in the 2 MCL cell lines Jeko-1 and Granta519 is shown in figure 4.1A. As mentioned previously, Jeko-1 had very low levels of basal Akt phosphorylation compared to Granta519. PTEN expression was intact in both cell lines and class Ia isoform expression was similar. Growth inhibition and cytotoxicity were determined in both cell lines using the Guava ViaCount and Annexin-V/PI assays respectively. GDC-0941 induced significant reduction in the viable cell number in Granta519 and Jeko-1 compared to both GS-1101 and the p110α selective inhibitor A66 (Figure 4.1 B). GDC-0941 also induced significant apoptosis in the Jeko-1 cell line, but only at concentrations >5μM, as demonstrated in figures 4.1C and D, while GS-1101 induced minimal apoptosis in both cell lines.

4.3.2 Primary samples

Western blotting was performed on 12 primary samples ('experimental cohort' in Table 4.1) to determine basal expression of p-Akt and PTEN. Samples were treated with increasing concentrations of GS-1101 and GDC-0941. Cytotoxicity was measured using the ATP assay at 72 hours. Variability was observed in the sensitivity of individual samples but overall the activity of GDC-0941 was significantly greater than that of GS-1101 starting at a concentration of 0.1μM (Figure 4.2A). Similar to observations in the two cell lines, PTEN expression and phosphorylation of Akt (Figure 4.2B) did not predict response to either inhibitor in primary samples. In addition, some primary samples were resistant to both GS-1101 and GDC-0941. The effect of these two drugs on individual primary samples is detailed later in this chapter.

Figure 4.1 Activity of GS-1101, A66 and GDC-0941 on MCL cell lines. (A) Western blot showing basal expression of p-Akt (thr308), PTEN and class Ia PI3K isoforms in Jeko-1 and Granta519. (B) Significantly greater growth inhibition seen using the Guava Viacount assay in both cell lines with GDC-0941 compared to both GS-1101 and A66. (C) The effect of both GS-1101 and GDC-0941 on apoptosis using flow cytometry with Annexin-V/PI staining is minimal although significant apoptosis is seen on treating Jeko-1 with ≥5μM GDC-0941. (D) Representative flow cytometry plots of AnnexinV/PI uptake in Granta519 and Jeko-1 cells treated with GDC-0941. Error bars represent standard deviation of three separate experiments.

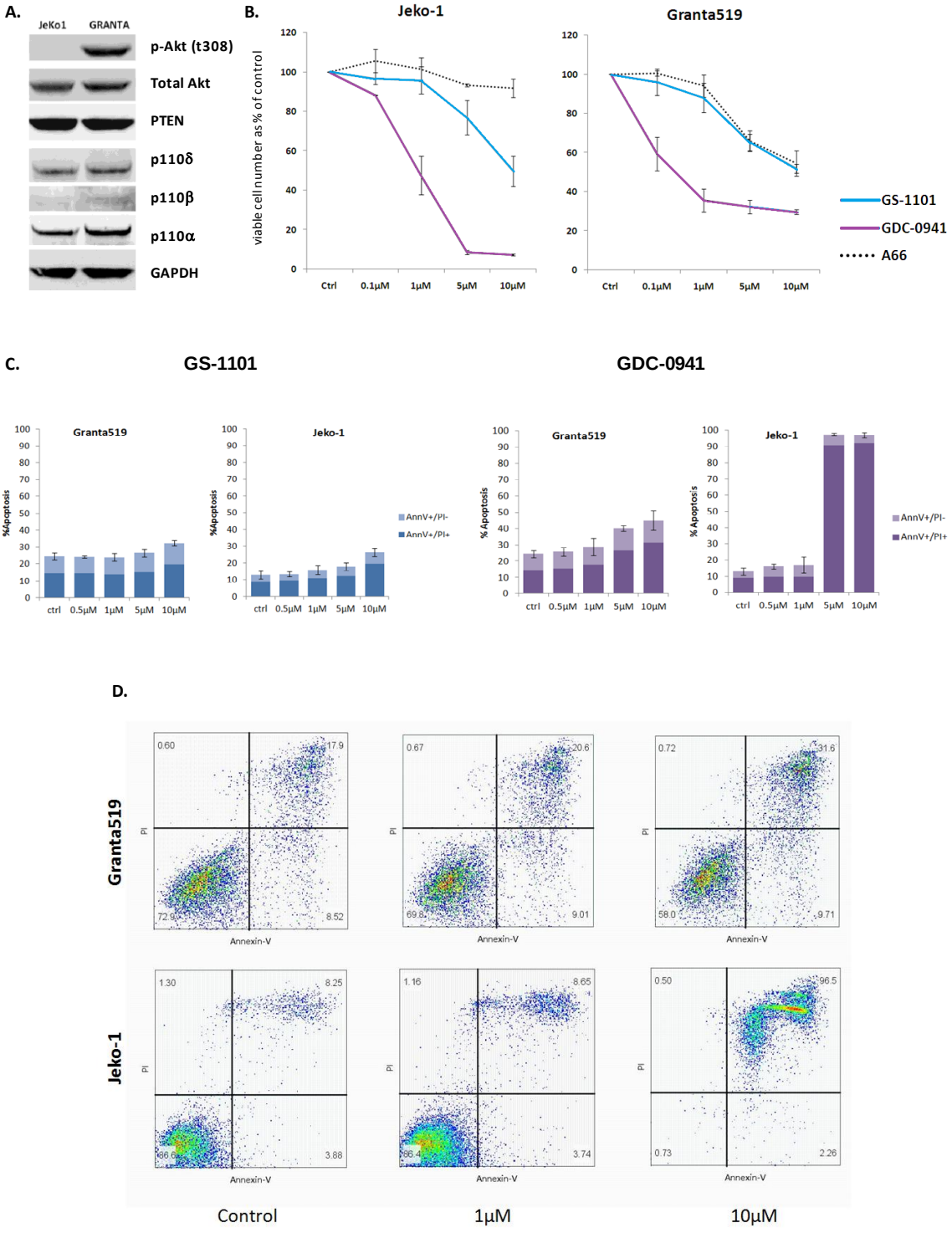

4.3.3 IL4 stimulated proliferation of MCL cells

The activity of GS-1101 and GDC-0941 was compared at 72 hours using the ATP cytotoxicity assay, in 3 primary MCL samples stimulated with IL4 (Figure 4.2C). Increase in ATP luminescence reflecting proliferation was seen in IL4 stimulated, untreated controls from all 3 samples. GDC-0941 appeared to be more cytotoxic than GS-1101 at all concentrations (means: 0.1μM=152.7 vs 132.7, 1μM=136.3 vs 106, 5μM=111 vs 89, 10μM=89.67 vs 71) in the presence of IL4 although these differences were not significant using an unpaired t-test. The difference in the degree of IL4 stimulated proliferation between untreated controls in the two groups was also not significant but mean proliferation was higher in the GS-1101 group (198.7 vs 175.7). This made it difficult to draw comparisons between the activity of the two inhibitors in the presence of IL4 but overall both appeared to counteract IL4 induced proliferation to a similar degree.

4.3.4 Healthy B-cells

The effect of GS-1101 and GDC-0941, at the concentrations used in MCL cells, was evaluated in B-cells isolated from healthy PBMCs. At 72 hours, GDC-0941 appeared to be more cytotoxic compared to GS-1101 but this was not statistically significant at any of the concentrations evaluated (Figure 4.2D).

4.4 BIOMARKERS PREDICTIVE OF RESISTANCE TO GS-1101

As would be expected, samples that were responsive to PI3K inhibition with GS-1101 showed similar sensitivity to treatment with GDC-0941. As sensitivity is relative and difficult to define, we elected to evaluate the parameters described below against their ability to predict resistance to GS-1101. Markers were evaluated in relation to the effect of the two drugs at 0.1 and 1μM, concentrations at which they are most likely to be faithful to their targets.

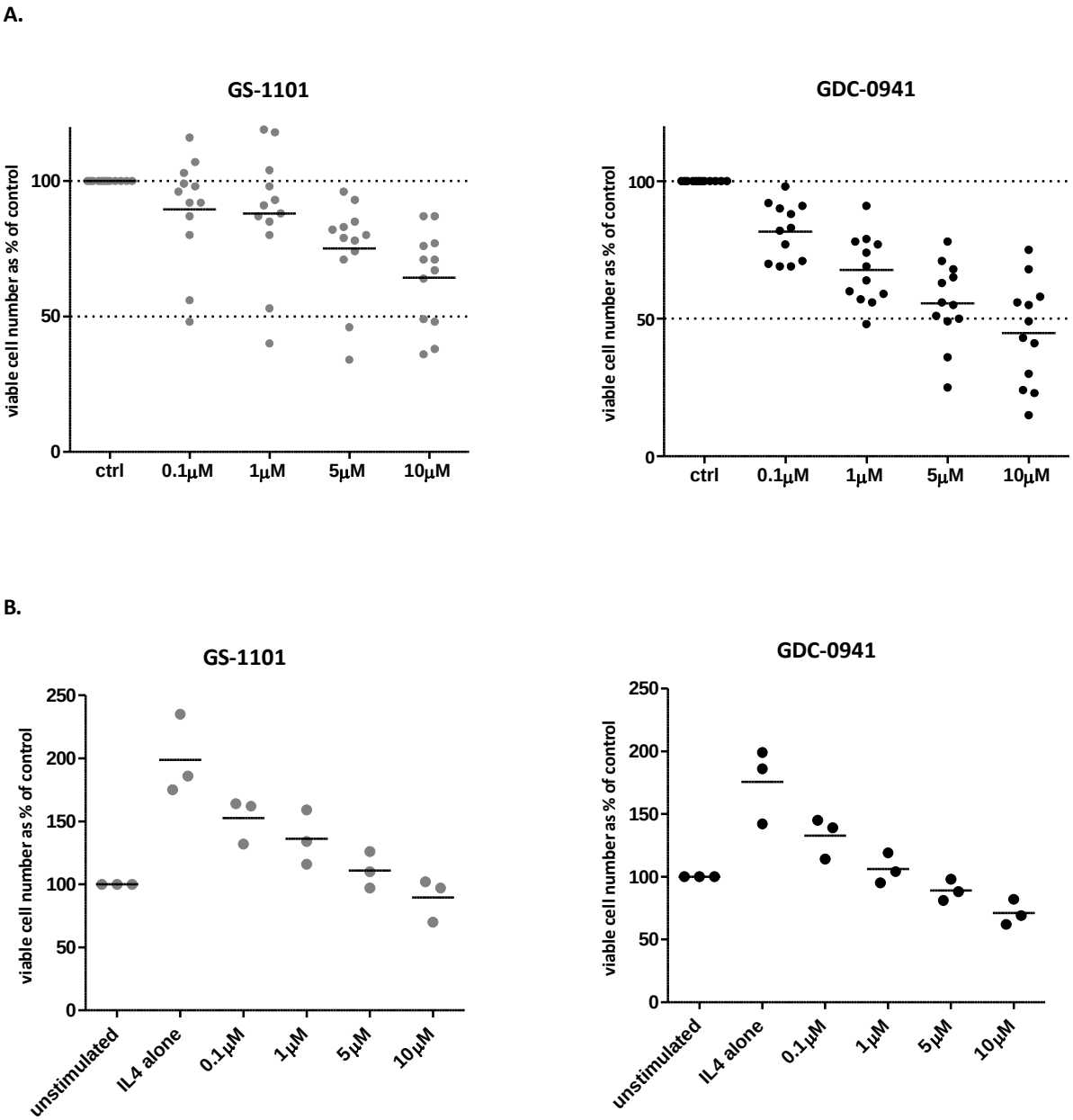

Figure 4.2 Activity of GS-1101 and GDC-0941 in primary MCL. (A) Dot plots showing greater cytotoxicity in the ATP assay with GDC-0941 compared to GS-1101 in 12 primary MCL samples with statistically significant toxicity at and above 0.1µM. Lines represent median viable cell number (B) Activity of GS-1101 and GDC-0941 on IL4 stimulated proliferation in 3 primary MCL samples. Lines represent mean viable cell number. (C) Activity of GS-1101 and GDC-0941 in healthy B-cell controls (n=3). Error bars represent standard deviation of 3 separate experiments.

4.4.1 PTEN and phosphorylation of downstream targets

Loss of PTEN expression did not predict sensitivity to either inhibitor. While samples M3 and M16 were minimally responsive to GS-1101 (figure 3.6), sample M16 was significantly more sensitive to GDC-0941. The two primary samples with the strongest basal phosphorylation of Akt (thr308) were M5 and M9. While both GS-1101 and GDC-0941 had minimal activity against M5, sample M9 appeared to be equally responsive to both drugs. Another primary sample M7 was equally responsive to both drugs but had weak phosphorylation of Akt. This is in keeping with the findings in the two cell lines where despite differences in basal phosphorylation of Akt both cell lines had similar responses to GS-1101 and GDC-0941.

Downstream phosphorylation of Akt and ribosomal S6 was evaluated in Jeko-1 and Granta519, as well as two primary samples (M8 and M9). In cell lines, downstream effects were evaluated at 2 hours and 24 hours, comparing effects of GS-1101 and GDC-0941 (Figure 4.4A). In Granta519, as described previously, PI3K inhibition with the p110α/δ inhibitor GDC-0941 resulted in more effective and sustained inhibition of Akt phosphorylation compared to p110δ selective inhibition with GS-1101. This was reflected in decreased downstream phosphorylation of p-S6. In the Jeko-1 cell line, basal phosphorylation of Akt was not detected and therefore could not be used to as a marker of PI3K inhibition. However, a decrease in phosphorylation of S6 was seen in a similar pattern to that seen with Granta519 and GDC-0941 treatment resulted in sustained inhibition of p-S6.

On evaluation with the ATP assay at 72 hours, primary sample M8 was relatively resistant to both GS-1101 and GDC-0941 while both inhibitors were found to induce significantly greater toxicity in primary sample M9. Interestingly, there was very little difference in the downstream effects of PI3K inhibition in both primary samples at the 2 hour time point and equal, near complete inhibition of Akt (thr308) and S6 phosphorylation was seen with both GS-1101 and GDC-0941. In sample M8, some residual phosphorylation of ribosomal S6 was observed in cells treated with GS-1101

compared to those treated with GDC-0941, but the cytotoxic effect of both drugs on M8 was minimal (Figure 4.4B). Due to limited cell numbers, western blots were not performed on primary samples at 24 hours.

Figure 4.3 Correlation of p-Akt (t308) and PTEN with response to GS-1101 and GDC-0941 in primary samples. (A) Western blot showing expression levels of p-Akt (t308) and PTEN in 12 primary samples. (B) Comparative activity of GS-1101 and GDC-0941 determined by the ATP assay. The X axis shows the viable cell number as a percentage of the untreated control. Error bars represent standard deviation of triplicates in the same experiment.

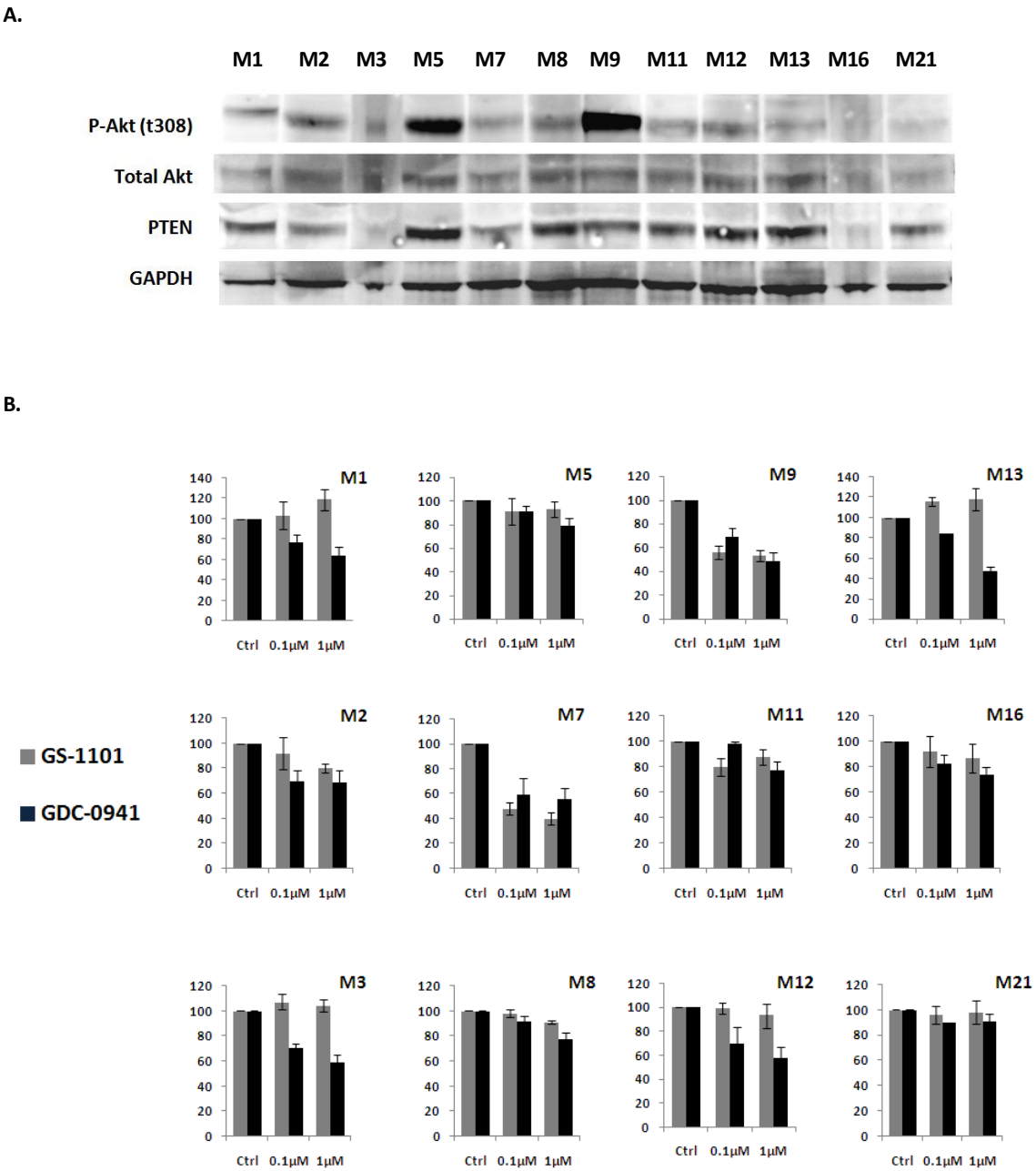

Figure 4.4 Comparative effects of GS-1101 and GDC-0941 on downstream targets of PI3K. (A) Western blots displaying downstream effects of GS-1101 and GDC-0941 in cell lines Granta519 and Jeko-1 at two time points 2 and 24 hours. The immunoblot for Granta519 is the same as shown in figure 3.4C. (B) Western blot displaying downstream effects of GS-1101 and GDC-0941 in 2 primary MCL samples at 2 hours. There is no marked difference between downstream effects even though sample M8 is resistant to both inhibitors while sample M9 is sensitive to both.

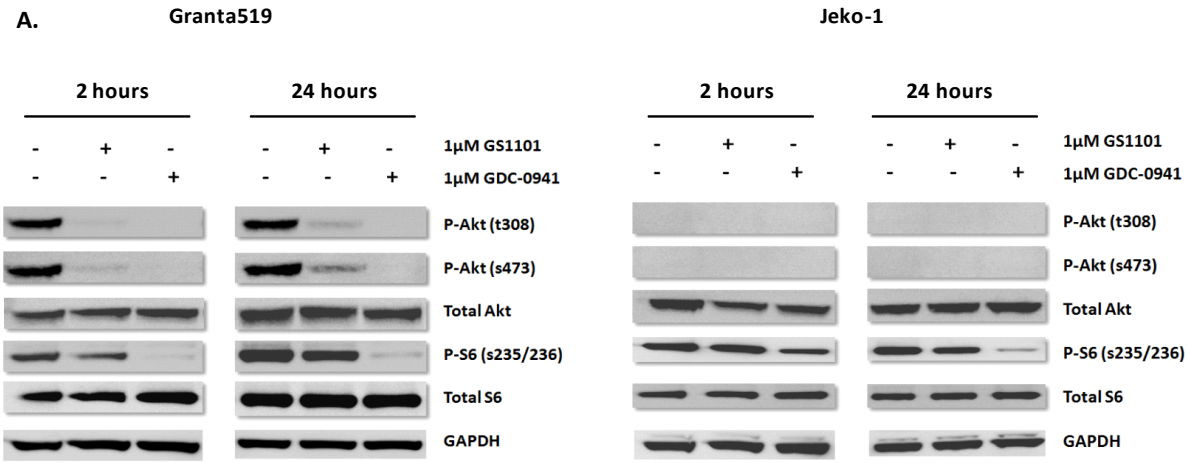

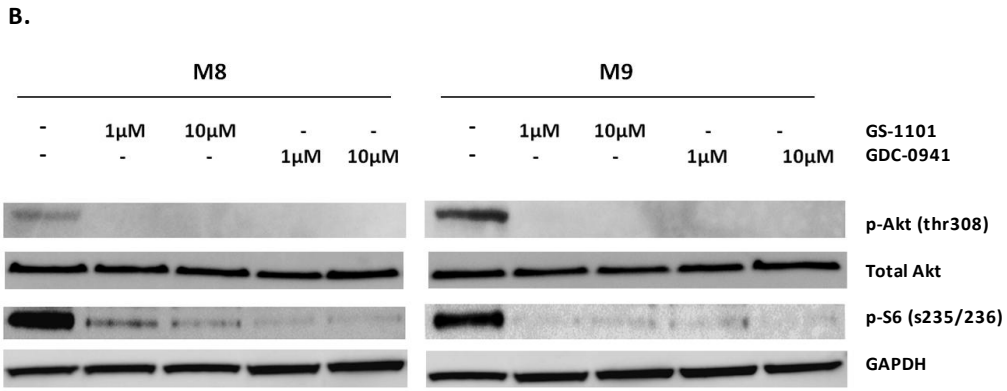

4.4.2 *PIK3CA* and *PIK3R1* mutations

DNA extracted from 2 MCL cell lines (Jeko-1 and Granta519) and 20 primary MCL samples was sequenced and screened for somatic mutations in the hotspot regions of *PIK3CA* (exons 9 and 20) and *PIK3R1* (exons 9, 10, 11, 13, 15 and 16). 12 of the 20 primary DNA samples screened were those in the experimental cohort while the remaining 8 DNA samples were obtained from diagnosis-relapse frozen biopsy pairs form 4 patients (clinical information for these samples can be found in figure 4.8). No mutations were detected suggesting that somatic mutations in class Ia PI3Ks leading to their constitutive activation are rare or absent in MCL.

4.4.3 Gene expression of class Ia isoforms and the *PIK3CA*/*PIK3CD* ratio

Relative gene expression of class Ia isoforms was determined by qRT-PCR on RNA extracted from 12 primary MCL samples (experimental cohort). In keeping with findings at the protein level, PIK3CD gene expression was the highest while PIK3CB gene expression was the weakest (Figure 4.5A). Compared to healthy B-cell controls, gene expression of isoforms *PIK3CA* and *PIK3CD* showed significant up-regulation ($p=0.0115$ for both using the Mann-Whitney test) in primary MCL samples.

When evaluated independently, relative gene expression ($2^{-\Delta\Delta Ct}$) of neither *PIK3CA* nor *PIK3CD* was able to predict resistance to GS-1101. In order to evaluate the importance of the relative contribution of these two isoforms, the ratio of their gene expression (*PIK3CA/PIK3CD)* was calculated. This ratio separated samples into two groups, one with ratios similar to that seen in healthy B-cell controls and another group with significantly higher expression (Figure 4.5B). *PIK3CA/PIK3CD* greater than twice the mean ratio in healthy B-cell controls identified a group of samples that were resistant to GS-1101 and showed a significantly greater response to GDC-0941 ($p=0.03$ at 0.1µM, $p=0.008$ at 1µM) (Figure 4.5B). The two samples that were most sensitive to GS-1101 reassuringly fell in the group with the lower ratios. These differences were seen at 0.1 and 1µM, concentrations at which these inhibitors are likely to be selective for their isoform targets.

Figure 4.5 Gene expression of class Ia isoforms and predictive value of the *PIK3CA/PIK3CD* ratio. (A) Gene expression of class Ia isoforms in healthy B-cells (grey bars) compared to expression in MCL (black bars). (B) A *PIK3CA/PIK3CD* ratio greater than twice that the mean ratio in healthy B-cells (dotted line) can identify primary samples that are resistant to GS-1101 but significantly more sensitive to GDC-0941. Bars represent median expression. The accompanying table displays the *PIK3CA/PIK3CD* values for each of the samples.

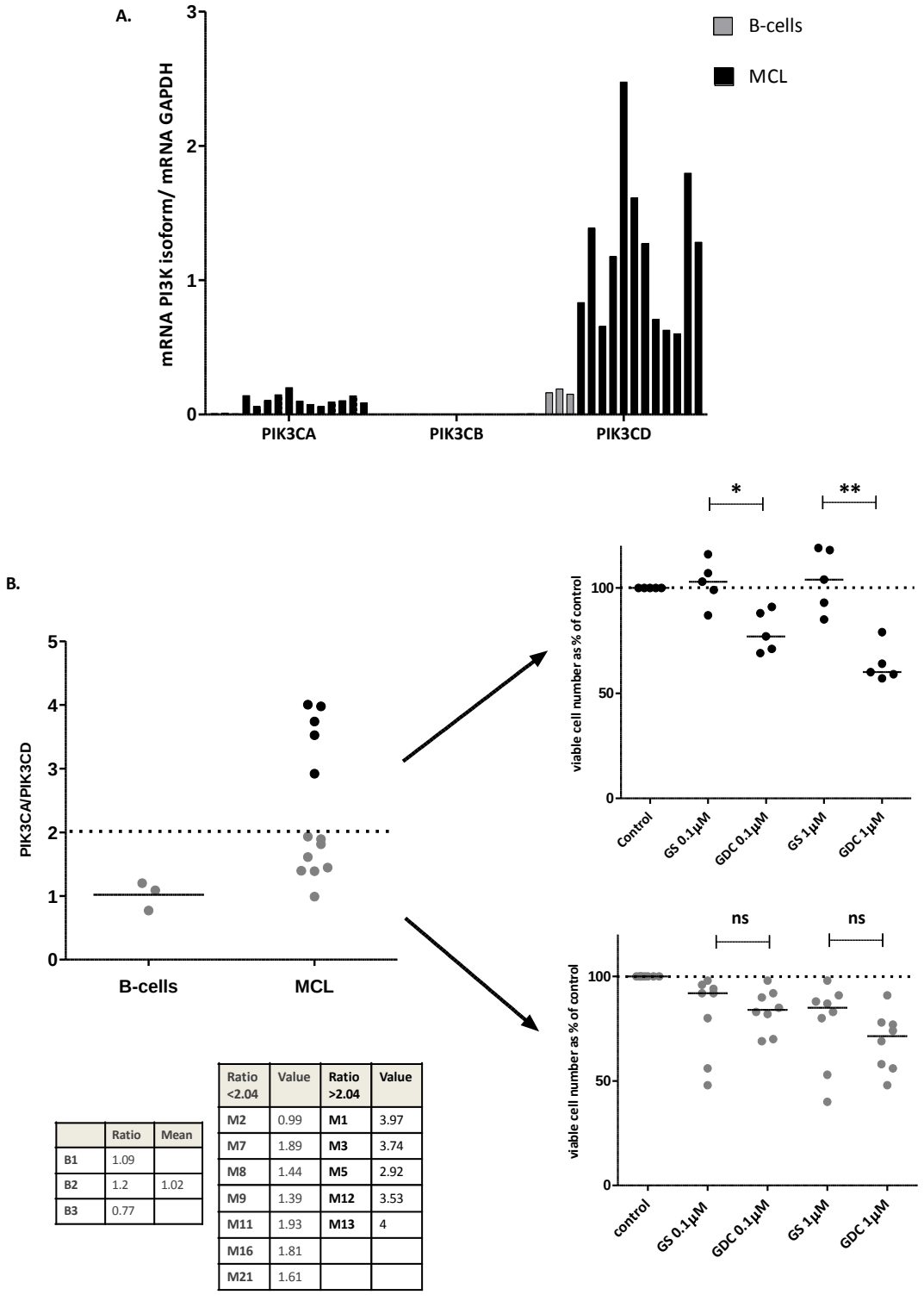

	Ratio	Mean
B1	1.09	
B2	1.2	1.02
B3	0.77	

Ratio <2.04	Value	Ratio >2.04	Value
M2	0.99	**M1**	3.97
M7	1.89	**M3**	3.74
M8	1.44	**M5**	2.92
M9	1.39	**M12**	3.53
M11	1.93	**M13**	4
M16	1.81		
M21	1.61		

An independent cohort of 10 primary MCL samples (Table 4.1) was used to validate these findings. RNA was extracted from these samples and qRT-PCR was performed together with RNA from three healthy B-cell controls. Relative gene expression of the class Ia isoforms was calculated and the *PIK3CA/PIK3CD* ratio was determined using the same methods as for the experimental cohort (Figure 4.6A).

Alongside the qRT-PCR studies, samples in the validation cohort were incubated with 1μM of GS-1101 or GDC-0941 and ATP luminescence was measured at 72 hours. Samples were also treated with 1μM A66 to determine the effect of p110α selective inhibition (Figure 4.6B). On plotting the ratios, the primary samples did not separate as distinctly as with the experimental cohort but on applying the cut-off (2 x mean ratio in healthy B-cells) once again samples above the cut-off were found to be resistant to GS-1101 but significantly more sensitive to GDC-0941 ($p=0.0079$). As with the experimental cohort, primary samples that were relatively sensitive to GS-1101 fell in the group of samples with low *PIK3CA/PIK3CD* ratios. P110α selective inhibition with A66 did not have a significant effect on any of the samples treated.

Figure 4.6 Validation of the *PIK3CA/PIK3CD* ratio as a predictor of resistance to GS-1101. (A) Validation of *PIK3CA*/PIK3CD ratio in an independent cohort of 10 MCL primary samples. Dot plot showing *PIK3CA*/PIK3CD ratios with a cut-off set at twice the ratio in healthy B-cell controls (dotted line). The accompanying table displays *PIK3CA/PIK3CD* values for each of the samples. Samples with a high ratio (black dots) are significantly more sensitive to GDC-0941 compared to GS-1101 while those with lower ratios have a similar sensitivity to both drugs. Lines represent median percentage viable cell number. (B) Bar graph comparing activity of GS-1101, GDC-0941 and A66 in the validation cohort. Error bars represent standard deviation of triplicate samples in the same experiment.

A.

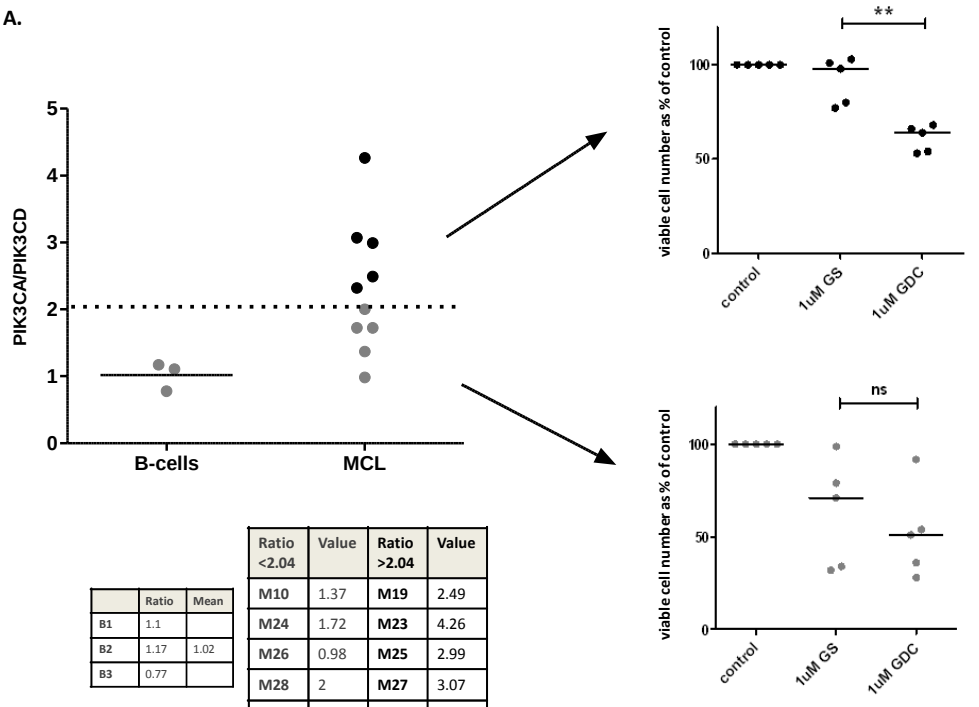

	Ratio	Mean
B1	1.1	
B2	1.17	1.02
B3	0.77	

Ratio <2.04	Value	Ratio >2.04	Value
M10	1.37	M19	2.49
M24	1.72	M23	4.26
M26	0.98	M25	2.99
M28	2	M27	3.07
M29	1.72	M30	2.32

B.

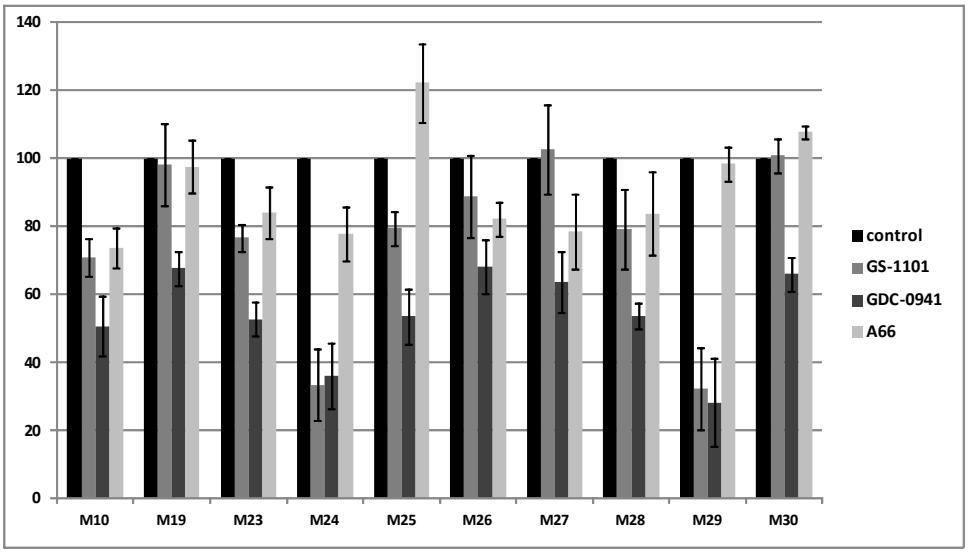

4.5 GENE EXPRESSION IN SEQUENTIAL MCL BIOPSIES

Quantitative RT-PCR was used to determine gene expression of class Ia isoforms in frozen sequential biopsies that were available in the tissue bank from four MCL patients. Complementary DNA derived from two tonsil controls was incorporated in the same run. Protein was extracted simultaneously to determine expression of isoforms by western blotting. These were the only frozen sequential MCL biopsies available and, unfortunately, were mutually exclusive from the sequential biopsies studied by IHC.

As would be expected, *PIK3CD* expression was the strongest in MCL samples but was also found to be up-regulated compared to expression in tonsil controls (Figure 4.7A). However, p110δ expression was comparable between tonsils and MCL samples by western blotting. Gene and protein expression of *PIK3CB* were the weakest among the three isoforms. Gene expression of *PIK3CA* was also weak but expression was significantly higher than tonsil controls (Figure 4.7B). This was reflected in protein expression of p110α on western blotting (Figure 4.7C).

Increase in p110α expression was seen with relapse in 2 out of 4 sequential biopsies by western blotting (Figure 4.7B). *PIK3CA* expression was also seen to increase in the same two biopsies with relapse (Figure 4.7C). Interestingly, on evaluating the ratio of *PIK3CA* to *PIK3CD*, we found that all 4 sequential biopsies showed a marked increase in the *PIK3CA*/*PIK3CD* ratio with relapse, relative to both diagnostic biopsies and tonsil controls (Figure 4.7D). Densitometry was performed on immunoblots of p110α and p110δ and corrected to densitometry of GAPDH (loading control). Although the ratios of p110α to p110δ showed wide variation, an increase with relapse was observed in all 4 cases, similar to that seen with gene expression (Figure 4.7E). Figure 4.8 indicates the timing of the biopsies in patients S1 to S4 in relation to disease course and treatment received.

A.

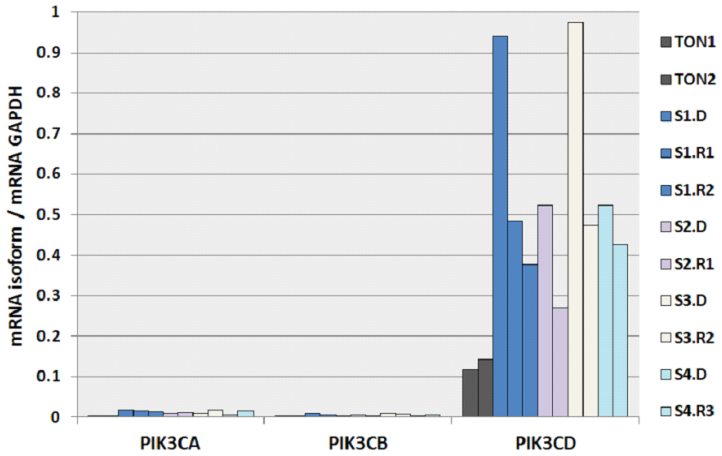

B.

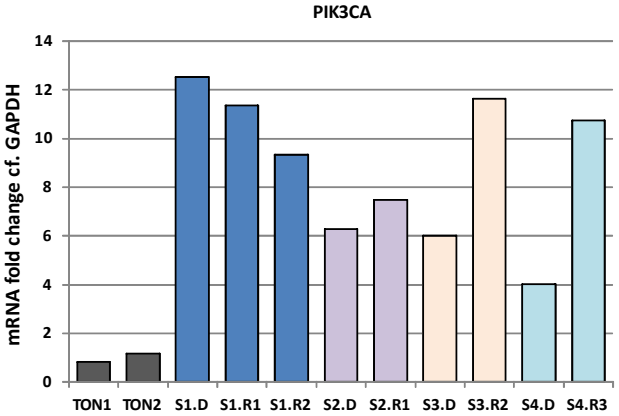

C.

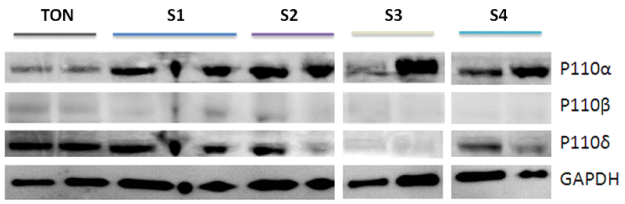

Figure 4.7 Gene expression and *PIK3CA*/*PIK3CD* ratio in sequential MCL biopsies (A) Gene expression of class Ia isoforms. Tonsil controls are in grey and sequential samples from the same patient share the same colour. Individual patients are represented as S1-S4 while the accompanying letter indicates timing of the biopsy for e.g. D indicates a biopsy at diagnosis, R1 at 1st relapse and so on. (B) Fold change in *PIK3CA* expression ($2^{-\Delta\Delta Ct}$) in MCL samples compared to tonsil controls. (C) Immunoblot of class Ia isoforms in tonsils and MCL. (D) Marked increase in *PIK3CA*/*PIK3CD* ratio in biopsies taken at relapse compared to diagnostic biopsies and tonsil controls. (E) Table displaying densitometry values for p110α and p110δ as well as the p110α/ p110δ ratio showing a similar trend.

D.

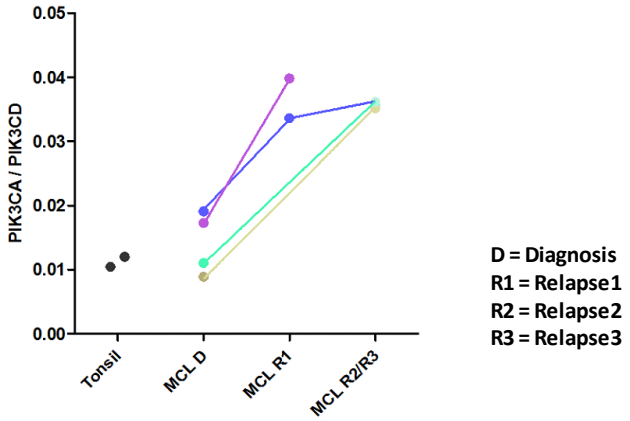

E.

	TON1	TON2	S1.D	S1.R1	S1.R2	S2.D	S2.R1	S3.D	S3.R2	S4.D	S4.R3
p110a	0.79	0.8	1.13	0.96	1.18	1.32	1.19	1.14	1.56	1.2	1.95
p110d	1.73	1.36	1.35	1.08	0.81	0.92	0.34	0.19	0.17	1.06	1.08
a/d	0.46	0.59	0.84	0.89	1.45	1.43	3.52	5.83	9.4	1.13	1.8

Figure 4.8 Graphical representation of the timing of biopsies in relation to disease course and treatment received in patients S1-S4.

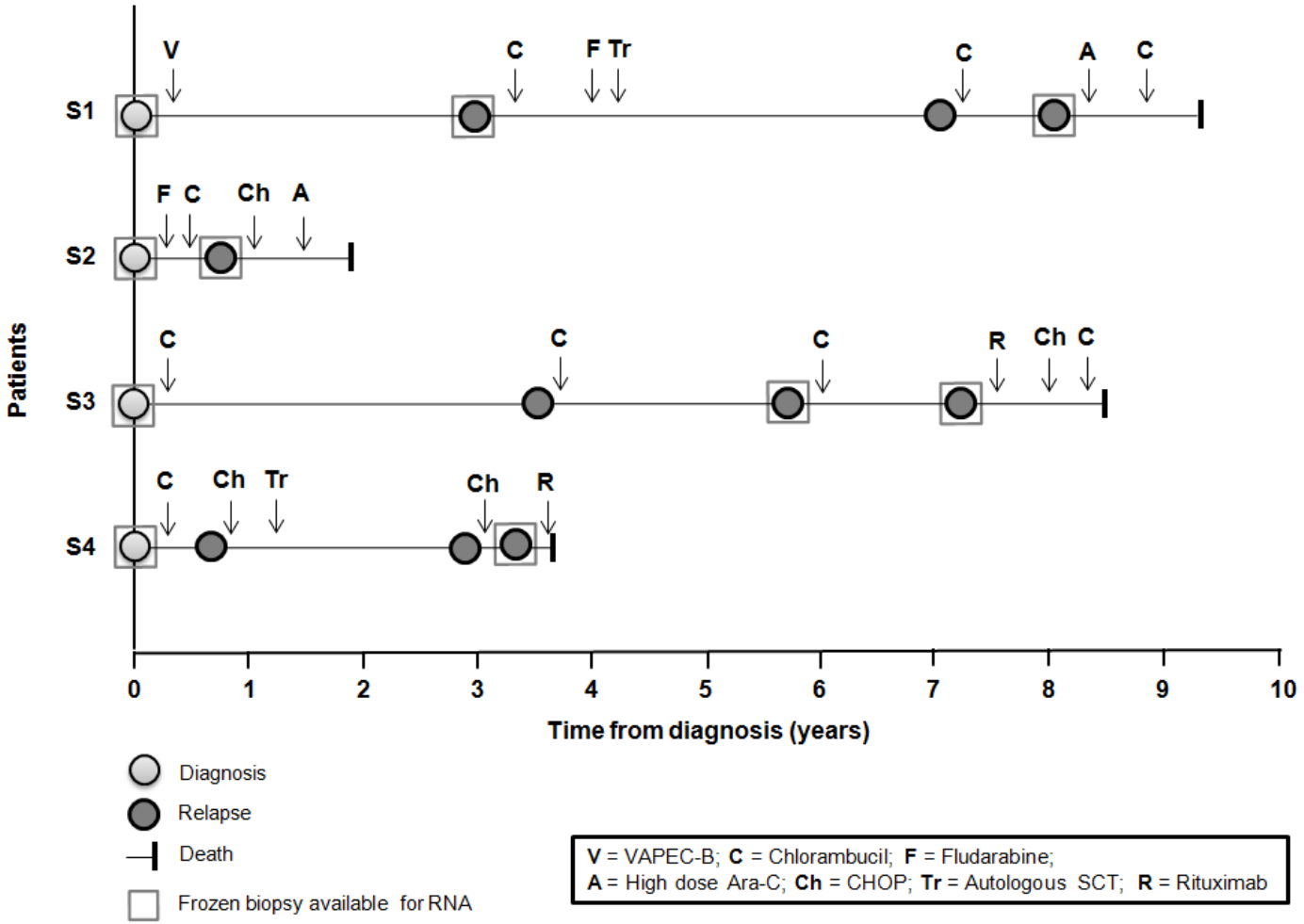

4.6 EXPRESSION OF CLASS IA ISOFORMS IN INDOLENT NHL

4.6.1 Data mining of public gene expression profiling data

In order to investigate whether differences existed in isoform expression between MCL and other NHL, we extracted PI3K class IA isoform expression from public gene expression profiling data (www.ebi.ac.uk) that was available from a study comparing diagnostic samples of MCL to indolent NHL (Figure 4.8A)[177] and analyse this data using the O-miner software.[178] Even in these samples, median expression of the *PIK3CA* isoform was significantly higher in MCL (n=15) compared to CLL (n=17), hairy cell leukaemia (n=5), splenic marginal zone lymphoma (n=4) and follicular lymphoma (n=7). This difference was not seen with *PIK3CB or PIK3CD* implying that the *PIK3CA/PIK3CD* ratio was higher in MCL than in CLL and indolent NHL. Benjamini-Hochberg multiple testing adjusted p values were as follows cMCL vs HCL=0.005, cMCL vs SMZL=0.0001 cMCL vs CLL=0.003 and cMCl vs FL= 0.05. There was no publicly available data comparing gene expression in relapsed lymphomas that we could analyze at the time of this study.

4.6.2 Follicular lymphoma sequential biopsies

Immunohistochemistry for p110α was performed in sequential biopsies from ten follicular lymphoma patients, four of whom had paired biopsies beyond first relapse. Sections were stained as for the MCL tissue microarray and were scanned and scored with the same protocols using the Ariol visual analysis software. There was no evidence of increase in p110α expression with relapse and in fact a decrease in expression was observed with progression in some sequential biopsies (Figure 4.8B, C).

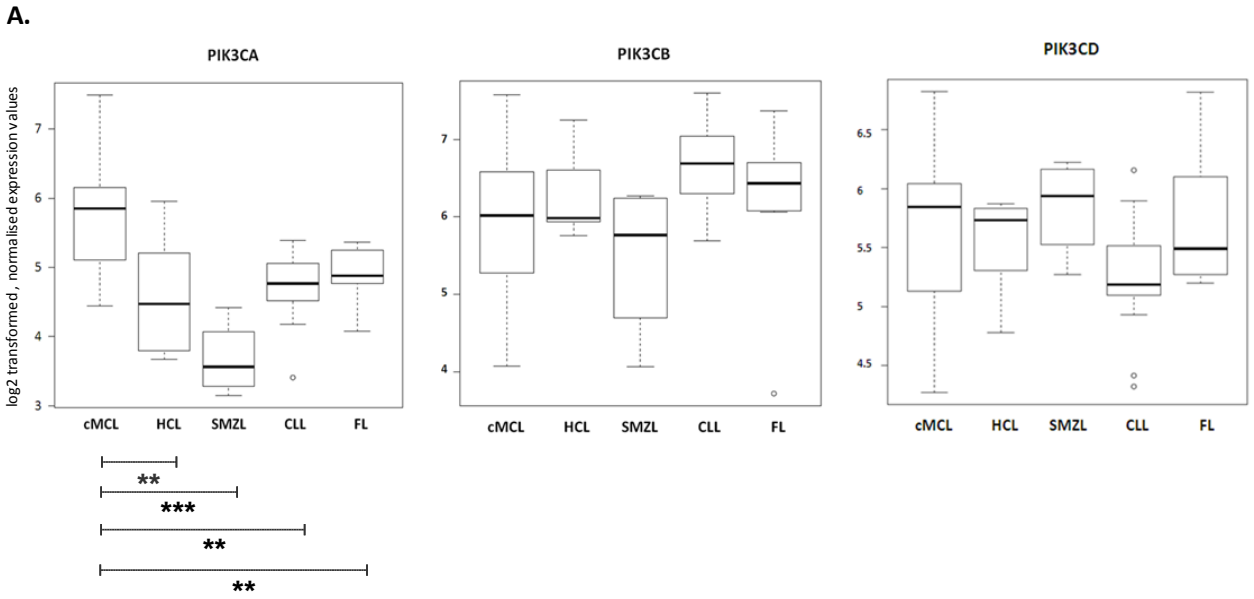

Figure 4.9 Gene expression of *PIK3CA* in MCL compared to indolent NHL and p110α expression in sequential biopsies of follicular lymphoma. (A) Gene expression of class IA PI3K isoforms at diagnosis in MCL was compared with indolent NHL. cMCL=conventional MCL, HCL=hairy cell leukemia, SMZL= splenic marginal zone lymphoma, CLL=chronic lymphocytic leukemia, FL=follicular lymphoma. (B) IHC images of 4 follicular lymphoma diagnosis-second relapse pairs showing no increase in p110α expression with relapse (original magnification x200). (C) Dot-plot comparing expression of p110α in sequential biopsies from follicular lymphoma patients (n=10). No evidence of increased p110α expression is seen with relapse. Pairs are connected by straight lines.

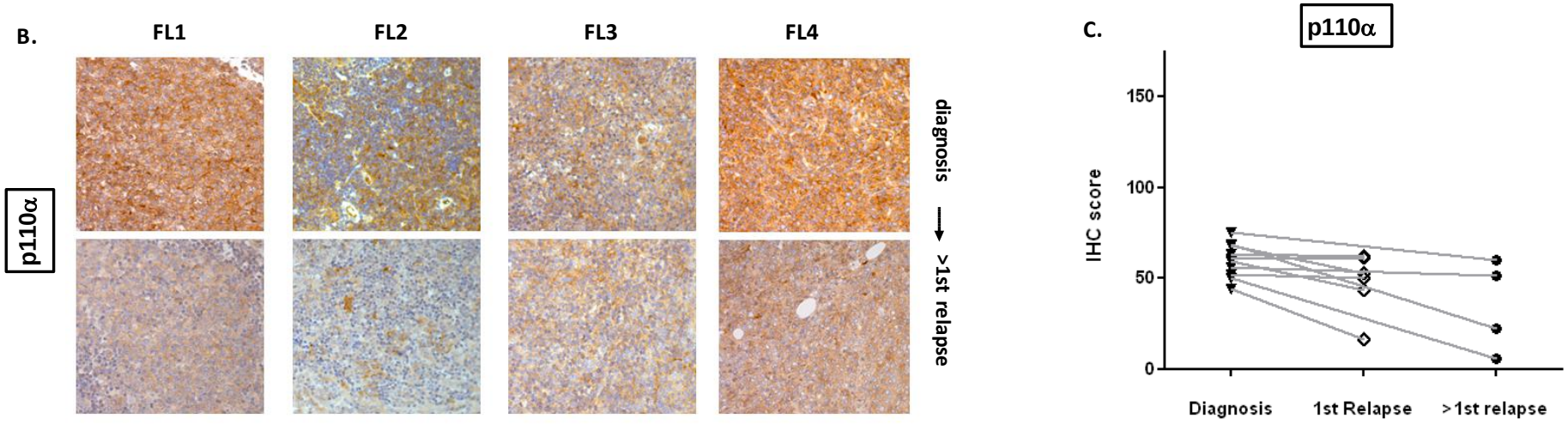

4.7 DISCUSSION

Dual inhibition of p110α and p110δ with GDC-0941 appears to result not only in more effective PI3K inhibition in MCL but also greater cytotoxicity towards MCL cells. These findings are unlikely to be influenced by p110γ, the only class IB catalytic unit isoform, as both GS-1101 and GDC-0941 have similar efficacy against p110γ. However, it is also important to note that some primary MCL samples showed similar sensitivity (or resistance) to GS-1101 and GDC-0941. In addition, these experiments show that GS-1101 was able to counteract IL4 induced proliferation in three primary MCL samples as effectively as GDC-0941. This finding highlights the importance of p110δ in IL4 stimulated proliferation of MCL cells and this may be similar to the importance of this isoform in BCR signalling. These findings appear to be consistent with the role of p110δ described in healthy B-cells.[140]

In both cell lines and primary samples, neither the degree of constitutive Akt phosphorylation nor PTEN status predicted resistance to GS-1101. Another interesting observation, although evaluated only in one primary sample, was that while effective inhibition of Akt appeared to be necessary, it did not necessarily predict cytotoxicity. This could be explained by activation of alternative pathways that may enable cells to survive despite PI3K inhibition. Activation of NOTCH signalling may be one such mechanism as shown in studies in T-ALL[176] and indeed NOTCH mutations are found in approximately 12% of MCL[27] suggesting an important role for this pathway.

It is reasonable to assume that inhibition of a greater number of target kinases is likely to result in greater toxicity with clinical use. In the experiments above, the difference in the *in vitro* toxicity of GDC-0941 and GS-1101 towards healthy B-cells is not statistically significant but appears to be slightly greater with GDC-0941. The important issue of course is the effect of p110α inhibition on non-haematopoietic tissues. Early phase trials with GDC-0941 have reported a favourable toxicity profile below a dose of 450mg QD in advanced solid tumour patients with activity seen starting at

100mg. Side effects were related to gastro-intestinal (GI) toxicity and a few grade 3-4 adverse events including fatigue, neutropenia and hyperglycemia were seen with higher doses (130mg and above).[154] On the other hand, hyperglycemia is not reported as a side-effect with GS-1101 although fatigue, GI side-effects and a reversible rise in ALT and AST have been reported.[153]

The *PIK3CA*/PIK3CD ratio appears to be a useful and reproducible marker in our *in vitro* studies. Primary samples with a high *PIK3CA*/PIK3CD ratio are resistant to inhibition with GS-1101 but also show significantly greater sensitivity to GDC-0941. A high ratio is therefore likely to identify tumors that can utilize p110α mediated constitutive PI3K signalling for survival and can maintain PI3K signalling despite p110δ inhibition. Interestingly, the PIK3CA/PIK3CD ratio was up-regulated with progression in all 4 sequential biopsies that were studied perhaps reflecting increased constitutive signalling through p110α with disease progression in MCL. The rise in *PIK3CA* with relapse, in conjunction with the proposed role of *PIK3CA* in mediating chemo-resistance[130] emphasize the potential benefit of targeting this isoform in MCL.

The MCL cell suspensions used in these studies were selected based on their viability and cell number rather than their source. The fact that the majority of primary samples used in these studies were derived from the peripheral blood of MCL patients at diagnosis Is a potential limitation as isolated leukaemic disease is considered a favourable prognostic factor in MCL and therefore these samples may represent a less aggressive cohort. However, it is also important to note that the majority of these patients had accompanying nodal disease (Table 4.1).

Another finding in these studies is that while Akt phosphorylation is a useful marker to study responses to PI3K inhibition the degree of phosphorylation does not predict sensitivity to PI3K inhibition and cells lacking constitutive Akt phosphorylation can still be responsive to PI3K inhibition. We find that constitutive Akt phosphorylation is not always seen in primary MCL exhibiting increased

PIK3CA/PIK3CD. This is not entirely surprising as Akt independent PI3K signalling has been found in cancers harboring *PIK3CA* mutations and similar mechanisms could operate in MCL exhibiting a high *PIK3CA*/*PIK3CD* ratio.

Finally, an important finding in relation to the background to these studies is the significantly higher gene expression of *PIK3CA* in MCL compared to CLL and other indolent NHL. This indirectly implies a higher *PIK3CA*/PIK3CD ratio in MCL as PIK3CB and PIK3CD expression are not significantly different in MCL compared to CLL and indolent NHL. Although it would be interesting to further explore the *PIK3CA*/PIK3CD ratio and sensitivity to isoform selective inhibitors in other indolent NHL, these studies would not have been possible to complete within the time frame for this research. However, in support of the theory that this phenomenon may be peculiar to MCL, we did not find an increase in p110α with relapse using immunohistochemistry on 10 sequential follicular lymphoma biopsies.

In summary, *PIK3CA* may be of particular significance in MCL, a disease characterized by frequent relapse and chemo-resistance. These studies highlight the potential benefit of dual p110α/δ inhibition, particularly in MCL exhibiting a high *PIK3CA*/PIK3CD ratio, but require confirmation *in vivo.* While *PIK3CA* may or may not be important in other lymphomas, these findings along with the discrepant results of early phase studies in relapsed/refractory MCL, compared to other NHL, suggest that dual inhibition of p110α and p110δ should be explored as a therapeutic option in MCL.

CHAPTER 5: ESTABLISHING A DISSEMINATED XENOGRAFT MODEL OF HUMAN PRIMARY MANTLE CELL LYMPHOMA IN NSG MICE

5.1 INTRODUCTION

The initial intention of carrying out xenograft studies as part of this research was to establish a model to validate our findings *in vivo*. As the Haemato-Oncology department had well established links with the Haematopoietic stem cell laboratory (London Research Institute, Cancer Research UK, Lincoln's Inn Fields) led by Dr Dominique Bonnet, a collaboration was set up to use their experience with NSG mice to establish a disseminated MCL mouse model. Subcutaneous or disseminated models of MCL cell lines in immunodeficient mice (SCID, NOD-SCID and NSG) are relatively easy to establish and have been widely employed for in vivo studies. However, these models have their limitations which include problems inherent to cell lines such as genetic instability and contamination, rapid progression of disease in mice and the difficulty in interpreting interactions with the microenvironment. The relatively large collection of MCL cell suspensions available in the tissue bank at Barts Cancer Institute led us to shift our focus to the possibility of establishing a NSG model of human primary MCL. The only primary human MCL mouse model described in the literature was established by injection of CD19 selected primary MCL cells into human embryonic bone grafts that were implanted subcutaneously in SCID mice (SCID-Hu). As SCID mice without subcutaneous human embryonic bone grafts did not show engraftment, the study concluded that a human bone marrow microenvironment was necessary for establishing MCL in SCID mice. However, access to the NSG model which allows engraftment of a wider range of primary human haematopoietic cells and the recent report of an NSG model of human primary CLL provided encouragement for our hypothesis.[179] The SCID-Hu model requires access to human embryonic bone grafts and therefore a primary human MCL xenograft NSG model, if viable, can provide a more easily reproducible model for both pre-clinical drug testing and *in vivo* studies of MCL biology.

Prior to undertaking studies with primary cells, we injected two concentrations of the Jeko-1 cell line into NSG mice to study the kinetics and homing of these cells with bioluminescent imaging. This was done in order to guide follow up of mice injected with primary cells.

5.2 MATERIALS AND METHODS

All animal experiments were performed in line with home office as well as CRUK guidelines, and under the home office license held by Dr Dominique Bonnet's Haematopoietic stem cell laboratory at the CRUK laboratories, Lincoln's Inn Fields. As mentioned in chapter 2, luciferase transduction of Jeko-1 cells, tail vein injection of cells into mice, bioluminescent imaging and flow cytometry on mouse derived cells were performed by Linda Ariza-McNaughton at the Haematopoeitic stem cell laboratory, CRUK at Lincoln's Inn Fields while characterisation/preparation of primary samples, immunohistochemistry on mouse derived tissue and processing of mouse spleens was done by me with assistance from Andrew Clear, Debra Lillington and Amy Roe at Barts Cancer Institute.

5.2.1 Luciferase transduction of the Jeko-1 cell line

The firefly luciferase gene encodes a 61KDa luciferase enzyme that converts D-lucifern to oxyluciferin in the presence of ATP, releasing light in the process. Quantification of this luminescence can be used as a reflection of cell number (as in the ATP cytotoxicity assay) or tumour burden in mice through bioluminescent imaging. As previously mentioned, the identity of the Jeko-1 cell line was confirmed by STR typing. Jeko-1 cells were transduced with a lentiviral vector expressing a double fusion reporter gene – green fluorescent protein (GFP) and firefly luciferase. This was followed by flow assisted sorting of GFP positive cells and injection of either $5x10^5$ or $2x10^6$ cells (in 200µlPBS + 2%FCS) by tail-vein into pre-irradiated NSG mice. Kinetics, disease burden and distribution were assessed by non-invasive bioluminescence imaging (BLI) following injection of D-luciferin.

5.2.2 Bioluminescent imaging

In vivo optical imaging was performed at 7, 14, 21 and 28 days using IVIS Spectrum bioluminescence-fluorescence optical imaging system (Caliper Life Science, Runcorn, UK). Before imaging, 125 mg/kg D-luciferin (Caliper Life Science) was administered intra-peritoneally to each mouse. Isoflurane (3%) was used to induce general anaesthesia and mice were placed in a light-tight heated chamber. After acquiring bright-field images of each mouse, anterior and posterior luminescent images were then successively acquired with 1- to 5-min exposure time. Optical images were displayed and analyzed with the IVIS Living Image software (Caliper Life Science). Regions of interest (ROI) were drawn manually around the bodies of the mice to assess the emitted signal intensity and sum of the anterior and posterior measurements were used as the total bioluminescence signal for each mouse.

5.2.3 Characterisation and preparation of primary samples

The Haemato-Oncology tissue bank at Barts Cancer Institute has a well established collection of MCL single cell suspensions, collected following informed consent from patients at diagnosis and/or relapse, which are linked to a clinical information database. At present, there are over 100 MCL patient samples in cell suspensions prepared from peripheral blood, lymph nodes, spleen and bone marrow that are cryopreserved in liquid nitrogen and can be accessed through a sample requisition process. The three samples that were used in our experiments (Table 5.1)were selected as each had over 50 cryopreserved vials available per patient episode containing approximately 5-10x10^7 cells per vial with good viability (>80%) on thawing. These were chosen to ensure we could test our hypothesis with sufficient replicates.

Following thawing, samples were characterised by flow cytometry for CD5/CD20 positive tumour cells and T-cell content (as described in chapter 2). Samples were also confirmed to have the *IGH: CCND1* translocation by FISH. A total of 4 x 10^7 T-cell depleted cells (10^7 per mouse) were re-

suspended in 800µl sterile PBS containing 2% FCS and transported on ice to the animal facility at Lincoln's Inn Fields for tail-vein injection into pre-irradiated NSG mice.

Table 5.1 Details of primary MCL samples injected into NSG mice

	Source	Timing	Morphology	t(11;14)	Viability
Primary1	PBMCs	1st relapse	Blastoid	Yes	96.5%
Primary2	PBMCs	Diagnosis	Blastoid	Yes	96.7%
Primary3	Lymph node cell suspension	2nd relapse	Classical	Yes	88.1%

T-cell depletion: T-cell depletion was performed using magnetic depletion with CD3 micro beads (Miltenyi Biotec) to obtain an untouched T-cell depleted population. Briefly, a cell count was performed before centrifuging cells at 400xg for 10 minutes and re-suspending them in 80µl of MACS buffer per 10^7 cells. 20µl of CD3 beads were then added for every 10^7 cells and the suspension was mixed well before incubation on ice for 15 minutes. Following this cells were washed with 1-2ml of MACS buffer per 10^7 cells and up to 10^8 cells were re-suspended in 500µl MACS buffer. LD columns (Miltenyi Biotec) were prepared in the magnetic field of a MACS separator (Miltenyi Biotec) by rinsing with 2ml of buffer. Cell suspensions were applied to the columns and columns were washed through with 2 x 1ml MACS buffer. The effluent containing the CD3 depleted fraction was collected and cell counts were performed. CD3 depletion was confirmed by flow cytometry. 4 x 10^7 T-cell depleted cells were re-suspended in 800µl of PBS + 2%FCS for injection into mice.

Fluorescent in situ hybridisation (FISH): FISH for the *IGH: CCNDI* translocation was performed at the cytogenetics laboratory at Barts Health NHS Trust. 5-10 x10^7 MCL cells were thawed and re-suspended in cytogenetics medium for interphase FISH analysis using the Vysis LSI *IGH/CCND1* XT Dual Color, Dual Fusion Translocation Probe (Abbott Laboratories, Abbott Park, Illinois, USA).

5.2.4 Preparation and injection of NSG mice

Eight to twelve week old NSG mice were γ-irradiated (3.75 Gy) within 24 hours of tail vein injection with T-cell depleted PBMCs. The recently described NSG models of human CLL were established by injecting 5-10x10^7 cells per mouse. We injected 10^7 cells per mouse (4 mice in each group) with a view to increasing cell numbers if we failed to see engraftment.

5.2.5 Monitoring of mice

Flow cytometry: Fluorochrome conjugated antibodies anti-human CD45-PerCP, anti-human CD33-APC, anti-human CD20-PE and anti-human CD5-PECy7 were purchased from BD biosciences while anti-mouse CD45-FITC was purchased from e-Bioscience (San Diego, CA, USA). Mice were bled at 3-4 weeks and then again at 10-12 weeks after injection of cells. Flow cytometric analysis was performed using DAPI staining for live/dead discrimination. Cells were then evaluated for mouse CD45 (mCD45) and human CD45 (hCD45) after which hCD45 gated cells were evaluated for hCD3, hCD5 and hCD20 positivity. Cells flushed out from bone marrow of mice at sacrifice were evaluated in the same manner. Analysis was performed on FlowJo software version 8.8.7 (TreeStar Inc, Ashland, OR, USA).

Immunohistochemistry: Mice were sacrificed at 20 weeks and dissection was carried out to look for evidence of gross organ involvement. Spleen, liver, bone marrow, ileo-caecal junction and any other organs that appeared affected were harvested and fixed in formalin. In addition, portions from the harvested spleens were placed in ice-cold PBS + 2% FCS for preparing cell suspensions. Home office criteria were used to judge if mice need to be sacrificed at any point before this. FFPE mouse tissue was stained for human CD3, CD20, cyclin D1 and Ki-67 (Table 5.2). For primary antibodies generated in mice (CD20 and Ki-67), a mouse-on-mouse blocking step for an hour, with a M.O.M Mouse Ig Blocking Reagent (Vectastain, Burlingame, CA, USA), was introduced prior to primary antibody application to prevent binding of secondary anti-mouse immunoglobulin antibody to mouse tissue.

Fluorescent in situ hybridisation for IGH: CCND1: Single cell suspensions were prepared from mouse spleens that showed MCL infiltration. Spleens were harvested and placed in 10ml ice-cold PBS+2% FCS. A 70µm filter (BD biosciences) was placed over a 50 ml falcon tube and spleens were mashed on the filter using the end of a plunger from a 1ml syringe. The filter was rinsed through with PBS+2%FCS. The effluent was washed once and incubated with 5ml of RBC Lysis Buffer (e-Bioscience, San Diego, CA, USA) on a roller at room temperature for 5 minutes after which the reaction was quenched with 20mls of PBS. After another wash, cell counts were performed and approximately 10^7 cells were transported to the cytogenetics laboratory at the Royal London Hospital for FISH analysis as previously detailed.

Table 5.2 Details of primary antibodies and IHC conditions used for staining of tissue harvested from NSG mice at sacrifice

Primary antibody	Supplier	Species (clone)	Antigen retrieval	Concentration	Incubation
CD3	Labvision	Rabbit monoclonal (SP7)	Citrate pH6	1:500	40”
CD20	Dako	Mouse monoclonal (L26)	Citrate pH6	1:2000	40”
Cyclin D1	Labvision	Rabbit monoclonal (SP4)	Citrate pH6	1:50	40”
Ki-67	Dako	Mouse monoclonal (MIB1)	Citrate pH6	1:1000	40”

Figure 5.1 Plan of investigation for establishing a NSG model of human primary MCL

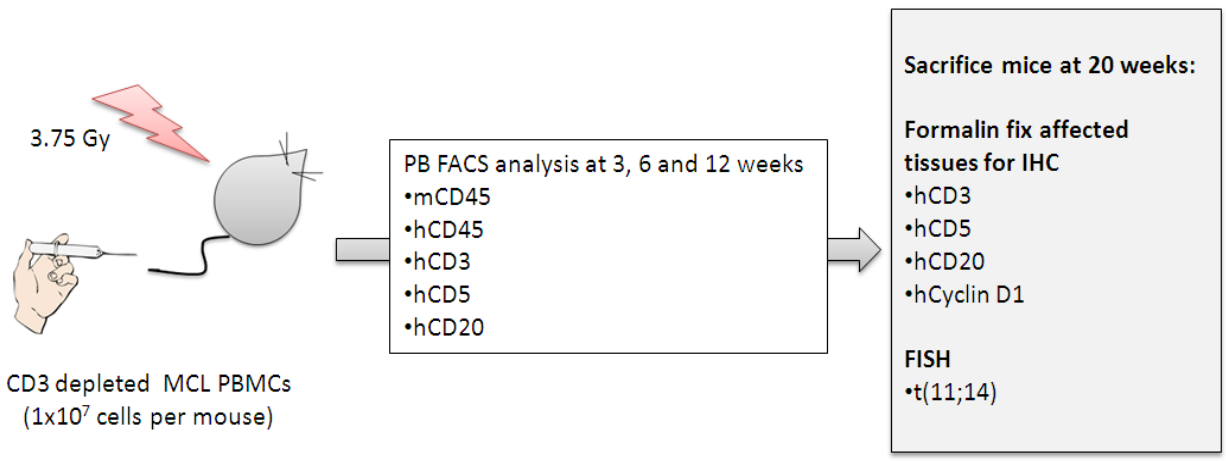

5.3 DISSEMINATED XENOGRAFT MODEL OF JEKO-1 IN NSG MICE

Luciferase-transduced Jeko-1 cells were injected at 2 concentrations (0.5×10^6 and 2×10^6) into a total of 6 mice. Mice were identified by ear marks (1, 2 or 3) on the left (L) or right (R) ears. For these experiments mice injected with 0.5×10^6 Jeko-1 cells were 1R, 2R and 3R while mice injected with 2×10^6 cells were 1L1R, 2L and 3L. By day 29, all mice were ill with marked weight loss and had to be sacrificed. Some hind leg weakness was noted in mice, particularly in those injected with the higher concentration of Jeko-1 cells. Until day 21, mice injected with the lower concentration (0.5×10^6) of Jeko-1 cells appeared to have a similar rate of dissemination as mice injected with 2×10^6 cells by BLI. *In vivo* imaging on day 29 showed markedly greater luminescence in mice injected with 2×10^6 cells. Bioluminescence was observed primarily in the bone marrow, spleen and spinal regions of all mice. Representative anterior and posterior luminescence images of mice injected with 2×10^6 cells on day 7 are displayed in figure 5.2. D-luciferin diffuses across the blood-brain barrier and enhancement of the spinal cord and brain indicates CNS infiltration of Jeko-1 cells which may account for hind leg weakness in the mice. Total bioluminescence (average of 3 replicates), reflecting the kinetics and disease burden with injection of the two concentrations of Jeko-1 cells are plotted in the graphs accompanying figure 5.3.

Figure 5.2 Images of bioluminescence in NSG mice on day 7 after injection of Jeko-1 cells. (A) Posterior images showing luminescence the pelvis, femurs, spine, cranial and splenic regions of mice. (B) Anterior images showing luminescence in the femoral and sternal regions. The regions of interest (ROI) for bioluminescent readings are marked in red.

A.

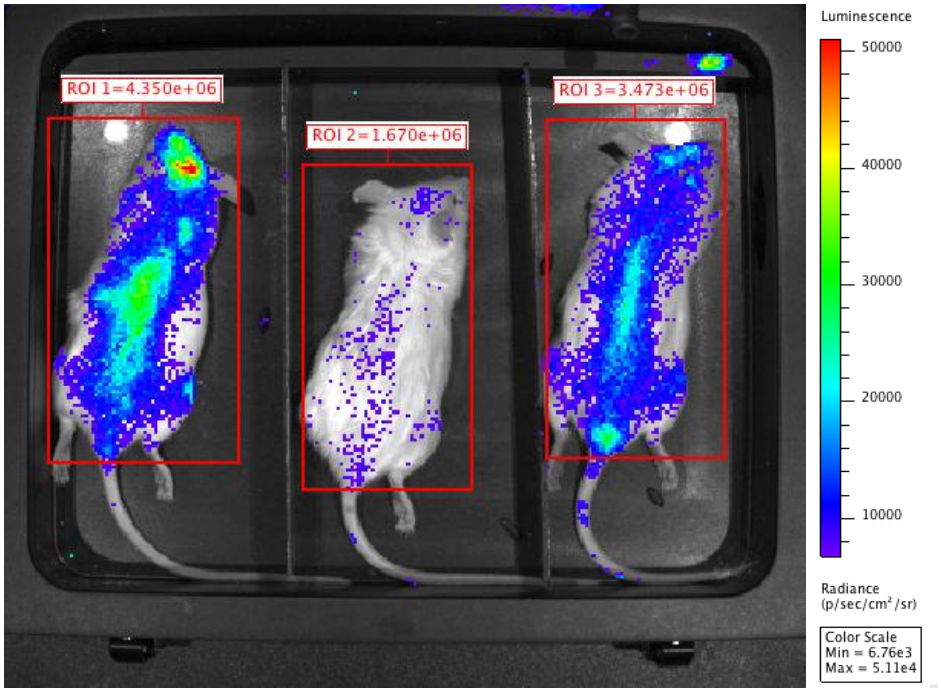

B.

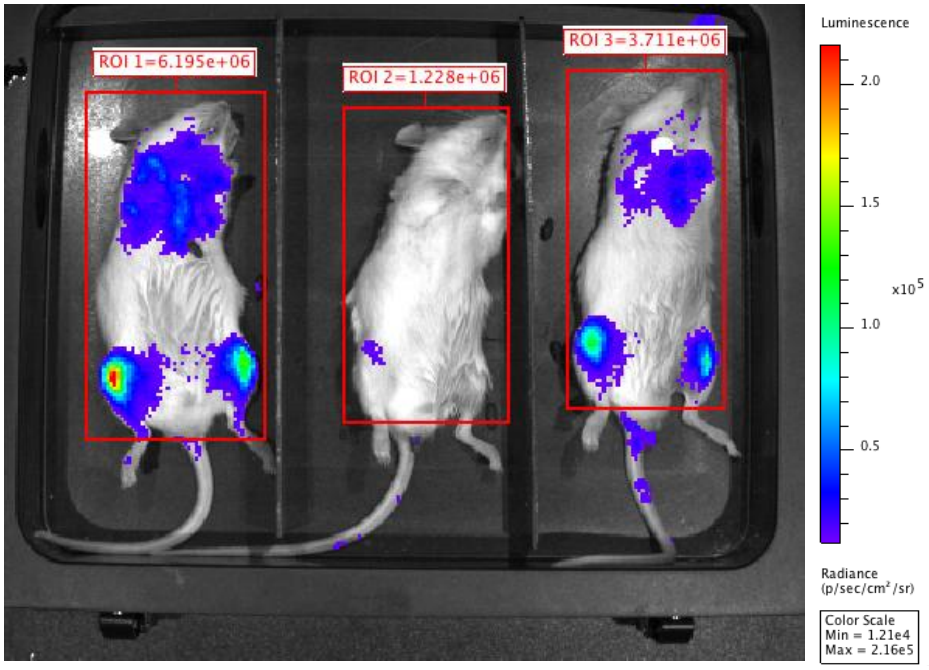

Figure 5.3 Growth kinetics of Jeko-1 cells in NSG mice estimated by *in vivo* bioluminescent imaging. (A) Graph showing progressive increase in bioluminescence over 4 weeks from 3 mice (3R, 2R and 1R) injected with 0.5 x 10^6 cells. (B) Graph of bioluminescence from 3 mice (3L, 2L, 1L1R) injected with 2x 10^6 cells. (C) A comparison of average bioluminescence in the 2 groups of mice showing a rapid increase after 21 days in mice injected with a higher concentration of Jeko-1 cells.

A.

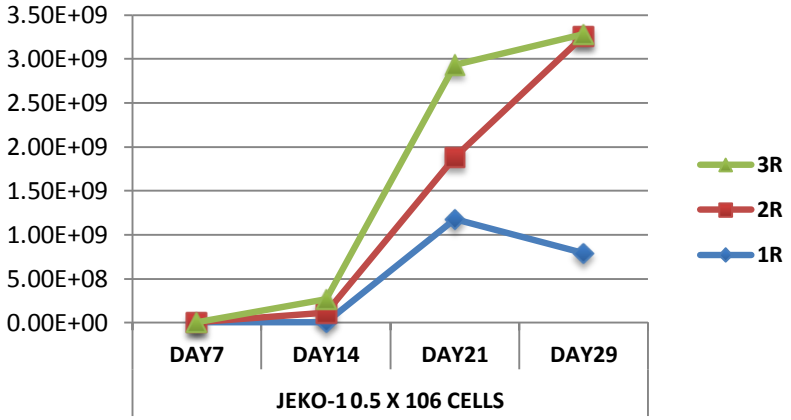

B.

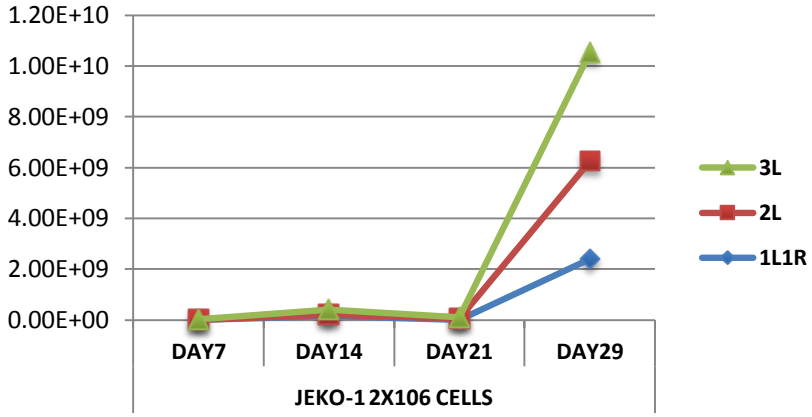

C.

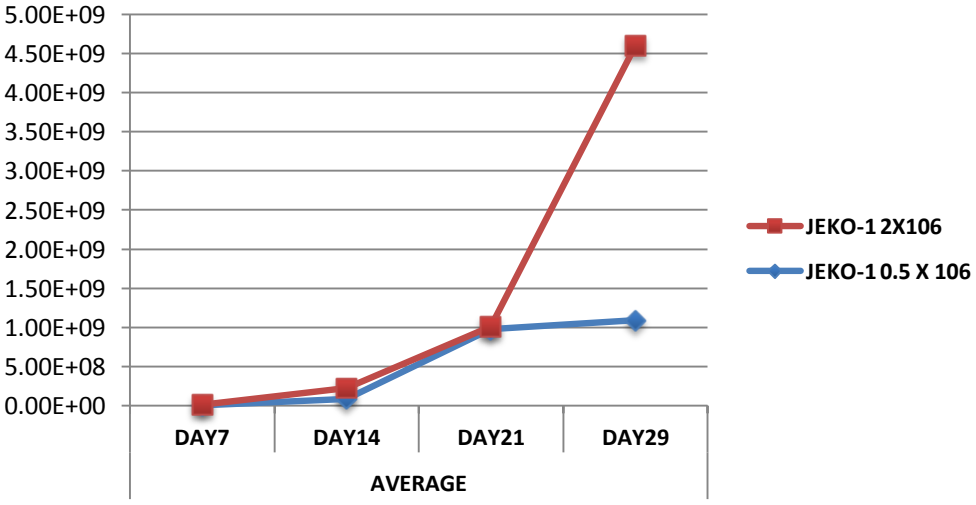

5.4 DISSEMINATED XENOGRAFT MODEL OF HUMAN PRIMARY MCL IN NSG MICE

5.4.1 Characterisation of primary samples

Flow cytometry was performed for immunophenotyping and assessment of T-cell content following magnetic T-cell depletion on the three primary MCL samples listed in table 5.1. While all 3 samples were positive by FISH for the IGH: CCND1 translocation, primary samples 1 and 3 had dual CD5 and CD20 expression and primary sample 2 had weak CD5 expression. This was consistent with lymph node histopathology for sample 2 at diagnosis. Samples had less than 10% T-cells and this fell to less than 1% with magnetic T-cell depletion. Of the three primary samples injected, only sample 1 was seen to engraft consistently. The results in this chapter will therefore focus on this primary sample and draw comparisons of this sample with samples 2 and 3 where relevant. Findings in mice injected with samples 2 and 3 are detailed in appendix C. Figure 5.4 shows immunohphenotyping plots and further clinical details for primary sample 1.

Figure 5.4 Clinical details and immunophenotypic characteristics of primary sample 1

Age (when sample taken)	60yrs
Sex	Male
Tissue diagnosis	Blastoid MCL t(11;14)
Source (sample date)	Peripheral blood at 1st relapse (Jan 2008)
Sites of involvement	Spleen, bone marrow, penile mass
Previous treatment	CHOP x 8 in 2005 to CR

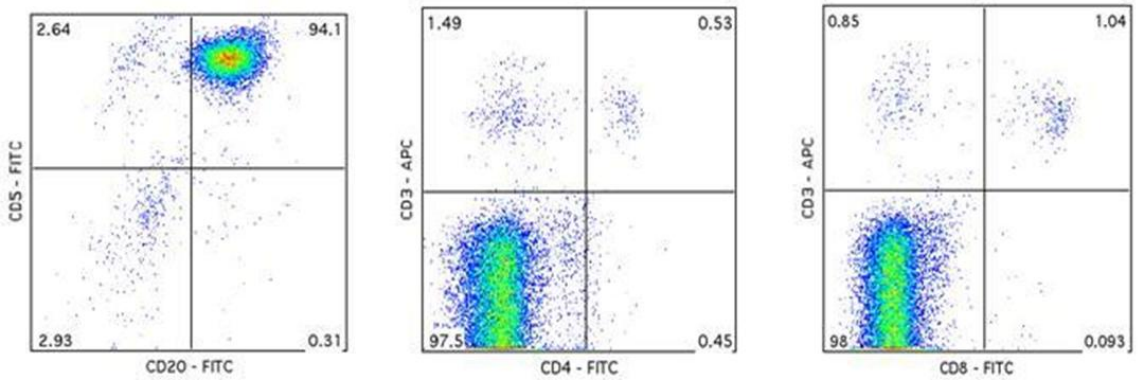

5.4.2 Evidence for engraftment of human primary MCL in NSG mice

T-cell depleted PBMCs from primary sample 1 were injected into a total of 4 mice identified as 1R, 2R, 3R and NEM (no ear mark). Mice were not visibly ill through the period of monitoring and up until sacrifice at 20 weeks. Peripheral blood sampling at 3 weeks revealed less than 1% human CD45 cells by flow cytometry in all mice. At 6 and 12 weeks a distinct human CD45 population was detected in all mice and more than 95% of these cells exhibited dual CD5 and CD20 expression. Results of peripheral blood flow cytometry at 12 weeks are shown in figure 5.5A. The growth kinetics of injected cells varied between the replicates (figure 5.6B).

Mice were sacrificed at 20 weeks and 2-3 cm splenomegaly was noted in all mice at autopsy, while spleen from mice that had no evidence of engraftment measured upto 1cm. Some mice had hepatomegaly in addition but no obvious lymphadenopathy or intra-abdominal masses were detected on exploratory dissection at sacrifice. Flow cytometry performed on flushed bone marrow showed a distinct CD5 and CD20 expressing population of tumour cells (Figure 5.6A). CD20 IHC performed on femoral and pelvic bone marrow of mice confirmed the presence of MCL cells in a scattered pattern (Figure 5.6B). Similar scattered CD20 expressing cells were seen on liver IHC.

Spleens from all mice showed heavily infiltration. Loss of splenic architecture was seen on comparing haematoxylin-eosin stained sections between normal spleens from NSG mice (injected with primary samples 2 and 3) and infiltrated spleen from mice injected with primary sample 1 (Figure 5.7). CD20 and cyclin D1 staining of the infiltrated spleens further confirmed engraftment (Figure 5.8). Ki-67 was performed on the spleens and ranged between 30 and 40% in all spleens. Finally, molecular confirmation for engraftment was obtained by performing FISH for the IGH: CCND1 translocation on a cell suspension prepared from one of the infiltrated spleens, and this was positive in over 90% of cells. No evidence of infiltration was seen in the ileo-caecal junctions of mice.

Figure 5.5 Peripheral blood flow cytometry monitoring of MCL engraftment in NSG mice. (A) Flow cytometry plots at 12 weeks from 4 NSG mice (1R, 2R, 3R, NEM) injected with primary sample 1. Gating of cells positive for human CD45 (hCD45, top row) was followed by detection of CD5/CD20 double staining cells (bottom row). (B) Dot plot showing progressive increase in the percentage of hCD45 cells in the 4 mice at 3, 6 and 12 weeks. Lines represent mean %hCD45.

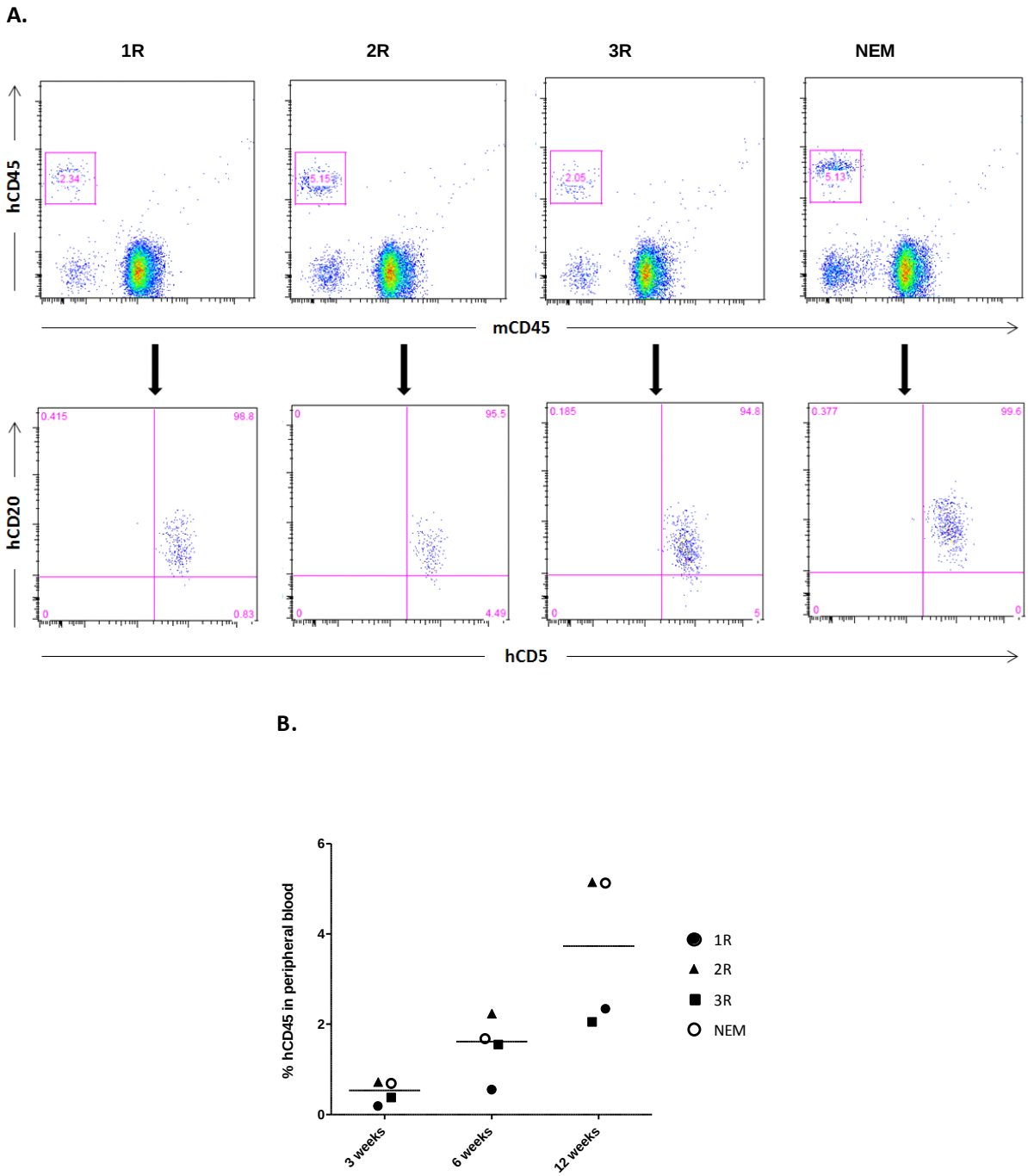

Figure 5.6 Immunophenotyping of bone marrow cells obtained from NSG mice at sacrifice. (A) Flow cytometry analysis showing a distinct human CD5/CD20 double staining population in cells flushed out from femurs of mice. (B) Scattered CD20 positive cells seen on IHC staining of decalcified, paraffin embedded femoral bone marrow of mice.

A.

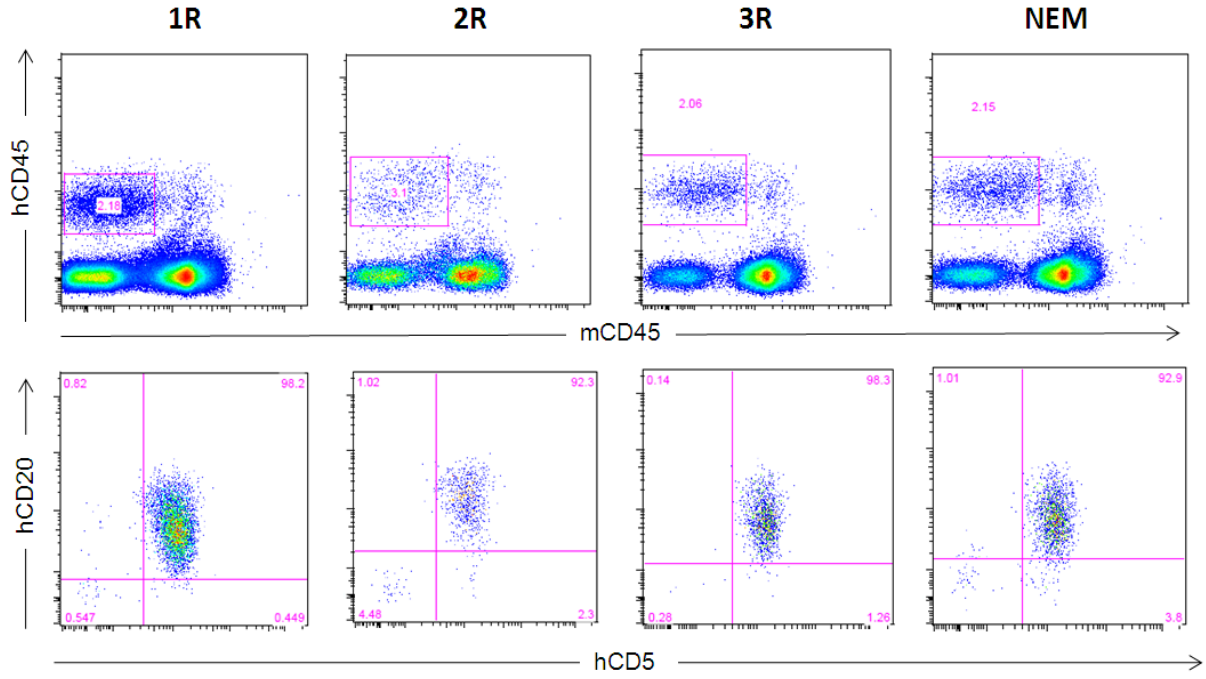

B.

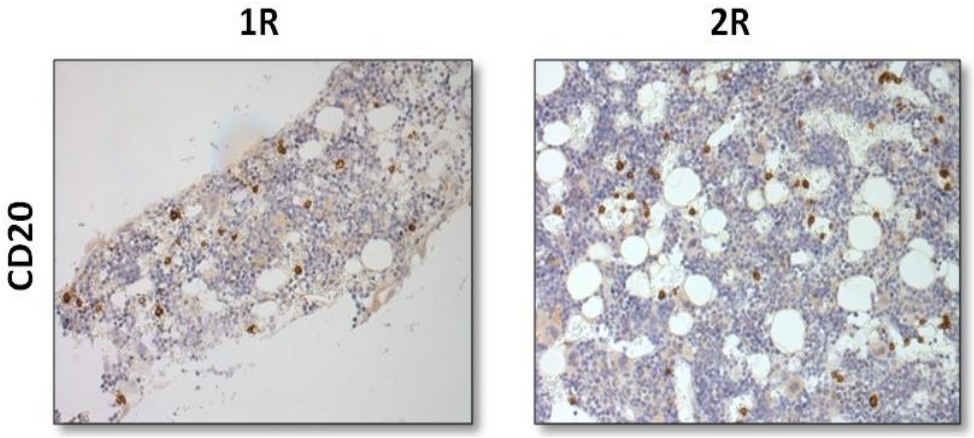

Figure 5.7 Disruption of splenic architecture by MCL infiltration. A haematoxylin and eosin stained section of **s**pleen harvested from a NSG mouse injected with primary sample 2 (left) showing normal splenic architecture compared to the image on the right from a mouse injected with primary sample 1. Areas of infiltration are seen as lighter staining regions and are most prominent around vascular structures in the spleen.

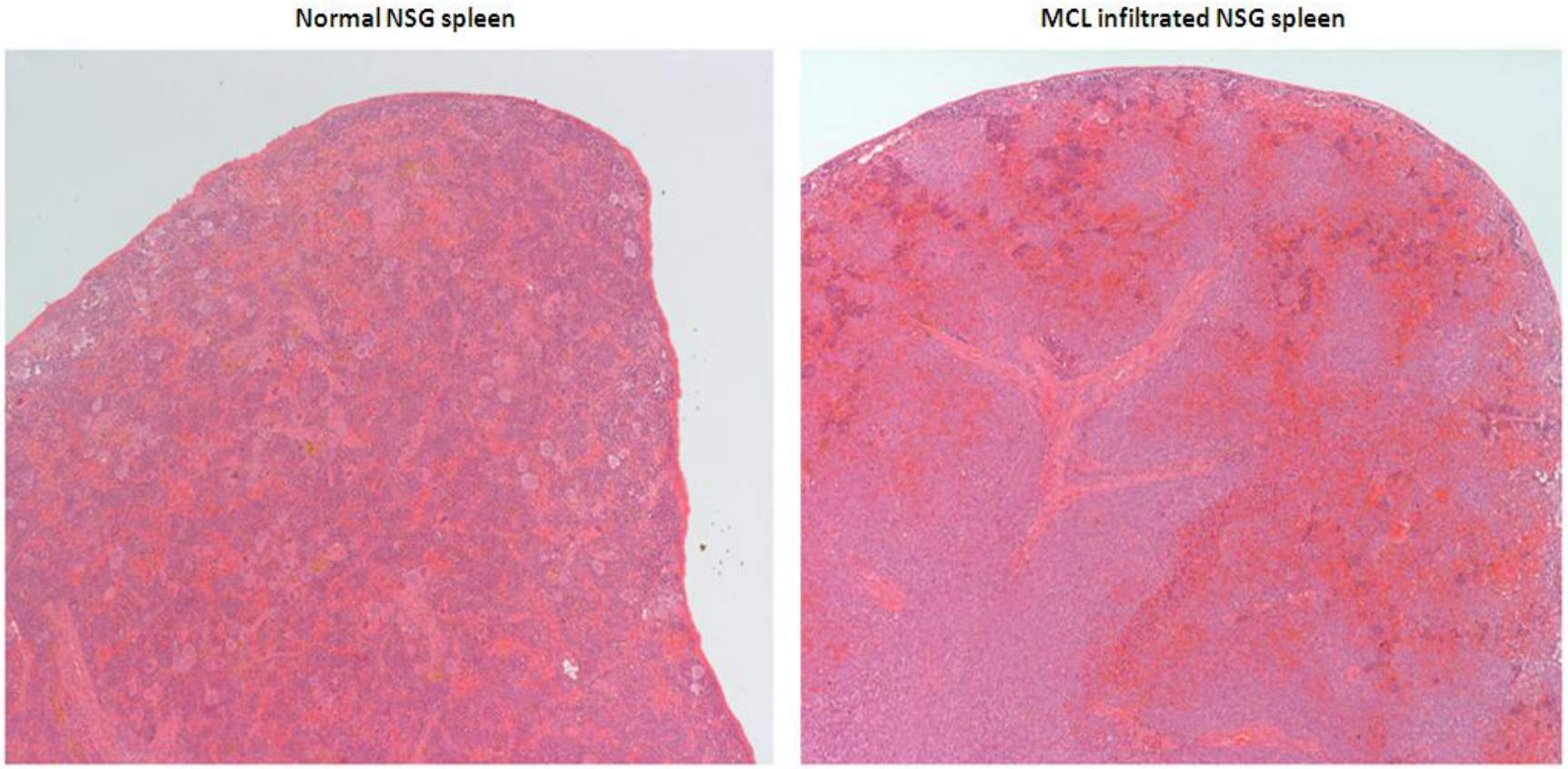

Figure 5.8 Images of CD20 and cyclin D1 IHC on spleen sections from NSG mice showing MCL infiltration. FFPE sections of spleens from 4 mice (1R, 2R, 3R and NEM) showing heavy infiltration with CD20 (top row) and cyclin D1 expressing cells. The inset in IHC images for 1R show CD20 and cyclin D1 staining at a higher magnification.

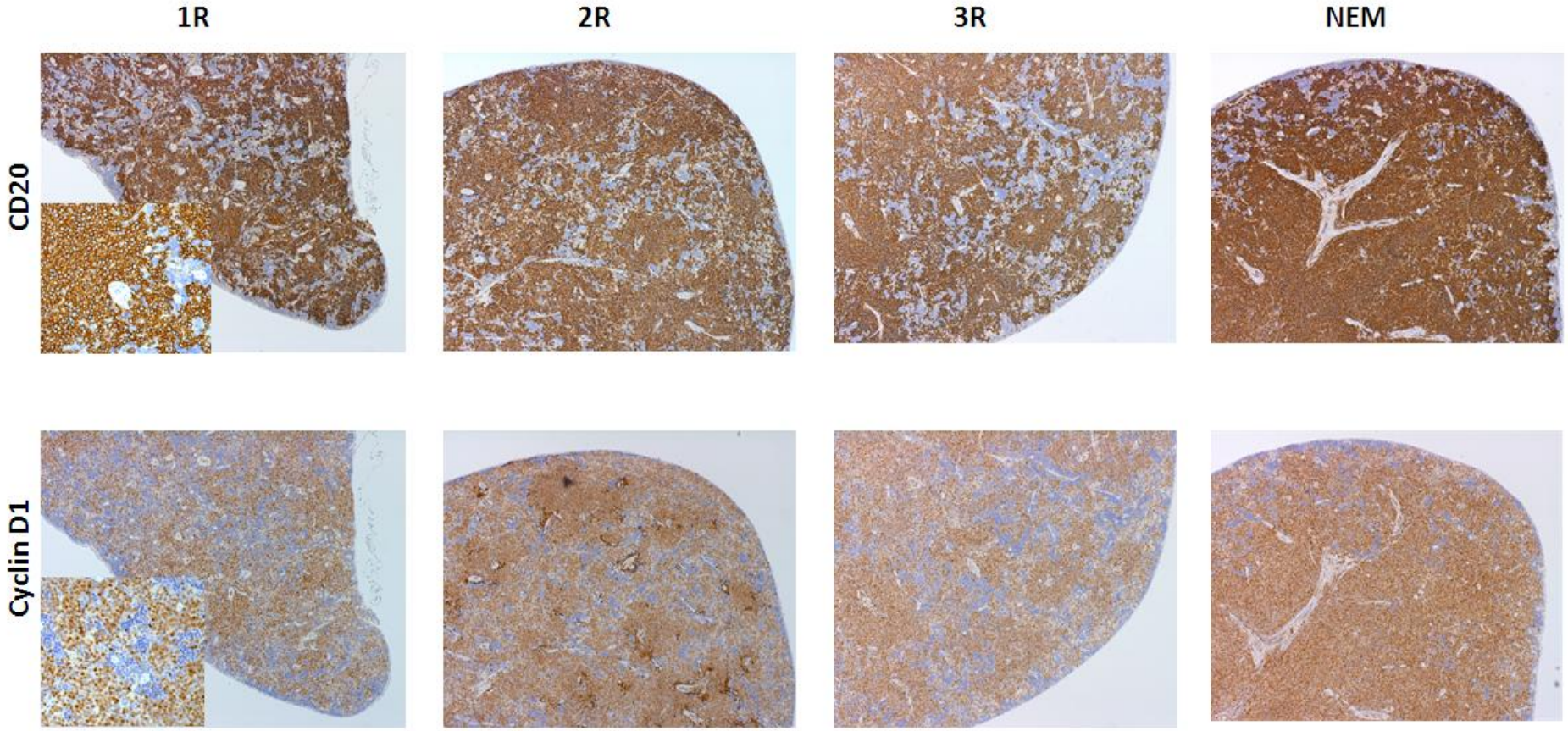

5.4.3 Secondary transplantation

Single cells suspensions prepared from spleens of NSG mice that showed engraftment with primary sample 1 were cryopreserved in 90% FCS and 10% DMSO. Cells were thawed in a water bath and re-suspended in RPMI+10% FCS for performing cell counts. For secondary transplantation, 3 x 10^7 cells were re-suspended in 600µl of PBS + 10%FCS and injected by tail-vein into 3 NSG mice (1R, 2R and NEM) that were irradiated within 24 hours of cell injection. Peripheral blood flow cytometry performed at 6 and 12 weeks showed a distinct CD5/CD20 double positive population (Figure 5.9A). Once again, mice showed no signs of illness until sacrifice. At 20 week sacrifice, 2 out of 3 mice (2R and NEM) had marked splenomegaly. No other obvious masses were found at autopsy. IHC for CD20 and cyclin D1 confirmed heavy infiltration of the spleen in all 3 mice. Flow cytometry of cells flushed out from the bone marrow showed a small population of CD5/CD20 double positive cells that was most obvious in 2R, less so in NEM and not detected in 1R. These differences are very likely due to a smaller cell dose injected into mouse 1R as it was the last mouse injected.

Figure 5.9 Engraftment of MCL cells with secondary transplantation of primary sample 1 at 20 weeks (A) CD5/CD20 double positive cells in peripheral blood. (B) and (C) CD20 positive cells in the bone marrow and spleen of mice. (D) Infiltration of spleen with cyclin D1 expressing cells.

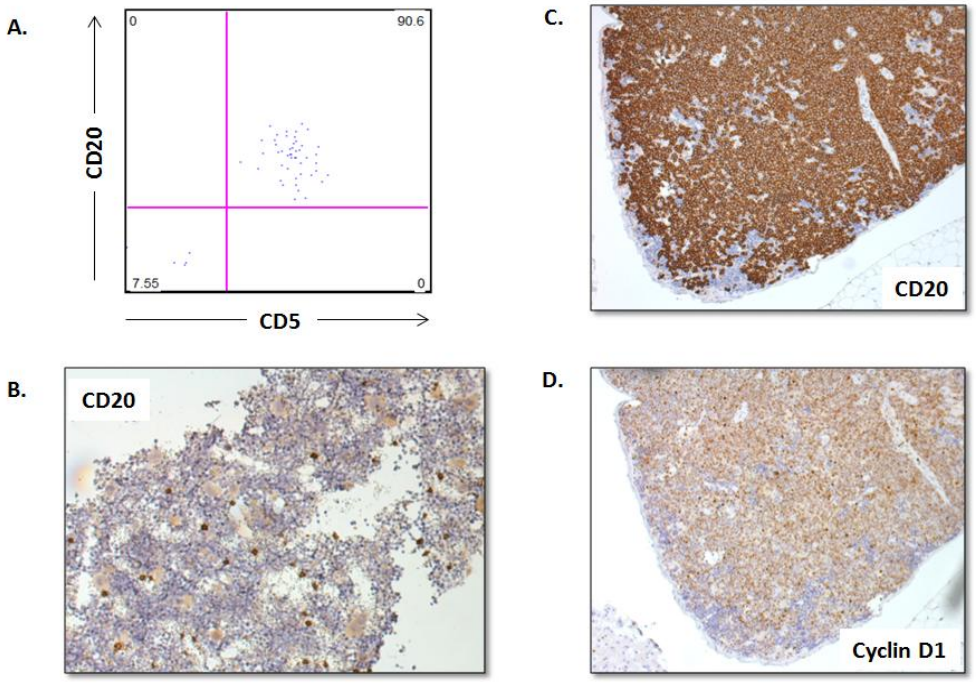

5.5 Discussion

This preliminary study demonstrates that human primary mantle cell lymphoma can be established in NSG mice. Disseminated models of MCL cell lines in immunodeficient mice have been previously used for pre-clinical testing of drugs. We used a disseminated model of Jeko-1 to predict kinetics and distribution with primary cells. This provided some insights – firstly, the cell dose injected appears to correlate with the kinetics and burden of engraftment and secondly the bone marrow and spleen were common sites of involvement. The aggressiveness of the Jeko-1 cell line in the NSG model is also of note with rapid dissemination in mice resulting in illness at 4-5 weeks.

We saw engraftment of only one of the three primary samples injected into the NSG mice. Although this is a limited number of samples, the sample that engrafted was from a patient with relapsed, blastoid disease suggesting that an aggressive phenotype is more likely to favour engraftment in this model. This is in keeping with observations from other NSG models of human malignancy such as acute myeloid leukaemia.[180] Engraftment of MCL was confirmed by immunophenotyping and FISH for *IGH: CCND1*. We saw MCL involvement of spleen, bone marrow and peripheral blood in the mice, similar to that seen in the patient from whom these cells were harvested. No tumour masses or lymphadenopathy was detected and the ileo-caecal junction showed no evidence of infiltration in these mice. Indeed, it is not known if lymphadenopathy can be expected in these mice that lack both B-cells and T-cells. Interestingly, mice were not visibly ill at 20 weeks despite widespread infiltration but this is likely to occur with longer observation. This may however be an advantage for pre-clinical testing as drugs can be administered for adequate periods of time in order to test their effect on reduction of disease burden compared to untreated controls.

The failure of engraftment of the two other samples also needs to be discussed. One option may be to increase the cell dose administered to mice but this is not as easy as with CLL where patient

samples are more readily available. The same argument holds for evaluating freshly isolated cells from patients compared to cryopreserved cells that were used in our study. A third option is to evaluate the effect of co-transplanting tumour cells with allogeneic T-cells as described in the NSG model of human primary CLL. While there is evidence for a protective role for T-cells in CLL, evidence for this in MCL is scant. We used a conservative strategy of depleting T-cells prior to injection of mice because an expansion of T-cells has often seen by our collaborators after injection of PBMCs into NSG mice and these often 'out-compete' tumour cells.

Finally, we were able to establish MCL in a new set of NSG mice by secondary transplantation of cells derived from spleens of mice that had engrafted. This supports the self-renewal and tumour-initiating capacity of MCL cells. While this NSG model needs further refining to improve the rate of engraftment, it is a promising *in vivo* model for both pre-clinical drug testing and for improving our understanding of MCL biology for e.g. through studies of tumour initiating cells or co-transplantation of allogeneic T-cells. A good understanding of the benefits and limitations of this model is necessary in order to interpret findings and use it effectively.

CHAPTER 6: FINAL DISCUSSION AND FURTHER WORK

6.1 Discussion and translational relevance

In vitro studies have demonstrated an important role for the PI3K pathway in MCL pathogenesis. The p110δ isoform of PI3K is highly enriched in leucocytes and is therefore an attractive target in lymphomas. However, relatively inferior responses to the p110δ inhibitor GS-1101 were reported in relapsed/ refractory MCL compared to indolent NHL. This may imply a role for other isoforms in the survival of MCL cells or may simply mean that this pathway is not as important as *in vitro* studies suggest. The hypothesis for this research was based on the former theory i.e. the contribution of other class Ia isoforms, particularly p110α, may explain the relatively inferior responses to GS-1101. This hypothesis was supported by evidence from a previous study that demonstrated *PIK3CA* amplification in approximately two-thirds of MCL cases (68%).[144] However, the relative expression of class Ia isoforms and the implications of *PIK3CA* amplification for MCL survival were not evaluated in this study. We therefore elected to evaluate the expression of class Ia isoforms in MCL and study their relative importance in the setting of *PIK3CA* amplification, B-cell receptor engagement, IL4 stimulation and loss of PTEN expression

Of the three class Ia isoforms (p110α, p110β and p110δ), immunohistochemistry for p110δ on human tissues had not been described at the time of starting these studies and therefore initial work focussed on validation and optimisation of an antibody against p110δ that could be used in human FFPE tissue. In parallel, MCL biopsies stored over a period of 36 years from patients treated at Barts hospital were incorporated into a TMA to study the expression of the important tumour suppressor phosphatase PTEN and the class Ia isoforms. Tonsils excised for non-malignant pathology were incorporated into the TMAs as benign controls.

There were some limitations to using this collection of MCL biopsies. Firstly, there was a relatively high number of poor quality cores and therefore loss of cores on the TMAs with repeated sections and secondly, the number of diagnostic samples was relatively small owing to the tertiary referral centre care provided at St. Bartholomew's hospital thereby limiting the ability to perform meaningful survival studies. On the other hand, this represents one of the largest MCL cohorts studied with respect to the PI3K pathway and provided the opportunity to study changes with disease progression in this rare lymphoma.

Studies in MCL have suggested an important role for suppression or inactivation of PTEN in MCL. In keeping with previous observations,[22,144] loss of PTEN expression was found in 17% of diagnostic and 16% of all biopsies. As there is evidence that p110β plays an important role in solid tumour cells exhibiting loss of PTEN expression,[145] the addition of a p110β inhibitor (TGX221) to GS1101 was evaluated in 2 primary samples exhibiting loss of PTEN expression. Although no increased cytotoxicity was found with addition of TGX221, it is difficult to draw firm conclusions from this limited number, particularly as other mechanisms of PTEN inactivation such as phosphorylation and microRNA induced suppression were not investigated. However, these studies confirm that loss of PTEN expression is a relatively common phenomenon in MCL. They also demonstrate a non significant increase of PTEN expression loss with blastoid transformation (15% of classical MCL vs. 20% blastoid MCL) and no significant change in isoform expression in these cases compared to MCL with intact PTEN expression. The implications of this molecular aberration in MCL are however not entirely clear and need further study.

Overall, the expression of the class Ia isoforms in MCL followed that seen in tonsil controls with p110δ showing the strongest expression. However, two differences between tonsils and MCL were observed – firstly, the expression of p110β in MCL was significantly lower than expression in tonsil controls and secondly, p110α expression showed wide variation within MCL samples. The first

important and interesting finding on correlating these findings to clinical information was that p110α was significantly higher in biopsies taken beyond 1st relapse compared to those taken at diagnosis while the expression of p110β and p110δ was not significantly different between diagnosis and relapse. The importance of increased p110α expression was studied in the Granta519 MCL cell line which exhibits constitutive Akt phosphorylation and increased p110α expression. Use of isoform selective inhibitors in this cell line revealed that p110δ inhibition with GS-1101 was insufficient for effective PI3K inhibition but addition of a p110α inhibitor (but not a p110β inhibitor) to GS-1101 resulted in complete PI3K inhibition. Further studies carried out with GDC-0941, a dual p110α and δ inhibitor showed that dual inhibition was necessary for not just complete but also sustained PI3K inhibition in the setting of increased p110α expression. Further, GDC-0941 treatment was found to have significantly greater activity in MCL cell lines and primary samples compared to GS-1101.

In relation to external stimuli, however, it appeared that p110δ inhibition was sufficient to abolish BCR induced PI3K activation and did not differ significantly from GDC-0941 in its ability to counteract the proliferative effects of IL4 in primary MCL cells. These findings suggest that while p110δ is important for PI3K activation mediated by external stimuli, p110α appears to primarily support constitutive PI3K activation in MCL. MCL cells exhibiting *PIK3CA/*p110α over-expression can therefore sustain PI3K signalling despite p110δ inhibition. These findings are unlikely to be influenced by p110γ as both GS-1101 and GDC-0941 have very similar activity against this isoform.

Two studies particularly relevant to these findings merit mention at this stage. The first by Ramadani *et al* provides evidence that although p110δ is the key isoform in relation to agonist-induced BCR signalling, p110α contributes to tonic BCR signalling in healthy lymphocytes.[169] So while p110δ appears to retain its role in MCL, increased expression of p110α, may confer a benefit through increased p110α-induced tonic signalling. The second study by Hui *et al* demonstrates a role for increased expression of *PIK3CA* in chemo-resistance.[130] Chronic exposure of K562 cells to

doxorubicin was found to induce nuclear accumulation of FOXO3a which in turn led to increased expression of *PIK3CA* (and p110α) through FOXO3a induced activation of the *PIK3CA* promoter region. Activation of the PI3K pathway through *PIK3CA* amplification conferred resistance to doxorubicin in these cells. This mechanism of *PIK3CA/*p110α amplification may explain the reason why increase in p110α is most significant with increasing chemotherapy exposure i.e. beyond 1st relapse in MCL. However, another possible mechanism is the selection and expansion of a pre-existing clone of high *PIK3CA*/p110α expressing cells by repeated cycles of chemotherapy that eliminates chemo-sensitive cells. Support for the latter mechanism can perhaps be found in the results of data mining of class Ia PI3K gene expression that demonstrated a significantly higher *PIK3CA* in MCL compared to indolent NHL even at diagnosis. Immunohistochemistry does not allow differentiation of these mechanisms and indeed, both mechanisms may co-exist. It is interesting that an increase in *PIK3CA* was not found in sequential follicular lymphoma biopsies and this may once again suggest a pre-existing clone of high *PIK3CA* expressing cells in MCL that selectively expands in response to chemotherapy. A further IHC study looking at the expression of nuclear FOXO3a with MCL progression as well as a study of p110α expression in diagnostic biopsies and its impact on survival can provide further insight into this process. A summary of the proposed mechanisms by which increased p110α may confer a survival advantage in MCL cells is depicted in figure 6.1.

The evaluation of phosphorylation of downstream targets of PI3K yielded inconsistent results. Neither the degree of Akt phosphorylation nor inhibition of phosphorylation in response to PI3K inhibition appeared to predict sensitivity. One interpretation could be that constitutive PI3K activation is not always associated with Akt phosphorylation and a more reliable marker is needed. This view is supported by observations that constitutive Akt phosphorylation is not always seen in cells harbouring activating mutations in *PIK3CA*.[181] However, Akt phosphorylation when detected is a useful marker to detect the degree of PI3K inhibition. Phosphorylation of ribosomal S6 may be a useful marker in the absence of detectable Akt phosphorylation. Another aspect of these studies

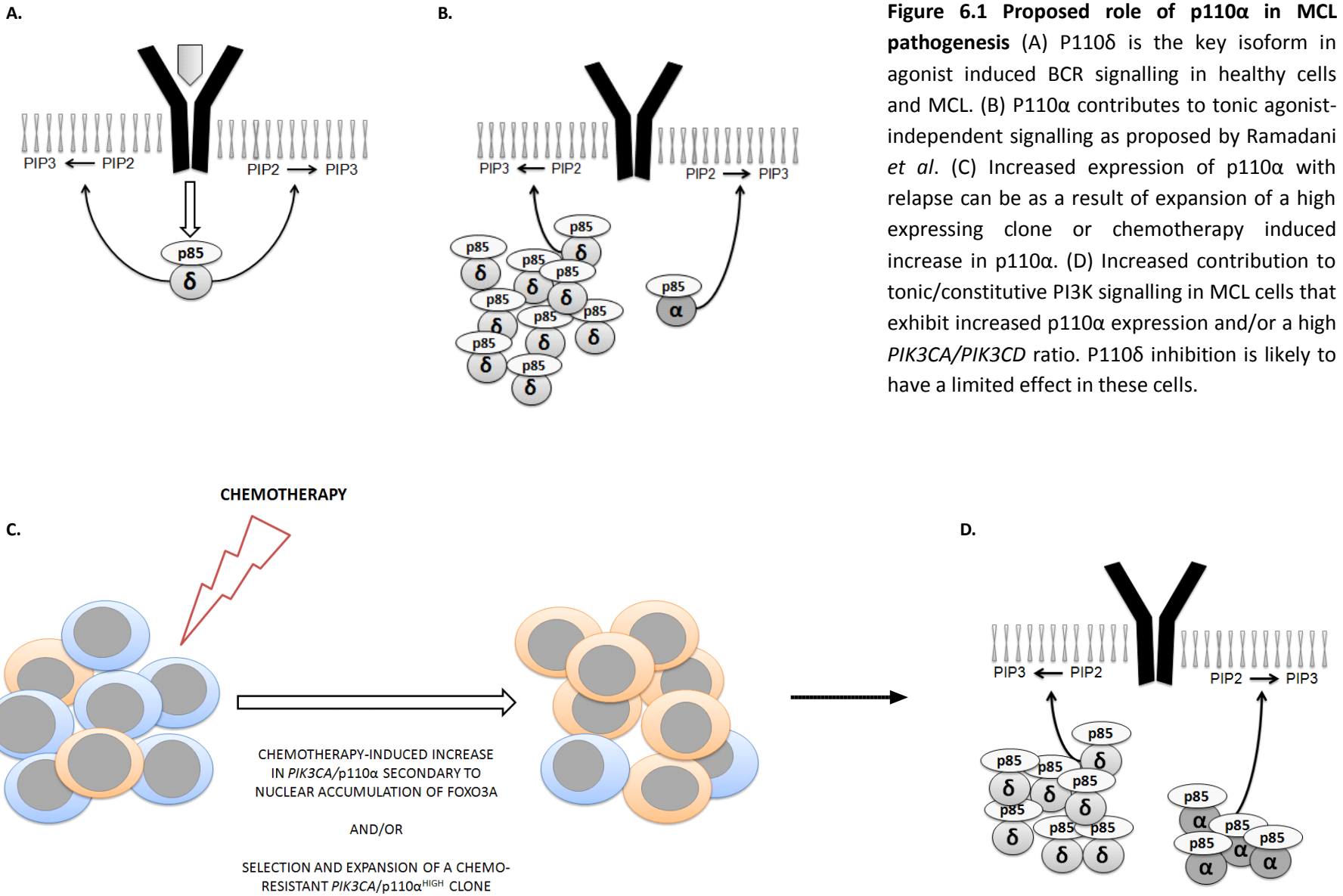

Figure 6.1 Proposed role of p110α in MCL pathogenesis (A) P110δ is the key isoform in agonist induced BCR signalling in healthy cells and MCL. (B) P110α contributes to tonic agonist-independent signalling as proposed by Ramadani *et al*. (C) Increased expression of p110α with relapse can be as a result of expansion of a high expressing clone or chemotherapy induced increase in p110α. (D) Increased contribution to tonic/constitutive PI3K signalling in MCL cells that exhibit increased p110α expression and/or a high *PIK3CA/PIK3CD* ratio. P110δ inhibition is likely to have a limited effect in these cells.

was the lack of association between successful PI3K inhibition with pharmacological inhibitors, as judged by inhibition of Akt phosphorylation, and their effect on growth inhibition or cytotoxicity. It is very likely that a subset of MCLs either do not rely on the PI3K pathway for survival or are able to activate alternate survival pathways in response to PI3K inhibition. A recent study in T-ALL suggests an important role for activation of the NOTCH pathway as a mechanism of resistance to PI3K/mTOR inhibition.[176] This may be a particularly interesting pathway for study in relation to resistance to PI3K inhibition in MCL as NOTCH mutations are found in approximately 12% of MCL cases and this pathway is therefore likely to play an important role in at least a subset of MCL.

In order to determine the potential implications of increased *PIK3CA* in MCL, we studied the gene expression of the class Ia isoforms using qRT-PCR. The ΔC_t method was used for relative quantitation of gene expression and B-cells from healthy PBMCs were used as controls. Although a higher *PIK3CA* expression by itself was not predictive of resistance to GS-1101, the *PIK3CA*/PIK3CD mRNA ratio was found to be predictive of resistance to GS-1101 *in vitro* in an initial cohort of 12 primary MCL samples. Resistant samples were found to have a ratio that was greater than twice the ratio found in healthy B-cells. This cut-off was validated in an independent cohort of 10 samples. As this marker of resistance employs an internal healthy control to determine the cut-off, it is less likely to suffer from variability and is therefore more likely to be reproducible. It also reflects the mechanism proposed for resistance of MCL cells to p110δ inhibition i.e. high relative expression of *PIK3CA*. The recent synthesis and availability of the selective p110α inhibitor A66[164] allowed us to evaluate the effect of p110α inhibition on its own in MCL. This inhibitor had no significant cytotoxicity in Jeko-1, Granta 519 and 10 primary MCL samples that were studied. This further supports the role for dual p110α/δ inhibition in MCL.

One of the limitations of the cytotoxicity studies was the lack of availability of sequential PBMCs from MCL patients. However, sequential frozen MCL lymph nodes were available and gene

expression of class Ia isoforms was therefore determined on these using qRT-PCR. In keeping with the IHC studies, the *PIK3CA*/PIK3CD ratio was higher at relapse compared to diagnosis in these sequential biopsies. Of note, gene expression of class Ia PI3K isoforms in frozen MCL was observed to differ from that seen in MCL PBMCs in that the expression of p110α appeared to be lower in relation to p110δ in frozen nodes compare to PBMCs. Gene expression on purified MCL cells from lymph node and peripheral blood samples taken simultaneously from a patient are required to confirm this finding but potential explanations are a higher proportion of non-tumour cells in lymph nodes compared to PBMCs and perhaps a reversible down-regulation of *PIK3CA* expression induced by the lymph node micro-environment.

Our observation that the *PIK3CA*/PIK3CD mRNA ratio increases with relapse as does p110α expression implies that these inhibitors may be particularly useful in relapsed MCL. However, as increased *PIK3CA*/p110α expression appears to be associated with relapse, and potentially chemo-resistance, it could be argued that there is a rationale for using dual p110α/δ inhibition either upfront or as maintenance therapy in patients who attain remission. On the other hand, as MCL is as yet an incurable disease, the *PIK3CA*/PIK3CD ratio may be useful to determine which patients would benefit most from dual inhibition. Those with a low *PIK3CA*/PIK3CD ratio may benefit equally from a p110δ inhibitor such as GS-1101 while dual inhibition could be reserved for relapsed disease or when a high *PIK3CA*/PIK3CD ratio becomes apparent.

The results obtained from data mining of class Ia PI3K isoform gene expression taken together with the finding that p110α expression appears not to change with disease progression in follicular lymphoma suggest that targeting p110α is particularly important in MCL. It is possible that the genetic instability seen with MCL, which is not as prominent with indolent NHL, lends itself to this phenomenon and it would be interesting to study changes in p110α with progression in aggressive lymphomas.

Although initially intended to provide in vivo validation for the results discussed above, the final aspect of this research moved away from this idea and towards the exciting possibility of establishing human MCL in NSG mice. From the perspective of a rapidly expanding armamentarium of potential therapies, a mouse model for pre-clinical drug testing is particularly valuable for a rare disease like MCL. Three MCL samples from three individual patients were injected into NSG mice in order to evaluate their ability to engraft in this model. Engraftment was seen in only one of the 3 samples injected but was seen consistently across all 4 replicate mice. This sample was from a patient with relapsed, blastoid disease suggesting that an aggressive phenotype may favour engraftment. Similar observations of favourable engraftment in cells from patients with a worse outcome have been reported in NSG models of human AML.[180] In addition, we found engraftment following serial transplantation of the spleen cells from affected mice. This supports the self-renewal and tumour initiation capacity of these MCL cells. Engraftment in mice was confirmed with both immunophenotyping (human CD20 and cyclin D1) and FISH analysis for t(11;14) in cells from NSG spleen.

While this data is preliminary, it demonstrates that it is possible to establish human primary MCL in NSG mice. This model can be used for pre-clinical testing of drugs as well as for studying certain aspects of MCL biology such as tumour-initiating cells. The obvious limitation of this model is the lack of micro-environment (B-cells, T-cells and NK cells). It is therefore important to develop this model keeping in mind its advantages and limitations. There may be ways to improve engraftment that need further exploration and these include using a higher cell dose, using a different cell source (for e.g. spleen, bone marrow) and using alternative conditioning of mice.

6.2 Further work

While further studies are required to establish the role of p110α in chemo-resistance and disease progression, these studies should not delay the evaluation of dual p110α/δ inhibition in a clinical trial with MCL patients, particularly as dual p110α/δ inhibitors like GDC-0941 have been relatively well tolerated in early phase clinical trials in solid tumours. The expression of p110α needs to be investigated in a large cohort of diagnostic MCL samples in relation to progression free and overall survival. Functional studies in MCL cell lines of the relationship between FOXO3a, *PIK3CA* and chemo-resistance in conjunction with an immunohistochemistry study of the localisation of FOXO3a in MCL cells in relation to p110α expression and disease progression may help to elucidate the mechanism behind the higher expression of this PI3K isoform in relapsed disease. Simultaneous studies in follicular lymphoma, which does not appear to exhibit an increase in p110α with relapse, would also be useful to investigate whether increased p110α expression with disease progression is in fact related to chemotherapy induced nuclear accumulation of FOXO3a.

Evaluation of the *PIK3CA*/PIK3CD ratio in MCL cells from GS-1101 treated patients and correlation with clinical response would provide a robust test of this ratio as a biomarker. A clinical trial with a dual p110α/δ inhibitor such as GDC-0941 could take the form of a phase II study in relapsed/refractory MCL patients where patients receive a cycle of the p110α/δ inhibitor prior to a salvage chemotherapy regimen followed by the option of maintenance with a p110α/δ inhibitor if a response is achieved. *PIK3CA*/PIK3CD ratio on tumour cells (blood, bone marrow or lymph node) prior to starting treatment can then be correlated with response to treatment.

Although important, PI3K inhibition is not always effective against MCL cells and other survival pathways may be able to sustain survival in the absence of PI3K signalling. In relation to haematological malignancy, targets that may be important in view of recent evidence are CDK4/6,

mTOR and NOTCH signalling pathways. Combining an mTOR inhibitor (Everolimus or Temsirolimus) or CDK4/6 inhibitor with GS-1101 has been shown to have a greater effect than GS-1101 alone[171,172] while a separate study describes promising activity with PI3K/mTOR inhibitors in MCL cells in vitro.[182] Another particularly attractive pathway to investigate is the NOTCH signalling pathway as its activation has been shown to impair responses to PI3K/mTOR inhibition in T-ALL[176] and approximately 12% of all MCL cases are found to carry NOTCH mutations.[27] As previously discussed, targeting a greater number of pathways is likely to lead to greater toxicity but the simultaneous evaluation of predictive markers may aid appropriate selection of patients.

In relation to the NSG model of human primary MCL, further work is required to investigate conditions that may favour engraftment of patient derived MCL cells. These could include changing cell conditions such as injecting a higher cell number, comparing fresh cells to cryopreserved cells, using a different cell source and injecting whole PBMCs instead of T-cell depleted PBMCs. Mouse conditions such as using more humanised mice or using alternative conditioning of mice could also be explored. The obvious limitation to using this model is the lack of immune cells (T-cells, B-cells and NK cells) and therefore lack of a representative tumour microenvironment. On the other hand, this is still a useful model to study the direct tumour toxicity of molecular therapies and is also potentially useful to study the role of other components of the tumour microenvironment such as angiogenesis and macrophages. Other potential uses for this model include the exploration and isolation of MCL-initiating cells by serial transplantation of lymphoma sub-populations. Further studies in the NSG mice that are on-going include injection of additional primary MCL cells from different sources (peripheral blood, lymph node, bone marrow or spleen), comparing engraftment between T-cell depleted and whole PBMCs from the same patient and evaluation of characteristics that may predict which samples will engraft in NSG mice.

In conclusion, despite advances in therapy, MCL remains an incurable disease characterised by frequent relapse. This research provides evidence for the potential role of p110α in disease progression and resistance to p110δ inhibitors in MCL. Further work should focus on investigating the role of p110α in MCL chemo-resistance and also evaluating dual p110α/δ inhibitors in the clinical setting with the incorporation of the *PIK3CA*/PIK3CD ratio as a biomarker. Finally, it is likely that a rational combination of molecular therapies will be required for optimal control or perhaps even cure in MCL but the rarity of this disease makes this challenging. We provide preliminary data for a mouse model of human MCL that can be used for pre-clinical testing of novel molecular therapies and their combinations. This model needs to be refined but is a potentially valuable tool for pre-clinical testing of novel therapies and also one that could advance our understanding of MCL biology and thereby take us a step further towards overcoming this rare but as yet incurable lymphoma.

REFERENCES:

1. Harris NL, Jaffe ES, Stein H, et al: A revised European-American classification of lymphoid neoplasms: a proposal from the International Lymphoma Study Group. Blood 84:1361-92, 1994
2. Weisenburger DD, Kim H, Rappaport H: Mantle-zone lymphoma: a follicular variant of intermediate lymphocytic lymphoma. Cancer 49:1429-38, 1982
3. Smedby KE, Hjalgrim H: Epidemiology and etiology of mantle cell lymphoma and other non-Hodgkin lymphoma subtypes. Semin Cancer Biol 21:293-8
4. Montserrat E, Bosch F, Lopez-Guillermo A, et al: CNS involvement in mantle-cell lymphoma. J Clin Oncol 14:941-4, 1996
5. Ferrer A, Bosch F, Villamor N, et al: Central nervous system involvement in mantle cell lymphoma. Ann Oncol 19:135-41, 2008
6. Herrmann A, Hoster E, Zwingers T, et al: Improvement of overall survival in advanced stage mantle cell lymphoma. J Clin Oncol 27:511-8, 2009
7. Andersen NS, Donovan JW, Borus JS, et al: Failure of immunologic purging in mantle cell lymphoma assessed by polymerase chain reaction detection of minimal residual disease. Blood 90:4212-21, 1997
8. Walsh SH, Thorselius M, Johnson A, et al: Mutated VH genes and preferential VH3-21 use define new subsets of mantle cell lymphoma. Blood 101:4047-54, 2003
9. Kienle D, Krober A, Katzenberger T, et al: VH mutation status and VDJ rearrangement structure in mantle cell lymphoma: correlation with genomic aberrations, clinical characteristics, and outcome. Blood 102:3003-9, 2003
10. Hadzidimitriou A, Agathangelidis A, Darzentas N, et al: Is there a role for antigen selection in mantle cell lymphoma? Immunogenetic support from a series of 807 cases. Blood 118:3088-95
11. Raty R, Franssila K, Jansson SE, et al: Predictive factors for blastoid transformation in the common variant of mantle cell lymphoma. Eur J Cancer 39:321-9, 2003
12. Swerdlow S. CE, Harris N. L., Jaffe E.S., Pileri S.A., Stein H., Thiele J., Vardiman J.W.: WHO Classification of Tumours of Haematopoietic and Lymphoid Tissues, (ed 4th). Lyon, IARCPress, 2008
13. Akiyama N, Tsuruta H, Sasaki H, et al: Messenger RNA levels of five genes located at chromosome 11q13 in B-cell tumors with chromosome translocation t(11;14)(q13;q32). Cancer Res 54:377-9, 1994
14. Fu K, Weisenburger DD, Greiner TC, et al: Cyclin D1-negative mantle cell lymphoma: a clinicopathologic study based on gene expression profiling. Blood 106:4315-21, 2005
15. Smith MR, Joshi I, Jin F, et al: Murine model for mantle cell lymphoma. Leukemia 20:891-3, 2006
16. Bodrug SE, Warner BJ, Bath ML, et al: Cyclin D1 transgene impedes lymphocyte maturation and collaborates in lymphomagenesis with the myc gene. EMBO J 13:2124-30, 1994
17. Fernandez V, Hartmann E, Ott G, et al: Pathogenesis of mantle-cell lymphoma: all oncogenic roads lead to dysregulation of cell cycle and DNA damage response pathways. J Clin Oncol 23:6364-9, 2005
18. Fang NY, Greiner TC, Weisenburger DD, et al: Oligonucleotide microarrays demonstrate the highest frequency of ATM mutations in the mantle cell subtype of lymphoma. Proc Natl Acad Sci U S A 100:5372-7, 2003
19. Schaffner C, Idler I, Stilgenbauer S, et al: Mantle cell lymphoma is characterized by inactivation of the ATM gene. Proc Natl Acad Sci U S A 97:2773-8, 2000

20. Espinet B, Salaverria I, Bea S, et al: Incidence and prognostic impact of secondary cytogenetic aberrations in a series of 145 patients with mantle cell lymphoma. Genes Chromosomes Cancer 49:439-51, 2010
21. Rizzatti EG, Falcao RP, Panepucci RA, et al: Gene expression profiling of mantle cell lymphoma cells reveals aberrant expression of genes from the PI3K-AKT, WNT and TGFbeta signalling pathways. Br J Haematol 130:516-26, 2005
22. Rudelius M, Pittaluga S, Nishizuka S, et al: Constitutive activation of Akt contributes to the pathogenesis and survival of mantle cell lymphoma. Blood 108:1668-76, 2006
23. Dal Col J, Zancai P, Terrin L, et al: Distinct functional significance of Akt and mTOR constitutive activation in mantle cell lymphoma. Blood 111:5142-51, 2008
24. Cecconi D, Zamo A, Bianchi E, et al: Signal transduction pathways of mantle cell lymphoma: a phosphoproteome-based study. Proteomics 8:4495-506, 2008
25. Fu L, Lin-Lee YC, Pham LV, et al: Constitutive NF-kappaB and NFAT activation leads to stimulation of the BLyS survival pathway in aggressive B-cell lymphomas. Blood 107:4540-8, 2006
26. Gelebart P, Anand M, Armanious H, et al: Constitutive activation of the Wnt canonical pathway in mantle cell lymphoma. Blood 112:5171-9, 2008
27. Kridel R, Meissner B, Rogic S, et al: Whole transcriptome sequencing reveals recurrent NOTCH1 mutations in mantle cell lymphoma. Blood 119:1963-71, 2012
28. Rinaldi A, Kwee I, Taborelli M, et al: Genomic and expression profiling identifies the B-cell associated tyrosine kinase Syk as a possible therapeutic target in mantle cell lymphoma. Br J Haematol 132:303-16, 2006
29. Castillo R, Mascarenhas J, Telford W, et al: Proliferative response of mantle cell lymphoma cells stimulated by CD40 ligation and IL-4. Leukemia 14:292-8, 2000
30. Kurtova AV, Tamayo AT, Ford RJ, et al: Mantle cell lymphoma cells express high levels of CXCR4, CXCR5, and VLA-4 (CD49d): importance for interactions with the stromal microenvironment and specific targeting. Blood 113:4604-13, 2009
31. Zhang L, Yang J, Qian J, et al: Role of the microenvironment in mantle cell lymphoma: IL-6 is an important survival factor for the tumor cells. Blood 120:3783-92, 2012
32. Farinha P, Opat S, Boyle M, et al: Number of Lymphoma-Associated-Macrophages (LAM) Is An Independent Predictor of Survival in Patients with Mantle Cell Lymphoma (MCL). ASH Annual Meeting Abstracts 114:3944-, 2009
33. Eve HE, Furtado MV, Hamon MD, et al: Time to treatment does not influence overall survival in newly diagnosed mantle-cell lymphoma. J Clin Oncol 27:e189-90; author reply e191, 2009
34. Martin P, Chadburn A, Christos P, et al: Outcome of deferred initial therapy in mantle-cell lymphoma. J Clin Oncol 27:1209-13, 2009
35. Ondrejka SL, Lai R, Smith SD, et al: Indolent mantle cell leukemia: a clinicopathological variant characterized by isolated lymphocytosis, interstitial bone marrow involvement, kappa light chain restriction, and good prognosis. Haematologica 96:1121-7, 2011
36. Del Giudice I, Messina M, Chiaretti S, et al: Behind the scenes of non-nodal MCL: downmodulation of genes involved in actin cytoskeleton organization, cell projection, cell adhesion, tumour invasion, TP53 pathway and mutated status of immunoglobulin heavy chain genes. Br J Haematol 156:601-11, 2012
37. Fernandez V, Salamero O, Espinet B, et al: Genomic and gene expression profiling defines indolent forms of mantle cell lymphoma. Cancer Res 70:1408-18
38. Nygren L, Baumgartner Wennerholm S, Klimkowska M, et al: Prognostic role of SOX11 in a population-based cohort of mantle cell lymphoma. Blood 119:4215-23
39. Thorselius M, Walsh S, Eriksson I, et al: Somatic hypermutation and V(H) gene usage in mantle cell lymphoma. Eur J Haematol 68:217-24, 2002

40. Lai R, Lefresne SV, Franko B, et al: Immunoglobulin VH somatic hypermutation in mantle cell lymphoma: mutated genotype correlates with better clinical outcome. Mod Pathol 19:1498-505, 2006
41. Schraders M, Oeschger S, Kluin PM, et al: Hypermutation in mantle cell lymphoma does not indicate a clinical or biological subentity. Mod Pathol 22:416-25, 2009
42. Greiner TC, Dasgupta C, Ho VV, et al: Mutation and genomic deletion status of ataxia telangiectasia mutated (ATM) and p53 confer specific gene expression profiles in mantle cell lymphoma. Proc Natl Acad Sci U S A 103:2352-7, 2006
43. Halldorsdottir AM, Lundin A, Murray F, et al: Impact of TP53 mutation and 17p deletion in mantle cell lymphoma. Leukemia 25:1904-8
44. Royo C, Navarro A, Clot G, et al: Non-nodal type of mantle cell lymphoma is a specific biological and clinical subgroup of the disease. Leukemia 26:1895-8
45. Navarro A, Clot G, Royo C, et al: Molecular Subsets of Mantle Cell Lymphoma Defined by the IGHV Mutational Status and SOX11 Expression Have Distinct Biologic and Clinical Features. Cancer Res 72:5307-5316
46. Rosenwald A, Wright G, Wiestner A, et al: The proliferation gene expression signature is a quantitative integrator of oncogenic events that predicts survival in mantle cell lymphoma. Cancer Cell 3:185-97, 2003
47. Katzenberger T, Petzoldt C, Holler S, et al: The Ki67 proliferation index is a quantitative indicator of clinical risk in mantle cell lymphoma. Blood 107:3407, 2006
48. Determann O, Hoster E, Ott G, et al: Ki-67 predicts outcome in advanced-stage mantle cell lymphoma patients treated with anti-CD20 immunochemotherapy: results from randomized trials of the European MCL Network and the German Low Grade Lymphoma Study Group. Blood 111:2385-7, 2008
49. Tiemann M, Schrader C, Klapper W, et al: Histopathology, cell proliferation indices and clinical outcome in 304 patients with mantle cell lymphoma (MCL): a clinicopathological study from the European MCL Network. Br J Haematol 131:29-38, 2005
50. Klapper W, Hoster E, Determann O, et al: Ki-67 as a prognostic marker in mantle cell lymphoma-consensus guidelines of the pathology panel of the European MCL Network. J Hematop, 2009
51. Hoster E, Dreyling M, Klapper W, et al: A new prognostic index (MIPI) for patients with advanced-stage mantle cell lymphoma. Blood 111:558-65, 2008
52. Pott C, Hoster E, Delfau-Larue MH, et al: Molecular remission is an independent predictor of clinical outcome in patients with mantle cell lymphoma after combined immunochemotherapy: a European MCL intergroup study. Blood 115:3215-23, 2010
53. Liu H, Johnson JL, Koval G, et al: Detection of minimal residual disease following induction immunochemotherapy predicts progression free survival in mantle cell lymphoma: final results of CALGB 59909. Haematologica 97:579-85, 2012
54. Hartmann E, Fernandez V, Moreno V, et al: Five-gene model to predict survival in mantle-cell lymphoma using frozen or formalin-fixed, paraffin-embedded tissue. J Clin Oncol 26:4966-72, 2008
55. Enjuanes A, Fernandez V, Hernandez L, et al: Identification of methylated genes associated with aggressive clinicopathological features in mantle cell lymphoma. PLoS One 6:e19736, 2011
56. Iqbal J, Shen Y, Liu Y, et al: Genome-wide miRNA profiling of mantle cell lymphoma reveals a distinct subgroup with poor prognosis. Blood 119:4939-48, 2012
57. Furtado M, Shah N, Levoguer A, et al: Abnormal serum free light chain ratio predicts poor overall survival in mantle cell lymphoma. Br J Haematol, 2012
58. Vandenberghe E, De Wolf-Peeters C, Vaughan Hudson G, et al: The clinical outcome of 65 cases of mantle cell lymphoma initially treated with non-intensive therapy by the British National Lymphoma Investigation Group. Br J Haematol 99:842-7, 1997

59. Leitch HA, Gascoyne RD, Chhanabhai M, et al: Limited-stage mantle-cell lymphoma. Ann Oncol 14:1555-61, 2003
60. Rosenbluth BD, Yahalom J: Highly effective local control and palliation of mantle cell lymphoma with involved-field radiation therapy (IFRT). Int J Radiat Oncol Biol Phys 65:1185-91, 2006
61. Rule S, Smith P, Johnson PW, et al: The Addition of Rituximab to Fludarabine and Cyclophosphamide (FC) Improves Overall Survival in Newly Diagnosed Mantle Cell Lymphoma (MCL): Results of the Randomised UK National Cancer Research Institute (NCRI) Trial. ASH Annual Meeting Abstracts 118:440-, 2011
62. Howard OM, Gribben JG, Neuberg DS, et al: Rituximab and CHOP induction therapy for newly diagnosed mantle-cell lymphoma: molecular complete responses are not predictive of progression-free survival. J Clin Oncol 20:1288-94, 2002
63. Lenz G, Dreyling M, Hoster E, et al: Immunochemotherapy with rituximab and cyclophosphamide, doxorubicin, vincristine, and prednisone significantly improves response and time to treatment failure, but not long-term outcome in patients with previously untreated mantle cell lymphoma: results of a prospective randomized trial of the German Low Grade Lymphoma Study Group (GLSG). J Clin Oncol 23:1984-92, 2005
64. Schulz H, Bohlius JF, Trelle S, et al: Immunochemotherapy with rituximab and overall survival in patients with indolent or mantle cell lymphoma: a systematic review and meta-analysis. J Natl Cancer Inst 99:706-14, 2007
65. Dreyling M, Lenz G, Hoster E, et al: Early consolidation by myeloablative radiochemotherapy followed by autologous stem cell transplantation in first remission significantly prolongs progression-free survival in mantle-cell lymphoma: results of a prospective randomized trial of the European MCL Network. Blood 105:2677-84, 2005
66. Geisler CH, Kolstad A, Laurell A, et al: Long-term progression-free survival of mantle cell lymphoma after intensive front-line immunochemotherapy with in vivo-purged stem cell rescue: a nonrandomized phase 2 multicenter study by the Nordic Lymphoma Group. Blood 112:2687-93, 2008
67. Hermine O, Hoster E, Walewski J, et al: Alternating Courses of 3x CHOP and 3x DHAP Plus Rituximab Followed by a High Dose ARA-C Containing Myeloablative Regimen and Autologous Stem Cell Transplantation (ASCT) Increases Overall Survival When Compared to 6 Courses of CHOP Plus Rituximab Followed by Myeloablative Radiochemotherapy and ASCT In Mantle Cell Lymphoma: Fnal Analysis of the MCL Younger Trial of the European Mantle Cell Lymphoma Network (MCL net). Presented at the ASH Annual Meeting Abstracts, Atlanta, GA, December 9, 2012, 2012
68. Romaguera JE, Fayad LE, Feng L, et al: Ten-year follow-up after intense chemoimmunotherapy with Rituximab-HyperCVAD alternating with Rituximab-high dose methotrexate/cytarabine (R-MA) and without stem cell transplantation in patients with untreated aggressive mantle cell lymphoma. Br J Haematol 150:200-8, 2010
69. Merli F, Luminari S, Ilariucci F, et al: Rituximab plus HyperCVAD alternating with high dose cytarabine and methotrexate for the initial treatment of patients with mantle cell lymphoma, a multicentre trial from Gruppo Italiano Studio Linfomi. Br J Haematol 156:346-53, 2012
70. Bosch F, Lopez-Guillermo A, Campo E, et al: Mantle cell lymphoma: presenting features, response to therapy, and prognostic factors. Cancer 82:567-75, 1998
71. Weisenburger DD, Vose JM, Greiner TC, et al: Mantle cell lymphoma. A clinicopathologic study of 68 cases from the Nebraska Lymphoma Study Group. Am J Hematol 64:190-6, 2000
72. Kluin-Nelemans HC, Hoster E, Hermine O, et al: Treatment of older patients with mantle-cell lymphoma. N Engl J Med 367:520-31

73. Maris MB, Sandmaier BM, Storer BE, et al: Allogeneic hematopoietic cell transplantation after fludarabine and 2 Gy total body irradiation for relapsed and refractory mantle cell lymphoma. Blood 104:3535-42, 2004
74. A. J. Wagner DHVH, P. M. LoRusso, R. Tibes, K. E. Mazina, J. A. Ware, Y. Yan, M. K. Derynck, G. D. Demetri: A first-in-human phase I study to evaluate the pan-PI3K inhibitor GDC-0941 administered QD or BID in patients with advanced solid tumors. Presented at the ASCO Annual Meeting, 2009
75. Inwards DJ, Fishkin PA, Hillman DW, et al: Long-term results of the treatment of patients with mantle cell lymphoma with cladribine (2-CDA) alone (95-80-53) or 2-CDA and rituximab (N0189) in the North Central Cancer Treatment Group. Cancer 113:108-16, 2008
76. Forstpointner R, Dreyling M, Repp R, et al: The addition of rituximab to a combination of fludarabine, cyclophosphamide, mitoxantrone (FCM) significantly increases the response rate and prolongs survival as compared with FCM alone in patients with relapsed and refractory follicular and mantle cell lymphomas: results of a prospective randomized study of the German Low-Grade Lymphoma Study Group. Blood 104:3064-71, 2004
77. Coleman M, Martin P, Ruan J, et al: Low-dose metronomic, multidrug therapy with the PEP-C oral combination chemotherapy regimen for mantle cell lymphoma. Leuk Lymphoma 49:447-50, 2008
78. Ansell SM, Inwards DJ, Rowland KM, Jr., et al: Low-dose, single-agent temsirolimus for relapsed mantle cell lymphoma: a phase 2 trial in the North Central Cancer Treatment Group. Cancer 113:508-14, 2008
79. Goy A, Bernstein SH, Kahl BS, et al: Bortezomib in patients with relapsed or refractory mantle cell lymphoma: updated time-to-event analyses of the multicenter phase 2 PINNACLE study. Ann Oncol 20:520-5, 2009
80. Kouroukis CT, Fernandez LA, Crump M, et al: A phase II study of bortezomib and gemcitabine in relapsed mantle cell lymphoma from the National Cancer Institute of Canada Clinical Trials Group (IND 172). Leuk Lymphoma 52:394-9, 2011
81. Morschhauser F, Depil S, Jourdan E, et al: Phase II study of gemcitabine-dexamethasone with or without cisplatin in relapsed or refractory mantle cell lymphoma. Ann Oncol 18:370-5, 2007
82. Whitman M, Kaplan DR, Schaffhausen B, et al: Association of phosphatidylinositol kinase activity with polyoma middle-T competent for transformation. Nature 315:239-42, 1985
83. Whitman M, Downes CP, Keeler M, et al: Type I phosphatidylinositol kinase makes a novel inositol phospholipid, phosphatidylinositol-3-phosphate. Nature 332:644-6, 1988
84. Druker BJ, Ling LE, Cohen B, et al: A completely transformation-defective point mutant of polyomavirus middle T antigen which retains full associated phosphatidylinositol kinase activity. J Virol 64:4454-61, 1990
85. Vanhaesebroeck B, Stephens L, Hawkins P: PI3K signalling: the path to discovery and understanding. Nat Rev Mol Cell Biol 13:195-203
86. Perez-Galan P, Mora-Jensen H, Weniger MA, et al: Bortezomib resistance in mantle cell lymphoma is associated with plasmacytic differentiation. Blood 117:542-52, 2011
87. Carpenter CL, Duckworth BC, Auger KR, et al: Purification and characterization of phosphoinositide 3-kinase from rat liver. J Biol Chem 265:19704-11, 1990
88. Morgan SJ, Smith AD, Parker PJ: Purification and characterization of bovine brain type I phosphatidylinositol kinase. Eur J Biochem 191:761-7, 1990
89. Hiles ID, Otsu M, Volinia S, et al: Phosphatidylinositol 3-kinase: structure and expression of the 110 kd catalytic subunit. Cell 70:419-29, 1992
90. Vanhaesebroeck B, Welham MJ, Kotani K, et al: P110delta, a novel phosphoinositide 3-kinase in leukocytes. Proc Natl Acad Sci U S A 94:4330-5, 1997

91. Chantry D, Vojtek A, Kashishian A, et al: p110delta, a novel phosphatidylinositol 3-kinase catalytic subunit that associates with p85 and is expressed predominantly in leukocytes. J Biol Chem 272:19236-41, 1997
92. Zvelebil MJ, MacDougall L, Leevers S, et al: Structural and functional diversity of phosphoinositide 3-kinases. Philos Trans R Soc Lond B Biol Sci 351:217-23, 1996
93. Vanhaesebroeck B, Leevers SJ, Panayotou G, et al: Phosphoinositide 3-kinases: a conserved family of signal transducers. Trends Biochem Sci 22:267-72, 1997
94. Escobedo JA, Navankasattusas S, Kavanaugh WM, et al: cDNA cloning of a novel 85 kd protein that has SH2 domains and regulates binding of PI3-kinase to the PDGF beta-receptor. Cell 65:75-82, 1991
95. Myers MG, Jr., Backer JM, Sun XJ, et al: IRS-1 activates phosphatidylinositol 3'-kinase by associating with src homology 2 domains of p85. Proc Natl Acad Sci U S A 89:10350-4, 1992
96. Backer JM, Myers MG, Jr., Shoelson SE, et al: Phosphatidylinositol 3'-kinase is activated by association with IRS-1 during insulin stimulation. EMBO J 11:3469-79, 1992
97. Maehama T, Dixon JE: The tumor suppressor, PTEN/MMAC1, dephosphorylates the lipid second messenger, phosphatidylinositol 3,4,5-trisphosphate. J Biol Chem 273:13375-8, 1998
98. Burgering BM, Coffer PJ: Protein kinase B (c-Akt) in phosphatidylinositol-3-OH kinase signal transduction. Nature 376:599-602, 1995
99. Hawkins PT, Eguinoa A, Qiu RG, et al: PDGF stimulates an increase in GTP-Rac via activation of phosphoinositide 3-kinase. Curr Biol 5:393-403, 1995
100. Stephens L, Anderson K, Stokoe D, et al: Protein kinase B kinases that mediate phosphatidylinositol 3,4,5-trisphosphate-dependent activation of protein kinase B. Science 279:710-4, 1998
101. Alessi DR, James SR, Downes CP, et al: Characterization of a 3-phosphoinositide-dependent protein kinase which phosphorylates and activates protein kinase Balpha. Curr Biol 7:261-9, 1997
102. Potter CJ, Pedraza LG, Xu T: Akt regulates growth by directly phosphorylating Tsc2. Nat Cell Biol 4:658-65, 2002
103. Kotani K, Yonezawa K, Hara K, et al: Involvement of phosphoinositide 3-kinase in insulin- or IGF-1-induced membrane ruffling. EMBO J 13:2313-21, 1994
104. Wymann M, Arcaro A: Platelet-derived growth factor-induced phosphatidylinositol 3-kinase activation mediates actin rearrangements in fibroblasts. Biochem J 298 Pt 3:517-20, 1994
105. Okada T, Kawano Y, Sakakibara T, et al: Essential role of phosphatidylinositol 3-kinase in insulin-induced glucose transport and antilipolysis in rat adipocytes. Studies with a selective inhibitor wortmannin. J Biol Chem 269:3568-73, 1994
106. Hara K, Yonezawa K, Sakaue H, et al: 1-Phosphatidylinositol 3-kinase activity is required for insulin-stimulated glucose transport but not for RAS activation in CHO cells. Proc Natl Acad Sci U S A 91:7415-9, 1994
107. Samuels Y, Wang Z, Bardelli A, et al: High frequency of mutations of the PIK3CA gene in human cancers. Science 304:554, 2004
108. Fruman DA, Snapper SB, Yballe CM, et al: Impaired B cell development and proliferation in absence of phosphoinositide 3-kinase p85alpha. Science 283:393-7, 1999
109. Suzuki H, Terauchi Y, Fujiwara M, et al: Xid-like immunodeficiency in mice with disruption of the p85alpha subunit of phosphoinositide 3-kinase. Science 283:390-2, 1999
110. Bi L, Okabe I, Bernard DJ, et al: Proliferative defect and embryonic lethality in mice homozygous for a deletion in the p110alpha subunit of phosphoinositide 3-kinase. J Biol Chem 274:10963-8, 1999
111. Okkenhaug K, Bilancio A, Farjot G, et al: Impaired B and T cell antigen receptor signaling in p110delta PI 3-kinase mutant mice. Science 297:1031-4, 2002
112. Foukas LC, Claret M, Pearce W, et al: Critical role for the p110alpha phosphoinositide-3-OH kinase in growth and metabolic regulation. Nature 441:366-70, 2006

113. Jou ST, Carpino N, Takahashi Y, et al: Essential, nonredundant role for the phosphoinositide 3-kinase p110delta in signaling by the B-cell receptor complex. Mol Cell Biol 22:8580-91, 2002
114. Arcaro A, Wymann MP: Wortmannin is a potent phosphatidylinositol 3-kinase inhibitor: the role of phosphatidylinositol 3,4,5-trisphosphate in neutrophil responses. Biochem J 296 (Pt 2):297-301, 1993
115. Vlahos CJ, Matter WF, Hui KY, et al: A specific inhibitor of phosphatidylinositol 3-kinase, 2-(4-morpholinyl)-8-phenyl-4H-1-benzopyran-4-one (LY294002). J Biol Chem 269:5241-8, 1994
116. Sadhu C, Masinovsky B, Dick K, et al: Essential role of phosphoinositide 3-kinase delta in neutrophil directional movement. J Immunol 170:2647-54, 2003
117. Jackson SP, Schoenwaelder SM, Goncalves I, et al: PI 3-kinase p110beta: a new target for antithrombotic therapy. Nat Med 11:507-14, 2005
118. Hu P, Mondino A, Skolnik EY, et al: Cloning of a novel, ubiquitously expressed human phosphatidylinositol 3-kinase and identification of its binding site on p85. Mol Cell Biol 13:7677-88, 1993
119. Gupta S, Ramjaun AR, Haiko P, et al: Binding of ras to phosphoinositide 3-kinase p110alpha is required for ras-driven tumorigenesis in mice. Cell 129:957-68, 2007
120. Delgado P, Cubelos B, Calleja E, et al: Essential function for the GTPase TC21 in homeostatic antigen receptor signaling. Nat Immunol 10:880-8, 2009
121. Jaiswal BS, Janakiraman V, Kljavin NM, et al: Somatic mutations in p85alpha promote tumorigenesis through class IA PI3K activation. Cancer Cell 16:463-74, 2009
122. Okkenhaug K, Vanhaesebroeck B: PI3K in lymphocyte development, differentiation and activation. Nat Rev Immunol 3:317-30, 2003
123. Okkenhaug K, Ali K, Vanhaesebroeck B: Antigen receptor signalling: a distinctive role for the p110delta isoform of PI3K. Trends Immunol 28:80-7, 2007
124. Vanhaesebroeck B, Ali K, Bilancio A, et al: Signalling by PI3K isoforms: insights from gene-targeted mice. Trends Biochem Sci 30:194-204, 2005
125. Philp AJ, Campbell IG, Leet C, et al: The phosphatidylinositol 3'-kinase p85alpha gene is an oncogene in human ovarian and colon tumors. Cancer Res 61:7426-9, 2001
126. Bi L, Okabe I, Bernard DJ, et al: Early embryonic lethality in mice deficient in the p110beta catalytic subunit of PI 3-kinase. Mamm Genome 13:169-72, 2002
127. Knight ZA, Gonzalez B, Feldman ME, et al: A pharmacological map of the PI3-K family defines a role for p110alpha in insulin signaling. Cell 125:733-47, 2006
128. Zhao JJ, Cheng H, Jia S, et al: The p110alpha isoform of PI3K is essential for proper growth factor signaling and oncogenic transformation. Proc Natl Acad Sci U S A 103:16296-300, 2006
129. Graupera M, Guillermet-Guibert J, Foukas LC, et al: Angiogenesis selectively requires the p110alpha isoform of PI3K to control endothelial cell migration. Nature 453:662-6, 2008
130. Hui RC, Gomes AR, Constantinidou D, et al: The forkhead transcription factor FOXO3a increases phosphoinositide-3 kinase/Akt activity in drug-resistant leukemic cells through induction of PIK3CA expression. Mol Cell Biol 28:5886-98, 2008
131. Yang N, Huang J, Greshock J, et al: Transcriptional regulation of PIK3CA oncogene by NF-kappaB in ovarian cancer microenvironment. PLoS One 3:e1758, 2008
132. Astanehe A, Arenillas D, Wasserman WW, et al: Mechanisms underlying p53 regulation of PIK3CA transcription in ovarian surface epithelium and in ovarian cancer. J Cell Sci 121:664-74, 2008
133. Jia S, Liu Z, Zhang S, et al: Essential roles of PI(3)K-p110beta in cell growth, metabolism and tumorigenesis. Nature 454:776-9, 2008
134. Martin V, Guillermet-Guibert J, Chicanne G, et al: Deletion of the p110beta isoform of phosphoinositide 3-kinase in platelets reveals its central role in Akt activation and thrombus formation in vitro and in vivo. Blood 115:2008-13

135. Kok K, Nock GE, Verrall EA, et al: Regulation of p110delta PI 3-kinase gene expression. PLoS One 4:e5145, 2009
136. Calvanese V, Fernandez AF, Urdinguio RG, et al: A promoter DNA demethylation landscape of human hematopoietic differentiation. Nucleic Acids Res 40:116-31, 2012
137. Srinivasan L, Sasaki Y, Calado DP, et al: PI3 kinase signals BCR-dependent mature B cell survival. Cell 139:573-86, 2009
138. Clayton E, Bardi G, Bell SE, et al: A crucial role for the p110delta subunit of phosphatidylinositol 3-kinase in B cell development and activation. J Exp Med 196:753-63, 2002
139. Jou ST, Carpino N, Takahashi Y, et al: Essential, nonredundant role for the phosphoinositide 3-kinase p110delta in signaling by the B-cell receptor complex. Mol Cell Biol 22:8580-91, 2002
140. Bilancio A, Okkenhaug K, Camps M, et al: Key role of the p110delta isoform of PI3K in B-cell antigen and IL-4 receptor signaling: comparative analysis of genetic and pharmacologic interference with p110delta function in B cells. Blood 107:642-50, 2006
141. Ali K, Bilancio A, Thomas M, et al: Essential role for the p110delta phosphoinositide 3-kinase in the allergic response. Nature 431:1007-11, 2004
142. Patton DT, Garden OA, Pearce WP, et al: Cutting edge: the phosphoinositide 3-kinase p110 delta is critical for the function of CD4+CD25+Foxp3+ regulatory T cells. J Immunol 177:6598-602, 2006
143. Bader AG, Kang S, Vogt PK: Cancer-specific mutations in PIK3CA are oncogenic in vivo. Proc Natl Acad Sci U S A 103:1475-9, 2006
144. Psyrri A, Papageorgiou S, Liakata E, et al: Phosphatidylinositol 3'-kinase catalytic subunit alpha gene amplification contributes to the pathogenesis of mantle cell lymphoma. Clin Cancer Res 15:5724-32, 2009
145. Wee S, Wiederschain D, Maira SM, et al: PTEN-deficient cancers depend on PIK3CB. Proc Natl Acad Sci U S A 105:13057-62, 2008
146. Kang S, Denley A, Vanhaesebroeck B, et al: Oncogenic transformation induced by the p110beta, -gamma, and -delta isoforms of class I phosphoinositide 3-kinase. Proc Natl Acad Sci U S A 103:1289-94, 2006
147. Manning BD, Cantley LC: AKT/PKB signaling: navigating downstream. Cell 129:1261-74, 2007
148. Perez-Galan P, Dreyling M, Wiestner A: Mantle cell lymphoma: biology, pathogenesis, and the molecular basis of treatment in the genomic era. Blood 117:26-38, 2011
149. Lannutti BJ, Meadows SA, Herman SE, et al: CAL-101, a p110delta selective phosphatidylinositol-3-kinase inhibitor for the treatment of B-cell malignancies, inhibits PI3K signaling and cellular viability. Blood 117:591-4, 2011
150. Herman SE, Gordon AL, Wagner AJ, et al: Phosphatidylinositol 3-kinase-delta inhibitor CAL-101 shows promising preclinical activity in chronic lymphocytic leukemia by antagonizing intrinsic and extrinsic cellular survival signals. Blood 116:2078-88, 2010
151. Hoellenriegel J, Meadows SA, Sivina M, et al: The phosphoinositide 3'-kinase delta inhibitor, CAL-101, inhibits B-cell receptor signaling and chemokine networks in chronic lymphocytic leukemia. Blood 118:3603-12, 2011
152. Rao E, Jiang C, Ji M, et al: The miRNA-17 approximately 92 cluster mediates chemoresistance and enhances tumor growth in mantle cell lymphoma via PI3K/AKT pathway activation. Leukemia 26:1064-72, 2012
153. Kahl B, Byrd JC, Flinn IW, et al: Clinical Safety and Activity In a Phase 1 Study of CAL-101, An Isoform-Selective Inhibitor of Phosphatidylinositol 3-Kinase P110{delta}, In Patients with Relapsed or Refractory Non-Hodgkin Lymphoma. ASH Annual Meeting Abstracts 116:1777-, 2010
154. V. Moreno Garcia RDB, K. J. Shah, B. Basu, N. Tunariu, M. Blanco, P. A. Cassier, J. V. Pedersen, M. Puglisi, D. Sarker, D. Papadatos-Pastos, A. G. Omlin, A. Biondo, J. A. Ware, H.

Koeppen, G. G. Levy, K. E. Mazina, J. S. De Bono: A phase I study evaluating GDC-0941, an oral phosphoinositide-3 kinase (PI3K) inhibitor, in patients with advanced solid tumors or multiple myeloma. Presented at the ASCO, 2011
155. Wang M, Zhang L, Han X, et al: Atiprimod inhibits the growth of mantle cell lymphoma in vitro and in vivo and induces apoptosis via activating the mitochondrial pathways. Blood 109:5455-62, 2007
156. Weston VJ, Oldreive CE, Skowronska A, et al: The PARP inhibitor olaparib induces significant killing of ATM-deficient lymphoid tumor cells in vitro and in vivo. Blood 116:4578-87
157. Wang M, Zhang L, Han X, et al: A severe combined immunodeficient-hu in vivo mouse model of human primary mantle cell lymphoma. Clin Cancer Res 14:2154-60, 2008
158. Shultz LD, Ishikawa F, Greiner DL: Humanized mice in translational biomedical research. Nat Rev Immunol 7:118-30, 2007
159. Carvalho S, Milanezi F, Costa JL, et al: PIKing the right isoform: the emergent role of the p110beta subunit in breast cancer. Virchows Arch 456:235-43
160. Abbott RT, Tripp S, Perkins SL, et al: Analysis of the PI-3-Kinase-PTEN-AKT pathway in human lymphoma and leukemia using a cell line microarray. Mod Pathol 16:607-12, 2003
161. Baker AF, Dragovich T, Ihle NT, et al: Stability of phosphoprotein as a biological marker of tumor signaling. Clin Cancer Res 11:4338-40, 2005
162. Burns JA, Li Y, Cheney CA, et al: Choice of fixative is crucial to successful immunohistochemical detection of phosphoproteins in paraffin-embedded tumor tissues. J Histochem Cytochem 57:257-64, 2009
163. Folkes AJ, Ahmadi K, Alderton WK, et al: The identification of 2-(1H-indazol-4-yl)-6-(4-methanesulfonyl-piperazin-1-ylmethyl)-4-morpholin-4-yl-t hieno[3,2-d]pyrimidine (GDC-0941) as a potent, selective, orally bioavailable inhibitor of class I PI3 kinase for the treatment of cancer. J Med Chem 51:5522-32, 2008
164. Jamieson S, Flanagan JU, Kolekar S, et al: A drug targeting only p110alpha can block phosphoinositide 3-kinase signalling and tumour growth in certain cell types. Biochem J 438:53-62, 2011
165. Skaletsky SRaHJ: Primer3 on the WWW for general users and for biologist programmers. Bioinformatics Methods and Protocols: Methods in Molecular Biology:365-386, 2000
166. Camp RL, Dolled-Filhart M, Rimm DL: X-tile: a new bio-informatics tool for biomarker assessment and outcome-based cut-point optimization. Clin Cancer Res 10:7252-9, 2004
167. McKay P, Leach M, Jackson R, et al: Guidelines for the investigation and management of mantle cell lymphoma. Br J Haematol 159:405-26, 2012
168. Jadayel DM, Lukas J, Nacheva E, et al: Potential role for concurrent abnormalities of the cyclin D1, p16CDKN2 and p15CDKN2B genes in certain B cell non-Hodgkin's lymphomas. Functional studies in a cell line (Granta 519). Leukemia 11:64-72, 1997
169. Ramadani F, Bolland DJ, Garcon F, et al: The PI3K isoforms p110alpha and p110delta are essential for pre-B cell receptor signaling and B cell development. Sci Signal 3:ra60, 2010
170. Gharbi SI, Zvelebil MJ, Shuttleworth SJ, et al: Exploring the specificity of the PI3K family inhibitor LY294002. Biochem J 404:15-21, 2007
171. Barr PM, Hernandez-Ilizaliturri FJ, Murante T, et al: Comprehensive in Vitro and in Vivo Analysis of Phosphatidylinositol-3-Kinase Delta (PI3K{delta}) Inhibition Using GS-1101 (CAL-101) in Combination with Mammalian Target of Rapamycin (mTOR) Inhibition Using Temsirolimus or Everolimus in Mantle Cell Lymphoma (MCL). ASH Annual Meeting Abstracts 120:3719-, 2012
172. Chiron D, Martin P, Liberto MD, et al: Induction of Early G1-Arrest by CDK4/CDK6 Inhibition Sensitizes Mantle Cell Lymphoma Cells to Selective PI3K{delta} Inhibition by GS-1101 Through Enhancing the Magnitude and Duration of p-AKT Inhibition. ASH Annual Meeting Abstracts 120:791-, 2012

173. O'Brien C, Wallin JJ, Sampath D, et al: Predictive biomarkers of sensitivity to the phosphatidylinositol 3' kinase inhibitor GDC-0941 in breast cancer preclinical models. Clin Cancer Res 16:3670-83, 2010
174. Janku F, Wheler JJ, Naing A, et al: PIK3CA mutation H1047R is associated with response to PI3K/AKT/mTOR signaling pathway inhibitors in early-phase clinical trials. Cancer Res 73:276-84, 2013
175. Stengel C, Cheung CW, Quinn J, et al: Optimal induction of myeloma cell death requires dual blockade of phosphoinositide 3-kinase and mTOR signalling and is determined by translocation subtype. Leukemia, 2012
176. Shepherd C, Banerjee L, Cheung CW, et al: PI3K/mTOR inhibition upregulates NOTCH-MYC signalling leading to an impaired cytotoxic response. Leukemia, 2012
177. Fernandez V, Salamero O, Espinet B, et al: Genomic and gene expression profiling defines indolent forms of mantle cell lymphoma. Cancer Res 70:1408-18, 2010
178. Cutts RJ, Dayem Ullah AZ, Sangaralingam A, et al: O-miner: an integrative platform for automated analysis and mining of -omics data. Nucleic Acids Res 40:W560-8, 2012
179. Bagnara D, Kaufman MS, Calissano C, et al: A novel adoptive transfer model of chronic lymphocytic leukemia suggests a key role for T lymphocytes in the disease. Blood 117:5463-72
180. Pearce DJ, Taussig D, Zibara K, et al: AML engraftment in the NOD/SCID assay reflects the outcome of AML: implications for our understanding of the heterogeneity of AML. Blood 107:1166-73, 2006
181. Vasudevan KM, Barbie DA, Davies MA, et al: AKT-independent signaling downstream of oncogenic PIK3CA mutations in human cancer. Cancer Cell 16:21-32, 2009
182. Kim A, Park S, Lee JE, et al: The dual PI3K and mTOR inhibitor NVP-BEZ235 exhibits anti-proliferative activity and overcomes bortezomib resistance in mantle cell lymphoma cells. Leuk Res 36:912-20, 2012

APPENDIX

APPENDIX A

Preparing cell blocks from cell suspensions

Two methods of cell block preparation, one using agar and the other using thrombin, were compared. The thrombin cell block method was superior at preserving cell morphology and was less time consuming. A comparison of the morphology obtained by using the two methods with the K562 cell line is shown in figure A1.

Agar cell block: 2% agar was prepared by adding 1g of powdered agar to 50ml PBS in a beaker. The solution was heated in a microwave at low power until all the agar had dissolved and a clear solution was obtained (approximately 2 minutes). The beaker was then placed in a pre-heated water bath at 50°C. Approximately 10-15 x 10^6 cells were centrifuged at 400xg for 5 minutes in a 15ml conical tube. The tube was inverted on filter paper for a minute and placed in the same water bath as the beaker for 1-2 minutes. The agar solution was then added in equal volume to the cells and the mixture was agitated. Following centrifugation at 100xg for 2 minutes, the agar was allowed to set by incubating the tube for 10-15 minutes at 4°C. The block was then gently teased out into formalin for fixation and subsequent embedding in paraffin.

Thrombin cell block: Approximately 10-15 x 10^6 cells were centrifuged at 400xg for 5 minutes in a 15ml conical tube. The tube was then inverted over filter paper for one minute following which the pellet was re-suspended in 3 to 5 drops each of human control plasma and thromboplastin. Once congealed into a fibrin clot, the block was left at 4°C for 15 minutes. This was then gently teased out into formalin for fixation and subsequent embedding in paraffin.

Figure A1 Comparative morphology of agar and thrombin cell blocks prepared from the K562 leukaemia cell line

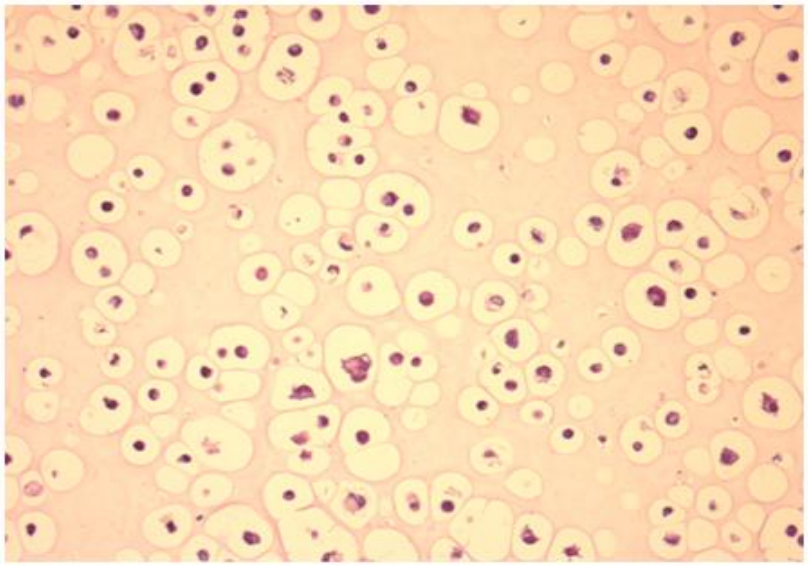

K562 in 2% agar

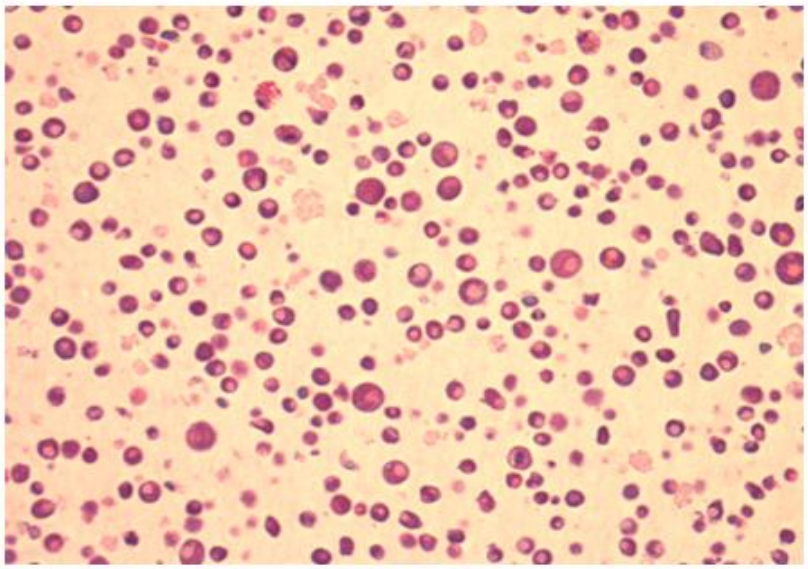

K562 in thrombin

APPENDIX B

A summary of clinical information and IHC scores for samples in the MCL TMA

As described in chapter 2, the large majority of MCL biopsies incorporated into the TMA were taken from patients with relapsed lymphoma. The cores were divided among 6 TMA slides 03A-2009 to 03F-2009. TMA slide maps were constructed with rows on the grid labelled alphabetically and columns labelled numerically. Each core could therefore be identified by the TMA slide number (e.g. TMA-03A-2009) and row/column co-ordinates (e.g. B12). Triplicate cores were arrayed consecutively, for e.g. A01-A03. The table on the following page (Table A1) displays average scores against the 1st core of the triplicate e.g. A01. Scores for the class Ia isoforms p110alpha, p110beta and p110delta were derived from visual analysis parameters obtained from Ariol SL-50 version 3.2 while PTEN and Ki67 were scored by eye (Dr Abigail Lee and Dr Sunil Iyengar).

Clinical information relating to timing of the biopsy and overall survival were kindly provided by Janet Mathews and Dr Rebecca Auer. Information on blastoid morphology was obtained from the original biopsy reports and confirmed on the TMA slides by Dr Maria Calaminici.

Table A1. Summary of IHC scores for class Ia PI3K isoforms, PTEN and Ki-67 and clinical information relating to MCL cores studied using the TMA technique (OS=overall survival).

TMA	SPOT	HOSP.NO	Biopsy at	OS (mths)	p110alpha	p110beta	p110delta	PTEN	Ki67 (%)	Blastoid?
03A-2009	A01	6358898	Relapse		55.72	82.86	70.39	1	93.7	yes
03A-2009	A04	F719526	1st relapse		39.11	5.51	76.86	1	23	
03A-2009	B03	M609903	Diagnosis/pretreatment	30	39.43	0.28	102.45	1	13	
03A-2009	B09	M508414	Relapse		22.45	7.28	78.21	neg	2.3	
03A-2009	B12	M658480	Relapse		16.4	0.92	81.20	1	20	
03A-2009	C01	6307612	Relapse		30.91	8.77	91.86	2	73.3	yes
03E-2009	F09	6517867	4th Relapse		44.36	0.72	82.72	1	21.7	
03E-2009	F12	6517867	4th Relapse		58.43	1.79	87.00	2	21.7	
03A-2009	C05	6043657	1st relapse		28.35	1.09	61.42	1	22.3	
03A-2009	C08	M87891	Diagnosis/pretreatment	65				neg		
03A-2009	C11	M87891	2nd relapse		5.78	0.44	44.45	neg	2	
03A-2009	D01	M502305	Relapse		60.06	19.73	68.34	1	21.3	
03A-2009	D04	M502305	Relapse		96.03	9.04	86.58		15.5	
03A-2009	D07	F616651	Diagnosis/pretreatment	25	6.87	15.17	66.57	1		
03A-2009	D10	M287253	Diagnosis/pretreatment	24	97.8	68.65	72.50	2	6.7	
03A-2009	D13	F624798	Diagnosis/pretreatment	60	53.23	26.32	95.81	1	17	
03A-2009	E03	F624798	1st relapse		95.68		87.70	1	3	
03A-2009	E06	F624798	2nd relapse		119.11	71.48	80.13	1	18.3	
03A-2009	E09	M631054	Diagnosis/pretreatment		46.6	20.8	92.07		51.7	yes
03A-2009	E12	M580030	Diagnosis/pretreatment	33	9.51	1.96	97.63	1	5	
03A-2009	F01	M580030	1st relapse		19.7	0.29	97.39	1	19	
03A-2009	F04	M580030	2nd relapse		84.3	4	79.38	1	22.7	
03E-2009	C06	6260113	Relapse		23.28		38.33		26	
03E-2009	C09	6260113	1st relapse		19.35	0.13	42.01	1	16	
03A-2009	F07	M581475	Diagnosis/pretreatment	58	21.69	1.15	82.57	1	3.3	
03A-2009	F10	M581475	3rd relapse		94.47	2.7	83.13	1	6.7	
03F-2009	B04	6174385	1st relapse		58.17	4.31	97.54		39	

TMA	SPOT	HOSP.NO	Biopsy at	OS (mths)	p110alpha	p110beta	p110delta	PTEN	Ki67 (%)	Blastoid?
03A-2009	F13	M684797	3rd Relapse		106.92	3.32	88.19	1	49.3	
03A-2009	G05	M768355	Not known		69.99	9.9	73.44	1	24	
03A-2009	G09	6176589	1st relapse		34.99	4.21	64.88	2	21.3	
03A-2009	G12	M600816	Diagnosis/pretreatment	5	29.48	2.51	13.72		17.7	
03A-2009	H01	PP	Not known		15.33	85.34	48.75		2.3	
03A-2009	H08	M640685	1st relapse		61.89	117.24	120.34	2	23.3	
03A-2009	H04	6107842	Diagnosis		90.07	40.2	85.82	1	16.7	
03F-2009	A11	6107842	Progression		58.63	1.32	96.16		14.7	
03A-2009	H11	6168205	Relapse		108.98	6.19	102.86	1	20	yes
03F-2009	B01	6168205	Relapse		77.49	0.14	81.52	1	41	yes
03A-2009	H14	F584365	Relapse		1.15	0.21	2.76	1	18.7	
03A-2009	I03	M526896	Relapse		84.55	3.12	94.34	1	10	
03A-2009	I06	M526896	Relapse		98.34	8.16	77.66	neg	6.7	
03B-2009	H07	M697593	Diagnosis/pretreatment	20	68.7	27.5	80.22	neg	18.3	yes
03E-2009	D01	6182106	Relapse		9.71	1.03	20.46	1	37.7	
03F-2009	B11	6358889	1st relapse blastoid		31.91	11.91	73.75	2	78.3	yes
03B-2009	A01	M697679	Diagnosis/pretreatment	27			11.30	2		
03B-2009	A11	M585844	1st relapse		74.1	32.6	87.77	1	11.5	
03B-2009	A14	M681984	Relapse		109.2	2.64	78.56		3.7	
03B-2009	B02	M681984	Relapse				95.69	1	18	
03B-2009	B05	6347968	Relapse		59.87	64.76	78.32	2	60.7	yes
03B-2009	B08	6281796	Diagnosis/pretreatment	28	42.87	6.12	80.52	neg	14	
03B-2009	B12	F840839	Not known		68.03	23.69	86.31		20.3	
03B-2009	B15	M594944	Diagnosis/pretreatment	8	33.52			1		
03B-2009	C03	M779624	Relapse		89.89	10.25	87.78	2	50.7	yes
03F-2009	A04	M650978	2nd relapse		79.76	4.59	97.05	1	18	
03B-2009	C12	M614054	Relapse					1		
03E-2009	A05	M783398	Relapsed / refractory			2.7	10.04	1	6	
03B-2009	C15	6227465	Diagnosis/pretreatment	108*	43.06	1.08	82.31	neg	21	
03E-2009	F02	6227465	2nd relapse		38.6	22.15	91.02	2	17	
03B-2009	D03	M563251	Relapse					1	21	

TMA	SPOT	HOSP.NO	Biopsy at	OS (mths)	p110alpha	p110beta	p110delta	PTEN	Ki67 (%)	Blastoid?
03B-2009	D07	M563251	Relapse				90.54	neg	7	
03B-2009	D10	M648098	Relapse		130.29	32.07	96.79		14.3	
03B-2009	D13	PP	Not known		103.7	49.05	76.20	1	21.3	
03E-2009	E11	6390360	Diagnosis/pretreatment	13	35.98	18.77	57.72		97.3	
03B-2009	E01	245367LC	Diagnosis/pretreatment	17	59.85	1.8	55.03		23	
03B-2009	E04	F523754	Diagnosis/pretreatment	61				1	15.5	
03B-2009	E07	F523754	3rd relapse				94.73	2	24.7	
03B-2009	E10	F648335	Diagnosis/pretreatment		33.99	12.91	107.93	1	15.5	
03B-2009	E13	M671739	Diagnosis/pretreatment	111	17.49	2.27	87.63	1	8	
03B-2009	F02	M671739	1st relapse		79.47	15.09	83.54	1	17.7	
03B-2009	F08	M671739	2nd relapse		128.96	3.32	88.54	1	18	
03B-2009	F14	M737477	Diagnosis/pretreatment	24	82.12	34.03	70.78		26.7	
03B-2009	G02	M737477	1st relapse		70.39	50.58	76.73		26.3	
03B-2009	G05	M685216	Diagnosis/pretreatment	3	32.06	1.79	45.89	2	13.7	
03B-2009	G12	M718014	Diagnosis/pretreatment	44	69.84	60.86	79.19		12	
03E-2009	A08	M579242	Diagnosis/pretreatment	nine		3.66	75.95	1	22	
03B-2009	H03	M599142	Diagnosis/pretreatment	6				1	20.7	
03B-2009	H10	M768402	Relapse		161.94	1.28	69.00	1	10.3	
03B-2009	H13	M768402	Relapse		113.89	3.58	76.21	1	15.3	
03B-2009	I01	M768402	Relapse		135.97	1.88	85.19	1	16.3	
03F-2009	C01	6437550	Diagnosis/pretreatment	9	37.91	6.78	58.41	2	70.3	yes
03E-2009	B12	6127836	Diagnosis/pre-treatment		9.37	1.39	72.78	1	17.3	
03C-2009	A01	6000212	Relapse		37.3	67.61	80.27	2	42.7	
03E-2009	C03	6026752	1st relapse		14.02		50.05		1	
03C-2009	A11	M597347	Diagnosis/pretreatment	40	4.99	0.11	30.39	2	23.7	
03C-2009	A14	M597347	post-treatment		4.78	0.77	65.00	1	13	
03C-2009	B02	M597347	2nd relapse		88.5	26.5	110.57	1	26	yes
03C-2009	B06	M604432	Diagnosis/pretreatment	41	24.45	7.26	104.59	1	22.7	yes
03C-2009	B09	M604432	1st relapse		2.26	7.36	66.10	2	13.7	yes
03C-2009	B12	M685565	Diagnosis/pretreatment	25	22.81	1.75	35.79	neg	14	yes
03C-2009	B15	M685565	Diagnosis/pretreatment		29.35	2.95	99.61		18	yes

TMA	SPOT	HOSP.NO	Biopsy at	OS (mths)	p110alpha	p110beta	p110delta	PTEN	Ki67 (%)	Blastoid?
03C-2009	C03	M685565	1st relapse - high grade		13.74	3.34	79.33	1	55	yes
03E-2009	F05	1216497WH	2nd Relapse		58.23	1.66	93.59	2	22	
03E-2009	G10	1216497WH	2nd relapse (later time point)		35.99	0.3	81.02	2	28	
03C-2009	C06	M532967	Relapse		44.67	7.94	74.37	1	15.7	
03C-2009	C09	M532967	Relapse		4.05	0.6	61.14	1	1	
03C-2009	C12	M756673	Diagnosis/pretreatment	44	27.8	1.58	12.87	1	1	
03C-2009	C15	M756673	1st relapse		60	25.61	63.42	2	53	yes
03C-2009	D04	104388HA	Relapse		53.59	2.61	92.52	1	17.3	yes
03C-2009	D07	104388HA	Relapse		4.46		94.87	2	33	yes
03C-2009	D10	F822553	Diagnosis/pretreatment	16	68.62	6.19	98.77	1	17.3	
03C-2009	D13	M504990	Diagnosis/pretreatment							
03C-2009	E01	M504990	Relapse		21.09	2.02	78.82	neg	30.5	yes
03C-2009	E04	M504990	Relapse		10.92	3.79	43.06	neg	28.7	yes
03C-2009	E07	6319093	Relapse		34.92	13.02	82.15	2	80.3	yes
03C-2009	E13	6182142	Relapse		57.7	1.17	89.28	1	9.3	yes
03C-2009	F01	M503906	Diagnosis/pretreatment	13	16.48	2.87	84.56		38.5	
03C-2009	F05	M790203	Diagnosis/pretreatment		53.7	10.23	100.58	1	8.7	
03C-2009	F08	M715889	Diagnosis/pretreatment		48.96	0.97	96.87	neg	20.3	
03C-2009	F11	M715889	Relapse		135.56	8.63	96.32	neg	4.3	
03C-2009	F14	6307615	Not known		30.61	3.06	76.03	2	20	
03C-2009	G02	M500046	Relapse		58.5	5.48	91.25	1	6.7	
03C-2009	G06	6023295	Relapse		48.35	0.5	101.07	1	14.3	
03C-2009	G09	M507789	Diagnosis/pretreatment	21	49.99	6.83	70.49	1	17.7	
03C-2009	G12	M507789	1st relapse		18.52	1.43	98.19	1	19.7	
03C-2009	G15	M638655	Diagnosis/pretreatment	35		2.77	116.98		5.3	
03C-2009	H04	PP	Relapse		41.32	1.23	99.87	1	37.3	
03C-2009	H07	6382107	Relapse					2		
03E-2009	E05	6382107	Relapse		21.83	0.16	74.85	2	67	
03E-2009	E08	6454531	1st relapse (2 previous Rx)		66.53	0.99	73.24	1	29	
03C-2009	H10	F721798	1st relapse		50.51	15.37	81.44	1	44	yes
03C-2009	H13	F721798	Diagnosis/pretreatment	14	36.76	5.41	94.88	1	29	yes

TMA	SPOT	HOSP.NO	Biopsy at	OS (mths)	p110alpha	p110beta	p110delta	PTEN	Ki67 (%)	Blastoid?
03F-2009	A01	F721798	Not known		36.8	0.32	65.19		24.5	yes
03D-2009	A07	6095348	Diagnosis/pretreatment	23	2.4	1.23	88.43		21	
03D-2009	A04	F605183	Relapse	15	32.57	114.86	109.32			
03D-2009	A01	M619107	Relapse		0.48	1.92	64.48	neg	10	
03D-2009	A10	F600214	Not known		69.25	2.7	107.17	neg	16.7	
03D-2009	A14	M529089	Diagnosis/pretreatment	14				neg		
03D-2009	B02	M529089	1st relapse		19.79	53.33	94.01	neg	40	yes
03D-2009	B05	M549401	Relapse		4.99	7.25	97.08	1	11.7	
03D-2009	B09	M549401	Relapse		1.44	5.34	38.93	neg	1	
03D-2009	B12	M584317	Relapse (n=2 or 3)		73.19	35.57	101.56	1	41	yes
03D-2009	B15	6311123	Relapse		52.04	80.56	80.41	2	47.7	
03D-2009	C03	PP	Not known		0.36	0.38	10.34	1	24.7	
03D-2009	C06	6003144	1st Relapse		72.79	8.41	115.15	2	21.7	
03D-2009	C09	44599HA	1st relapse		61.93	14.82	92.07	2	67.3	
03D-2009	C12	44599HA	1st relapse		70.06	4.83	35.68	2	67.3	
03E-2009	A01	F853428	1st relapse				15.74	1	13.3	
03D-2009	C15	F686876	1st relapse		1.23	0.19	7.92	1	51.7	
03D-2009	D03	F686876	2nd relapse		28.41	82.1	78.20	1	40	
03D-2009	D06	M721728	Not known		66.18	43.28	93.02		10.3	
03D-2009	D10	6382378	Relapse		9.57	0.43	59.03	2	13	
03D-2009	D13	M596357	Relapse		66.29	45.05	85.46	1	15	
03D-2009	E07	M718147	Diagnosis/pretreatment	33	66.42	49.35	111.00	2	24.3	
03D-2009	E10	M721068	1st relapse		82.09	67.24	102.44		20.3	
03F-2009	B08	6386925	Relapse		20.84	0.76	22.62	1	26	
03D-2009	E13	M532973	Diagnosis/pretreatment	16	59.33	42.75	88.15	1	10.3	
03D-2009	F01	1018763WH	Not known		45.04	14.61	109.43	1	17	
03D-2009	F04	6105456	Relapse		45.57	94.63	69.86	1	44.7	
03D-2009	F07	6330509	Relapse							
03D-2009	F10	6330509	Relapse		15.17	3.39	65.40	2	18.7	
03D-2009	F13	M715301	Not known					2		
03D-2009	G01	M715301	Not known		11.76	14.8	70.03	neg	1	

TMA	SPOT	HOSP.NO	Biopsy at	OS (mths)	p110alpha	p110beta	p110delta	PTEN	Ki67 (%)	Blastoid?
03E-2009	E02	6330509	Relapse		5.07	1.03	41.09	2	22.7	
03F-2009	A08	M715301	2nd Relapse				94.85			
03D-2009	G04	M621647	Relapse		5.45	62.13	74.87	neg	11.7	
03D-2009	G08	M621647	Relapse		45.15	55.93	95.78	1	10.3	
03E-2009	B09	M700928	Not known							
03D-2009	G11	M675633	Diagnosis/pretreatment	6	46.54	63.12	74.60	1	65.3	yes
03E-2009	E14	6306724	2nd Relapse							
03E-2009	G07	6306724	3rd Relapse		67.6	4.9	82.88		29	
03E-2009	D07	6346692	3rd Relapse		67.5		74.85		24.5	
03E-2009	D14	6346692	4th relapse		24.55	1.42	38.13	2	44.3	
03F-2009	C04	6346692	3rd Relapse		71.82	16.37	82.00	2	24.3	
03E-2009	H01	9031243	Diagnosis/pretreatment		61.88		35.96		25.5	
03E-2009	H04	9031243	Primary refractory		39.28	0.25	23.20	2	7.5	
03D-2009	G14	M578752	Relapse				0.20	1		
03D-2009	H03	M578752	Relapse		7.04	12.17	96.52	1	13	
03D-2009	H06	M578752	Relapse		6.53	6.05	98.63	1	22.3	
03D-2009	H09	F590185	1st relapse		66.24	3.56	64.46	neg	11	
03D-2009	H12	M654123	Diagnosis/pretreatment	18	53.52	2.74	89.59	1	7.3	
03D-2009	I03	M508453	Not known		10.03	4.31	56.03		6	
03D-2009	I06	M508453	1st relapse		15.07	26.15	87.07		22.7	
03D-2009	I09	6140686	Diagnosis/pretreatment	64	6.98	4.03	91.10	2	12.3	
03E-2009	B03	M705674	Diagnosis/pretreatment	244*			93.01			
03E-2009	B06	M667385	Not known		7.04	1.78	87.41	2	14.3	

APPENDIX C

Findings in NSG mice injected with MCL samples 2 and 3

Figure A2. A) Clinical information and B) immunophenotypic characteristics of peripheral blood MCL sample 2. CD5 expression was weak or absent in the majority of CD20 positive cells. This was consistent with the lymph node histology from this patient which also demonstrated cells exhibiting blastoid morphology. C) There were no detectable MCL cells on peripheral blood flow cytometry at 12 weeks on 4 NSG mice injected with sample 2. D) CD20 positive cells were not found on IHC of bone marrow from the femur. Representative image shown. E) No CD20 positive cells were found in NSG spleen as shown in the representative image.

Figure A3. A) Clinical information and B) immunophenotypic characteristics of MCL sample 3. A high tumour cell content was found in this lymph node suspension prepared from this biopsy taken at second relapse. C) There were no detectable MCL cells on peripheral blood flow cytometry at 12 weeks on 4 NSG mice injected with sample 2. D) CD20 positive cells were not found on IHC of bone marrow from the femur. Representative image shown. E) No CD20 positive cells were found in NSG spleen as shown in the representative image.

Figure A2

A.

Age (when sample taken)	71yrs
Sex	Male
Tissue diagnosis	CD5 negative, Blastoid MCL t(11;14)
Sample	Peripheral blood at diagnosis
Sites of involvement	Tonsil, bone marrow, cervical and mesenteric lymph nodes
Previous treatment	None

B.

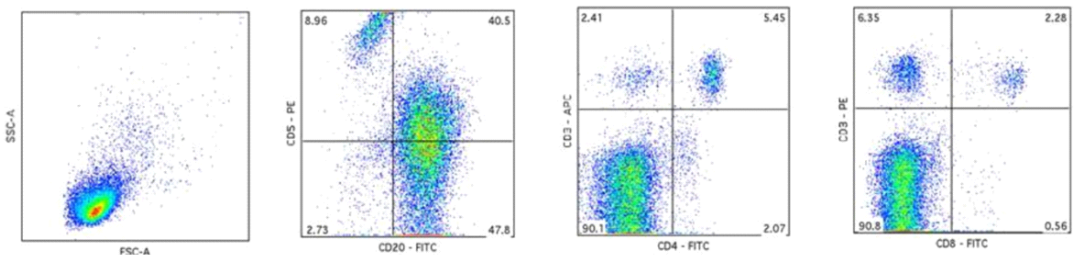

C.

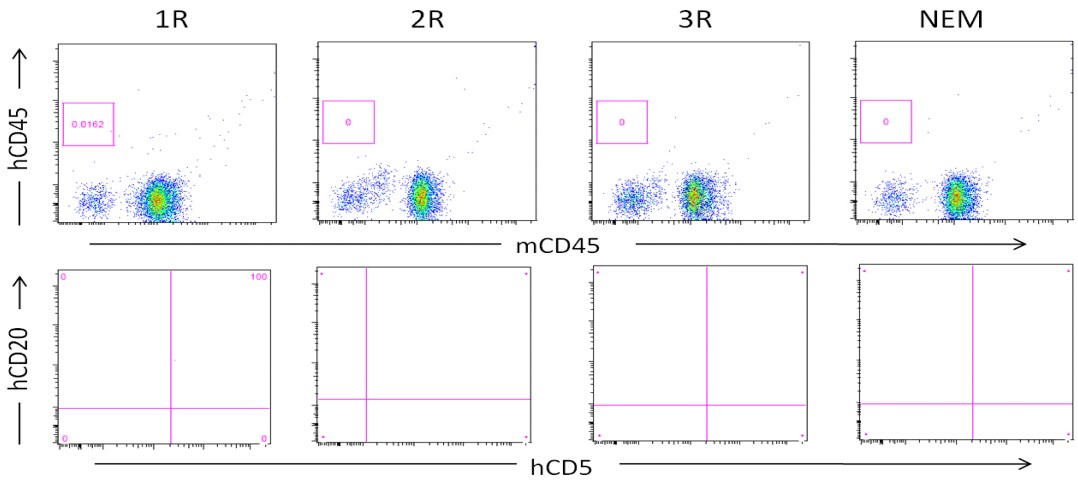

D.

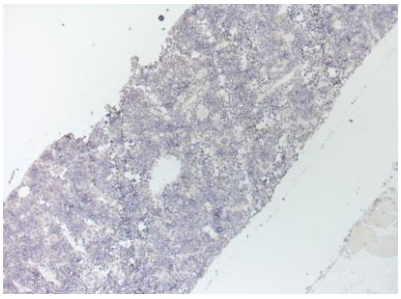

E.

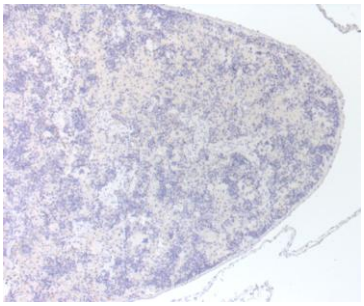

Figure A3

A.

Age (when sample taken)	69yrs
Sex	Male
Tissue diagnosis	MCL t(11;14)
Sample	Lymph node suspension at 2nd relapse
Sites of involvement	Not known
Previous treatment	Fludarabine (1999,2000)

B.

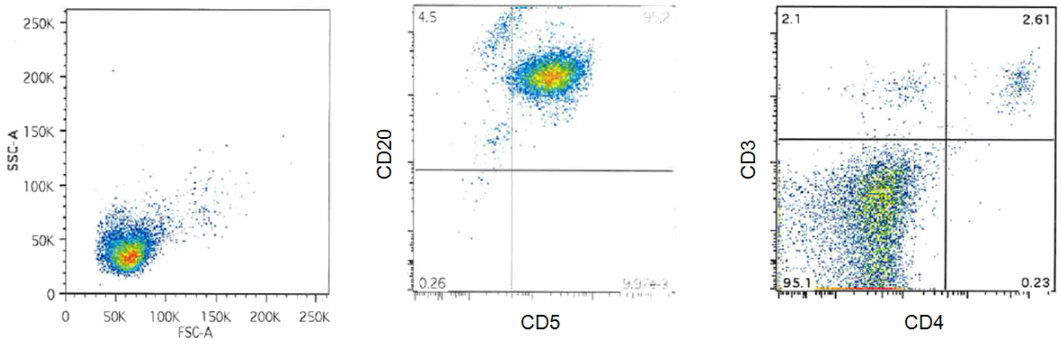

C.

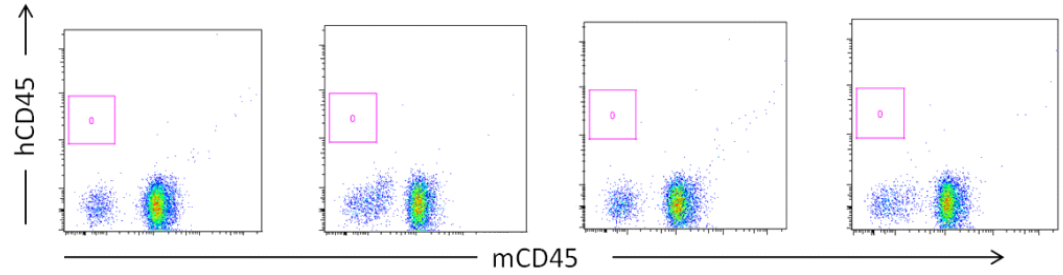

D.

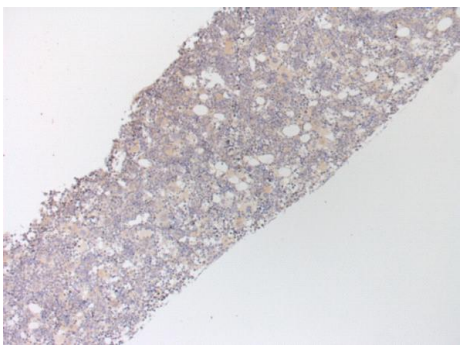

E.

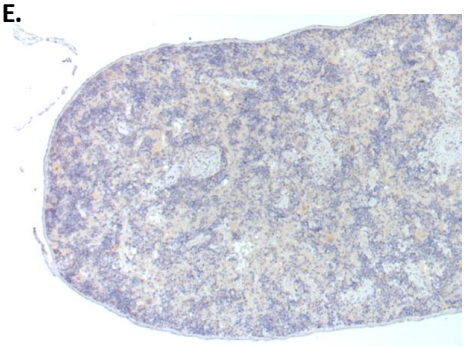

APPENDIX D

blood

2013 121: 2274-2284
Prepublished online January 22, 2013;
doi:10.1182/blood-2012-10-460832

P110α-mediated constitutive PI3K signaling limits the efficacy of p110δ -selective inhibition in mantle cell lymphoma, particularly with multiple relapse

Sunil Iyengar, Andrew Clear, Csaba Bödör, Lenushka Maharaj, Abigail Lee, Maria Calaminici, Janet Matthews, Sameena Iqbal, Rebecca Auer, John Gribben and Simon Joel

Blood (print ISSN 0006-4971, online ISSN 1528-0020), is published weekly by the American Society of Hematology, 2021 L St, NW, Suite 900, Washington DC 20036.

Regular Article

LYMPHOID NEOPLASIA

P110α-mediated constitutive PI3K signaling limits the efficacy of p110δ-selective inhibition in mantle cell lymphoma, particularly with multiple relapse

Sunil Iyengar, Andrew Clear, Csaba Bödör, Lenushka Maharaj, Abigail Lee, Maria Calaminici, Janet Matthews, Sameena Iqbal, Rebecca Auer, John Gribben, and Simon Joel

Centre for Haemato-Oncology, Barts Cancer Institute, Queen Mary University of London, Charterhouse Square, London, United Kingdom

Key Points

- The increased expression of PI3K p110α in mantle cell lymphoma, particularly at relapse, suggests a role for p110α in disease progression.
- A high *PIK3CA*/*PIK3CD* ratio identifies patients unlikely to respond to p110δ inhibitors and supports use of dual p110α/p110δ inhibitors in MCL.

Phosphoinositide-3 kinase (PI3K) pathway activation contributes to mantle cell lymphoma (MCL) pathogenesis, but early-phase studies of the PI3K p110δ inhibitor GS-1101 have reported inferior responses in MCL compared with other non-Hodgkin lymphomas. Because the relative importance of the class IA PI3K isoforms p110α, p110β, and p110δ in MCL is not clear, we studied expression of these isoforms and assessed their contribution to PI3K signaling in this disease. We found that although p110δ was highly expressed in MCL, p110α showed wide variation and expression increased significantly with relapse. Loss of phosphatase and tensin homolog expression was found in 16% (22/138) of cases, whereas *PIK3CA* and *PIK3R1* mutations were absent. Although p110δ inhibition was sufficient to block B-cell receptor–mediated PI3K activation, combined p110α and p110δ inhibition was necessary to abolish constitutive PI3K activation. In addition, GDC-0941, a predominantly p110α/δ inhibitor, was significantly more active compared with GS-1101 against MCL cell lines and primary samples. We found that a high *PIK3CA*/*PIK3CD* ratio identified a subset of primary MCLs resistant to GS-1101 and this ratio increased significantly with relapse. These findings support the use of dual p110α/p110δ inhibitors in MCL and suggest a role for p110α in disease progression. (*Blood*. 2013;121(12):2274-2284)

Introduction

Mantle cell lymphoma (MCL) is an aggressive disease in the vast majority of patients and is incurable with conventional therapy. Although there has been an improvement in median overall survival (OS), from the 2- to 4-year range cited in earlier series to between 5 and 7 years more recently,[1] outcome is still one of the poorest among B-cell lymphomas. MCL is characterized by t(11;14), which results in juxtaposition of the *IgH* enhancer on chromosome 14 to the *cyclin D1* locus on chromosome 11, leading to the characteristic overexpression of cyclin D1. Secondary hits primarily leading to defective DNA damage repair and cell -cycle dysregulation occur in MCL,[2] and a number of studies have implicated activation of the phosphoinositide-3 kinase (PI3K) pathway, one of the most commonly dysregulated pathways in human cancer, in the pathogenesis of this disease.[3-5] The serine-threonine kinase AKT, which is the major downstream target of PI3K, is thought to be important in MCL survival through its role in stabilizing cyclin D1 messenger RNA (mRNA), preventing nuclear export of cyclin D1 by phosphorylation of GSK-3b and increasing cyclin D1 translation through mammalian target of the rapamycin (mTOR) activation.[6-8]

PI3Ks are heterodimeric lipid kinases that have a regulatory and a catalytic subunit. Class IA PI3Ks primarily signal downstream of the B-cell receptor (BCR) and tyrosine kinase receptors to mediate downstream effects that lead to increased cell metabolism, proliferation, and survival. They have 3 catalytic subunit isoforms—p110α, p110β, and p110δ (encoded by *PIK3CA*, *PIK3CB*, and *PIK3CD*, respectively)—that dimerize with a p85 regulatory subunit. The p85 subunits (p85α, p85β, p55γ, p55α, and p50α) recognize phosphorylated tyrosine motifs.[9] These motifs are found in the intracellular domains of CD19 and BCAP (the B-cell adaptor for PI3K) and are phosphorylated upon BCR stimulation via phosphorylation of Syk and Lyn.[10] On binding to these sites, the p110 catalytic subunits are activated and convert cell membrane–bound PIP2 (phosphatidylinositol 4,5 biphosphate) to the important second messenger PIP3 (phosphatidylinositol 3,4,5 triphosphate). PIP3 binds and activates proteins that have a pleckstrin homology domain, such as AKT and PDK1. Full activation of Akt requires PI3K-induced phosphorylation at threonine 308 and mTOR complex 2–induced phosphorylation at serine 473. PTEN (phosphatase and tensin homolog) is a lipid phosphatase that opposes activation of this pathway by converting PIP3 back to PIP2.[11]

The p110δ isoform is a key messenger in BCR signaling and is highly enriched in leukocytes,[12,13] making it an attractive target in

Submitted October 7, 2012; accepted December 18, 2012. Prepublished online as *Blood* First Edition paper, January 22, 2013; DOI 10.1182/blood-2012-10-460832.

J.G. and S.J. contributed equally to this study.

The online version of this article contains a data supplement.

The publication costs of this article were defrayed in part by page charge payment. Therefore, and solely to indicate this fact, this article is hereby marked "advertisement" in accordance with 18 USC section 1734.

Table 1. Details of primary antibodies used for immunohistochemistry

Primary antibody	Supplier/code	Species (clone)	Antigen retrieval	Concentration	Incubation
P110α	Cell Signaling #4249	Rabbit polyclonal (C73F8)	Citrate pH6	1:250	40 seconds
P110β	Abcam ab65593	Mouse monoclonal	Citrate pH6	1:250	40 seconds
P110δ	Santa Cruz sc-55589	Mouse monoclonal (A-8)	Citrate pH6	1:500	40 seconds
PTEN	Cascade ABM-2052	Mouse monoclonal (6H2.1)	Citrate pH6	1:25	60 seconds

B-cell malignancies. However, in addition to quantitative isoform expression, the mechanism of PI3K activation may predict sensitivity to isoform selective inhibition. P110α (*PIK3CA*) is the only PI3K catalytic unit isoform that harbors cancer-associated somatic mutations and these occur at a high frequency in solid tumors.[14] *PIK3CA* mutations have not been found in 2 separate studies of MCL primary samples, but interestingly, gene amplification of *PIK3CA* related to increased copy number has been described in this disease.[3,15] Loss of PTEN expression is another mechanism leading to constitutive activation of the PI3K pathway, and studies in solid tumors have demonstrated a key role for p110β in PTEN-deficient tumors.[16-18] Loss of PTEN expression has been described in approximately 15% of MCLs.[15] Other mechanisms of PTEN inactivation that have been suggested in MCL include phosphorylation of PTEN and negative regulation by the microRNA-17–92 cluster.[4,19] More recently, activation of all 3 class IA isoforms has been described in association with somatic mutations in the gene encoding the regulatory p85α subunit (*PIK3R1*) in solid tumors.[20] These mutations have not been studied in MCL.

Preclinical studies have demonstrated the potential of inhibiting the PI3K pathway in MCL,[3,4,15,21] but early-phase studies of the first p110δ selective inhibitor, GS-1101, demonstrated more modest responses in patients with MCL compared with the impressive results seen in indolent non-Hodgkin lymphoma (NHL) and chronic lymphocytic leukemia.[22] Because loss of PTEN expression (~15%) and gene amplification of p110α (~68%) have been described in MCL,[15] understanding the relative contribution of the class IA isoforms in this disease may help in targeting this important oncogenic pathway more effectively.

We therefore studied the expression of class IA isoforms in MCL and evaluated their contribution to PI3K signaling in relation to BCR activation, loss of PTEN expression, and increased *PIK3CA* expression. We demonstrate that although p110δ remains highly expressed in MCL, tumor cells with increased *PIK3CA* expression can sustain constitutive PI3K signaling despite p110δ inhibition. Further, a *PIK3CA/PIK3CD* ratio greater than twice that in healthy B-cell controls identified primary MCL cases that were resistant to p110δ inhibition but significantly more sensitive to GDC-0941, a p110α/δ inhibitor in vitro. We also demonstrate a significant increase in both p110α expression and the *PIK3CA/PIK3CD* ratio with MCL progression.

Materials and methods

Cell lines

Granta519 and Jeko-1 MCL cell lines were used after confirmation of their identity by short tandem repeat profiling (LGC standards, Teddington, UK). Jeko-1 was cultured in RPMI (Sigma, St. Louis, MO) and Granta519 in Dulbecco's modified Eagle medium (Sigma). Both were supplemented with 10% heat-inactivated FCS (Sigma) and 1% gentamicin (GIBCO, Life Technologies, Paisley, UK).

Patient samples

In accordance with the updated Declaration of Helsinki, all samples were obtained following ethical approval, and after informed consent from patients treated at St Bartholomew's hospital. Solid tissue used in tissue microarray construction was fixed in formalin-fixed paraffin-embedded (FFPE) tissue. Snap-frozen tissue was evaluated for tumor content using CD20 staining of sections and homogenized using the Qiagen TissueLyserII (Qiagen, Hilden, Germany) for DNA and RNA extraction. Mononuclear cells from peripheral blood (PBMCs), bone marrow, and spleen-derived cell suspensions were isolated using Ficoll-paque density gradient centrifugation, and 22 primary MCL cell suspensions confirmed to have greater than 85% CD20-positive cells by flow cytometry were used in experiments. Clinical details of these primary samples are listed in supplemental Table 1. Cell suspensions were cultured in Iscove modified Dulbecco medium (Sigma) supplemented with 10% human serum, 1% gentamicin, 5 μg/mL bovine insulin, 50 μg/mL human transferrin, and 1 mM sodium pyruvate. PBMCs for control B cells were obtained from healthy volunteers and tonsil controls were obtained from tonsillectomies performed for nonmalignant pathology.

Antibodies and reagents

Primary antibodies for western blotting against p110α (#4249), glyceraldehyde-3-phosphate dehydrogenase (GAPDH, #2118), total Syk (#2712), phospho-Syk thr525/526 (#2710), total Akt (#9272), phospho-Akt ser473 and thr308 (#9271, #2965), phospho-GSK3b ser9 (#9323), total ribosomal S6 (#2217), and phospho-S6 ser235/ser236 (#2211) were purchased from Cell Signaling Technologies (Danvers, MA). Antibodies against p110β (sc-602) and p110δ (sc-55589) were purchased from Santa Cruz Biotechnology (Santa Cruz, CA) and anti-human PTEN (ABM-2052) from Cascade Bioscience (Winchester, MA). Goat anti-human immunoglobulin (Ig)M F(ab')$_2$ fragments were purchased from Southern Biotech (Cambridge, UK). GDC-0941,[23] A66,[24] and TGX221[25] were purchased from Selleck Chem (Houston, TX) and CAL-101/GS-1101 from Active Biochem (Maplewood, NJ). For cytotoxicity studies, cells were treated in triplicate with increasing concentrations of inhibitor (0.1-10 μM) for 72 hours while an inhibitor concentration of 1 μM was used to assess downstream effects by western blotting.

Immunohistochemistry

Tissue microarrays (TMA) were constructed using triplicate 1-mm cores of FFPE tissue. Clinical details of samples included in the tissue microarray are listed in supplemental Table 2. Although antibodies against p110α, p110β, and PTEN have previously been validated on FFPE tissue,[26] there was no previous literature describing the use of a p110δ-selective antibody for immunohistochemistry (IHC) at the time of performing these experiments. We therefore constructed a cell block microarray with high and low p110δ–expressing cell lines to optimize and validate this antibody (supplemental Figure 1). Details of antibodies used, concentrations, and antigen retrieval methods are listed in Table 1. All slides were scanned using an Olympus scanning microscope to obtain high-resolution images that were analyzed on Ariol SL-50 version 3.2 (Genetix, San Jose, CA) visual analysis software. Briefly, images of cores were screened individually to exclude nontumor tissue and the software was trained to calculate the percentage of positive

cells and staining intensity of cores. Biopsies with only 1 evaluable core on the TMA were excluded and IHC scores for duplicates and triplicates were averaged. The IHC score was calculated as the product of percentage positive cells and mean intensity. PTEN expression was scored independently by 2 authors (S.I. and A.L.) as 2+ (strong), 1+ (moderate) or 0 (no expression) based on expression in tumor cells compared with blood vessels or nontumor cells in the TMA cores.

Western blotting

Briefly, cell lysates were prepared by resuspending cell pellets in lysis buffer containing protease and phosphatase inhibitors (Roche, Basel, Switzerland). Total protein was estimated using the Pierce BCA protein assay kit (Thermo Scientific, Waltham, MA). Lysates were resolved on a NuPAGE 4% to 12% gel (Invitrogen, Life Technologies, Paisley, UK) and transferred onto a polyvinylidene difluoride membrane using the iBlot dry transfer method (Invitrogen). Membranes were incubated with primary antibody either overnight at 4°C or at room temperature for 2 hours at the recommended dilutions. Membranes were then washed and incubated with horseradish peroxidase-labeled secondary antibody (Dako, Denmark) for an hour at room temperature. Electrochemiluminescence reagent (GE Health Care, Uppsala, Sweden) was applied to visualize the blots using the Fuji LAS 2000 digital imager (Fujifilm, Japan).

Quantitative real-time PCR

Total RNA was extracted from cell suspensions and frozen tissue using the RNeasy mini kit (Qiagen, Hilden, Germany). A total of 2 μg RNA was reverse transcribed using the high-capacity reverse transcription kit (Applied Biosystems, Life Technologies, Paisley, UK) as per manufacturer's recommendations. Quantitative real-time polymerase chain reaction (qRT-PCR) was performed on the ABI HT-7900 instrument (Applied Biosystems) using Taqman gene expression assays (Applied Biosystems) for *PIK3CA* (Hs00192399_m1), *PIK3CB* (Hs00927728_m1), and *PIK3CD* (Hs00180679_m1). Data were analyzed using SDS 2.1 software and relative expression values were calculated using the ΔCt method with *GAPDH* (Hs99999905_m1) as endogenous control. All reactions were run in triplicate.

PIK3CA and *PIK3R1* mutation analysis

Genomic DNA was extracted from frozen lymph nodes (verified to have >80% tumor content) and PBMCs of MCL patients using the DNeasy mini kit (Qiagen). Primers used for PCR amplification of *PIK3CA* exons 9 and 20 and *PIK3R1* exons 9, 10, 11, 13, 15, and 16 are listed in supplemental Table 3. After DNA purification, bidirectional Sanger sequencing was performed on the purified PCR products.

Cytotoxicity assays

Growth inhibition was measured with the Guava ViaCount assay (Millipore, Billerica, MA). The ViaCount reagent was added to cells treated in triplicate in a 96-well plate, and cell count and viability was determined on a Guava express plus instrument (Millipore). The adenosine triphosphate (ATP) cytotoxicity assay kit (Lonza, Basel, Switzerland) was used to measure the cytotoxic effects of PI3K inhibitors on primary MCL cell suspensions. Briefly, cells were plated in triplicate in a 96-well format and treated with PI3K inhibitors at increasing concentrations before measurement of ATP luminescence in a plate reader at 72 hours.

Statistical analysis

Prism version 5.03 (GraphPad, La Jolla, CA) was used for statistical analysis. Normally distributed data sets were tested with paired or unpaired *t* tests, as appropriate, whereas for 3 data sets, 1-way analysis of variance followed by a Bonferroni multiple comparison post-hoc analysis was used. Data sets that were not normally distributed were analyzed using the Mann-Whitney test for unpaired samples or the Wilcoxon matched-pairs signed-rank test for paired samples. A P value below .05 was considered significant.

Results

P110α expression in MCL is significantly higher beyond first relapse

Expression of p110α, β, and δ was evaluated by IHC analysis of 144 evaluable biopsies from 109 MCL patients. P110δ was consistently expressed at high levels in MCL. P110β expression was the weakest, whereas p110α showed a wide variation in expression across biopsies (Figure 1A). Median expression of p110α (median IHC score = 44.5 vs 33.7, $P = .15$) and p110δ (median IHC scores = 77.4 vs 81.1, $P = .2$) in MCL was not different from that seen in the germinal center area of tonsil controls, whereas PI110β expression was significantly lower in MCL ($P = .01$). As shown in Figure 1B, p110α expression was significantly higher in biopsies taken beyond first relapse compared to those taken at diagnosis ($P = .04$). These differences were even more striking in sequential biopsies ($P = .008$) with 5 of 6 lymphoma samples showing increased p110α expression beyond first relapse (Figure 1B-D). Expression of p110α beyond first relapse was also significantly higher than expression in tonsil controls ($P = .024$). No significant change in expression of p110β or p110δ was seen with relapse. We also did not find a significant difference in expression of the individual isoforms between blastoid and classical MCL (data not shown).

Loss of PTEN expression is relatively common in MCL, whereas *PIK3CA* and *PIK3R1* mutations are rare or absent

We assessed PTEN protein expression by IHC (Figure 2). In keeping with a previous report,[15] we found loss of PTEN expression in 17% of diagnostic (6/35) and 16% of all (22/138) biopsies (Figure 2C). A higher proportion of tumors exhibiting blastoid morphology had loss of PTEN expression compared to cases with classical histology, but this was not statistically significant (20% vs 15%, $P = .55$ by Fisher's exact test). No significant change was found in the pattern of isoform expression, particularly for p110β, in biopsies that had loss of PTEN expression (Figure 2D). Loss of PTEN expression was seen by western blotting in 2 of 12 primary MCL samples (Figure 2E), and the results seen on western blotting corresponded to those seen by IHC. Unlike reports in solid tumors,[16] we did not find significant additional cytotoxicity in these 2 samples using the combination of GS-1101 and TGX221 (p110β selective inhibitor) compared to GS-1101 alone (Figure 2F). Exons 9 and 20 of *PIK3CA* and exons 9, 11, 12, 13, 15, and 16 of *PIK3R1* were sequenced in a total of 20 primary MCL samples and 2 cell lines (Granta519, Jeko-1); no mutations were found, suggesting these are rare or do not occur in MCL.

P110δ inhibition prevents BCR-induced PI3K activation in MCL, whereas additional p110α inhibition is required to abolish constitutive PI3K activation

The Jeko-1 MCL cell line exhibits low or undetectable levels of *p*-Akt and was therefore used to study the effect of isoform selective inhibition on agonist-induced BCR signaling. Whereas the p110δ inhibitor GS-1101 prevented phosphorylation of Akt (thr308) in response to BCR stimulation with IgM $F(ab')_2$ fragments, the p110α inhibitor A66[24] and the p110β inhibitor TGX221[25] had minimal effects on *p*-Akt (thr308) (Figure 3A). We then studied the effect of isoform-selective inhibition on the Granta519 MCL cell line, which exhibits constitutive Akt phosphorylation in association with increased p110α expression as a result of increased *PIK3CA* copy number and gene expression[15] (Figure 3B). Interestingly, GS-1101

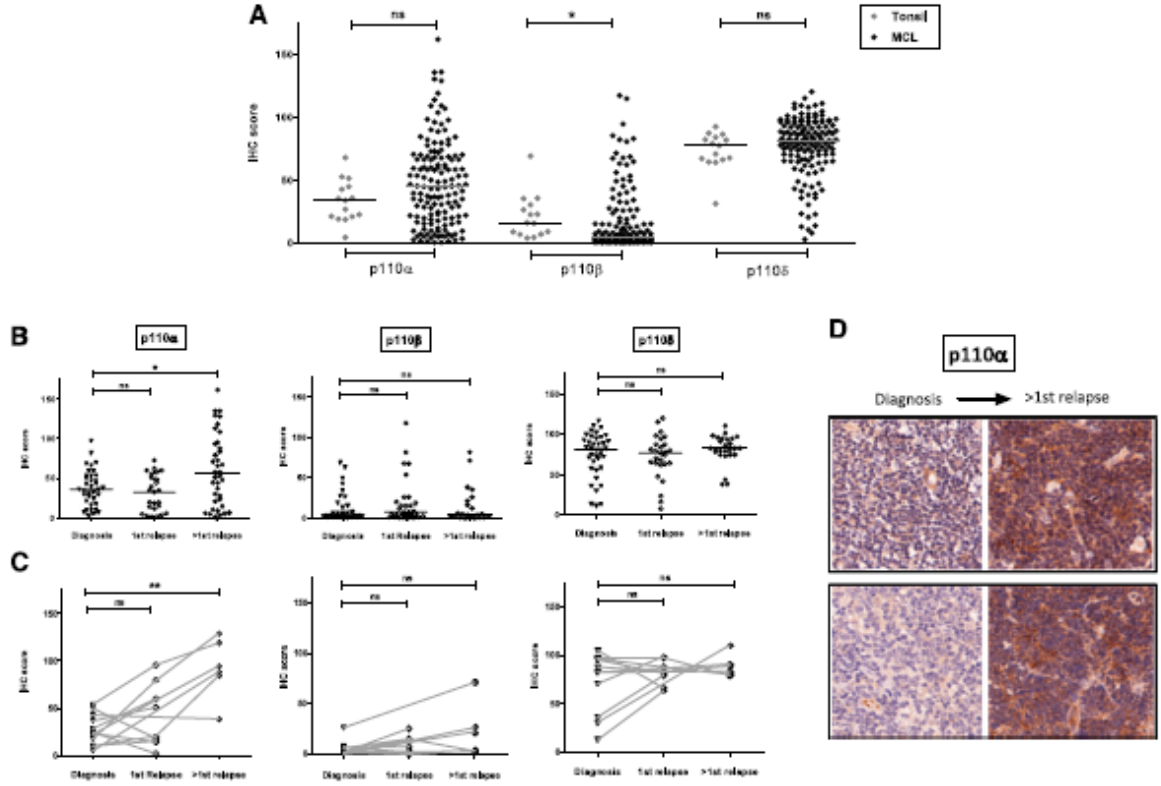

Figure 1. IHC expression of class IA PI3K isoforms in mantle cell lymphoma. (A) Dot plot showing expression of class IA isoforms in MCL biopsies (144 biopsies evaluable for all 3 isoforms from 109 patients) compared with tonsil controls (n = 14). Each dot represents the average IHC score of triplicate cores and bars represent median expression. P110δ is highly expressed in MCL and p110α shows a wide range of expression, whereas p110β expression is the weakest. (B) Dot plots showing significant increase in p110α expression, but not p110β or p110δ, beyond first relapse. (C) This finding is more striking in 12 sequential cases, 6 of whom had biopsies beyond first relapse (connected by gray lines). (D) Representative IHC images (original magnification ×200) of sequential biopsies from 2 patients showing a significant increase in p110α expression with relapse *$P < .05$, **$P < .01$. ns, not significant.

(1 μM) was unable to abolish Akt phosphorylation in Granta519, whereas at equimolar concentrations GDC-0941, a predominantly p110α/δ inhibitor, blocked Akt phosphorylation in a sustained manner over 24 hours. This was reflected in reduced downstream phosphorylation of ribosomal S6 as a result of mTOR inhibition (Figure 3C). To establish that this effect on constitutive PI3K activation was related to activity of the p110α isoform, we combined GS-1101 separately with the p110α inhibitor A66 and a p110β inhibitor TGX221 and tested these combinations along with GS-1101 and GDC-0941 alone in serum-starved Granta519 cells. Combining GS-1101 with A66 had a similar effect as GDC-0941, whereas combining GS-1101 with TGX221 made no significant difference, confirming that residual constitutive PI3K signaling in GS-1101–treated cells is attributable to p110α (Figure 3D).

PI3K inhibition with GDC-0941 results in greater cytotoxicity to MCL cells compared with GS-1101

We compared the cytotoxicity of GS-1101 and GDC-0941 on growth and survival of MCL cell lines and primary samples. GDC-0941 induced significantly higher growth inhibition at 72 hours in 2 MCL cell lines with intact PTEN expression (Granta519 and Jeko-1) compared with GS-1101, whereas the p110α-selective inhibitor A66 had a minimal effect on both cell lines (Figure 3F-G). Using an ATP cytotoxicity assay, a similar significant effect was observed on treating 12 primary MCL samples (Figure 3H) and GDC-0941 was significantly more cytotoxic than GS-1101 above concentrations of 0.1 μM ($P = .046$ at 0.1 μM, .008 at 1 μM, .005 at 5 μM, and .035 at 10 μM). Basal phospho-Akt levels were not predictive of sensitivity to either inhibitor in both cell lines and primary samples. We also treated B cells isolated from 3 healthy donors with GS-1101 and GDC-0941 and found no statistically significant difference in cytotoxicity even at higher concentrations.

A high *PIK3CA*/*PIK3CD* mRNA ratio can predict resistance to p110δ-selective inhibition

Our findings in the Granta519 MCL cell line led us to hypothesize that gene expression of the PI3K isoforms in MCL cells can predict sensitivity to isoform selective inhibition. We measured *PIK3CA*, *PIK3CB*, *PIK3CD*, and *GAPDH* mRNA levels by qRT-PCR in the same 12 MCL cell suspensions that we previously treated with GS-1101 and GDC-0941 and compared them with healthy B-cell controls. *PIK3CD* was highly expressed with gene expression of both *PIK3CA* and *PIK3CD* significantly up-regulated compared with healthy B-cell controls. *PIK3CB* showed the weakest expression (Figure 4A). Neither *PIK3CA* nor *PIK3CD* levels predicted sensitivity or resistance to the inhibitors independently. However, by plotting the ratio of *PIK3CA* to *PIK3CD* (*PIK3CA*/*PIK3CD*),

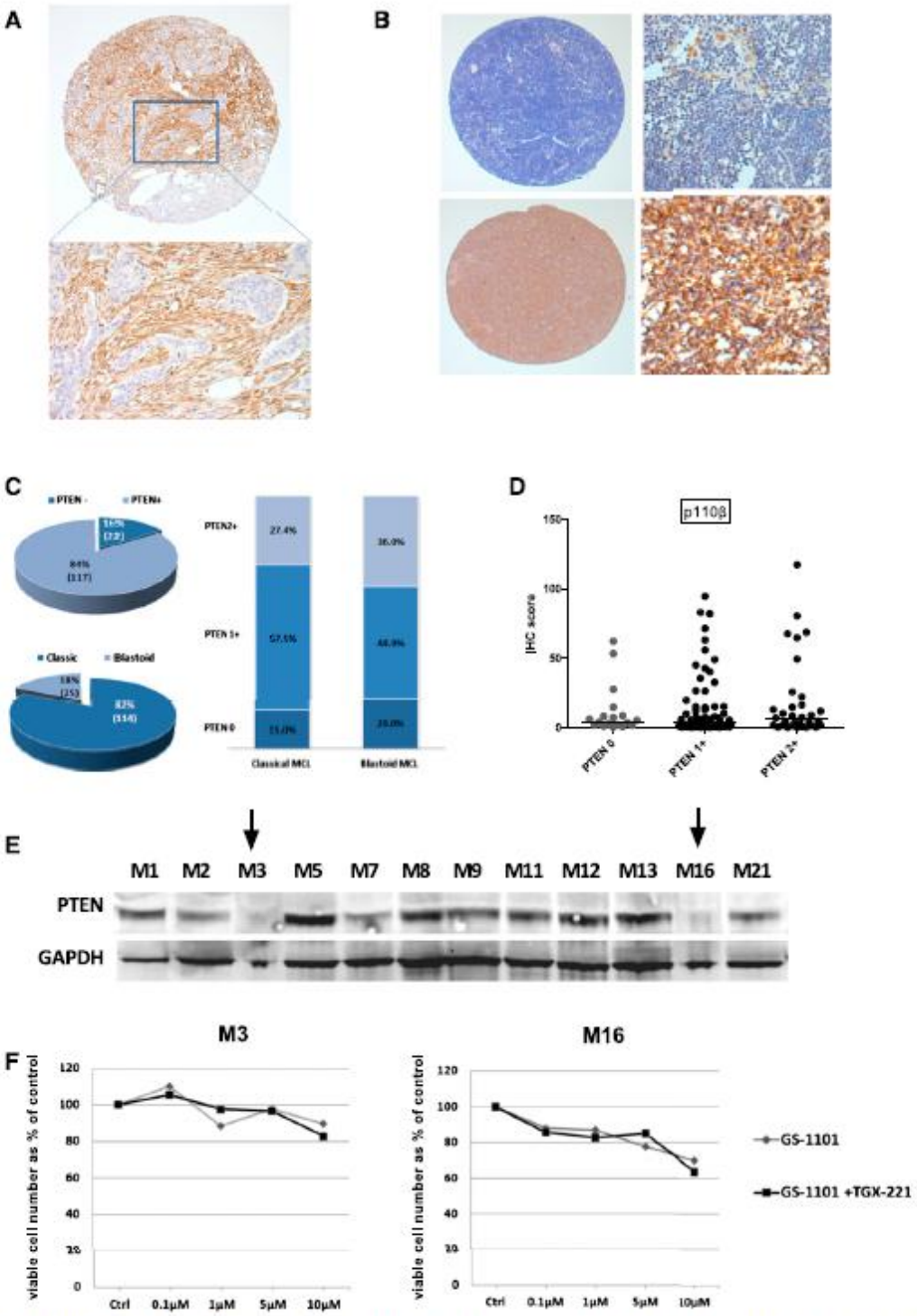

Figure 2. Loss of PTEN expression in MCL. (A) Core from a *PTEN*-null adenocarcinoma control showing PTEN-negative tumor islands surrounded by PTEN-positive stroma by IHC (original magnifications ×50 and ×200). (B) Representative images of MCL cores with and without loss of PTEN expression (original magnifications ×50 and ×200). Macrophages and blood vessels were used as internal controls. (C) Pie chart showing the proportion of all biopsies with PTEN loss and blastoid morphology accompanied by a bar graph of distribution of PTEN loss in blastoid and nonblastoid MCL. (D) Dot plot comparing p110β expression levels between cores with and without loss of PTEN expression showing no difference among the 3 groups (PTEN−, PTEN 1+, and PTEN2+). There was also no significant difference in expression of p110α and δ between these groups (data not shown). (E) Western blot for PTEN expression in 12 MCL cell suspensions showing loss of expression in 2 samples (indicated by arrows). (F) Results of ATP cytotoxicity assay after 72 hours' treatment showing no benefit from addition of a p110β-selective inhibitor to GS-1101 in 2 MCL suspensions exhibiting loss of PTEN expression.

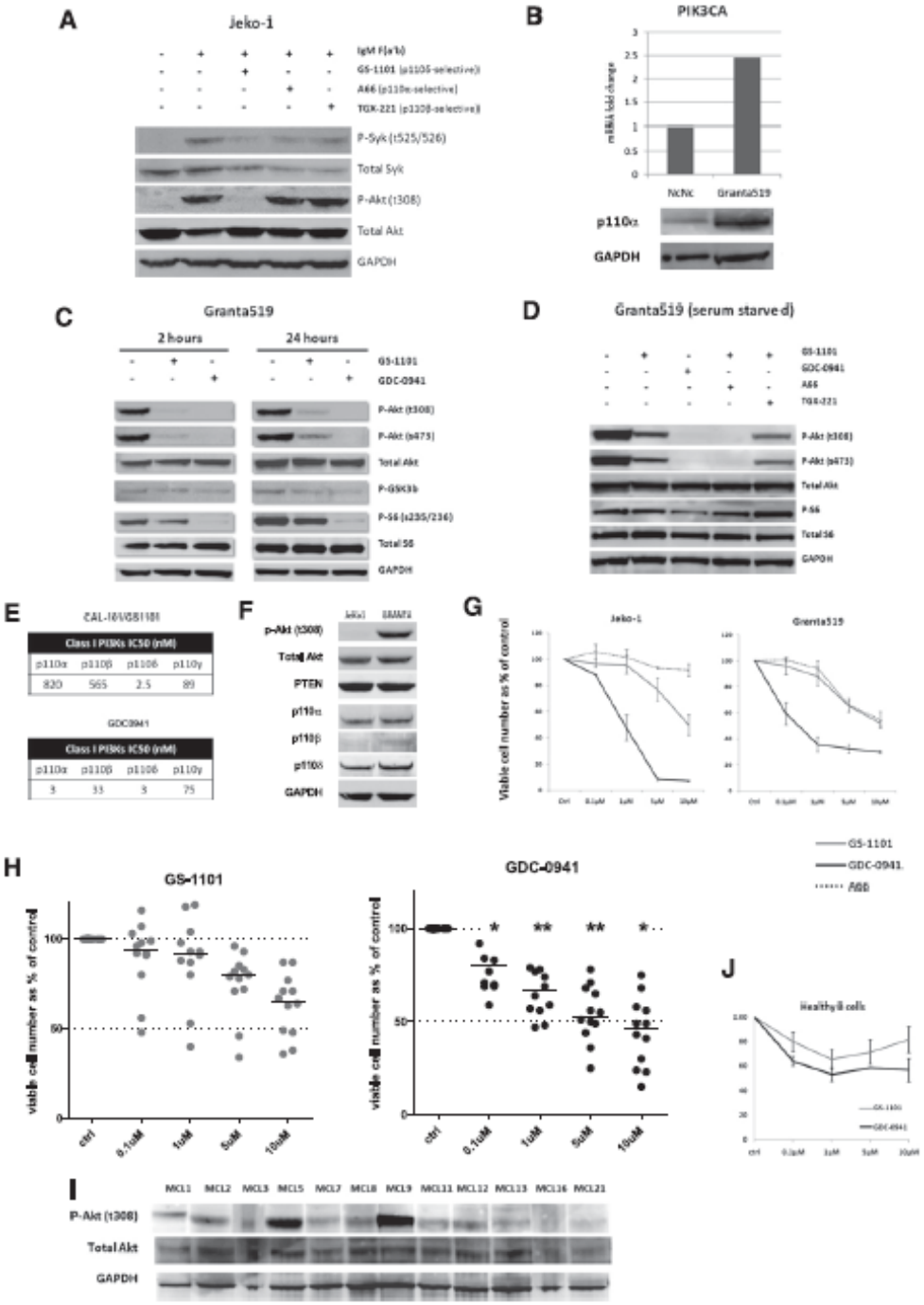

Figure 3. Role of class IA isoforms in BCR-induced and constitutive PI3K signaling. (A) Jeko-1 cells were pretreated for an hour with isoform-selective inhibitors (1 μM) as indicated, followed by IgM stimulation with 10 μg/mL anti-human IgM F(ab') fragments for 10 minutes. Phospho-Akt (thr308) levels were compared by western blotting with nonstimulated and IgM-stimulated Jeko-1 controls. P-Syk (tyr525/526) was used as a marker of BCR activation. GS-1101 (p110δ-selective) blocked *p*-Akt production, whereas A66 (p110α-selective) and TGX-221 (p110β-selective) did not. (B) Real-time PCR and western blotting confirming increased expression of *PIK3CA* and p110α in Granta519 MCL cell lines compared with the lymphoblastoid cell line NcNc. (C) Western blot comparing downstream effects of GS-1101 (1 μM) and GDC-0941 (1 μM), at 2 time points demonstrating incomplete and nonsustained effect of GS-1101 on *p*-Akt, *p*-GSK3β, and *p*-S6. (D) Western blots were performed with serum-starved (4 hours) Granta519 cells treated with GS-1101, GDC-0941, and combinations of GS-1101 with A66 or TGX-221 (all 1 μM), for 2 hours, confirming the effect of p110α on constitutive PI3K activation. (E) Comparison of 50% inhibition/inhibitory concentration of GS-1101 and GDC-0941 for the 4 class I isoforms. GS-1101 is highly p110δ-selective, whereas p110α is predominantly p110α/δ-selective. The activity of both inhibitors against p110γ is comparable. (F) Western blot showing expression of *p*-Akt (t308) and the class IA catalytic unit isoforms in Jeko-1 and Granta519. (G) Greater growth inhibition is seen in Granta519 and Jeko-1 with GDC-0941 compared with GS-1101, whereas A66 has a minimal effect. (H) Dot plots showing greater cytotoxicity (ATP assay) with GDC-0941 compared with GS-1101 in 12 primary MCL samples with significant toxicity at and above 0.1 μM. (I) Western blot showing *p*-Akt (thr308) expression in the same 12 MCL cell suspensions. (J) Comparative cytotoxicity (ATP assay) of GDC-0941 and GS-1101 in 3 healthy B cells showing somewhat greater, but not statistically significant, cytotoxicity at all concentrations with GDC-0941. **P* < .05, ***P* < .01.

we were able to separate the samples into 2 groups—1 with ratios similar to healthy B cells that had similar responses to GS-1101 and GDC-0941 and 1 with significantly higher expression. *PIK3CA/PIK3CD* greater than twice that seen in healthy B-cell controls identified a group that was resistant to GS-1101 and showed a significantly greater response to GDC-0941 ($P = .03$ at 0.1 μM, $P = .008$ at 1 μM) (Figure 4B). The 2 samples that were most sensitive to GS-1101 reassuringly fell in the group with the lower ratios. These differences were seen at 0.1 and 1 μM, concentrations at which the drugs are likely to be most selective for their targets. We validated our findings in a second independent cohort of 10 primary MCL samples using 1 μM GS-1101 and GDC-0941 (Figure 4C). We also treated these 10 samples with the p110α inhibitor A66 (1 μM) alone but found no significant cytotoxicity in any of the samples treated (supplemental Figure 2). As may be expected, we found some primary samples, mainly in the low-ratio group, that were relatively resistant to both GS-1101 and GDC-0941 at these lower concentrations, even when phosphorylation of Akt was blocked, suggesting alternative survival pathways were active in these tumors (data not shown).

A high *PIK3CA/PIK3CD* mRNA ratio is frequently associated with MCL progression

To investigate whether disease progression was associated with a change in *PIK3CA/PIK3CD*, qRT-PCR was performed on RNA extracted from frozen serial biopsies from 4 MCL patients and 2 tonsil controls. Protein was extracted simultaneously for western blotting from these biopsies. Whereas *PIK3CD* was highly expressed and up-regulated compared with tonsil controls (Figure 5A), *PIK3CA/PIK3CD* was higher in all 4 cases at relapse compared with diagnosis (Figure 5C). Compared with PBMCs, *PIK3CA* expression, and as a result *PIK3CA/PIK3CD*, was relatively lower in lymph nodes. However, protein expression by western blotting showed upregulation of p110α compared with tonsil controls and also showed a marked increase with relapse in 2 of 4 serial biopsies (Figure 5B).

To investigate whether differences existed in isoform expression between MCL and other NHL, we extracted PI3K class IA isoform expression data from publicly available gene expression profiling (www.ebi.ac.uk) from a study comparing diagnostic samples of MCL to indolent NHL.[27] Even in these diagnostic samples, median expression of only the *PIK3CA* isoform, and therefore *PIK3CA/PIK3CD*, was significantly higher in MCL compared with chronic lymphocytic leukemia and indolent NHL (Figure 6A). There was no publicly available data comparing gene expression in relapsed lymphomas that we could analyze at the time of this study, but we performed immunohistochemistry for p110α in sequential biopsies from 10 follicular lymphoma patients, 4 of whom had paired biopsies beyond first relapse, and did not find evidence of increase in expression with relapse (Figure 6B-C).

Discussion

Several studies have described the importance of the PI3K pathway in the pathogenesis of MCL.[3-5] The relatively inferior effects seen in MCL in early-phase trials of the PI3K p110δ selective inhibitor GS-1101 emphasize the need to study the contribution of the other class IA PI3K isoforms to MCL survival.

In keeping with previous observations,[3,15] we did not find *PIK3CA* mutations in 20 MCL primaries, and PTEN loss occurred at a frequency of about 16%, with an apparently, but not significantly, higher incidence in blastoid MCL. In addition, activating *PIK3R1* mutations were shown to be rare or absent in MCL. Although gene amplification of *PIK3CA* related to increased copy number has been previously described in MCL, we demonstrate for the first time that a high *PIK3CA/PIK3CD* mRNA ratio can predict resistance to p110δ-selective inhibition and is frequent with relapse. The mechanism for this increase of expression with relapse is unclear. Our observation that the increase in p110α expression is particularly significant beyond first relapse may imply a chemotherapy-induced phenomenon or selection and expansion of a chemotherapy-resistant clone with high *PIK3CA* expression, but this needs further study.

We demonstrate that although p110δ continues to be the predominant isoform in terms of expression and agonist-induced BCR signaling in MCL, an increase in p110α expression can maintain constitutive PI3K signaling in MCL cells despite p110δ inhibition. We explored the option of an small interfering RNA study to demonstrate the reliance of Granta519 on p110α but it has been found that knocking down the expression of any 1 of the class I PI3K isoforms can result in a compensatory increase or decrease in activity of other isoforms and lead to artifacts.[28-31] We therefore elected to use a highly selective p110α inhibitor, A66, for our studies.[24] Studies in healthy mouse lymphocytes have demonstrated that although PI3K p110δ plays a predominant role in both agonist-dependent and agonist-independent BCR signaling, p110α contributes to agonist-independent signaling.[32] The increased expression of p110α in MCL, particularly with relapse, may therefore allow tumor cells to survive independent of agonist-induced activation of the PI3K pathway. Of note, a similar phenomenon has been observed in immortalized macrophages, where p110α takes on a more prominent role in PI3K signaling, in contrast to primary macrophages where p110δ is the predominantly active isoform.[33] It is possible that PI3K inhibitors may also have an effect on the tumor microenvironment; this issue is not explored here. However, the clear effect in MCL cell lines and primary MCL cells in the absence of the microenvironment, together with the relative increase of *PIK3CA* in MCL cells themselves, strongly suggest that this is likely to result in a differential effect with greater toxicity to the tumor cells compared with an effect on the microenvironment.

P110β shows the weakest expression at both the RNA and protein level in MCL and we found no additional effect on PI3K-induced Akt phosphorylation on combining a highly selective p110β inhibitor (TGX-221) with GS-1101. We also demonstrate that, unlike observations in solid tumors,[16] there is a lack of additional cytotoxicity from combining TGX-221 and GS-1101 in MCL samples that exhibit loss of PTEN expression, but this requires confirmation on a larger number of samples. GDC-0941, an inhibitor with high selectivity for p110α and p110δ, was significantly more cytotoxic in both MCL cell lines and primary samples. Although inhibiting additional PI3K isoforms is likely to be associated with greater toxicity, this inhibitor has shown favorable toxicity profiles in early-phase clinical trials in solid tumors.[34] Our findings are unlikely to be influenced by p110γ, the only class IB catalytic unit isoform, because both GS-1101 and GDC-0941 have similar efficacy against p110γ (Figure 3E). The greater contribution of p110α to PI3K signaling with MCL relapse can explain the relatively modest effects seen in relapsed/refractory MCL patients recruited into early-phase trials of GS-1101.

We propose that *PIK3CA/PIK3CD* is a potential biomarker that can identify patients who are resistant to p110δ inhibition and may benefit most from combined p110α/δ inhibitor therapy. This ratio may identify tumors that can use p110α-mediated constitutive PI3K signaling for microenvironment-independent survival. Our data also

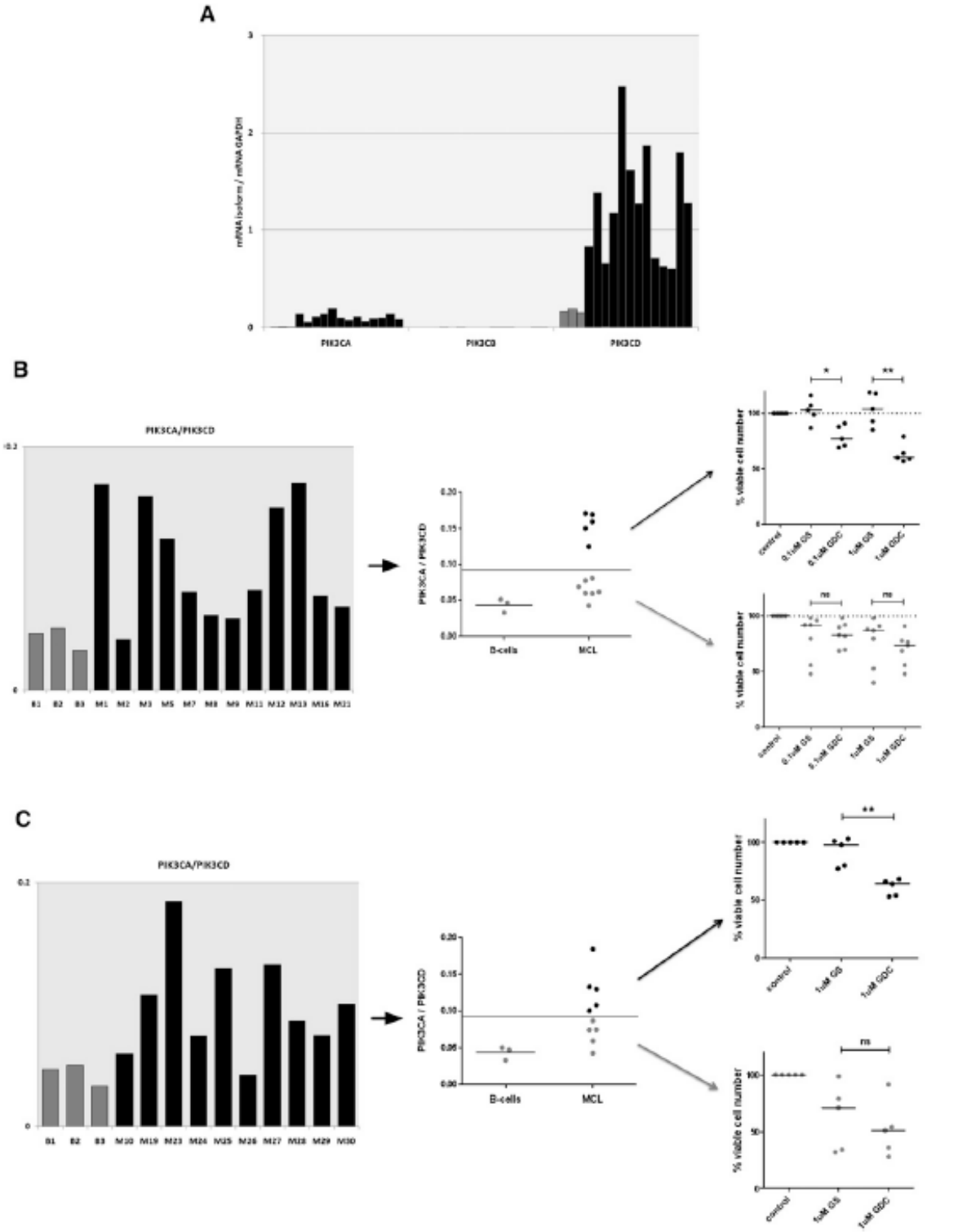

Figure 4. The *PIK3CA*/*PIK3CD* mRNA ratio can predict resistance to GS-1101. (A) Gene expression of class IA PI3K isoforms, relative to GAPDH, in 12 diagnostic MCL PBMCs and 3 healthy B-cell controls, showing significant increase in *PIK3CA* and *PIK3CD* compared with controls (gray) and very low levels of *PIK3CB*. (B) A *PIK3CA*/*PIK3CD* greater than twice the mean ratio in healthy B cells identifies a subset of primary samples (5/12) that are resistant to 0.1 μM and 1 μM GS-1101 (GS), but show significantly higher toxicity with equimolar concentrations of GDC-0941 (GDC). (C) This cutoff, when applied to an independent validation cohort (n = 10), was able to identify GS-1101–resistant samples (primary samples treated with 1 μM of GS-1101 and GDC-0941).

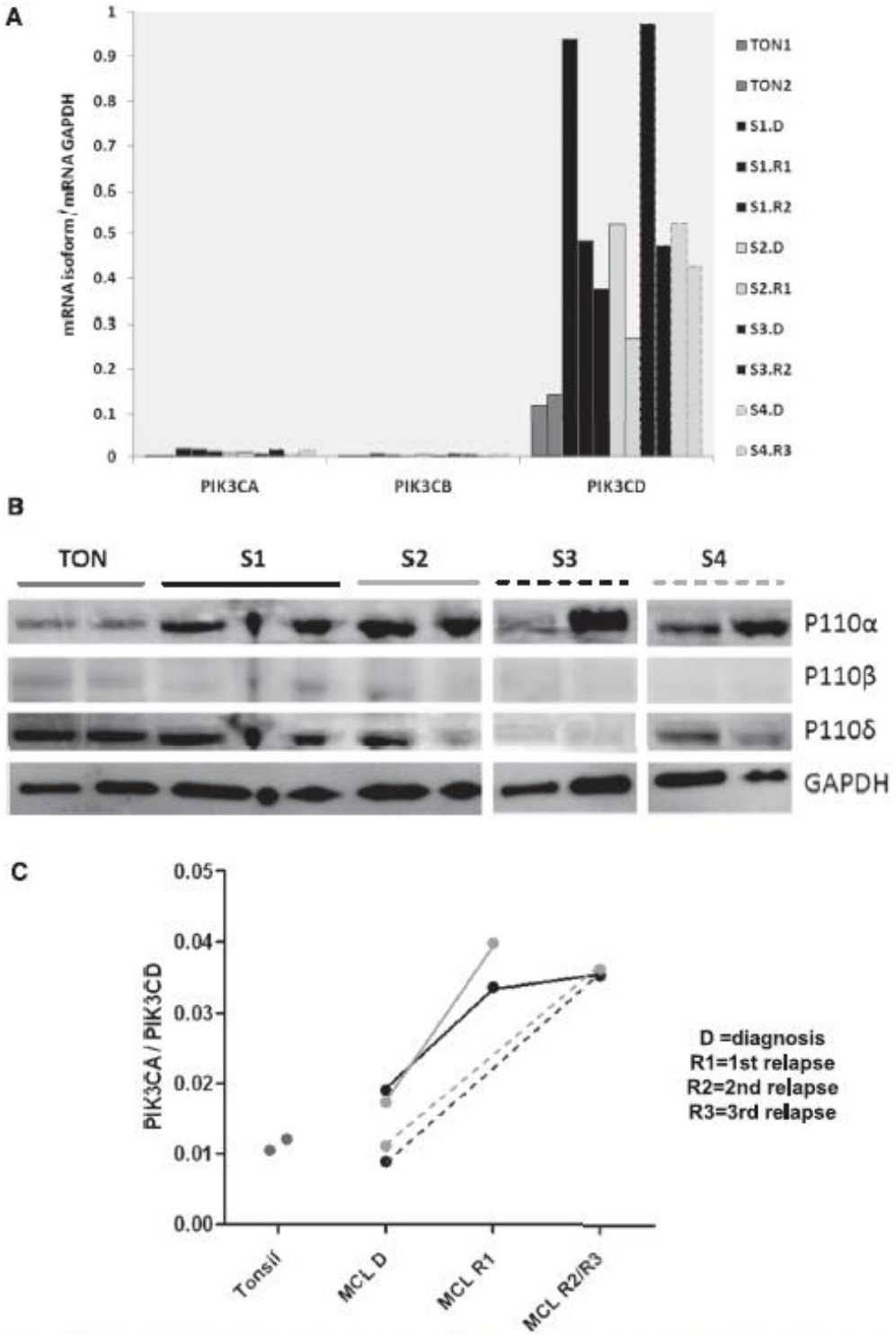

Figure 5. *PIK3CA/PIK3CD* increases with relapse in MCL. (A) Gene expression of the PI3K class IA isoforms compared with 2 tonsil controls (gray). Serial biopsies from the same patient are in the same color (B) western blot showing very weak expression of p110β and a clear increase in MCL p110α compared with tonsil while p110δ protein expression in MCL is similar to tonsil controls. Increase in p110α with relapse is apparent in 2 out of 4 serial biopsies (C) Dot plot showing a significantly higher *PIK3CA/PIK3CD* ratio in all relapsed samples compared with matched diagnostic samples and tonsil controls.

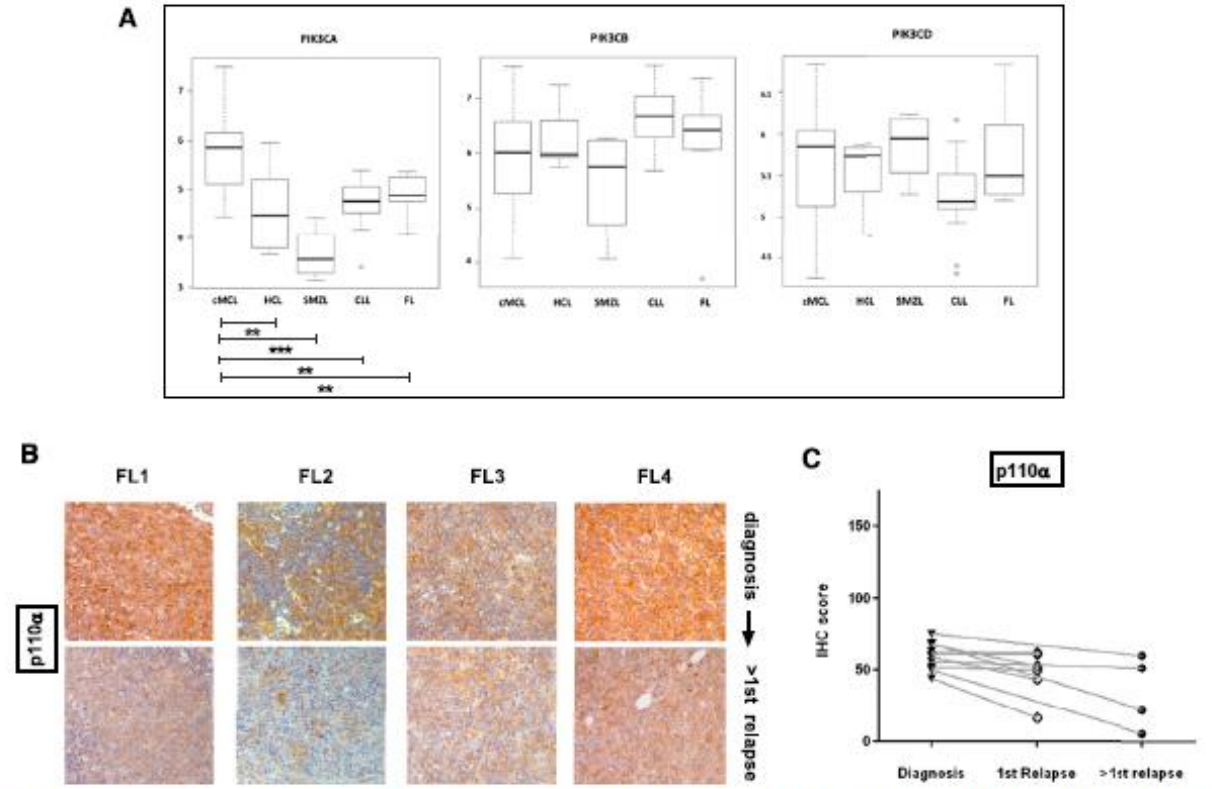

Figure 6. P110α expression does not increase with relapse in follicular lymphoma and gene expression of *PIK3CA* is significantly higher in MCL compared with indolent NHL and CLL. (A) Gene expression of class IA PI3K isoforms at diagnosis in MCL was compared with indolent NHL using publicly available Affymetrix data (European Bioinformatics Institute, www.ebi.ac.uk ref: E-GEOD-16455) with the web-based software *O-miner*. cMCL, conventional MCL; CLL, chronic lymphocytic leukemia; FL, follicular lymphoma; HCL, hairy cell leukemia, SMZL, splenic marginal zone lymphoma. *PIK3CA* expression is significantly higher in MCL compared with indolent NHLs (Benjamini-Hochberg multiple testing adjusted *P* values: cMCL vs HCL = .005, cMCL vs SMZL = .0001 cMCL vs CLL = .003, cMCl vs FL = .05) In this study, whereas *PIK3CB* and *PIK3CD* expression is not. (*$P < .05$, **$P < .01$, ***$P < .001$). (B) IHC images of 4 follicular lymphoma diagnosis: second-relapse pairs showing no increase in p110α expression with relapse (original magnification ×200). (C) Dot plot comparing expression of p110α in sequential biopsies from follicular lymphoma patients (n = 10). No evidence of increased p110α expression is seen with relapse. Pairs are connected by straight lines.

suggest that Akt phosphorylation, when present, is a useful marker to study responses to PI3K inhibition but absence of phosphorylation does not preclude sensitivity to PI3K inhibition. Also, we did not find higher Akt phosphorylation in MCL exhibiting increased *PIK3CA/PIK3CD*. This is not entirely surprising because, for instance, Akt-independent PI3K signaling has been found in cancers harboring *PIK3CA* mutations[35,36] and a similar mechanism could operate in MCLs that have a high *PIK3CA/PIK3CD* ratio.

In summary, our findings suggest that MCL requires blockade of both p110α and p110δ, particularly at relapse, for effective PI3K inhibition. This will require testing in a clinical trial, but the assessment of the relative gene expression of these isoforms may help identify those patients that are most likely to respond to these exciting agents.

Acknowledgments

The authors thank Bart Vanhaesebroeck, Ezra Aksoy, the European Hematology Association (EHA)-ASH Translational Research Training in Hematology faculty, particularly Donna Neuberg, David Williams, and Linda Burns, for their valuable advice and suggestions. The authors also thank Jacek Marzec for bioinformatics, John Riches and Eleni Kiotsiu for providing healthy B cells, and all the patients at Barts Cancer Centre who kindly consented to provide samples for this research.

This work was supported by grants from the David Pitblado Foundation, National Cancer Institute (P01 CA81538) (J.G.), Cancer Research UK (C1574/A6806), and an EHA Partner Fellowship awarded by the European Hematology Association (2009/01) (C.B.).

Authorship

Contribution: S.I., J.G., and S.J. designed experiments; S.I., A.C., and C.B. performed the experiments; R.A., L.M., S.I., and J.M. provided essential reagents, clinical samples, and related clinical information; M.C. and A.L. assisted with tissue microarray construction and immunohistochemistry scoring. S.I. prepared the manuscript with input from all authors.

Conflict-of-interest disclosure: J.G. and R.A. have received honoraria from Gilead for attendance at advisory boards. J.G. has received honoraria from Roche for attendance at advisory boards. The remaining authors declare no competing financial interests.

Correspondence: John Gribben, Centre for Haemato-Oncology, Barts Cancer Institute, London EC1M 6BQ, UK; e-mail: j.gribben@qmul.ac.uk.

References

1. Martin P, Coleman M, Leonard JP. Progress in mantle-cell lymphoma. *J Clin Oncol*. 2009;27(4):481-483.
2. Fernandez V, Hartmann E, Ott G, Campo E, Rosenwald A. Pathogenesis of mantle-cell lymphoma: all oncogenic roads lead to dysregulation of cell cycle and DNA damage response pathways. *J Clin Oncol*. 2005;23(26):6364-6369.
3. Rudelius M, Pittaluga S, Nishizuka S, et al. Constitutive activation of Akt contributes to the pathogenesis and survival of mantle cell lymphoma. *Blood*. 2006;108(5):1668-1676.
4. Dal Col J, Zancai P, Terrin L, et al. Distinct functional significance of Akt and mTOR constitutive activation in mantle cell lymphoma. *Blood*. 2008;111(10):5142-5151.
5. Rizzatti EG, Falcão RP, Panepucci RA, et al. Gene expression profiling of mantle cell lymphoma cells reveals aberrant expression of genes from the PI3K-AKT, WNT and TGFbeta signalling pathways. *Br J Haematol*. 2005;130(4):516-526.
6. Prasad A, Park IW, Allen H, et al. Styryl sulfonyl compounds inhibit translation of cyclin D1 in mantle cell lymphoma cells. *Oncogene*. 2009;28(12):1518-1528.
7. Dal Col J, Dolcetti R. GSK-3beta inhibition: at the crossroad between Akt and mTOR constitutive activation to enhance cyclin D1 protein stability in mantle cell lymphoma. *Cell Cycle*. 2008;7(18):2813-2816.
8. Pérez-Galán P, Dreyling M, Wiestner A. Mantle cell lymphoma: biology, pathogenesis, and the molecular basis of treatment in the genomic era. *Blood*. 2011;117(1):26-38.
9. Vanhaesebroeck B, Waterfield MD. Signaling by distinct classes of phosphoinositide 3-kinases. *Exp Cell Res*. 1999;253(1):239-254.
10. Okkenhaug K, Vanhaesebroeck B. PI3K in lymphocyte development, differentiation and activation. *Nat Rev Immunol*. 2003;3(4):317-330.
11. Vanhaesebroeck B, Stephens L, Hawkins P. PI3K signalling: the path to discovery and understanding. *Nat Rev Mol Cell Biol*. 2012;13(3):195-203.
12. Vanhaesebroeck B, Welham MJ, Kotani K, et al. P110delta, a novel phosphoinositide 3-kinase in leukocytes. *Proc Natl Acad Sci USA*. 1997;94(9):4330-4335.
13. Bilancio A, Okkenhaug K, Camps M, et al. Key role of the p110delta isoform of PI3K in B-cell antigen and IL-4 receptor signaling: comparative analysis of genetic and pharmacologic interference with p110delta function in B cells. *Blood*. 2006;107(2):642-650.
14. Samuels Y, Wang Z, Bardelli A, et al. High frequency of mutations of the PIK3CA gene in human cancers. *Science*. 2004;304(5670):554.
15. Psyrri A, Papageorgiou S, Liakata E, et al. Phosphatidylinositol 3'-kinase catalytic subunit alpha gene amplification contributes to the pathogenesis of mantle cell lymphoma. *Clin Cancer Res*. 2009;15(18):5724-5732.
16. Wee S, Wiederschain D, Maira SM, et al. PTEN-deficient cancers depend on PIK3CB. *Proc Natl Acad Sci USA*. 2008;105(35):13057-13062.
17. Edgar KA, Wallin JJ, Berry M, et al. Isoform-specific phosphoinositide 3-kinase inhibitors exert distinct effects in solid tumors. *Cancer Res*. 2010;70(3):1164-1172.
18. Jia S, Liu Z, Zhang S, et al. Essential roles of PI(3)K-p110beta in cell growth, metabolism and tumorigenesis. *Nature*. 2008;454(7205):776-779.
19. Rao E, Jiang C, Ji M, et al. The miRNA-17 approximately 92 cluster mediates chemoresistance and enhances tumor growth in mantle cell lymphoma via PI3K/AKT pathway activation. *Leukemia*. 2012;26(5):1064-1072.
20. Jaiswal BS, Janakiraman V, Kljavin NM, et al. Somatic mutations in p85alpha promote tumorigenesis through class IA PI3K activation. *Cancer Cell*. 2009;16(6):463-474.
21. Lannutti BJ, Meadows SA, Herman SE, et al. CAL-101, a p110delta selective phosphatidylinositol-3-kinase inhibitor for the treatment of B-cell malignancies, inhibits PI3K signaling and cellular viability. *Blood*. 2011;117(2):591-594.
22. Kahl B, Byrd JC, Flinn IW, et al. Clinical safety and activity in a phase 1 study of CAL-101, an isoform-selective inhibitor of phosphatidylinositol 3-kinase P110δ, in patients with relapsed or refractory non-Hodgkin lymphoma [abstract]. *Blood (ASH Annual Meeting Abstracts)*. 2010;116(21):1777.
23. Folkes AJ, Ahmadi K, Alderton WK, et al. The identification of 2-(1H-indazol-4-yl)-6-(4-methanesulfonyl-piperazin-1-ylmethyl)-4-morpholin-4-yl-thieno[3,2-d]pyrimidine (GDC-0941) as a potent, selective, orally bioavailable inhibitor of class I PI3 kinase for the treatment of cancer. *J Med Chem*. 2008;51(18):5522-5532.
24. Jamieson S, Flanagan JU, Kolekar S, et al. A drug targeting only p110α can block phosphoinositide 3-kinase signalling and tumour growth in certain cell types. *Biochem J*. 2011;438(1):53-62.
25. Jackson SP, Schoenwaelder SM, Goncalves I, et al. PI 3-kinase p110beta: a new target for antithrombotic therapy. *Nat Med*. 2005;11(5):507-514.
26. Carvalho S, Milanezi F, Costa JL, Amendoeira I, Schmitt F. PIKing the right isoform: the emergent role of the p110beta subunit in breast cancer. *Virchows Arch*. 2010;456(3):235-243.
27. Fernández V, Salamero O, Espinet B, et al. Genomic and gene expression profiling defines indolent forms of mantle cell lymphoma. *Cancer Res*. 2010;70(4):1408-1418.
28. Vanhaesebroeck B, Ali K, Bilancio A, et al. Signalling by PI3K isoforms: insights from gene-targeted mice. *Trends Biochem Sci*. 2005;30(4):194-204.
29. Vanhaesebroeck B, Rohn JL, Waterfield MD. Gene targeting: attention to detail. *Cell*. 2004;118(3):274-276.
30. Vanhaesebroeck B, Guillermet-Guibert J, Graupera M, et al. The emerging mechanisms of isoform-specific PI3K signalling. *Nat Rev Mol Cell Biol*. 2010;11(5):329-341.
31. Geering B, Cutillas PR, Nock G, et al. Class IA phosphoinositide 3-kinases are obligate p85-p110 heterodimers. *Proc Natl Acad Sci USA*. 2007;104(19):7809-7814.
32. Ramadani F, Bolland DJ, Garcon F, et al. The PI3K isoforms p110alpha and p110delta are essential for pre-B cell receptor signaling and B cell development. *Sci Signal*. 2010;3(134):ra60.
33. Papakonstanti EA, Zwaenepoel O, Bilancio A, et al. Distinct roles of class IA PI3K isoforms in primary and immortalised macrophages. *J Cell Sci*. 2008;121(Pt 24):4124-4133.
34. Wagner AJ, Von Hoff DH, LoRusso PM, et al. A first-in-human phase I study to evaluate the pan-PI3K inhibitor GDC-0941 administered QD or BID in patients with advanced solid tumors [abstract]. *J Clin Oncol*. 2010;28(15s):suppl. Abstract 2541.
35. Vasudevan KM, Barbie DA, Davies MA, et al. AKT-independent signaling downstream of oncogenic PIK3CA mutations in human cancer. *Cancer Cell*. 2009;16(1):21-32.
36. Morrow CJ, Gray A, Dive C. Comparison of phosphatidylinositol-3-kinase signalling within a panel of human colorectal cancer cell lines with mutant or wild-type PIK3CA. *FEBS Lett*. 2005;579(23):5123-5128.